MODELING, SIMULATION AND OPTIMIZATION OF PYROLYSIS OF BIOMASS

THESIS

Submitted in partial fulfillment
of the requirements for the degree of
DOCTOR OF PHILOSOPHY

By

ASHISH SUBHASH CHAURASIA

Under the supervision of

Prof.(Dr.) B.V. Babu
Assistant Dean - Engineering Services Division and
Group Leader - Chemical Engineering &
Engineering Technology Departments

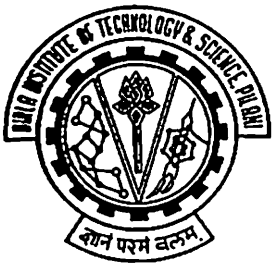

BIRLA INSTITUTE OF TECHNOLOGY AND SCIENCE
PILANI (RAJASTHAN)
2003

BIRLA INSTITUTE OF TECHNOLOGY AND SCIENCE
PILANI (RAJASTHAN)

CERTIFICATE

This is to certify that the thesis entitled "**Modeling, Simulation and Optimization of Pyrolysis of Biomass**" and submitted by **Ashish Subhash Chaurasia** ID No. **2001PHXF404** for award of Ph D Degree of the Institute, embodies the original work done by him under my supervision.

Signature in full of the Supervisor

Name in capital block letters B. V. Babu

Date: 09-12-2005

Designation
Professor of Chemical Engineering
Group Leader - Chemical Engineering & Engineering Technology Departments and
Assistant Dean - Engineering Services Division

ACKNOWLEDGEMENTS

I wish to express deep sense of gratitude and sincere thanks to my thesis supervisor Prof (Dr) B. V. Babu - Group Leader of Chemical Engineering & Engineering Technology Departments and Assistant Dean of ESD for his valuable guidance, encouragement, suggestions, and moral support throughout the period of this research work. It has been a privilege for me to work under his valuable guidance.

Much appreciation is expressed to Dr. V. S. Moholkar and Dr. M. K. Deshmukh who were the members of Doctoral Advisory Committee (DAC), for their kind suggestions, moral support, and assistance.

Gratitude is also accorded to BITS, Pilani for providing all the necessary facilities to complete the research work. My special thanks to Prof. S. Venkateswaran, the Vice-Chancellor of the Institute for allowing me to pursue my research work successfully. My sincere thanks to Prof. L. K. Maheshwari - Director, Prof. K. E. Raman - Deputy Director (Administration), Prof. V. S. Rao - Deputy Director (Off-Campus Programmes), and Prof. A. K. Sarkar - Dean (Instruction Division and Faculty Division I), for providing the necessary infrastructure and other facilities.

I also express my gratitude for the kind and affectionate enquiries about the work and the encouragement given by Prof. Ravi Prakash - Dean (Research and Consultancy Division) and Mr. S. D. Pohekar of the same Division.

Special thanks and appreciation is extended to Prof. R. P. Vaid, Prof. B. R. Natrajan, Prof. T. N. S. Mathur, Mr. S. D. Manjare, Mr. Rakesh Angira, Mr. B. D. Munshi, Mr. H. K. Mohanta, Mrs. Manjuri Kumar and other members of Chemical Engineering Group for their valuable advice and moral support throughout the study. I also thank to Mr. V. Ramakrishna of Civil Engineering Group for his cooperation and encouragement in completing my research work.

I sincerely thank anonymous reviewers of International Journals of 'Chemical Engineering Science', 'Energy Conversion and Management' and 'Arid Land Studies' for accepting seven research papers for publication in their journals based on the present study. Special thanks is also extended to Prof. A. T. Bell - Executive Editor (Chemical Engineering Science Journal) & Prof. of Chemical Engineerng Department (University of California) and Dr. Jesse C. Denton - Editor in chief (Energy Conversion and Management Journal) for their valuable suggestions while the reviewing the research papers based on the present work.

Sincere thanks to Dr M Ishwara Bhat, Librarian, BITS as well as to librarian at IIT, Delhi for providing literature useful for the present study. Special thank to my friends Mr Ravindra Marathe - Research scholar (National University of Singapore) and Amit Gaikwad - Research scholar (IIT, Delhi) for sending various research papers throughout the study I thank my co-researchers Mr Rahul Ralegaonkar, Mr Rajendra Khapre and Mr Shrikant Charde for their cooperation and encouragement in completing my research work

I express my thanks to Mr. Babulal Saini, Mr. Jangvir, Mr. Shankar, Mr Amarlal and other non-teaching staff of Chemical Engineering Group for their cooperation during the preparation of this thesis. I also wish to acknowledge Mr. Jamunadhar Saini, Mr. Mathuram Jangid, Mr. Gopi, Mr. Mahavir, Mr. Dilbag, Mr. Ashok and other members of Instruction Division for their help and cooperation. I express my thanks to Mr. V. N. Sharma, Mr. Mahendra Saini and Mr. Rajkumar Saini of ESD (Workshop) for their help while sending research papers related to thesis work.

I would like to thank members of Reprography, Xerox and Printing Sections for their prompt services. I would like to thank one and all who have helped me in myriad ways throughout the course of this work.

Last but not the least, this work would not have been completed without the moral support I got from my Param Pujya Gurudev - Sant Shri Asaramji Bapu, Sant Shri Saibaba and my loving parents - Shri Subhash S. Chaurasia & Smt. Shobha S. Chaurasia.

ABSTRACT

For energy applications, biomass has either been processed to increase its energy content or burned directly in furnaces. Energy produced from biomass or its conversion products represents an important part among today's energy sources. As biomass is renewable, abundant, and has domestic usage, the sources of biomass can help the world to reduce its dependence on petroleum products and natural gas. The pyrolysis of biomass is considered as one of the viable means for overcoming the so-called "energy-crisis". It is a renewable source of energy and has many advantages from ecological point of view. An understanding of the chemical processes and transport mechanisms of biomass pyrolysis is important for many applications including optimization of boilers and large scale furnaces, estimating the dominant design variable in pyrolysis reactor, determining the forest fire behavior, and predicting the resistance of buildings to fire.

The pyrolysis process consists of the thermal degradation of biomass feedstock, in the absence of oxygen/air, leading to the formation of solid (charcoal), liquid (tar and other organics) and gaseous products (methane, ethane, carbon monoxide, etc). Pyrolysis can be used as an independent process for the production of useful energy (fuels) and/or chemicals. It also occurs as the first step in gasification or combustion process. The knowledge on kinetics of pyrolysis of a solid particle is very significant in designing a fluid-solid gasifier. In spite of these many advantages, little work has been reported in literature on the mechanistic modeling of such kinetics. This may be attributed to the extreme complexity of pyrolysis process due to the presence of homogeneous and heterogeneous reactions.

The understanding of physical phenomena of pyrolysis and representing it with an appropriate mathematical model is essential in the design of pyrolysis reactors and biomass gasifiers. In the present study, the description of chemical processes of pyrolysis is coupled to an unsteady-state, one-dimensional, variable property model of transport phenomena including heat transfer (by all the three modes, i.e., convection, conduction & radiation), mass transfer (transport of volatiles & gases by diffusion & convection), and momentum transfer. A generalized reference model (Model-I) incorporating all the above effects is proposed. This is further improved by proposing two simplified models (Model-II & Model-III) incorporating additional assumptions. Finite difference pure implicit scheme utilizing Tri-Diagonal Matrix Algorithm (TDMA) is employed for solving heat transfer and mass transfer model equations. Runge-Kutta 4^{th} order method is used for solving chemical kinetics model equations. Simulations are carried out considering different geometries of biomass (slab, cylinder, and sphere) of

equivalent radius ranging from 0.0000125 m to 0.05 m, and temperature ranging from 303 K to 2800 K. The results obtained using the model developed are in excellent agreement with many experimental studies, much better than the agreement with the earlier models reported in the literature.

Based on the importance and promising nature of the pyrolysis of biomass process, the modeling and simulation has been carried out in this study for finding out the optimum parameters of the pyrolysis process. The model results reported in literature indicate a decrease in final pyrolysis time as the net heating rate or temperature is increased. But the results obtained using a wide range of operating conditions in the present study show that the final pyrolysis time initially decreases and then increases as the net heating rate or temperature is increased. This interesting phenomenon, which is not reported by earlier investigators, could be well explained both qualitatively and quantitatively by proposing appropriate realistic models and through simulations.

The improved validated model is utilized to investigate the influence of particle size, particle shape, product distribution, conversion time, convective & radiative heat transfer, and heat of reaction. Operating conditions are identified (by increasing convective heat transfer under controlled conditions) at which it is possible to get the same extent of conversion of biomass with lesser pyrolysis time that could be obtained when radiation is present at higher temperature ranges. Dominant design variables are identified for pyrolysis process through sensitivity analysis. Wide ranges of heat transfer coefficient (8.4-126.0 W/m^2K), thermal conductivity (0.03-0.40 W/mK), reactor temperature (303-2800 K), emissivity (0.0-1.0) and heat of reaction number (-0.7 to -0.1 for exothermic reactions and 0.001 to 1.0 for endothermic reactions) are considered. The highest sensitivity is associated with reactor temperature and emissivity. The least sensitive parameter is the convective heat transfer coefficient. The sensitivity for all the parameters is highest for the slab geometry and is lowest for the spherical geometry. The heat source from the surrounding environment which is utilized to initiate the pyrolysis reaction is not required at the later stage as the reaction is exothermic. This situation is termed the '*self-sustaining reaction*' which is identified in the present work. This is the major advantage of pyrolysis process.

The models on pyrolysis of biomass are corrected, updated, and also new models are proposed by incorporating the shrinkage effect. This resulted in an accurate prediction of yield of a wide range of products obtained during pyrolysis. The earlier models under-predict the product yields. The improved validated model incorporating shrinkage effect is used to examine the impact of shrinkage on particle size, pyrolysis time, product yields, specific heat capacity, and Biot number. Shrinkage affects both the pyrolysis time and the product yield in thermally thick regime. However, it is found that shrinkage has negligible affect on pyrolysis in the thermally thin regime. The improved validated model is also coupled with the optimization of pyrolysis time and heating rate under the restriction on concentration of biomass (a non-linear functional relationship) using a population-based search algorithm (Differential Evolution).

Keywords: Pyrolysis; Biomass; Modeling; Optimum parameters; Kinetics; Heat transfer; Mass transfer; Momentum transfer; Simulation; Thermal property; Thermodynamic property; Shrinkage; Gasification; Thermally thick regime; Differential Evolution; Sensitivity analysis.

TABLE OF CONTENTS

LIST OF TABLES

LIST OF FIGURES

A_1, A_2, A_3	frequency factor, s^{-1}
b	geometry factor (slab=1, cylinder=2, sphere=3)
B	virgin biomass
G_1	$(\text{gases and volatiles})_1$
C_1	$(\text{char})_1$
G_2	$(\text{gases and volatiles})_2$
C_2	$(\text{char})_2$
C_B	concentration of B, kg m^{-3}
$\overline{C}_B$	concentration of B, dimensionless
C_{G1}	concentration of G_1, kg m^{-3}
$\overline{C}_{G1}$	concentration of G_1, dimensionless
C_{C1}	concentration of C_1, kg m^{-3}
$\overline{C}_{C1}$	concentration of C_1, dimensionless
C_{G2}	concentration of G_2, kg m^{-3}
$\overline{C}_{G2}$	concentration of G_2, dimensionless
C_{C2}	concentration of C_2, kg m^{-3}
$\overline{C}_{C2}$	concentration of C_2, dimensionless
C_p	specific heat capacity, J kg^{-1} K^{-1}
C_{pG1}	heat capacity of $(\text{gases and volatiles})_1$, C_{pG10} at initial condition, J/mol K
d	pore diameter, m
D_1, D_2	constants defined by expressions of k_1 and k_2 respectively, K
D_{eG1}	effective diffusivity of $(\text{gases and volatiles})_1$, D_{eG10} for initial effective diffusivity, m^2/s
E_3	activation energy defined by expression of k_3, J mol^{-1}
E_{pa}	average percentage error, dimensionless
h	convective heat transfer coefficient, W m^{-2} K^{-1}

H	modified Biot number
HR	heating rate K s^{-1}
$\overline{HR}$	heating rate, dimensionless
k	thermal conductivity, W m^{-1} K^{-1}
k_{mass}	mass transfer coefficient of (gases and volatiles)$_1$ across the film, m/s
k_1, k_2, k_3	rate constants, s^{-1}
l	axial length of cylinder, m
L_1, L_2	constants defined by expressions of k_1 and k_2 respectively, K^2
M	mass, kg
N	total number of equations used in the simulation of the model
n_1, n_2, n_3	orders of reactions
p	gas pressure, N m^{-2}
P_1, P_2	variation constants
Q	$\left(-\Delta H + C_p T\right)/\left(\rho C_p (T_0 - T_f)\right)$, m^3 kg^{-1}
r	radial distance, m
R	radius for cylinder and sphere; half thickness for slab, m
R_c	universal gas constant, J mol^{-1}
SD	standard deviation, dimensionless
t	time, s
T	temperature, K
u	gas velocity, m s^{-1}
V	total particle volume, sum of the volume occupied by pores and by the solid phase, m^3
V_g	volume occupied by the pores i.e. by the gases and volatiles, m^3
V_S	solid-phase (wood and char) volume, m^3
V_{S0}	initial effective solid volume, m^3
W_i	molecular weight of species i, kg mol^{-1}
x	dimensionless radial distance
X	conversion of biomass

Greek letters

ΔH	heat of reaction, J kg^{-1}
$\Delta\tau$	axial grid length
Δx	radial grid distance
ρ	density, ρ_0 at initial condition, kg m^{-3}
α	thermal diffusivity, m^2 s^{-1}
τ	dimensionless time
θ	normalized temperature
ε	emissivity coefficient
ε''	void fraction of particle, ε_0'' at initial condition
σ	Stefan Boltzmann constant, W m^{-2} K^{-4}

φ	permeability, m^2
η	reaction progress variable
μ	viscosity, kg m^{-1} s^{-1}
α'	shrinkage factor
β'	shrinkage factor
γ'	shrinkage factor

Dimensionless numbers

Bi	Biot number
Bi_M	Modified Biot number
Le	Lewis number
Pr	Prandtl number
Q''	Heat of reaction number
Re	Reynolds number
Sh	Sherwood number

Subscripts

g	gas
0	initial
f	final
V	water vapor
L	light hydrocarbons
B	wood
C	char
eff	effective
m	mean

CHAPTER 1

INTRODUCTION

There are many different ways by which the energy available in abundance around us can be stored, converted and amplified for both industrial and our normal day-to-day requirements. Energy sources will play an important role in the world's future. The energy sources are categorized under three groups: fossil fuels, renewable sources and the nuclear sources. The fossil fuels are coal, petroleum and the natural gas. The sources of renewable energy are solar, hydroelectric, wind, biomass and the geothermal power. The nuclear powered sources are fission and fusion.

The cost of producing energy from the biomass fuels is less than that from the fossil fuels (Demirbaş, 2001a). The electricity generated by biomass gasifier power plants (say 2 MW or larger capacity) is quite competitive with the fossil fuels (coal) electricity. The purchasing price of coal electricity does not reflect the full social cost. Coal-fired power generation often produces pollutant gas emissions such as SO_x, NO_x, CO_2. If these externalities are internalized, the purchase price of coal-fired electricity should be higher, that would add the competitiveness with biomass gasifier power.

Biomass is the name given for the material derived from the growing plants or from the animal manure (which is actually a processed form of plant material) It is rather a effective term for all the organic material, trees and crops. Energy from biomass is derived from the animal and plant material, such as wood from natural forests; the wastes from forestry and the agricultural processes, the animals (that eat plants or other animals) or the human wastes. The production of biomass in the world is estimated at 146 billion metric tons a year, mostly due to the wild plant growth.

The energy in biomass from plant matter originally comes from the solar energy through the process known as the photosynthesis. This energy can be recovered by burning biomass as a fuel. Biomass releases heat and carbon dioxide during combustion that is absorbed while the plant is growing. Essentially, the use of biomass is the reversal of photosynthesis. All the biomass ultimately decomposes to its molecules with the release of heat, in nature. The release of energy from the combustion of biomass imitates the natural processes. Biomass energy is therefore, a renewable form of energy and, in principle, using this energy does not add carbon dioxide to the environment if proper energy plantation is done, in contrast to fossil fuels (Twidell, 1998). It is effectively stored solar energy. It is the only renewable source of carbon and is able to convert into the convenient solid, liquid and gaseous fuels.

Biomass can be utilized directly (e.g. burning wood for heating and cooking) or indirectly by converting it into a liquid or gaseous fuel (e.g. alcohol from sugar crops or biogas from animal waste). The net amount of energy obtained from biomass when it is combusted ranges from about 8 MJ/kg for green wood, to 20 MJ/kg for dry plant matter (Demirbaş, 1998a), to 55 MJ/kg for methane, as compared with about 27 MJ/kg for coal

(Twidell, 1998). The yield of volatile materials from biomass can be increased by increasing the heating rate and the temperature of pyrolysis.

Many biomass fired electricity generators use waste materials, such as the domestic refuse or straw. There are several techniques based on the idea of cultivating crops of various kinds, especially to provide biomass for fuel.

1.1. Importance of biomass

Biomass is the oldest form of energy used by human beings, mainly in the form of wood. It has either been burned directly in furnaces, or processed to increase its energy content (Haykiri-Açma, 2003). It has historically been a dispersed, land intensive and labor intensive source of energy. Therefore, as industrial development activities had increased in countries, more concentrated and convenient sources of energy had substituted the biomass.

In industrialized countries, biomass mainly represents only 3% of the primary energy consumption (Demirbaş, 2001a). However, much of the rural population in developing countries, which represents about 50% of the world's population, is reliant on biomass, mainly in the form of wood, for fuel. In developing countries, biomass accounts for 35% of primary energy consumption, raising the world total to 14% of primary energy consumption (Demirbaş, 2001a).

Natural biomass of the earth represents an energy supply of around 3000 EJ (3×10^{21} J) a year, of which just under 2% is currently used as a fuel. However, it is not possible, to use all of the annual production of biomass in a sustainable manner. The analysis provided by the United Nations Conference on Environment and Development (UNCED)

estimates that the biomass could potentially supply about half of the present world primary energy consumption by the year 2050 (Demirbaş, 2001a).

As a renewable energy source, biomass has great potential both for the richer countries and for the developing world. Biomass as a fuel is still in the experimental stage and provides only about 0.25% of the total electricity generating capacity in UK (Demirbaş, 2001a). This is likely to increase for a number of reasons. One reason is that the biomass power systems will become more affordable as the technology improves. Another reason is that, UK and European legislation aims to encourage less polluting methods of waste disposal, and one viable option is to burn the waste to generate power.

In some member states of the European Union (EU), like Spain, Italy, Germany, France, Belgium and Austria, liquid biofuels such as sugar, wheat, root, sunflower oil and rapeseed, are currently being used (Demirbaş, 2000a, 2000b).

Potential benefits are also there in growing biomass exclusively for converting it into fuel. If the right crops are chosen, it is possible to use poor quality land which is unsuitable for growing food.

1.2. Biomass energy

Biomass energy is one of the earliest sources of energy. Biomass is useful to meet different kinds of energy needs, including fueling vehicles, providing process heat for industrial facilities, generating electricity and heating homes. The substantial increase in oil prices in recent years, together with its progressive exhaustion, has generated a great interest in biomass utilization as a renewable energy source (Figueiredo, Valenzuela,

Bernalte, & Encinar, 1989). Biomass is only an organic petroleum substitute which is renewable

The one renewable energy source on which mankind has relied since the discovery of fire is photosynthesis process It is the process in which solar energy is converted into an energy rich biomass. The solar energy absorbed by green plant tissue, provides energy to reduce CO_2 and form carbohydrates which are then utilized as energy sources and raw materials for all other synthetic reactions in the plant. Solar energy thus stored and captured in the plant, provides food, fiber, fuel and shelter for mankind. However, this photosynthesis uses only a small portion of the sun's energy to fix 200 billion tons of carbon into terrestrial and aquatic biomass with an energy content of 3000 billion GJ/yr. Yet, only 1/10th of the world's biomass energy is consumed, while the rest goes unutilized (Reddy, 1994). Every year, plants store 10 times the present annual consumption of energy. This huge amount of energy not only can contribute to the country's energy resources but also can effectively provide a wide range of chemical feed stocks for the organic chemical industry, thus saving the consumption of precious non-renewable petroleum products. Moreover, it is environmental friendly and prevents ecological imbalance. The stored plant energy can be utilized by burning it directly or using various processes to obtain potential fuels, such as methane, ethanol etc.

The energy obtained from the forest involves the use of biomass of the forest which is currently not being used in the traditional forest product industries. Actually, this implies that the forest biomass is nothing but the forest residues left after forest harvesting, residual trees and scrub or under-managed wood land. The residues of the forest alone accounts for around 50% of the total forest biomass and are currently left in the forest to

rot (Kaygusuz, 1996). The combination of the fuelwood production with the effluent disposal has many potential environmental benefits. The economic feasibility of woody biomass plantations is difficult to justify at present. But if full costing of externalities (such as CO_2 emissions) are to be applied in the future, then the acceptable payback periods for boiler conversions and handling and storage facilities could be achieved.

1.3. Resources of biomass

Resources of biomass include wood and wood wastes, agricultural crops and their waste byproducts, municipal solid waste (MSW), animal wastes, waste from food processing and aquatic plants and algae. The biomass energy is produced from wood and wood wastes (64%); followed by MSW (24%), landfill gases (5%) and agricultural waste (5%) and other (2%) (Demirbaş, 2000a, 2000b).

Biomass supplies only 4% of the energy to the industrialized countries. As mentioned earlier, it is burned in a special waste to energy plant to produce electricity. Biomass energy comes from burning organic matter and biomass fuel comes from landfill and agricultural waste. Landfill gas is widely used in power generation schemes to produce electricity for export to the generating companies (McKendry, 2002). The burning of waste for converting it into energy reduces 60-90% of the trash dumped in the landfills. This also reduces landfill cost. Biomass can be converted to energy through many conversion processes.

Resources of biomass that can be used for energy production cover a wide range of materials. Energy from biomass can be separated into two categories, mainly modern biomass and traditional biomass. Modern biomass includes large scale uses and aims to

substitute for conventional energy sources. It usually involves wood and agricultural residues, urban wastes and biofuels, such as biogas and energy crops. Traditional biomass is generally confined to developing countries and small scale uses. It includes charcoal and fuelwood for domestic use, rice husks and other plant residues and animal wastes. The most widely used biomass energy resources can be categorized into the following groups:

1.3.1. Wastes

- Agricultural production wastes
- Crop residues
- Urban wood wastes
- Agricultural processing wastes
- Mill wood wastes
- Urban organic wastes

1.3.2. Forest products

- Logging residues
- Wood
- Sawdust, bark etc. from forest clearings
- Trees and shrubs
- Wood residues

1.3.3. Energy crops

- Herbaceous woody crops
- Short rotation woody crops

- Starch crops (corn, wheat and barley)
- Grasses
- Sugar crops (cane and beet)
- Forage crops (grasses and clover)
- Oilseed crops (soyabean, sunflower, safflower)

1.3.4. Aquatic plants

- Water weed
- Algae
- Water hyacinth
- Reed
- Rushes

Due to the exponential growth of world population, the demand for energy is increasing at an exponential rate. This, combined with widespread depletion of the fossil fuels and gradually emerging consciousness about environmental degradation, suggests that the energy supply in the future has to come from renewable energy sources. Total renewable energy sources now account for nearly 18% of global energy supply. Out of this, over 55% is supplied by traditional biomass and about 30% by large hydro. Modern biomass, solar, wind, small hydro (below 10 MW), geothermal and ocean energy all put together account for only 12% of the total renewable sources. The new renewable sources contribute to only 2% of the world primary energy supply. In the today's world primary energy supply, biomass contributes about 12%, while in the developing countries, its contribution varies from 40% to 50% (Demirbaş, 2001a).

1.4. Energy content in biomass

Biomass is not in ideal form for fuel use. The heat content calculated on a dry basis must be corrected for the natural water content that can reduce the net heat available by as much as 20% in direct combustion applications. Gasification to low calorific gas carries an additional net energy loss and its subsequent conversion to synthetic natural gas, and liquid fuels results in still greater reduction of net energy, to perhaps 30% of the original heat content.

In many non-OPEC (Organization of the Petroleum Exporting Countries), tropical, developing countries, wood is still a predominant fuel and it will continue to be so for at least next 40-50 years. Because it is renewable, it competes well with fossil fuels, and with soft energies like solar and wind, on account of its energy storage capacity. It is being used in the commercial (water heating), industrial (for water heating and process heat) and domestic (for cooking) sectors and also in rural industries, like potteries, brick kilns etc.

Wood is a composite of cellulose, lignin and hemicellulose (42%, 36% and 22% respectively). A typical analysis of the dry wood yields carbon (52%), hydrogen (6.3%), oxygen (40.5%), nitrogen (0.4%) and others (0.8%). The proximate analysis of wood shows the following components (Demirbaş, 2000a, 2000b):

- Wood: volatile matter (80%), fixed carbon (19.4%) and ash (0.6%).
- Bark: volatile matter (74.7%), fixed carbon (24%) and ash (1.3%).

The energy content of different plant materials determines their calorific value (heat content). This calorific value depends on the percentage of carbon and hydrogen, which are the main contributors to the heat energy value of a biomass material. The

characteristics of important fuelwoods indicate that the energy content (kcal/kg) of the wood varies between 4200 and 5400, and the density varies between 400 and 900 kg/m^3. In order to get the maximum energy, the plant materials should be air dried, because the amount of energy contained in the plant varies with the amount of moisture content. The variations of calorific value of Indian firewoods indicate that with an increasing moisture content, the calorific value decreases linearly (Reddy, 1994). Energy can be obtained from biomass in five different ways:

(1) Solid waste which can be burnt.

(2) Production of crops which yield starch, sugar, cellulose and oil.

(3) Landfill production for methane.

(4) Anaerobic digesters which produce biogas which can be used to generate heat/electricity.

(5) Biofuel production which includes ethanol, methanol, biodiesel and their derivatives.

Ethanol can be used in the fuel cells. It is blended with the gasoline in the ratio of 1:9 to produce the fuel gasohol. Biodiesel production has also gone up from 11,000 tons in 1991 to 1,286,000 tons in 1997. The raw materials are oils from rapeseed (84%), sunflower (13%), soyabean (1%), palm (1%) and others (1%) (Jain & Singh, 1999).

In some developed countries (such as Sweden) with a high land to population ratio and an active forest industry, although the wastes are still largely under utilized, their use is increasing rapidly, whilst costs (in real terms) drop significantly, resulting in as much as 15-18% contribution to national energy needs. It has been suggested by the predictions that in countries such as New Zealand, biomass energy mixed with the hydro and wind energies could make the country self reliant on renewables within the next 26

years, if the right financial support is given. It has been indicated by the reports from US, UK, Sweden, New Zealand and covering the European Union (EU) that the efforts which are being made by the governments to establish biomass as a long term resource within the framework of a environmentally acceptable, sustainable, cost effective policy linked to specific fiscal and legislative measures (Demirbaş, 2000a, 2000b).

1.5. Benefits of biomass

Biomass is potentially sustainable, renewable and environmentally acceptable source of energy. It is carbon dioxide neutral, if grown and utilized properly. The energy production with biomass will result in a net reduction in greenhouse gas emissions and the replacement of a non-renewable energy source. Many large power producers in industrialized countries are looking to biomass as a means of meeting the greenhouse gas reduction targets.

The sulfur content of biomass fuels are negligible and, therefore, do not contribute to the sulfur dioxide emissions, which cause the acid rain. The combustion of biomass produces less ash than the coal combustion, and the ash produced can be used as a soil additive on farm targets. The energy production by the combustion of the agricultural and forestry residues and MSW, is an effective use of waste products that reduces the significant problem of waste disposal, particularly in municipal areas.

Biomass is a domestic resource, which is not subject to the world price fluctuations or the supply uncertainties of the imported fuels. In developing countries in particular, the use of liquid biofuels, such as biodiesel and ethanol, reduces the economic pressures of

importing the petroleum products. The benefits of biomass are as discussed below in brief

1.5.1. Benefits of biomass energy

As compared to fossil fuels, biomass energy generates very less air emissions, reduces the amount of waste sent to landfills and decreases our reliance on foreign oil. Biomass provides a clean, renewable energy source that could dramatically improve our environment, economy and energy security. Biomass energy also creates thousands of jobs and helps in revitalizing the rural communities.

1.5.2. Environmental impacts of biomass energy

As with the other forms of energy production, the biomass energy systems raise some environmental issues that must be addressed. In biomass energy projects, issues such as air pollution, impacts due to crop cultivation and impacts on forests must be addressed on a case by case basis. Biomass energy can be produced and consumed in a sustainable fashion, and there is no net contribution of carbon dioxide to global warming (Kaygusuz, 2002). Fears of climate change and increasing concern over the global warming have prompted a search for new, cleaner methods for electrical power generation. Co-firing of biomass fuels (e.g. wood chips, straw, bagasse, peat and municipal solid waste) is presently considered as an effective means of reducing the global CO_2 emissions (Meesri & Moghtaderi, 2002). There would be very little or no net contribution to the atmospheric carbon dioxide as a greenhouse gas due to such bioenergy crops. On the other hand, carbon is released when fossil fuels are burned. It has been stored underground for millions of years, making a net contribution to the atmospheric greenhouse gases. Hence, the biomass energy can have significant environmental

advantages over the use of fossil fuels, if managed carefully. An appropriate level of biomass energy use can have less environmental impacts than our current means of energy production.

1.5.3. Industrial and home use

Most of the biomass energy is consumed by homeowners and wood related industries. In our homes, we burn wood in fireplaces and stoves to cook meals and warm our residences. The lumber, paper and pulp industries burn their own wood wastes in large boilers and furnaces to supply 60% of the energy needed to run the factories.

In electricity production, biomass is burned by direct combustion to produce steam, the steam turns a turbine and the turbine drives a generator. Only certain types of biomass materials are used for direct combustion, because of potential ash build-up which fouls the boilers, reduces the efficiency and increase the costs.

Gasifiers are used to convert biomass into a combustible gas i.e., biogas (Jorapur & Rajvanshi, 1997; Fletcher, Haynes, Chen, & Joseph, 1998; Khraisha, 2000; Warnecke, 2000; Zhuo, Messenböck, Collot, Megaritis, Paterson, Dugwell, & Kandiyoti, 2000; Midilli, Dogru, Howarth, Ling, & Ayhan, 2001; Zainal, Ali, Lean, & Seetharamu, 2001; Mathieu & Dubuisson, 2002). The biogas is then used to drive high efficiency, combined cycle gas turbine. Heat is used to convert the biomass chemically into the pyrolysis oil. It is burned like petroleum to generate the electricity. It is also easier to store and transport than the solid biomass material. Pyrolysis also can convert the biomass into phenol oil, a chemical used to make molded plastics, wood adhesives and foam insulation. Wood adhesives are used to glue together the plywood and the other composite wood products.

1.5.4. The future of biomass

Biomass has the potential to provide a cost effective and sustainable supply of energy in the future, while at the same time, aiding countries in meeting their greenhouse gas reduction targets. It is estimated that by the year 2050, 90% of the world population will live in developing countries (Demirbaş, 2001a). It is critical, therefore, that the biomass processes used in these countries are sustainable. The modernization of biomass technologies, leading to more efficient biomass production and conversion, is one possible direction for biomass use in the developing countries.

The main biomass processes utilized in the future in industrialized countries are expected to be (i) direct combustion of residues and wastes for electricity generation, (ii) production of bio-ethanol and biodiesel as liquid fuels, and (iii) the combined heat and power generation from energy crops. In the short to medium term, biomass waste and residues are expected to dominate biomass supply, to be substituted by energy crops in the longer term. The future of biomass electricity generation lies in the biomass integrated gasification/gas turbine technology, which offers the high energy conversion efficiencies.

The success of the biomass derived chemical industries will depend on the supply and demand for feedstock, primary chemicals and key intermediates (cellulose, lactic acid and levulinic acid) that cannot be manufactured by the petrochemical industry. The first synthetic fibers and thermoplastics are made from the cellulose derivatives. Lactic acid can be used to make acetaldehyde, a major petrochemical key intermediate. Levulinic acid salts have been proposed to replace ethylene glycol as an engine coolant.

1.6. Biomass conversion processes

There are two broad pathways for biomass conversion, i.e., the chemical decomposition and the biological digestion. The conversion technologies for utilizing biomass can be separated into five basic categories: (i) direct combustion processes, (ii) thermochemical processes, (iii) biochemical processes, (iv) agrochemical processes, and (v) hydrogen manufacture process.

Thermochemical decomposition can be used for energy conversion of all the five categories of biomass materials, but low moisture herbaceous (small grain field residues) and woody (woody industry wastes) are the most suitable ones. The biological processes involved are essentially the microbic digestion and the fermentation. Marine crops, manure and high moisture herbaceous plants such as vegetables, sugar cane, sugar beet, corn, sorghum, cotton, etc. are the most suitable for biological digestion.

Another process for producing an energy carrier from biomass is extraction (e.g. rapeseed oil from rapeseed). With regard to the energy carrier produced from biomass, a distinction can be made between the production of heat, electricity and fuels. There are numerous ongoing technological developments in the field of biomass energy conversion. Some of these technologies are described below:

1.6.1. Direct combustion processes

On various scales, combustion is widely used to convert biomass energy to heat and/or electricity with the help of a steam cycle (stoves, boilers and power plants). Combustion is used to produce heat, power and process steam which is applied for a wide variety of fuels and from very small scale (for domestic heating) up to a scale in the range of 100 MW. An especially attractive option is the co-combustion of biomass in large and

efficient coal fired power plants because of the high conversion efficiency of these plants. It is a proven technology, although further improvements in the performance are still possible. Net electrical efficiencies for biomass combustion power plants range from 20% to 40%. The higher efficiencies are obtained when the biomass is co-combusted in coal fired power plants (Brock, Faaij, & Wijk, 1996).

Direct combustion is the main process adopted for utilizing biomass energy. Biomass such as forestry residues, fuelwood, bagasse and MSW, can be combusted in furnaces and boilers to produce process heat, or steam for a steam turbine generation. The size of the power plant is constrained by the local feedstock availability and is generally less than 25 MW. However, by using dedicated feedstock supplies, such as short rotation plantations or herbaceous energy crops, the capacity can be increased to 50-75 MW, gaining significant economy of scale (Overend, 1998).

1.6.2. Thermochemical conversion processes

Thermochemical conversion processes can be subdivided into five categories consisting of gasification, pyrolysis, direct liquefaction, supercritical fluid extraction, and hydro thermal upgrading process. A brief description of these processes is given below:

1.6.2.1. Gasification

Gasification is a form of pyrolysis. It is performed at high temperatures in order to optimize the gas production. The gas produced, known as producer gas, is a mixture of carbon monoxide, hydrogen and methane, together with carbon dioxide and nitrogen. The gas is more versatile than the original solid biomass (usually wood or charcoal). It can be burnt to produce process heat and steam, or used in gas turbines to produce electricity.

Biomass gasification comes under the category of the latest generation of biomass energy conversion processes. It is used to improve the efficiency and to reduce the investment costs of biomass electricity generation through the use of gas turbine technology (Kaltschmitt & Bridgwater, 1997; Bridgwater, 2003). High efficiencies up to about 50% are achievable through the use of combined cycle gas turbine systems. Economic studies show that the biomass gasification plants can be as economical as conventional coal fired plants (Badin & Kirschner, 1998).

Commercial gasifiers are available in a wide range of sizes and types, and run on a variety of fuels, including charcoal, wood, coconut shells and rice husks. The power output is determined by the economic supply of biomass, which is limited to 80 MW in most regions (Overend, 1998).

1.6.2.2. Pyrolysis

A promising route for processing biomass is pyrolytic conversion, which has been conducted under variety of experimental conditions (Demirbaş, 2002a). Pyrolysis is the thermal degradation of biomass in the absence of air to produce liquid (bio-oil or bio-crude), charcoal and non-condensable gases. The process can be adjusted to maximize charcoal, pyrolytic oil, gas or methanol production with a 95.5% fuel-to-feed efficiency. Flash pyrolysis can be used for the production of bio-oil, and it is currently at the pilot stage (Demirbaş, 2001a). Pyrolysis is the most efficient process for biomass conversion as it produces energy fuels with high fuel-to-feed ratios (Bridgwater, 2001). It is the method that is most capable of competing with and eventually replacing non-renewable fossil fuel resources. The conversion of biomass to crude oil can have an efficiency up to 70% for flash pyrolysis processes. The bio-crude thus obtained can be used in engines

and turbines. Its use as a feedstock for refineries is also being considered (Demirbaş & Güllü, 1998; Güllü & Demirbaş, 2001a).

Pyrolysis is the basic thermochemical process for converting biomass to a more useful fuel (Demirbaş, 1998b). It is used to produce hydrogen rich gaseous products (Çağlar & Demirbaş, 2002a; 2002b) and more useful liquid products (Çağlar & Demirbaş, 2000). Biomass conversion by pyrolysis has many environmental and economic advantages over fossil fuels. Recent years have brought an increased concern with the environment, and this led to the importance of pyrolysis. The reductions in oxygen levels and/or flame temperatures in the vicinity of the burners have proven to efficiently reduce NO_x emissions (Alonso, Borrego, Alvarez, & Menéndez, 1999).

The process of pyrolysis has been used since the dawn of the civilization. The process is also known as the wood distillation. The ancient Egyptians practiced wood distillation by collecting tars and pyroligneous acid for use in their embalming industry. In the 1800s, pyrolysis of wood to produce charcoal was a major industry, supplying the fuel for the industrial revolution, until it was replaced by coal. The wood distillation industry declined in the 1930s due to the advent of the petrochemical industry. However, pyrolysis of wood to produce charcoal for the charcoal briquette continued (Demirbaş, 1999).

Pyrolysis of wood has been studied as a zonal process. Zone A is the easily degrading zone occurring at temperatures up to 473 K. At this temperature, the surface of wood becomes dehydrated. The water vapor, carbon dioxide, formic acid, acetic acid and glyoxal are given off. The wood is said to be in zone B when the temperatures of 473-533 K are attained, and gives water vapor, carbon dioxide, formic acid, acetic acid

glyoxal and some carbon monoxide. The reactions to this point are mostly endothermic. Pyrolysis actually begins between 535 K and 775 K, which is called zone C. The reactions are exothermic. Combustible gases, such as carbon monoxide, methane, formaldehyde, formic acid, acetic acid, methanol and hydrogen are liberated and charcoal is formed. Before escaping the reaction zone, the primary products react with each other giving rise to secondary reactions and are classified as zone D.

Automobile shredder residue (ASR) produced in the conventional disposal process comprises of plastics, fabrics, rubber, glass and other materials. Pyrolysis, offers an environmentally attractive method for the treatment of ASR (Galvagno, Fortuna, Cornacchia, Casu, Coppola, & Sharma, 2001). The process uses medium to high temperatures and an oxygen-free environment to decompose ASR chemically, thus producing minimum emissions of nitrogen oxide and sulphur oxide compared to the commonly practiced conventional technology, the incineration. Pyrolysis also allows the recovery of valuable materials.

For high yield of liquid products resulting from biomass pyrolysis, a low temperature, high heating rate, short gas residence time process is required. If the purpose is to maximize the char production, a low temperature, low heating rate process would be chosen. A high temperature, low heating rate, long gas residence time process would be preferred, if the purpose is to maximize the yield of fuel gas resulting from pyrolysis.

Above all, biomass pyrolyzing technology is a mature and excellent applied technology. It is a comprehensive utilization technology being advantageous to environment, society and economy (Bridgwater, 2002). Its application has an extraordinary bright future in the world.

1.6.2.3. Liquefaction

Liquefaction is a thermochemical process that takes place at low temperature, and high pressure in the presence of a catalyst. It produces a marketable liquid product. It takes place at moderate temperatures and high pressure with the addition of hydrogen. The products of various kinds can be produced by wood liquefaction (Rustamov, Kerimov, Schachbazov, Kerimov, & Rustamova, 2002). Aqueous liquefaction of lignocellulosics involves segregation of the wood ultrastructure, followed by the partial depolymerization of the constitutive compounds (Demirbaş, 2000a, 2000b; 2001c). The interest in liquefaction is low because the fuel feeding systems and reactors are more complex and more expensive than for pyrolysis processes.

1.6.2.4. Supercritical fluid extraction

Conversion by supercritical fluid extraction of biomass to liquids has been demonstrated with the use of a number of processing configurations (Akdeniz & Küçük, 1998; Demirbaş, Tüzen, & Özdemir, 1999; Küçük & Tunç, 1999; Çağlar & Demirbaş, 2001; Demirbaş, 2001b). These different processing techniques tend to emphasize different mechanism subsets within the large group of potential chemical mechanisms by which biomass is converted to the primary products and thereafter further converted by varying degrees to final products.

1.6.2.5. Hydro thermal upgrading process

Another way to produce bio-crudes is by the hydro thermal upgrading (HTU) process. HTU converts biomass in a wet environment at high pressure to partly oxygenated hydrocarbons. The process development is almost at the pilot plant scale.

1.6.3. Biochemical processes

1.6.3.1. Anaerobic digestion

The decomposition of biomass through bacterial action in the absence of oxygen is known as anaerobic digestion. It is essentially a fermentation process and produces a mixed gas output of carbon dioxide and methane. The anaerobic digestion of MSW buried in landfill sites produces a gas known as landfill gas. Biogas is the product generated by the decay, in the absence of air, of sewage or animal waste.

1.6.3.2. Alcoholic fermentation

Biomass materials which contain sugars, starch or cellulose can be used to produce ethanol. The best known source of ethanol is the sugar cane, but other materials including sugar beet, wheat and other cereals, jerusalem artichoke and wood, can be used. The choice of biomass is important as feedstock costs typically make up 55-80% of the final alcohol selling price. As compared to sugar based biomass, starch based biomass is cheaper, but requires additional processing. Similarly, cellulose materials, such as wood and straw, are readily available but require expensive preparation.

A process known as fermentation is used to produce ethanol. Typically, sugar is extracted from the biomass crop by crushing, mixed with water and yeast, and kept warm in large tanks called fermenters. The yeast breaks down the sugar and converts it into methanol. A distillation process is required to remove the water and other impurities in the diluted alcohol product (10-15% ethanol). The concentrated ethanol (95% by volume with a single step distillation process) is drawn off and condensed to a liquid form.

1.6.4. Agrochemical processes

The energy content of vegetable oils is 39.3-40.6 MJ/kg (Demirbaş, 1998c) Seed crops, which contain high proportion of oil, can be crushed and the oils extracted and used directly to replace diesel (called biodiesel) or as a heating oil. There are varieties of crops that can be used for biodiesel production, but the most common crop is rapeseed. Other raw materials used are sunflower oil, palm oil, soyabean oil and recycled frying oils. The cost of the raw material is the most important factor affecting the overall cost of production. There are currently 85 biodiesel plants around the world (including one in Malaysia using palm oil) with a combined capacity of over 1.28 million tons (Korbitz, 1998). In the Philippines, diesel is blended with coconut oil and used in lorries and tractors.

There are number of advantages associated with biodiesel. It includes a reduction in greenhouse gases of at least 3.2 kg of carbon dioxide-equivalent per kilogram of biodiesel, a 99% reduction of sulfur dioxide emissions, a 39% reduction in particulate matter, a high biodegradability and energy supply security (Korbitz, 1998).

1.6.5. Hydrogen from biomass

It is a clean burning fuel. It must be manufactured from water with either fossil or non-fossil energy sources. Hydrogen is produced from pyroligneous oils produced from the pyrolysis of lignocellulosics biomass (Demirbaş & Çağlar, 1998). Gasification of solid wastes and sewage is a recent innovation. The synthesis gas formed with air or oxygen is converted to hydrogen. The solid waste concept solves two problems: (1) disposal of urban refuse and sewage and (2) a source of hydrogen fuel for hydrogen

powered vehicles. Hydrogen from biomass has generally been based on the following reactions (Demirbaş, Karslioğlu, & Ayas, 1996).

$$\text{solid waste} + \text{Air} \longrightarrow CO + H_2$$

$$\text{biomass} + H_2O + \text{Air} \longrightarrow H_2 + CO_2$$

$$\text{cellulose} + H_2O + \text{Air} \longrightarrow H_2 + CO + CH_4$$

1.7. Background

With increasing urbanization all over the world, in both developing and developed countries, the quantity of municipal solid waste generated every day is increasing very rapidly, leading to more biomass formation. The study of pyrolysis is gaining increasing importance as it is not only an independent process, but is also a first step in gasification and combustion process (Srivastava & Jalan, 1994). Pyrolysis is defined as the process by which biomass feedstock is thermally degraded in the absence of air/oxygen (Soltes, Wiley, & Kenny Lin, 1981). It is used for the production of solid (char), liquid (tar and other organics) and gaseous components (methane, ethane, carbon monoxide, etc), which can all be utilized as possible alternatives for fuels (Srivastava, Sushil, & Jalan, 1996).

Pyrolysis has an important role in the combustion of biomass since the products of this stage, namely volatiles and char, subsequently undergo combustion, to release thermal energy (Sinha, Jhalani, Ravi, & Ray, 2000). It is relatively easy to convert biomass into synthetic fuels (Reed, Milne, Diebold, & Desrosiers, 1981). It is important to model the phenomenon of this pivotal role of pyrolysis mathematically. The primary objectives of these models are to identify the system characteristics, to evaluate the importance of

various system parameters, and to provide the valuable quantitative information about the process (Soltes, Wiley, & Kenny Lin, 1981; Sinha, Jhalani, Ravi, & Ray, 2000).

The world's production of oil and gas is expected to decline, and one should start thinking about alternate/substitute fuels. Biomass is available abundantly so one can expect the future fuels from biomass. Pyrolysis is one of the technologies which upgrade the biomass as a fuel. As mentioned above, biomass conversion by pyrolysis has many environmental and economic advantages over fossil fuels. It is the latest generation of biomass energy conversion processes (Demirbaş, 2001a). The pyrolysis of biomass is considered as one of the viable means for overcoming the so-called "energy-crisis". It is a renewable source of energy and has many advantages from ecological point of view.

1.8. Modeling of Pyrolysis

Modeling of pyrolysis implies the representation of the chemical and physical phenomena constituting the pyrolysis in mathematical form. In other words, pyrolysis is to be represented as the system of equations which taken together can provide valuable quantitative information about the process (Sinha, Jhalani, Ravi, & Ray, 2000). A general mathematical model of the pyrolysis process is not only difficult to formulate, but also tedious to solve.

1.9. Limitations of the model of pyrolysis

The existing literature on pyrolysis modeling suggests that great strides have been made in understanding and modeling pyrolysis in the last three decades. But, the models which are presently available in literature have some limitations. The limitations are:

(1) The secondary pyrolysis reactions are not considered.

(2) The model does not consider the effect of density as a function of time.

(3) The effect of specific heat capacity and thermal conductivity of char, which are the functions of temperature, is neglected.

(4) Instead of considering the convective heat transfer coefficient as a function of Reynolds number and Prandtl number, constant value is used.

(5) Convective and diffusive transport of volatiles and gases is neglected.

(6) Practically significant kinetic scheme consisting of physically measurable parameters is not considered.

(7) Effect of auto-catalysis secondary reactions, residence time, shrinkage, particle size distribution, etc., on pyrolysis yield are neglected.

(8) Some of the models are not applicable for different biomass geometries (slab, cylinder and sphere).

(9) The effect of thermal and transport properties (porosity, thermal conductivity, specific heat, mass diffusivity) on pyrolysis are not considered.

Though a few models are available in which some of the anomalies listed above are rectified, the detailed model for pyrolysis rectifying all the above anomalies is not available.

1.10. Motivation

The understanding of physical phenomena of pyrolysis and representing it with an appropriate mathematical model is essential in the design of pyrolysis reactors, biomass gasifiers and industrial pyrolysis units. The knowledge on modeling of pyrolysis of a

biomass particle is also very significant in optimization of boilers and large scale furnaces. The detailed description of chemical processes of pyrolysis - coupling to an unsteady-state, one-dimensional, variable property model of transport phenomena including heat convection, conduction and radiation, volatile and gas transport by diffusion & convection, and momentum transfer - is necessary for proper designing of the industrial pyrolysis units. It is also useful to predict the effects of the widely variable properties such as density, thermal conductivity, specific heat capacity, convective heat transfer coefficient, emissivity and temperature in the pyrolysis of biomass. In spite of these many advantages, little work has been reported in literature on the mechanistic modeling of such kinetics. This may be attributed to the extreme complexity of pyrolysis process due to the presence of homogeneous and heterogeneous reactions consecutively along with heat, mass, and momentum transfer operations occurring simultaneously during the process.

1.11. Objectives

Based on the importance and application of pyrolysis process and the background work reported in literature with their limitations (details are given in chapter 2), the objectives of the present study given in brief are as follows:

(1) Understanding of physical aspects of pyrolysis in modeling of biomass gasification.

(2) Improvement on the existing models considering auto-catalysis secondary pyrolysis reactions, residence time effects, shrinkage, particle size distribution, different geometries, changes in material properties during the course of pyrolysis, etc.

(3) Validating the proposed models with the actual experimental data obtained from the literature.

1.12. Scope

Biomass, being a readily available renewable energy source that reduces the sulfur dioxide and carbon dioxide emissions, is an attractive option as a fuel for power generation. Biomass has the potential to provide a cost effective and sustainable supply of energy in the future, while at the same time, aiding countries in meeting their greenhouse gas reduction targets. The intensive research is carried out on thermal conversion techniques for biomass like combustion, gasification and pyrolysis. Pyrolysis is one of the promising routes for the production of charcoal, medium heating value gases and condensable organic components. It is a renewable source of energy and has many advantages from ecological point of view. It also occurs as the first step in gasification or combustion process. There has been an increasing interest for thermochemical conversion of biomass through pyrolysis for upgrading energy in terms of more easily handled fuels, namely gases, liquids, and charcoal. Each product can be commercially interesting depending upon the type of application. The understanding of the interaction between chemical and physical mechanisms during pyrolysis of biomass is of fundamental importance, for the optimal design of chemical pyrolysis reactors and combustors. The pyrolysis of biomass has a lot of practical importance and physical significance in industrial pyrolysis applications. The pyrolysis process has a great future in the world.

1.13. Conclusions

- Biomass has the potential to provide a cost effective and sustainable supply of energy in the future, while at the same time, aiding countries in meeting their greenhouse gas reduction targets.
- Biomass conversion may be conducted on two broad pathways: chemical decomposition and biological digestion.
- Thermochemical conversion processes can be subdivided into gasification, pyrolysis and direct liquefaction.
- Liquefaction is a low temperature, high pressure thermochemical process using a catalyst. The process produces a marketable liquid product.
- There is also the process of pyrolysis, which is the destructive distillation of wood. It is a process which has been known from ancient times. It is a promising route for biomass conversion, which has been conducted under variety of experimental conditions, resulting in production of charcoal, tarry material, aqueous fraction and gaseous products (Demirbaş, 2002a).
- Pyrolysis basically is the thermal degradation of biomass in the absence of air to produce liquid (bio-oil or bio-crude), charcoal and non-condensable gases.
- The pyrolysis can be adjusted to maximize charcoal, pyrolytic oil, gas or methanol production with a 95.5% fuel-to-feed efficiency.
- Pyrolysis is the method that is most capable of competing with and eventually replacing non-renewable fossil fuel resources.
- The fuels obtained based on the biomass conversion by pyrolysis have many environmental and economic advantages over the fossil fuels.

- Gasification is a form of pyrolysis. It is performed at high temperatures in order to optimize gas the production.
- Biomass gasification through pyrolysis comes under the category of the latest generation of biomass energy conversion processes.
- It is used to improve the efficiency and to reduce the investment costs of biomass electricity generation through the use of gas turbine technology.
- The process of pyrolysis has a great future in the world.

1.14. Structure of thesis

The thesis is organized as follows:

Chapter-2 gives a brief introduction to pyrolysis, key issues in modeling pyrolysis, modeling of pyrolysis, contributions to pyrolysis modeling, limitations of earlier models, and objectives of present study.

Chapter-3 deals with the estimation of optimum parameters in the pyrolysis of biomass for both non-isothermal and isothermal conditions. A wide range of heating rates (25 – 360 K/s) and temperatures (773 – 1773 K) has been considered.

Chapter-4 focuses on the development of mathematical model to describe the pyrolysis of a single solid particle by incorporating improvements in the existing model reported in literature. It couples heat transfer equation with chemical kinetics equations. The pyrolysis rate has been simulated by a kinetic scheme involving three reactions (primary and secondary): two parallel reactions and a third for secondary interactions between volatile & gaseous products and the char.

Chapter-5 chemical processes of pyrolysis is coupled to an unsteady-state, one-dimensional, variable property model of transport phenomena including heat convection, conduction and radiation, volatile and gas transport by diffusion & convection, and momentum transfer. A generalized reference model (Model-I) incorporating all the above effects is proposed. This is further improved by proposing two simplified models (Model-II & Model-III) incorporating additional assumptions.

Chapter-6 deals with the prediction of the effects of the most important physical and thermal properties (thermal conductivity, heat transfer coefficient, emissivity, reactor temperature and heat of reaction number) of the feedstock on the convective-radiant pyrolysis of biomass fuels by using simultaneous chemical kinetics and heat transfer model. The effects of these parameters have been analyzed for different geometries such as slab, cylinder, and sphere.

Chapter-7 discusses the impact of shrinkage on the pyrolysis of biomass particles. A kinetic model coupled with heat transfer model using a practically significant kinetic scheme consisting of physically measurable parameters is used to examine the impact of shrinkage on particle size, pyrolysis time, product yields, specific heat capacity, and Biot number considering cylindrical geometry.

Chapter-8 deals with the modeling and simulation of the pyrolysis process coupled with the optimization of a non-linear function using Differential Evolution. Optimal time of pyrolysis and heating rate under the restriction on concentration of biomass are estimated.

Chapter-9 gives summary of the thesis.

CHAPTER 2

MODELING OF PYROLYSIS OF BIOMASS: A REVIEW

Pyrolysis is a process by which a biomass feedstock is thermally degraded in the absence of oxygen/air. The pyrolysis of biomass is a promising route for the production of solid (charcoal), liquid (tar and other organics) and gaseous products (H_2, CH_4, CO). These products are of interest as they are possible alternate sources of energy. The study of pyrolysis is gaining increasing importance, as it is not only an independent process, but it is also a first step in the gasification or combustion process. The pivotal role of pyrolysis has prompted many researchers to attempt to model this phenomenon mathematically. The primary objectives of these models are to provide a diagnostic tool for evaluating the importance of the various system parameters and to identify the system characteristics useful to experimentalists. However, the inherent complexity of the pyrolysis process has posed formidable challenges to modeling attempts. The pyrolytic decomposition of biomass involves a complex series of reactions, and consequently, changes in the experimental heating conditions or sample composition and preparation may affect not only the rate of reaction, but also the actual course of

reactions. In this chapter, the chemical and physical aspects of the pyrolysis process and the various issues that complicate the modeling of the pyrolysis process are discussed. The focus of the chapter would be on the modeling of pyrolysis of biomass. The models available for the pyrolysis of biomass and the limitations of these models are discussed.

2.1. Pyrolysis: the process

2.1.1. Physical process

The basic steps and processes that take place during the pyrolysis are: (1) heat transfer from a heat source leading to an increase in temperature inside the fuel, (2) initiation of pyrolysis reactions due to this increased temperature leading to the release of volatiles and the formation of the char, (3) flow of volatiles towards the ambient resulting in heat transfer between hot volatiles and cooler unpyrolysed fuel, (4) condensation of some of the volatiles in the cooler parts of the fuel to produce tar, and (5) autocatalytic secondary pyrolysis reactions due to these interactions.

2.1.2. Chemical process

The pyrolysis chemistry is strongly influenced by the chemical composition of the fuel. The elemental composition of the fuel may be obtained from the ultimate analysis. The average values obtained from the ultimate analysis of two broad classes of wood is listed in Table-2.1 (Krishna Prasad, Sangen, & Visser, 1985). A fair idea of the percentage of the major products of pyrolysis (volatiles and char) is obtained from the proximate analysis. Table-2.2 gives the proximate analysis by percentage weight (Krishna Prasad, Sangen, & Visser, 1985). It is to be noted that volatiles are almost 77%

by weight of dry wood. Thus, a weight loss of this order may be expected after pyrolysis is complete and all the volatile matter is released.

Table-2.1. Typical ultimate analysis of dry wood by weight (%) (Krishna Prasad, Sangen, & Visser, 1985)

Type of wood	Hydrogen	Carbon	Nitrogen	Oxygen	Ash
Hardwood	6.4	50.5	0.4	41.8	0.9
Softwood	6.3	52.9	0.1	39.7	1.0

Table-2.2. Typical proximate analysis of dry wood by weight (%) (Krishna Prasad, Sangen, & Visser, 1985)

Type of wood	Volatile matter	Fixed carbon	Ash
Hardwood	77.3	19.5	3.2
Softwood	77.2	21.2	1.6

The major constituents of wood are cellulose, hemicellulose and lignin. There is some variation in the relative occurance of these constituents in different species of wood but as a rough guideline cellulose is taken to be 50% and the other two to be 25% each by dry weight (Krishna Prasad, Sangen, & Visser, 1985). Most fuels of biological origin such as woods of different species of plants and agro-wastes contain the same principal constituents and differ only in their percentage composition.

The reaction products of pyrolysis are a combination of the products expected from the separate pyrolysis of each of the three major constituents. Pyrolysis of each individual constituent is itself a complex process depending on many factors. A process with a combination of all the three constituents is even more complex with many more factors governing the rate of the numerous reactions leading to an enormous range of possible products. The pyrolysis characteristics of individual constituents, i.e., cellulose, hemicellulose and lignin are described below.

2.1.2.1. Cellulose

Cellulose is a polymer of glucan consisting of linear chains of β-(1,4)-D-glucopyranose units. It is characterized by the general elementary formula, $C_6H_{10}O_5$. Its average molecular weight is 1,00,000. Cellulose component normally constitutes 45-50% of the dry wood. Shafizadeh (1982) has studied the effect of temperature on cellulose pyrolysis and reported the following results. At low temperatures (less than 300^0C), the dominant process is the reduction in degree of polymerization. In the second step, at high temperatures (more than 300^0C), there is a formation of char, tar and gaseous products. The major component of the tar is 'laevoglucosan' that vaporizes and then decomposes with increasing temperature.

The following mechanism (Demirbaş, 2002d) appears, in compliance with the facts, to account for the course of hydrogenolysis of cellulose.

$$(C_6H_{10}O_5)_x \xleftrightarrow{535K} x(C_6H_{10}O_5)$$

cellulose levoglucosan

$$C_6H_{10}O_5 \longleftrightarrow H_2O + 2CH_3 - CO - CHO$$

levoglucosan (methyl glyoxal)

$$2CH_3 - CO - CHO + 2H_2 \longleftrightarrow 2CH_3 - CO - CH_2OH$$

(acetal)

$$2CH_3 - CO - CH_2OH + 2H_2 \longleftrightarrow 2CH_3 - CHOH - CH_2OH$$

(propylene glycol)

$$CH_3 - CHOH - CH_2OH + H_2 \longleftrightarrow CH_3 - CHOH - CH_3 + H_2O$$

(isopropyl alcohol)

The kinetics of the reaction permit three distinct stages of pyrolysis to be identified: in the first stage, a rapid decomposition takes place with a weight loss that increases with rising temperature; in the second stage, a decomposition and volatilization occur.

2.1.2.2. Hemicellulose

Hemicellulose is a mixture of polysaccharides mainly consisting of glucose, mannose, galactose, xylose, arabinose, methylglucuronic acid and galacturonic acid residues. It is characterized by the same elementary formula as that for cellulose, i.e., $C_6H_{10}O_5$. Its molecular weight is much lower than cellulose and is amorphous in structure unlike cellulose. It is thermally most sensitive and decomposes in the temperature range 200-260^{0}C (Soltes & Elder, 1981). This decomposition may occur in the following two steps: (1) Decomposition of the polymer into soluble fragments and/or conversion into monomer units. (2) Further decomposition of monomer units into volatile products. Hemicellulose gives rise to more volatiles, less tar and char as compared to cellulose. The components of the tar include organic acids such as acetic acid, formic acid, and a few furfural derivatives.

The hemicelluloses, which are present in deciduous woods chiefly as pentosans and in coniferous woods almost entirely as hexosanes, undergo thermal decomposition very rapidly. It is therefore expected that furan derivatives would readily be found among the decomposition products.

2.1.2.3. Lignin

The term lignin is used to mean the complex, naturally occurring phenolic phenylpropanoid polymer or 'protolignin' characterized by the general empirical formula, $C_9H_{8-x}O_2[H_2]$ [< 1.0 $[OCH_3]_x$]. It can be processed to yield aromatics. It is considered as the main binder for agglomeration of the fibrous components. In the biomass, its content varies between 17% and 30%. It decomposes when heated between 280^{0}C and 500^{0}C (Soltes & Elder, 1981). The major product of lignin pyrolysis is char

with a yield of 55%. A liquid product known as pyroligneous acid consists of 20% aqueous components and 15% tar residue on dry lignin basis. The aqueous portion is composed of methanol, acetic acid, acetone, and water. The tar residue consists mainly of homologous phenolic compounds. The gaseous products represent 10% of the lignin and are composed of methane, ethane, and carbon monoxide (CO).

The aromatic nature of lignin is shown by its pyrolysis products, of which is guaiacol, that is chiefly obtained from coniferous wood & guaiacol and pyrogallol dimethyl ether from deciduous woods. An outline of the following reaction mechanism (Demirbaş, 2002d) of the thermal cleavage of guaiacol has been suggested:

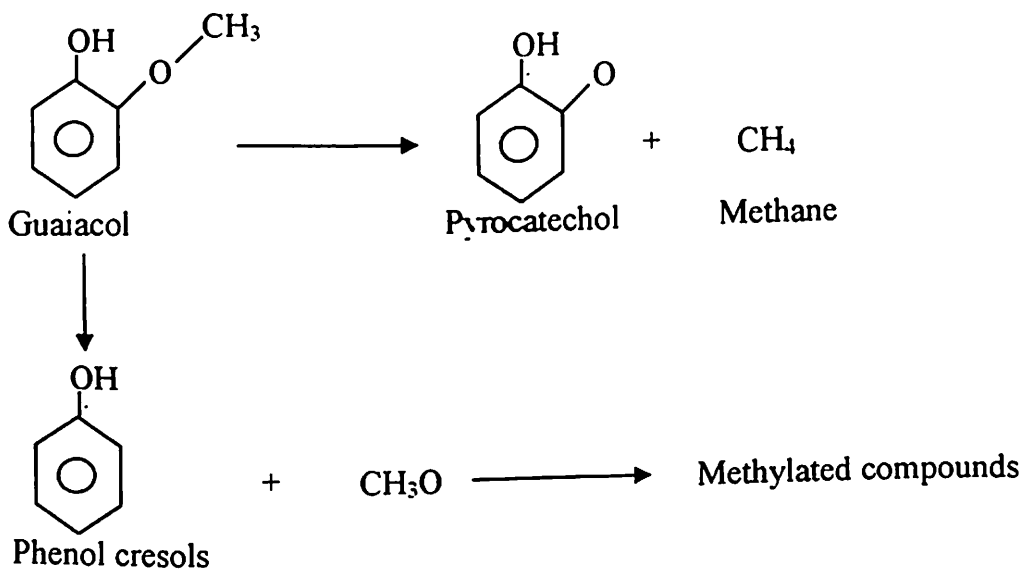

According to the above mechanism, the first step in the reaction is evidently a monomolecular dissociation of guaiacol into the corresponding radicals. The selectivity of pyrocatechol formation remains low, < 20 %. The breakdown of guaiacol is further observed by the presence of carbon oxides in the gas phase.

2.1.3. Overall process of pyrolysis

The overall process of pyrolysis of biomass is believed to proceed as follows (Roberts,

1971) The removal of all moisture (dehydration) is complete at around 160^{0}C. Over the temperature range of 200-280^{0}C, all the hemicellulose decomposes, yielding predominantly volatile products such as carbon dioxide, carbon monoxide, and condensable vapors. From 280-500^{0}C the decomposition of cellulose picks up and reaches a peak around 320^{0}C. The decomposition of lignin increases rapidly at temperatures beyond 320^{0}C. This is accompanied by a comparatively rapid increase in the carbon content of the residual solid material.

The thermal decomposition of cellulosic materials such as wood proceeds through a complex series of chemical reactions, coupled with heat and mass transfer processes. It is estimated that over 200 intermediate products are formed during the pyrolysis of biomass (Emmons & Atreya, 1983). Since cellulose is the major constituent of biomass (wood) and pyrolyses over almost the entire range of temperature, several researchers (Maa & Bailie, 1973; Bradbury, Sakai, & Shafizadeh, 1979; Shafizadeh, 1982; Koufopanos, Maschio, & Lucchesi, 1989; Di Blasi, 1993a, 1996a) have studied cellulose pyrolysis in detail, in order to understand the mechanism of pyrolysis of wood. The general set of reactions suggested by Shafizadeh (1982) for the cellulose pyrolysis is as shown below.

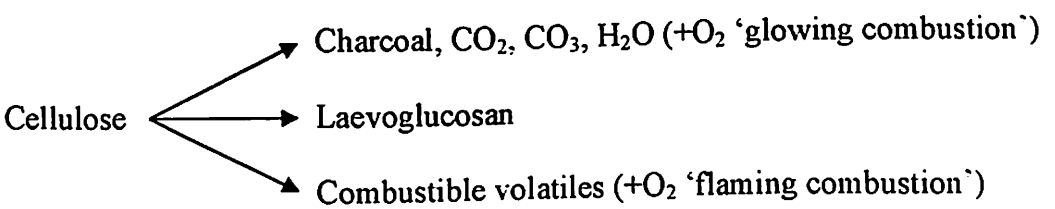

(2.1)

A more detailed description of possible pathways that may contribute to weight loss during pyrolysis of cellulose matrix is as shown in the Fig. 2.1 below (Lewellen, Peters, & Howard, 1969)

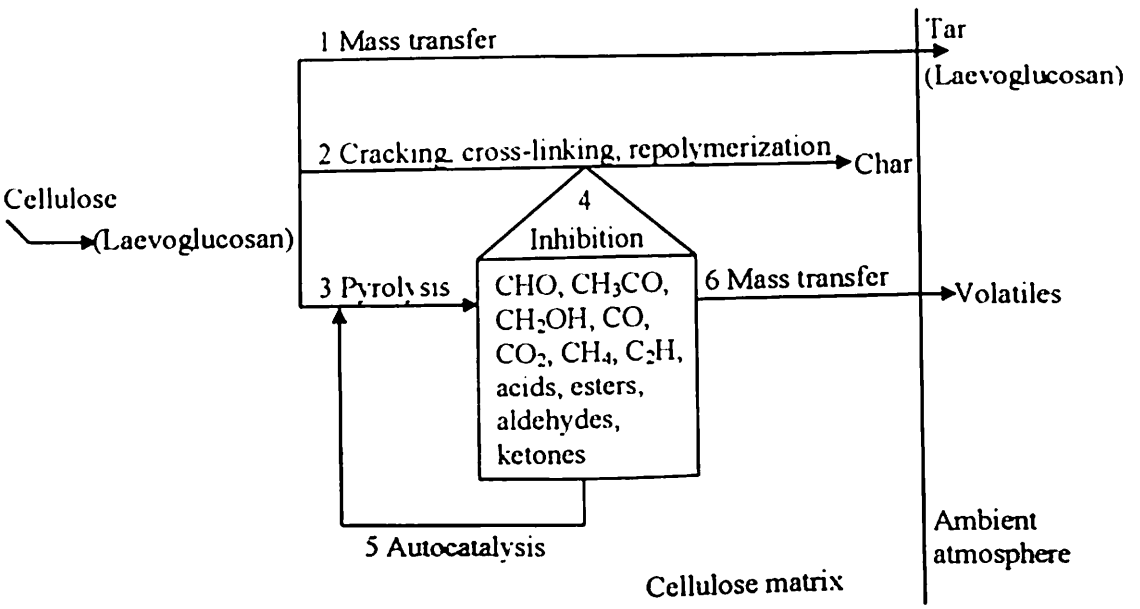

Fig. 2.1. Possible pathways in pyrolysis of cellulose matrix

In this scheme, cellulose decomposes rapidly to an intermediate product, laevoglucosan. Through path 1, it may be transported from the cellulose matrix to give tar; or may repolymerize, crack, or become cross-linked to give char through path 2. It may be pyrolysed through path 3 to lighter volatile products including CO, CO_2, fixed gases, organic acids, ketones, esters, aldehydes, and free radicals, some of which inhibit char formation through path 4 or autocatalyze step 3 through path 5. Lighter stable products would escape the matrix through path 6 to yield volatiles. Thus, there are numerous possible pathways for the pyrolysis of cellulose alone, which reflects the complex mechanism of pyrolysis of biomass (wood) as a whole.

Di Blasi (1993a) presents the different classes of mechanisms proposed for the pyrolysis of wood and other cellulosic materials. The models are classified into three categories:

(1) One-step global models.

(2) Two-stage semi-global models.

(3) One-stage multi-reaction models.

The first category of models considers pyrolysis as a single step first order reaction given as

$$\text{Solids} \xrightarrow{k} \text{a Gases} + \text{b Tar} + \text{c Char} \qquad (2.2)$$

where k is the rate constant of the reaction and a, b, and c are the yield coefficients of the different products of pyrolysis. Reaction rate constant k is written in terms of the frequency factor A and the activation energy E according to the Arrhenius equation as $k=A \exp(-E/RT)$. Table-2.3 gives the values of A and E presented by Di Blasi (1993a), quoted from different sources in the literature, for different species of wood. It can be seen that the values span a wide range for different species of wood. Even for a given species, the kinetic contants depend very strongly on the experimental conditions under which the values are obtained.

Table-2.3. Kinetic constants for different species of wood (Di Blasi, 1993a)

Sample	Temperature (K)	E (kJ/mol)	A (s^{-1})	Source
Wood	321-720	125.4	1.0×10^{8}	Nolan *et al.* (1973)
Beech sawdust	450-700	18 (T<600) 71 (T>600)	0.0053 2.3×10^{4}	Barooah & Long, (1976)

The second category of models considers pyrolysis to be a two-stage reaction, in which the products of first stage break up further in the presence of each other to produce secondary pyrolysis products. Such models are presented for cellulose by Bradbury, Sakai, & Shafizadeh (1979) and for lignin by Antal (1985). Koufopanos, Papayannakos, Maschio, & Lucchesi (1991) proposed the following two-step mechanism for virgin biomass (wood) which is given below:

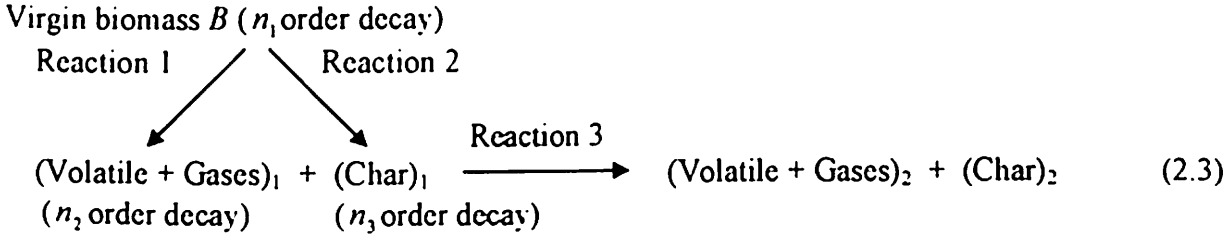

(2.3)

The virgin biomass decomposes to volatiles, gases and char. The volatiles and gases may further react with char to produce different types of volatiles, gases, and char where the compositions are different. Therefore, the primary pyrolysis products participate in secondary interactions (Reaction 3), resulting in modified final product distribution. A condensable fraction is termed as volatiles. It includes acetal, furfural, aldehydes, ketones, phenolic compounds, carboxylic acid, tar, etc. The gases include H_2O, CO, CH_4, C_2H_6, etc.

The third category of models discusses those mechanisms, which considers simultaneous and competing first order reactions in which virgin wood decomposes into the different constituents of pyrolysis products, namely, tar, char, and gases. Such studies have been conducted for small particles of wood (Nunn, Howard, Longwell, & Peters, 1985a, 1985b; Samolda & Vasalos, 1991).

2.2. Important issues in modeling of pyrolysis

The pyrolysis modeling implies the representation of the chemical and physical phenomena constituting pyrolysis in a mathematical form. In other words, pyrolysis is to be represented as a system of equations which taken together can provide valuable quantitative information about the process. Pyrolysis, chemically represented, is a huge series of inter-linked reactions. Besides the range of pyrolysis reactions, several other issues complicate the modeling of pyrolysis. These issues are inter-linked making it extremely difficult to separate the influence of one from another. The major issues are discussed in the following section. However, at some places it has been found more fruitful to discuss overlapping issues together, to bring out their connection.

2.2.1. Reaction scheme

Several reaction schemes have been suggested for the mechanism of pyrolysis. The pyrolysis of biomass consists of two types, i.e., primary and secondary. Primary pyrolysis refers to the decomposition of any of the three major constituents of biomass (wood). Thus, in primary reactions depending on the temperature, there is simultaneous decomposition of lignin, cellulose, and hemicellulose in different regions of the fuel. The primary reactions depend on the local solid temperature. It has a very low enthalpy change (Zaror & Pyle, 1984). Secondary reactions involve the decomposition of primary products. The products of primary reactions, mainly char and volatiles, also catalyze the secondary reactions. Such autocatalytic reactions are initiated when the hot volatile products come in physical contact with unpyrolysed biomass.

A one-step first order global reaction scheme has been used by most of the earlier models (Bamford, Crank, & Malan, 1946; Matsumoto, Fujiwara, & Kondo, 1969; Kansa,

2.2. Important issues in modeling of pyrolysis

The pyrolysis modeling implies the representation of the chemical and physical phenomena constituting pyrolysis in a mathematical form. In other words, pyrolysis is to be represented as a system of equations which taken together can provide valuable quantitative information about the process. Pyrolysis, chemically represented, is a huge series of inter-linked reactions. Besides the range of pyrolysis reactions, several other issues complicate the modeling of pyrolysis. These issues are inter-linked making it extremely difficult to separate the influence of one from another. The major issues are discussed in the following section. However, at some places it has been found more fruitful to discuss overlapping issues together, to bring out their connection.

2.2.1. Reaction scheme

Several reaction schemes have been suggested for the mechanism of pyrolysis. The pyrolysis of biomass consists of two types, i.e., primary and secondary. Primary pyrolysis refers to the decomposition of any of the three major constituents of biomass (wood). Thus, in primary reactions depending on the temperature, there is simultaneous decomposition of lignin, cellulose, and hemicellulose in different regions of the fuel. The primary reactions depend on the local solid temperature. It has a very low enthalpy change (Zaror & Pyle, 1984). Secondary reactions involve the decomposition of primary products. The products of primary reactions, mainly char and volatiles, also catalyze the secondary reactions. Such autocatalytic reactions are initiated when the hot volatile products come in physical contact with unpyrolysed biomass.

A one-step first order global reaction scheme has been used by most of the earlier models (Bamford, Crank, & Malan, 1946; Matsumoto, Fujiwara, & Kondo, 1969; Kansa,

Perlee & Chaiken, 1977; Fan, Fan, Miyanami, Chen, & Walawender, 1977; Maa & Bailie, 1973). However, based on their experimental work Lee, Chaiken, & Singer, (1976) concluded that such a simple scheme is unlikely to result in an accurate model. They suggested the following multi-step scheme:

$$\text{Wood} \xrightarrow{\text{Heat}} \text{Char} + \text{Tar} + \text{Gas} \qquad (2.4)$$

$$\text{Tar} \xrightarrow{\text{Char}} \text{Char} + \text{Gas} + \text{Heat} \qquad (2.5)$$

The decomposition catalysed by char would account for the apparent residence time dependency of the exothermic pyrolysis reactions and secondary char formation. Other researchers share this view of the inadequacy of a single-step reaction. Similar scheme is suggested by Panton & Rittman (1971) based on their investigation. Murty & Blackshear (1967), and Broido & Nelson (1975) also suggested the similar scheme. It has been shown that for the special case of flash pyrolysis under rapid heating, a single-reaction scheme is adequate (Lewellen, Peters, & Howard, 1969) since in such cases the residence time is very small and autocatalytic secondary reactions are absent.

The modeling of secondary pyrolysis reaction is necessary to narrow down the difference between experimental observations and model predictions (Roberts, 1971; Kansa, Perlee, & Chaiken, 1977). Koufopanos, Maschio, & Lucchesi (1989) proposed a two step mechanism model, where an 'Intermediate' product is formed in primary pyrolysis, which breaks up into the final pyrolysis products in the secondary stage. Since it is difficult to establish the composition of components of the intermediates experimentally, the mechanism is modified to that shown above in equation (2.3) for

two-stage semi-global models (Koufopanos, Papayannakos, Maschio, & Lucchesi, 1991) which is utilized by Jalan & Srivastava (1999).

2.2.2. Residence time of volatiles

The residence time of volatile products within the pyrolysing cellulose matrix is extremely important in determining conversion (Lewellen, Peters, & Howard, 1969). Residence time decides the extent of secondary pyrolysis. Competitive pathways such as escape from the matrix, inhibition of char formation, and autocatalysis of secondary pyrolysis may exist whose rates and extent depends upon the residence time of certain products within cellulose.

2.2.3. Heating rate

The reaction pathway and hence, the final products depends on the heating rate. Pyrolysis is classified into slow pyrolysis, with heating rates of the order of 10^0C/min, and rapid/fast/flash pyrolysis, with heating rates approaching 1000^0C/min. The char yield is supported at low heating rates whereas the yield of volatiles increases markedly at fast heating rates. The reaction pathways in the reaction scheme differ depending on the heating rate (Lewellen, Peters, & Howard, 1969). Under rapid heating rates and thin specimen conditions, pathways 1, 3, 4 and 6 as shown in Fig. 2.1 would be expected to dominate yielding little char. At low heating rates, particularly those involving large samples, the residence time of all primary products within the pyrolysing matrix would dominate, accounting for large char yields.

The intermolecular condensation reactions of cellulose are favored at low heating rates (Shafizadeh, 1982). With the slower heating rate experienced at the particle interior, any pressure-driven flow rate is reduced, increasing the intra-particle residence

time of volatiles and increasing the opportunity for condensation and char formation reaction.

2.2.4. Heat of reaction

In modeling, the issue of whether pyrolysis reactions are exothermic or endothermic plays an important role. It has been observed during the experiments (Lee, Chaiken, & Singer, 1976) that the overall heat of reaction at higher heat fluxes is more and resulting in exothermic reaction. The exothermicity of the reaction is greater when the heating is perpendicular to the grain orientation than when it is parallel. This may be explained as follows. For heating perpendicular to the grain orientation, pyrolysis gases have a much higher residence time in the solid matrix leading to an increase in secondary pyrolysis reactions, which are believed to be exothermic. The exothermic behavior is strongly influenced by lignin content (Roberts, 1971).

2.2.5. Particle size

In large particles, the fluid residence times are sufficiently long to result in secondary reactions of the volatiles produced by primary reactions (Bamford, Crank, & Malan, 1946; Chan, Kelbon, & Krieger, 1985). Large particle size implies large thermal gradient. If the moisture is present in a fuel particle, it escapes violently. Local condensation of volatiles and moisture may also take place in the fuel.

The particle size should be sufficiently small to enhance the rate of heat and mass transfer, and the external surface available for reaction. For small particles, it is less likely that internal mass or heat transfer would be rate controlling.

2.2.6. Thermal and thermodynamic properties

Thermal and thermodynamic properties are extremely important as parameters in modeling. The most important thermal and thermodynamic properties are thermal conductivity, heat transfer coefficient, emissivity, heat of reaction number, and reactor temperature. The dependence of average product concentrations and conversion time on these properties during convective/radiant pyrolysis is applicable to both gasification (devolatilization stage) and pyrolysis units. These properties are important mainly for large particles (thermally thick regime). In many cases the desired product is char. High char concentration is associated with high thermal conductivity. Kung (1972) has noted that the temperatures and mass loss predictions are quite sensitive to the thermal conductivity of char.

2.2.7. Shrinkage

The shrinking of the solid particle affects the pyrolysis in several ways (Di Blasi, 1996b; Hagge & Bryden, 2002). The medium properties (porosity, permeability, density, mass diffusivity, specific heat capacity and thermal conductivity), the volume occupied by the volatiles (gas and tar), the volume occupied by the solid (wood and char), and consequently the total volume of the particle also change continuously. As a result of the chemical restructuring during pyrolysis, the density of the char increases. The temperature profile of the particle changes due to increased density and decreased distance across the pyrolysis region (Hagge & Bryden, 2002). The product yield is also affected by the thinner and hotter char layer.

2.2.8. Surface cracks

The effect of surface cracking is to alter the heating characteristics. While the total heat transfer remains the same, heat is transported more quickly to the interior due to the presence of cracks on the surface. Internal failures result in changed local porosity and permeability, affecting the fluid flow inside. Curry & Cox (1973, as in Kansa, Perlee, & Chaiken, 1977) have found that the internal heat transfer coefficient had its greatest effect on the fluid temperature at temperatures around 700 K and pore size or cracks 1mm in diameter. At fire intensity levels where the temperature exceed 1200 K, and the cracks tend to become large, radiation transfer through the solid matrix may become more important than thermal conduction.

2.3. Modeling approach

2.3.1. Chemical kinetics model

The actual reaction scheme of pyrolysis of biomass is extremely complex because of the formation of over a hundred intermediate products. Pyrolysis of biomass is, therefore, generally modeled on the basis of apparent kinetics. Ideally, the chemical kinetics model should account for the primary decomposition reactions as well as the secondary reactions. The model should take heating rate into account to determine the scheme of reactions and should consider the possibility of autocatalysis of certain secondary reactions depending on the residence time of volatiles. However, till date, models have generally accounted for primary reactions through apparent kinetics and in some cases, some of the secondary reactions through multi-step reaction schemes. Other issues are yet to be accounted for in the existing models.

Zaror & Pyle (1984) suggest a single pseudo-first order reaction scheme. Bamford, Crank, & Malan (1946) have used a single reaction scheme and first order kinetics with a fixed heat of reaction. Matsumoto, Fujiwara, & Kondo (1969) used Bamford, Crank, & Malan (1946) model but, in addition, considered the rate of char removal by oxidation. But, none of the above models considered the secondary pyrolysis reactions.

It is well known that the large number of complex reactions taking place in the pyrolysis process, and therefore, even today, it is difficult to develop a precise kinetic model taking into account all the parameters. It is generally accepted that the most important parameters are temperature, concentration, time and heating conditions. Keeping the above view, Koufopanos, Papayannakos, Maschio, & Lucchesi (1991) proposed kinetic model as given by equation (2.3), which indicates that the biomass decomposes to volatiles, gases and char. The volatiles and gases may further react with char to produce different types of volatiles, gases and char where the compositions are different. The scheme of reactions of this model is adapted by Srivastava & Jalan (1994), Srivastava, Sushil, & Jalan (1996) and Jalan & Srivastava (1999). Chan (1983, as given in Sinha, Jhalani, Ravi, & Ray, 2000) proposed a mechanism as shown below where volatiles and tar formed by primary pyrolysis undergo secondary pyrolysis. The other

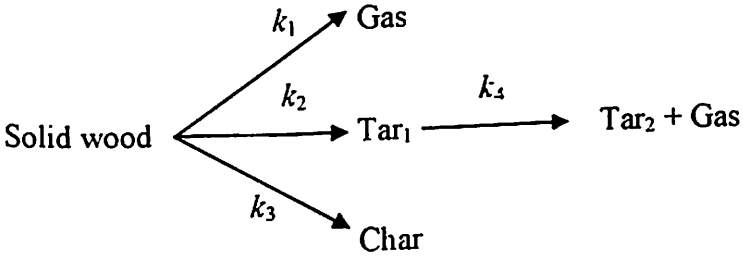

(2.6)

primary reactions of formation of char and gas from wood are parallel and competing with the tar formation reaction.

The chemical processes of biomass pyrolysis are described through a primary and a secondary stage (Shafizadeh & Chin, 1977; Thurner and Mann, 1981; Chan, Kelbon & Krieger, 1985; Font, Marcilla, Verdu, & Devesa, 1990) as given by equation (2.7). Wood undergoes thermal degradation according to primary reactions (k_1, k_2, k_3) giving gas, tar and char as products. Tar may undergo secondary reactions (k_4, k_5).

(2.7)

Broido-Shafizadeh scheme of cellulose pyrolysis (with kinetic constants k_1, k_2, and k_3 as in Bradbury, Sakai & Shafizadeh, 1979), extended to include secondary reaction with kinetic constant k_4 (Liden, Berruti & Scott, 1988) in which the formation of "active" cellulose precedes the formation of gas, tar, and char is given by equation (2.8). This scheme is also utilized by Di Blasi (1996a).

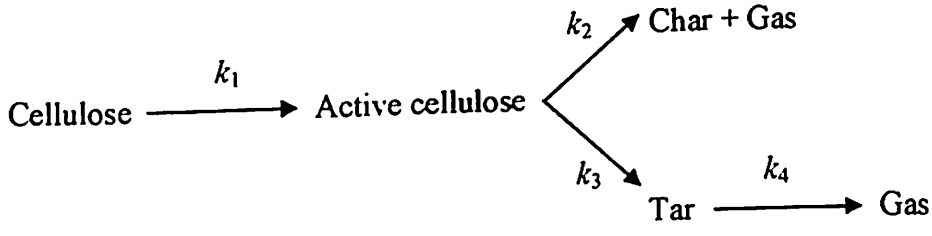

(2.8)

It is necessary to know the values of kinetic parameters of the biomass under a particular set of conditions, in the view of the importance of kinetics in the pyrolysis of biomass. However, difficulty arises in studying the thermal behavior of biomass due to lack of exact knowledge of the course of reactions and their degree of completion. Moreover, the vast number of products resulting from the thermal degradation of biomass hinders a thorough understanding of the process. Thus, several different values

of the kinetic reaction constants, the pre-exponential factor, and the activation energy have been used in literature for numerical simulation using the models. Few researchers have used the values of kinetic constants in their simulation that have been estimated from the same sample of biomass that is used for experimental corroboration. Koufopanos, Papayannakos, Maschio, & Lucchesi (1991), have determined both primary and secondary reaction rate constants and heat of pyrolysis by matching models with measured mass loss and temperature profile data. This approach is to be favored since it enhances the reliability of the model validation.

2.3.2. Heat transfer model

The heat transfer model determines the temperature profiles that serve as an input to the kinetic model. Hence, the details of the heat transfer model often determine the accuracy of prediction of the overall model. The ideal heat transfer model should account for the following phenomena/issues: heat transfer to the surface fuel, conduction to the interior, internal convection, effect of internal structural changes on fluid flow, heat of reaction, and changes in thermal & thermodynamic properties during the course of pyrolysis. However, the existing models excluded many of the above mentioned important aspects in modeling. The first model of pyrolysis of wood is developed by Bamford, Crank, & Malan (1946). But, the model does not consider residence time of volatiles, secondary pyrolysis reactions and thermal conductivity as a function of temperature.

In the later model, Matsumoto, Fujiwara, & Kondo (1969) used temperature dependent thermal conductivity and included internal convective heat transfer. This model is further enhanced by Kung (1972) who studied the effects of slab thickness of

wood, char conductivity, and decomposition endothermicity. However, no specific kinetic mechanism is suggested to predict the concentration of the various components produced during pyrolysis. Maa & Bailie (1973) have developed the unreacted shrinking core model for high temperatures. This model differed from earlier models in the manner in which chemical kinetics is combined with heat transfer. Kansa, Perlee, & Chaiken (1977) included momentum equation for the motion of pyrolysing gases within the solid. A suitable kinetic mechanism has not been utilized and the solution to the heat and momentum balance equation is based on arbitrary boundary conditions. Fan, Fan, Miyanami, Chen, & Walawender (1977) have used a volume reaction model, which accounts for simultaneous heat and mass transfer in the particle. The reaction is considered to be first order with respect to initial particle concentration. Also product concentrations cannot be analyzed from the above model as the secondary reactions are not considered.

Chan, Kelbon, & Krieger (1985) described the unsteady rise of temperature in the particle interior by using a time-varying global porosity to characterize the internal energy change of the gas and solid. A variable thermal conductivity, dependent on the wood density and temperature, has been used. Di Blasi (1997) modeled the momentum conservation in the domain using Darcy's law, in order to relate pressure gradients to velocities, and used the ideal gas equation of state to relate the gas phase density, pressure and temperature. Jalan & Srivastava (1999) developed the model for a single cylindrical biomass pellet, but neglected the effect of specific heat and thermal conductivity of char, which are the functions of temperature. Also, instead of considering convective heat transfer coefficient as a function of Reynolds number &

Prandtl number, a constant value is used.

Table-2.4. Important contributions to pyrolysis modeling literature

Researchers	Important contributions & assumptions made
Bamford, Crank, & Malan (1946)	First model of pyrolysis; only conductions, constant thermal conductivity (k), first order single step reaction
Tinney (1965)	Two consecutive reaction schemes
Matsumoto, Fujiwara, & Kondo (1969)	Temperature dependent thermal conductivity (k), internal convection char removal by oxidation
Roberts (1971)	Compared presence and absence of internal heat transfer, considered constant thermal conductivity (k) and density of biomass (ρ).
Kung (1972)	Importance of thermal conductivity of char
Maa & Bailie (1973)	Unreacted shrinking core model
Lee, Chaiken, & Singer (1976)	Purely experimental work on type and extent of heat of reaction (exothermic & endothermic)
Fan, Fan, Miyanami, Chen, & Walawender (1977)	Volume reaction model for simultaneous heat and mass transfer
Kansa, Perlee, & Chaiken (1977)	Momentum equation for motion of pyrolysis gases; modeled anisotropicity
Chan, Kelbon, & Krieger (1985)	Multi-step reaction schemes, time-varying global porosity, variable thermal conductivity (k), fluid flow, contribution of evaporation of inherent moisture to weight loss, volatile properties based on CO and H_2O
Koufopanos, Papayannakos, Maschio, & Lucchesi (1991)	Competing and consecutive reactions to account for both primary and secondary pyrolysis
Bilbao, Mastral, Aldea, & Ceamanos (1996, as given in Sinha, Jhalani, Ravi, & Ray, 2000)	Work on small samples of sawdust; used TGA to determine frequency factor (A) and the activation energy (E) used in the model
Di Blasi (1998)	Physico-chemical processes occurring inside a degrading two-dimensional anisotropic porous medium
Jalan & Srivastava (1999)	Studies on pyrolysis of a single biomass cylindrical pellet-kinetic and heat transfer effects
Hagge & Bryden (2002)	Modeling the impact of shrinkage on the pyrolysis of dry biomass

2.3.3. Mass transfer model

The ideal mass transfer model should consider the effect of particle size, shrinkage, mass diffusivity and the residence time of pyrolysis gases. The mass transfer model is heavily dependent on the extent of detailing in chemical kinetics model. This is so because it is the kinetics model that identifies various species that the mass transfer model must work with. Single step reaction models predict only the lumped gas species and hence, the product distribution is unaffected by a finite mass transfer rate. However, for more complex multi-step reaction schemes, mass transfer does affect the secondary pyrolysis. Various studies on this aspect show that mass transfer effects may be neglected for the case of heating parallel to the grain orientation since the residence time is low in this case. For developing a good mass transfer model the information on secondary pyrolysis reactions is very important. Table-2.4 above presents a summary of the important contributions to pyrolysis modeling in the literature.

2.4. Objectives

Based on the background work reported in literature with their limitations as discussed above and the importance & useful applications of pyrolysis process (given in chapter 1), the objectives of the present study also discussed briefly in chapter 1 are as follows:

(1) To understand the physical aspects of pyrolysis in modeling of biomass gasification.

(2) To incorporate the effect of convective heat transfer coefficient as a function of Reynolds number & Prandtl number and specific heat capacity & thermal conductivity of char as functions of temperature.

(3) To incorporate autocatalytic secondary pyrolysis reactions and density of char as a

function of time.

(4) Incorporating the effect of thermal and transport properties such as porosity, thermal conductivity, specific heat and mass diffusivity on pyrolysis.

(5) Improvement on the existing models considering residence time effects, shrinkage, particle size distribution, different geometries, changes in material properties, heat of reaction during the course of pyrolysis, etc.

(6) Validating the proposed models with the actual experimental data obtained from the literature.

2.5. Conclusions

- The primary objectives of the models of pyrolysis of biomass are to provide a diagnostic tool for evaluating the importance of the various system parameters and to identify system characteristics.
- The pyrolysis modeling implies the representation of the chemical and physical phenomena constituting pyrolysis in a mathematical form. In other words, pyrolysis is to be represented as a system of equations which taken together can provide valuable quantitative information about the process.
- The modeling of autocatalytic secondary pyrolysis reaction is necessary to narrow down the difference between experimental observations and model predictions.
- Residence time decides the extent of secondary pyrolysis. The residence time of volatile products within the pyrolysing cellulose matrix is extremely important in determining conversion.
- The reaction pathway and hence, the final products depends on the heating rate.

Pyrolysis is classified into slow pyrolysis reactions, with the heating rates of the order of 10^0C/min, and rapid/fast/flash pyrolysis reactions, with heating rates approaching 1000^0C/min.

- The issue of whether pyrolysis reactions are exothermic or endothermic plays an important role in modeling.
- Large particle size implies large thermal gradient. In large particles, the fluid residence times are sufficiently long to result in secondary reactions of the volatiles produced by primary reactions.
- The most important thermal and thermodynamic properties affecting the pyrolysis modeling are thermal conductivity, heat transfer coefficient, emissivity, heat of reaction number, and reactor temperature.
- Shrinking of the solid particle of biomass affects the pyrolysis in several ways. The medium properties, the volume occupied by the volatiles, the volume occupied by the solid, and consequently the total volume of the particle change continuously.
- Presence of cracks on the surface alters the heating characteristics. While the total heat transfer remains the same, heat is transported more quickly to the interior due to the presence of cracks on the surface.
- The existing literature on pyrolysis modeling suggests that great strides have been made in understanding and modeling pyrolysis in the last three decades. The models which are presently available exclude some of the important effects as mentioned above.
- It is essential that more detailed models taking into account of all these effects, should be attempted paving the way for improved simulation of actual processes.

CHAPTER 3

MODELING, SIMULATION AND ESTIMATION OF OPTIMUM PARAMETERS IN PYROLYSIS OF BIOMASS

3.1. Introduction

The thermochemical conversion of biomass (pyrolysis, gasification, combustion) is one of the most promising non-nuclear forms of future energy. It is a renewable form of energy with many ecological advantages. Pyrolysis of biomass is an important process for producing energy with a promising future for the production of solid (charcoal), liquid (tar and other organics) and gaseous products (methane, ethane and carbon monoxide). These products are of interest as possible alternate fuels.

It is well known that there are a large number of complex reactions involved in the process of pyrolysis, and therefore, it is impossible to develop a precise kinetic model taking into account the various parameters. In many cases the description of the pyrolysis kinetics by relatively simple, rationally-based models, is extremely useful. The models employed in this kind of study do not necessarily represent the detailed physicochemical mechanism of the process, but they predict the overall yield.

The development of thermochemical processes for the biomass conversion and the proper equipment design requires the knowledge of several process features such as: a good understanding of the governing pyrolysis mechanisms, the determination of the most significant pyrolysis parameters & their effect on the process and knowledge of the kinetics. It is generally accepted that the most important parameters affecting the process of pyrolysis of biomass are temperature, concentration, time and heating conditions.

3.2. Background

Studies have been carried out on pyrolysis of biomass and other substances by several researchers (Fan, Fan, Miyanami, Chen, & Walawender, 1977; Miyanami, Fan, Fan, & Walawender, 1977; Pyle & Zaror, 1984; Nunn, Howard, Longwell, & Peters, 1985a, 1985b; Koufopanos, Papayannakos, Maschio, & Lucchesi, 1991; Di Blasi, 1998; Jalan & Srivastava, 1999; Hawboldt, Monnery, & Svrcek, 2000; Li, Kennedy, & Dlugogorski, 2000; Sørum, Grønli, & Hustad, 2001; Demirbaş, 2002b). The actual reaction scheme of pyrolysis of biomass is extremely complex because of formation of over hundred intermediate products. Pyrolysis of biomass is, therefore, generally modeled on the basis of apparent kinetics. Ideally, the chemical kinetics model should account for primary decomposition reactions as well as secondary reactions. Significant contributions have been made on kinetic modeling by Roberts (1970), Kanury (1972), Anthony & Howard (1976), Bradbury, Sakai, & Shafizadeh (1979), Shafizadeh (1982), Jegers & Klein (1985), Matsui, kunii, & Furusawa (1987), Wang & Kinoshita (1993), Wiktorsson & Wanzl (2000), Castets, Daguerre, & Py (2001), etc. However, none of the above studies

have been able to develop a universal model that can predict the rate of pyrolysis, final conversions and concentrations over a wide range of operation conditions. The major shortcomings of the models are that they are useful for a particular type of biomass only, as indicated in the work done by Mellottee & Richard (1983) and Ward & Braslaw (1985).

For a complete understanding of the pyrolysis process, it is essential to obtain concentration profiles and other related information for the biomass material. The kinetic model proposed by Koufopanos, Maschio, & Lucchesi (1989) introduced the concept of "intermediate". This model is also utilized by Srivastava & Jalan (1994) in their studies. However, it is later highlighted that it is very difficult to define physically the components or the composition of intermediates, and consequently it is not possible to measure its concentration experimentally in order to test the model rigorously. Therefore, Koufopanos, Papayannakos, Maschio, & Lucchesi (1991) utilized a different kinetic model which did not have an "intermediate" product. This model is utilized by Srivastava, Sushil, & Jalan (1996) in their studies. The optimum values of the parameters affecting the pyrolysis process are not estimated in the studies reported so far.

3.3. Motivation

As discussed above, temperature, concentration, time and heating conditions is generally accepted as the most important parameters affecting the process of pyrolysis of biomass. The optimum values of these parameters play a very important role in designing biomass gasifer and pyrolysis units. But, the optimum values of these

parameters are not estimated in the studies reported so far. This provided motivation to examine the problem in greater detail. The purpose of this work is to find the optimum values of these parameters for both non-isothermal and isothermal heating conditions.

3.4. Problem formulation

Koufopanos, Papayannakos, Maschio, & Lucchesi (1991) proposed the following two-step mechanism scheme [equation (2.3), chapter 2] for describing the kinetics of the pyrolysis of biomass:

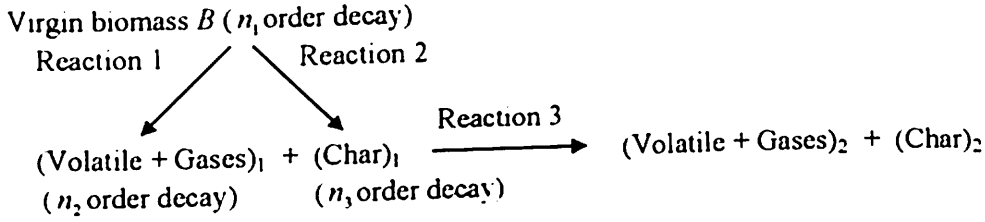

The kinetic equations for the mechanism shown above are as follows:

$$\frac{\partial \overline{C}_B}{\partial t} = -k_1 \overline{C}_B^{n_1} - k_2 \overline{C}_B^{n_1} \tag{3.1}$$

$$\frac{\partial \overline{C}_{G1}}{\partial t} = k_1 \overline{C}_B^{n_1} - k_3 \overline{C}_{G1}^{n_2} \overline{C}_{C1}^{n_3} \tag{3.2}$$

$$\frac{\partial \overline{C}_{C1}}{\partial t} = k_2 \overline{C}_B^{n_1} - k_3 \overline{C}_{G1}^{n_2} \overline{C}_{C1}^{n_3} \tag{3.3}$$

$$\frac{\partial \overline{C}_{G2}}{\partial t} = k_3 \overline{C}_{G1}^{n_2} \overline{C}_{C1}^{n_3} \tag{3.4}$$

$$\frac{\partial \overline{C}_{C2}}{\partial t} = k_3 \overline{C}_{G1}^{n_2} \overline{C}_{C1}^{n_3} \tag{3.5}$$

where,

$$k_1 = A_1 \exp[(D_1/T) + (L_1/T^2)]$$

$k_2 = A_2 \exp[(D_2/T)+(L_2/T^2)]$

$k_3 = A_3 \exp[(-E_3/RT)]$

$A_1 = 9.973 \times 10^{-5}\ s^{-1}$; $A_2 = 1.068 \times 10^{-3}\ s^{-1}$; $A_3 = 5.7 \times 10^{5}\ s^{-1}$

$D_1 = 17254.4$ K; $D_2 = 10224.4$ K

$L_1 = -9061227\ K^2$; $L_2 = -6123081\ K^2$

$E_3 = 81$ kJ/mol

Srivastava, Sushil, & Jalan (1996) assumed that in the thermo-gravimetric analysis, temperature and time have a linear relationship, and consequently it is appropriate to describe the above phenomenon as follows:

$$T = (HR)\, t + T_0 \tag{3.6}$$

where, T_0 is the initial temperature in K. HR is the heating rate in K/s, and t is time in s.

3.5. Method of solution and simulation of model equations

The equations (3.1) – (3.6) are used for non-isothermal conditions with an initial temperature of $T_0 = 773$ K and with different heating rates of 25 K/s, 40 K/s, 50 K/s, 60 K/s, and 80 K/s. Also the heating rates beyond 80 K/s are used in the simulation over a wide range between 125 K/s and 360 K/s with a heating rate interval of 15 K/s (step size) for finding out the optimum heating rate. In addition, the simulation is also carried out at the optimum heating rate corresponding to the minimum pyrolysis time to find out the corresponding optimum parameters. The equations (3.1) – (3.5) are used for isothermal conditions ($T = T_0 =$ constant) with different temperatures of 773 K, 873 K, 973 K, 1023 K, and 1073 K. Similarly, in this case also, simulation is carried out with a wide range of temperatures ranging from 773 K to 1773 K with a maximum step size of 100 K

initially to a very small step size of 0.1 K to ensure not to miss out the optimum parametric values. In addition, the model equations are solved at the optimum temperature also to find out the corresponding optimum parameters. For both the non-isothermal and isothermal cases, the corresponding equations are solved numerically using the fourth order Runge-Kutta method (Appendix-A) and the results are simulated. The pyrolysis process is very slow below a temperature of 773 K (Srivastava, Sushil, & Jalan, 1996), and hence the lower values of initial temperature are not considered in the simulations of the present study (Babu & Chaurasia, 2003a). The following initial conditions are used for solving the coupled ordinary differential equations.

At $t = 0$, $\overline{C}_B = 1$, $\overline{C}_{G1} = \overline{C}_{C1} = \overline{C}_{G2} = \overline{C}_{C2} = 0$.

The final dimensionless concentration of biomass is assumed to be equal to 0.03, because beyond that concentration, pyrolysis is found to be very slow and of little practical importance. The iterations are continued till $C_B \geq 0.03$. The optimum values of the parameters are found using $n_2 = n_3 = 1.5$ with two values of n_1 (i.e., for $n_1 = 0$ and $n_1 = 1$) for both the non-isothermal and isothermal conditions. The Computer Codes in C++ for both non-isothermal and isothermal conditions are given in Appendix-A.

3.6. Results and discussion

3.6.1. Nonisothermal conditions

The concentration profiles for a particular type [wood sawdust (0.30-0.85mm)] of biomass with $n_1 = 1$ and $n_2 = n_3 = 1.5$ for the heating rates of 25 K/s and 60 K/s are shown in Figs. 3.1 and 3.2 respectively. By substituting units of various quantities in

equations (3.1) – (3.5), the unit of pyrolysis time is found to be in second, but probably by mistake it is reported to be in minutes (Srivastava, Sushil, & Jalan, 1996).

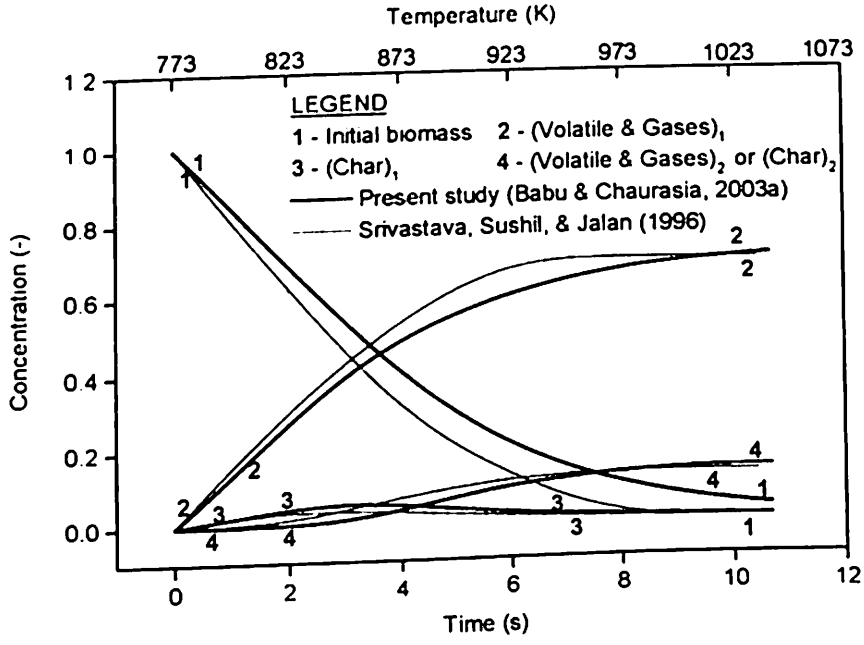

Fig. 3.1. Concentration profile as a function of time and temperature for pyrolysis under non-isothermal condition (HR=25 K/s, n_1=1, n_2=n_3=1.5).

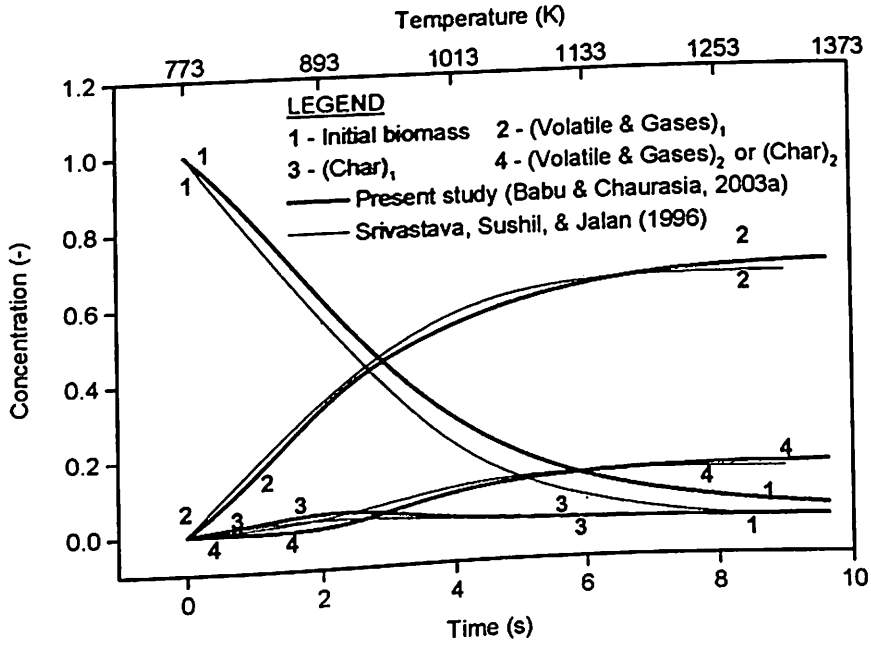

Fig. 3.2. Concentration profile as a function of time and temperature for pyrolysis under non-isothermal condition (HR=60 K/s, n_1=1, n_2=n_3=1.5).

Accordingly, the unit of heating rate should be in K/s but not K/min as reported. The trends observed in figures are qualitatively same as those reported. But, quantitatively there is slight difference in the final values. It may be due to the different methods adopted for the solution and the assumptions made. Srivastava, Sushil. & Jalan (1996) used the fourth order Runge-Kutta Predictor-Corrector method to simulate the model and assumed maximum time for simulation to be 20 s, while in the present study (Babu & Chaurasia, 2003a) the simulation is carried out not based on stopping criteria of time of 20 s but the final dimensionless concentration of the biomass of 0.03. The final pyrolysis time, final temperature and final concentrations for the above orders of reactions and for heating rates of 40, 50 and 80 K/s obtained in the present study (Babu & Chaurasia, 2003a) are compared with those reported (Srivastava, Sushil. & Jalan, 1996) as given in Table-3.1.

Table-3.1. Comparison of the simulated results obtained for pyrolysis under non-isothermal condition in the present study (Babu & Chaurasia, 2003a) with those reported in literature (Srivastava, Sushil, & Jalan, 1996) (n_1=1; n_2=n_3=1.5)

Final	40 K/s		50 K/s		80 K/s	
	P	R	P	R	P	R
t	9.707	9.58	9.532	9.28	10.792	9.08
T	1161.28	1156.2	1249.6	1237.0	1636.36	1494.6
C_B	0.030010	0	0.030005	0	0.030001	0
C_{C_1}	0.001131	0.0002	0.000731	0	0.000168	0
C_{G_1}	0.692126	0.671	0.686190	0.666	0.663411	0.648
C_{C_2}	0.138367	0.133	0.141538	0.135	0.153210	0.143
C_{G_2}	0.138367	0.133	0.141538	0.135	0.153210	0.143

P – Present study (Babu & Chaurasia, 2003a); R – Srivastava, Sushil, & Jalan (1996)

It is seen from Table-3.1 that, as the heating rate increases, final pyrolysis temperature increases, and final concentrations of (volatile & gases)$_1$ and (char)$_1$ decrease while the final concentrations of (volatile & gases)$_2$ or (char)$_2$ increase. The trends obtained in

final temperature and final concentrations of biomass in the present study (Babu & Chaurasia, 2003a) are same as those reported (Srivastava, Sushil, & Jalan, 1996). But the trend in final pyrolysis time is not matching. It is seen from Table-3.1 that for the heating rates of 40 K/s and 50 K/s, final pyrolysis time decreases. It is noted that for 80 K/s the final pyrolysis time increases but (Srivastava, Sushil, & Jalan, 1996) reported decreasing value. To have a clear and better understanding of this contradiction, the model is simulated for different values of heating rates with smaller step size in the range of 50 - 80 K/s. The final pyrolysis time vs. heating rates are plotted and shown in Fig. 3.3. It is found that the final pyrolysis time first decreases with increasing heating rate, reaches the optimum value and then increases as heating rate is further increased. For the above orders of reactions the optimum values of heating rate & final pyrolysis time are found to be 51 K/s and 9.53 s respectively. As Srivastava, Sushil, & Jalan (1996) did not carry out the simulation of the model in between the heating rates of 50 K/s and

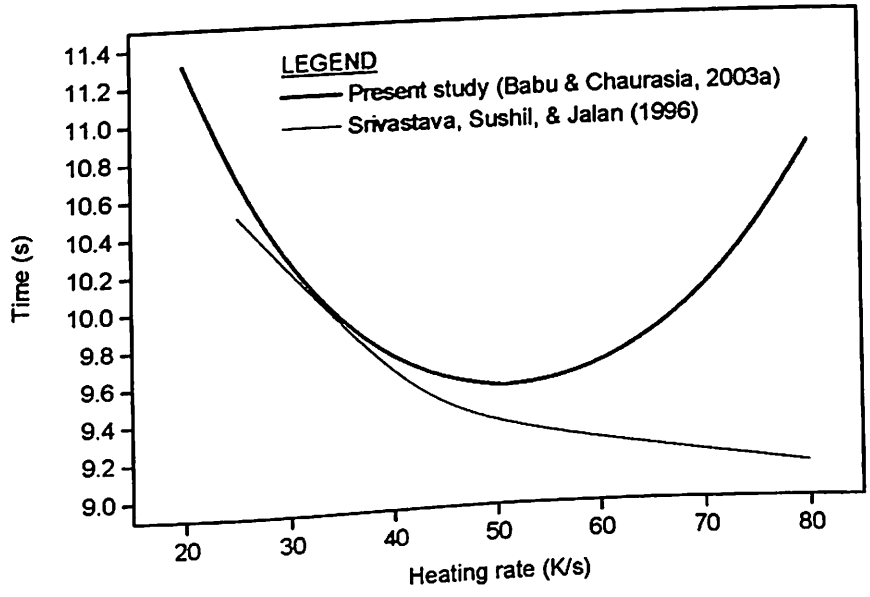

Fig. 3.3. Time as a function of heating rate for pyrolysis under non-isothermal condition (n_1=1, n_2=n_3=1.5).

80 K/s, they could not notice this decreasing and increasing trend.

In order to explain this interesting decreasing and increasing trend in final pyrolysis time with heating rate or temperature, the simulated data for optimum heating rate (51 K/s) and heating rate of 80 K/s are used as shown in Tables 3.2 and 3.3 respectively. It is seen that as the pyrolysis proceeds (i) temperature increases, (ii) concentration of biomass decreases and reaches the final value, (iii) concentration of (volatile & gases)$_1$

Table-3.2. Simulated results with the optimum heating rate (51 K/s) for pyrolysis under non-isothermal condition (n_1=1; n_2=n_3=1.5)

t	T	C_B	C_{G_1}	C_{C_1}	C_{G_2}	C_{C_2}
0.000000	773.000000	1.000000	0.000000	0.000000	0.000000	0.000000
0.100000	778.100000	0.984444	0.013370	0.002186	0.000000	0.000000
1.800000	864.800000	0.666499	0.283709	0.042532	0.003630	0.003630
1.900000	869.900000	0.646787	0.299580	0.044153	0.004740	0.004740
2.000000	875.000000	0.627204	0.315098	0.045522	0.006088	0.006088
2.200000	885.200000	0.588554	0.344865	0.047397	0.009592	0.009592
2.300000	890.300000	0.569549	0.359027	0.047861	0.011781	0.011781
2.400000	895.400000	0.550794	0.372664	0.047994	0.014274	0.014274
2.500000	900.500000	0.532316	0.385754	0.047793	0.017068	0.017068
3.100000	931.100000	0.428431	0.452937	0.040561	0.039036	0.039036
3.200000	936.200000	0.412433	0.462433	0.038653	0.043241	0.043241
3.300000	941.300000	0.396842	0.471527	0.036651	0.047490	0.047490
4.000000	977.000000	0.299518	0.526486	0.022800	0.075598	0.075598
5.000000	1028.00000	0.195522	0.586404	0.010409	0.103833	0.103833
6.000000	1079.00000	0.126164	0.628144	0.005079	0.120306	0.120306
7.000000	1130.00000	0.081744	0.655061	0.002697	0.130249	0.130249
8.000000	1181.00000	0.053790	0.671731	0.001519	0.136480	0.136480
9.000000	1232.00000	0.036213	0.681929	0.000895	0.140482	0.140482
9.530000	1259.03000	0.030004	0.685557	0.000699	0.141870	0.141870

increases, (iv) concentration of (char)$_1$ increases up to certain value of time and then decreases, and (v) concentrations of (volatile & gases)$_2$ and (char)$_2$ increase. It may be noted that the decrease in concentration of biomass is more for 80 K/s up to certain time (7 s). The maximum concentration of (char)$_1$ is obtained at 2.4 and 1.9 s for heating rates of 51 and 80 K/s respectively. After 1.9 s, the concentration of (char)$_1$ starts

Table-3.3. Simulated results with the heating rate = 80 K/s for pyrolysis under non-isothermal condition (n_1=1; n_2=n_3=1.5)

t	T	C_B	C_{G_1}	C_{G_1}	C_{G_2}	C_{G_2}
0.000000	773.000000	1.000000	0.000000	0.000000	0.000000	0.000000
0.100000	781.000000	0.984002	0.013754	0.002244	0.000000	0.000000
1.800000	917.000000	0.619522	0.318944	0.044262	0.008636	0.008636
1.900000	925.000000	0.597060	0.335530	0.044785	0.011313	0.011313
2.000000	933.000000	0.574944	0.351302	0.044778	0.014488	0.014488
2.200000	949.000000	0.531948	0.380276	0.043187	0.022295	0.022295
2.300000	957.000000	0.511153	0.393489	0.041675	0.026841	0.026841
2.400000	965.000000	0.490875	0.405905	0.039773	0.031724	0.031724
3.100000	1021.00000	0.365117	0.476451	0.022603	0.067914	0.067914
3.200000	1029.00000	0.349578	0.484943	0.020413	0.072532	0.072532
3.300000	1037.00000	0.334646	0.493153	0.018399	0.076901	0.076901
4.000000	1093.00000	0.246239	0.543283	0.008955	0.100761	0.100761
5.000000	1173.00000	0.160908	0.593360	0.003752	0.120990	0.120990
6.000000	1253.00000	0.108788	0.623367	0.001831	0.133007	0.133007
7.000000	1333.00000	0.076824	0.640868	0.000985	0.140662	0.140662
8.000000	1413.00000	0.056744	0.651157	0.000571	0.145764	0.145764
9.000000	1493.00000	0.043710	0.657332	0.000352	0.149303	0.149303
10.000000	1573.00000	0.034947	0.661127	0.000228	0.151849	0.151849
10.792000	1636.36000	0.030001	0.663411	0.000168	0.153210	0.153210

decreasing for heating rate of 80 K/s, so rate of consumption of biomass also decreases. After 7 s, the decrease in concentration of biomass is less for 80 K/s as compared to 51 K/s, because the $(char)_1$ left for 80 K/s is less as compared to 51 K/s. So the reaction between $(volatile\ \&\ gases)_1$ and $(char)_1$ is slow for 80 K/s as compared to 51 K/s time, and hence it takes more time to reach the desired final concentration of biomass. Hence the final pyrolysis time is more for 80 K/s as compared to 51 K/s.

The final concentrations of $(volatile\ \&\ gases)_1$, $(char)_1$ and $(volatile\ \&\ gases)_2$ or $(char)_2$ are plotted against heating rates as shown in Figs. 3.4-3.6. As the heating rate increases, the concentration of $(volatile\ \&\ gases)_2$ or $(char)_2$ increases, while the concentrations of $(volatile\ \&\ gases)_1$ and $(char)_1$ decrease as they react with each other to produce $(volatile\ \&\ gases)_2$ or $(char)_2$, i.e. the primary pyrolysis products participate in

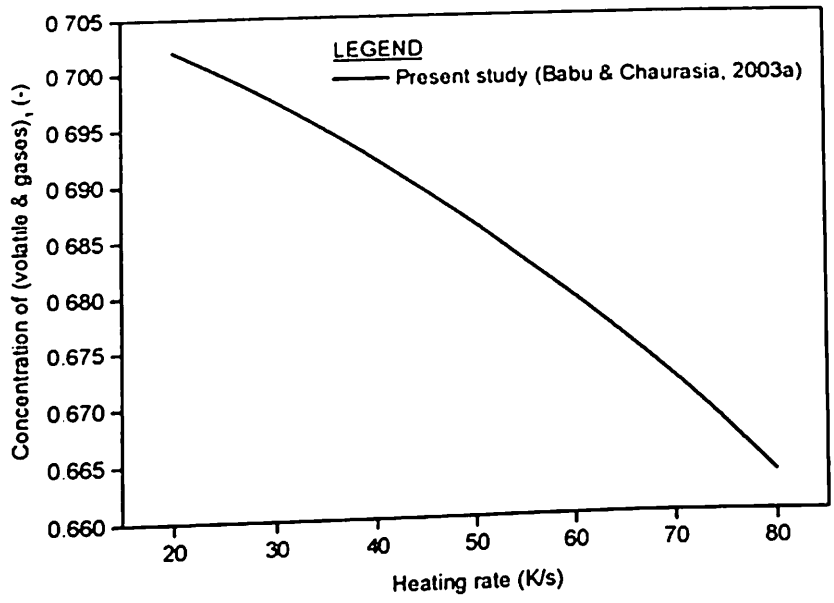

Fig. 3.4. Concentration of (volatile & gases)$_t$ as a function of heating rate for pyrolysis under non-isothermal condition (n_1=1, n_2=n_3=1.5).

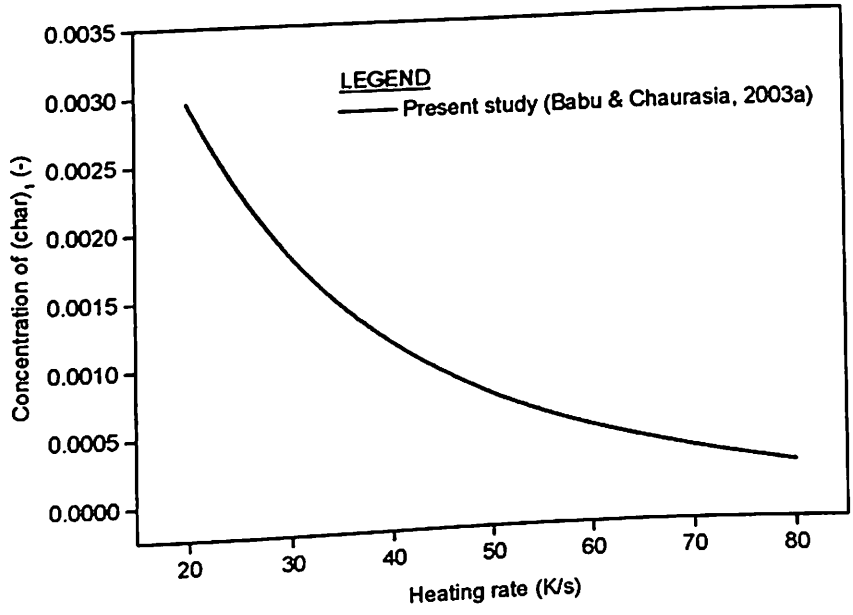

Fig. 3.5. Concentration of (char)$_t$ as a function of heating rate for pyrolysis under non-isothermal condition (n_1=1, n_2=n_3=1.5).

the secondary interactions, resulting in a modified final product distribution. The optimum values of parameters for the above orders of reactions are shown in Table-3.4.

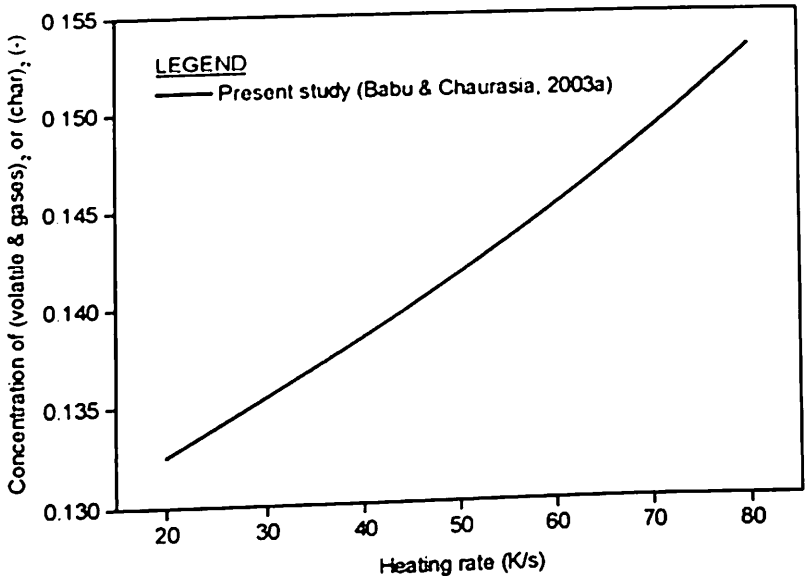

Fig. 3.6. Concentration of (volatile & gases)$_2$ or (char)$_2$ as a function of heating rate for pyrolysis under non-isothermal condition (n_1=1, n_2=n_3=1.5)

Table-3.4. Optimum Parametric values for different orders of reactions for pyrolysis under non-isothermal condition

Optimum Parameters	n_1=1; n_2=n_3=1.5	n_1=0; n_2=n_3=1.5
Heating rate (K/s)	51	184.38
Final pyrolysis time (s)	9.53	2.636
Final pyrolysis temperature (K)	1259.03	1259.03
Final concentration of initial biomass (-)	0.030004	0.030045
Final concentration of (char)$_1$ (-)	0.000699	0.007357
Final concentration of (volatile & gases)$_1$ (-)	0.685557	0.662166
Final concentration of (char)$_2$ (-)	0.141870	0.150216
Final concentration of (volatile & gases)$_2$ (-)	0.141870	0.150216

Similarly, the concentration profiles for orders of reactions of $n_1 = 0$ and $n_2 = n_3 = 1.5$ for heating rates of 25 K/s and 60 K/s are presented in Figs. 3.7 and 3.8 respectively. Again, the trends are same as reported Srivastava, Sushil, & Jalan (1996). The final pyrolysis time, final temperature and final concentrations for the heating rates of 40, 50 and 80 K/s are given in Table-3.5. It is seen that the trends in final pyrolysis

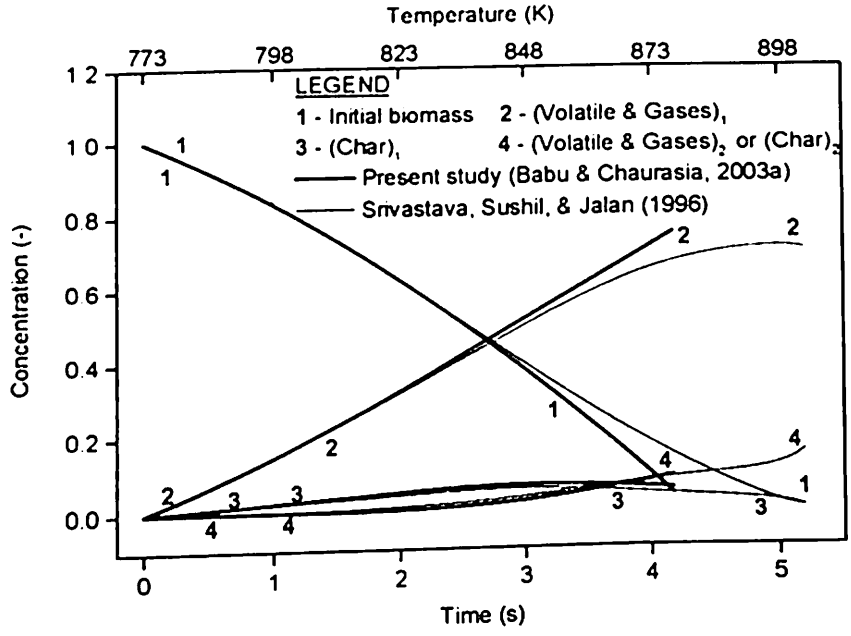

Fig. 3.7. Concentration profile as a function of time and temperature for pyrolysis under non-isothermal condition (HR=25 K/s, n_1=0, n_2=n_3=1.5).

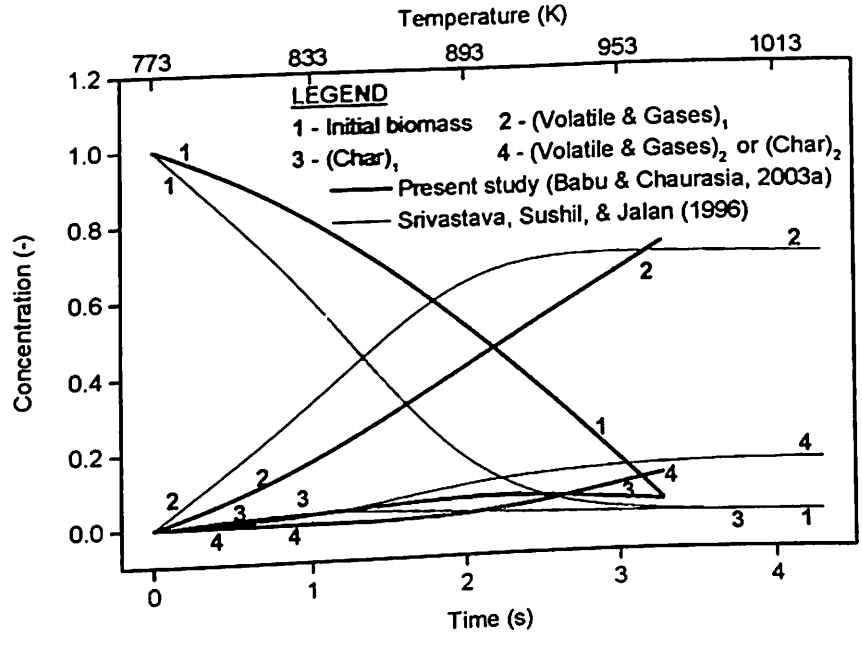

Fig. 3.8. Concentration profile as a function of time and temperature for pyrolysis under non-isothermal condition (HR=60 K/s, n_1=0, n_2=n_3=1.5).

time, final pyrolysis temperature and final concentrations of the biomass are same qualitatively. It may be noted that Srivastava, Sushil, & Jalan (1996) did not simulate

the model beyond a heating rate value of 80 K/s, while in the present study (Babu & Chaurasia, 2003a), a wide range of heating rates of 25 K/s to 360 K/s has been used for simulating the model equations, to find the optimum values as observed in the previous case. In this case also, it is found that final pyrolysis time decreases up to certain heating rate and then increases as the heating rate is increased as shown in Fig. 3.9.

Table-3.5. Comparison of the simulated results obtained for pyrolysis under non-isothermal condition in the present study (Babu & Chaurasia, 2003a) with those reported in literature (Srivastava, Sushil, & Jalan, 1996) (n_1=0; n_2=n_3=1.5)

Final	40 K/s		50 K/s		80 K/s	
	P	R	P	R	P	R
t	3.692	4.68	3.467	4.48	3.045	4.08
T	920.68	960.20	946.35	997.0	1016.60	1099.4
C_B	0.030024	0	0.030056	0	0.030202	0
C_{C_1}	0.040922	0.006	0.035923	0.004	0.024598	0.001
C_{G_1}	0.740931	0.700	0.734284	0.700	0.716064	0.700
C_{C_2}	0.094061	0.132	0.099869	0.136	0.114568	0.143
C_{G_2}	0.094061	0.132	0.099869	0.136	0.114568	0.143

P – Present study (Babu & Chaurasia, 2003a). R – Srivastava, Sushil, & Jalan (1996)

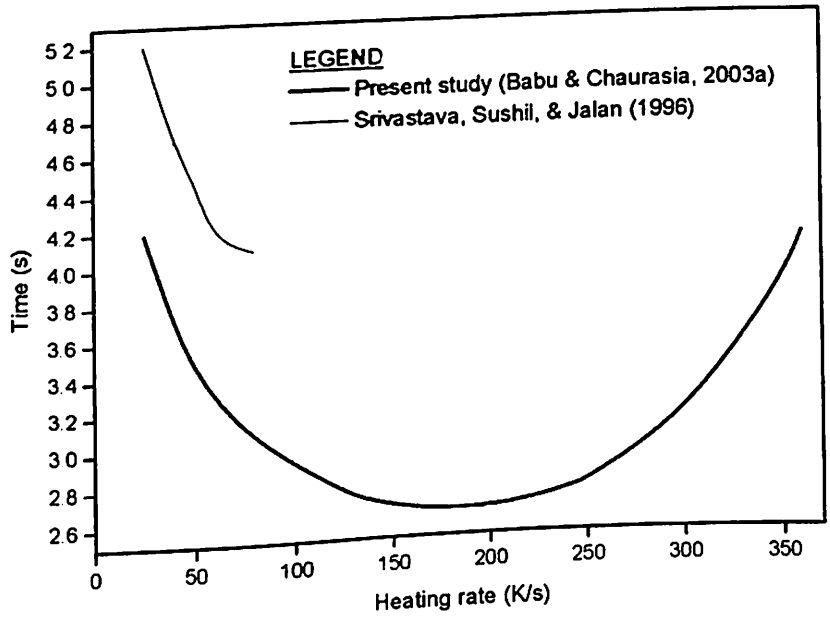

Fig. 3.9. Time as a function of heating rate for pyrolysis under non-isothermal condition (n_1=0, n_2=n_3=1.5).

The optimum values of heating rate and the final pyrolysis time for above orders of reactions are found to be 184.38 K/s and 2.636 s respectively. This interesting phenomenon can be explained using the simulated results shown in Tables-3.6 & 3.7 by

Table-3.6. Simulated results with the optimum heating rate (184.38 K/s) for pyrolysis under non-isothermal condition (n_1=0; n_2=n_3=1.5)

t	T	C_B	C_{G_1}	C_{C_1}	C_{G_2}	C_{C_2}
0.000000	773.000000	1.000000	0.000000	0.000000	0.000000	0.000000
0.100000	791.438000	0.982233	0.015291	0.002476	0.000000	0.000000
0.200000	809.876000	0.961516	0.033144	0.005340	0.000000	0.000000
0.300000	828.314000	0.937842	0.053553	0.008600	0.000003	0.000003
0.400000	846.752000	0.911274	0.076448	0.012251	0.000013	0.000013
0.500000	865.190000	0.881934	0.101695	0.016276	0.000047	0.000047
0.600000	883.628000	0.849998	0.129092	0.020630	0.000140	0.000140
0.700000	902.066000	0.815682	0.158366	0.025228	0.000362	0.000362
0.800000	920.504000	0.779232	0.189156	0.029922	0.000845	0.000845
0.900000	938.942000	0.740915	0.220999	0.034475	0.001805	0.001805
1.000000	957.380000	0.701009	0.253320	0.038542	0.003564	0.003564
1.100000	975.818000	0.659794	0.285450	0.041687	0.006534	0.006534
1.200000	994.256000	0.617544	0.316711	0.043451	0.011147	0.011147
1.300000	1012.69400	0.574526	0.346549	0.043495	0.017715	0.017715
1.400000	1031.13200	0.530987	0.374696	0.041745	0.026285	0.026285
1.500000	1049.57000	0.487163	0.401239	0.038469	0.036565	0.036565
1.600000	1068.00800	0.443264	0.426549	0.034200	0.047993	0.047993
1.700000	1086.44600	0.399485	0.451107	0.029560	0.059924	0.059924
1.800000	1104.88400	0.355995	0.475316	0.025077	0.071806	0.071806
1.900000	1123.32200	0.312946	0.499406	0.021084	0.083282	0.083282
2.000000	1141.76000	0.270467	0.523427	0.017720	0.094193	0.094193
2.100000	1160.19800	0.228671	0.547301	0.014980	0.104524	0.104524
2.200000	1178.63600	0.187649	0.570891	0.012780	0.114340	0.114340
2.300000	1197.07400	0.147479	0.594048	0.011017	0.123728	0.123728
2.400000	1215.51200	0.108223	0.616644	0.009593	0.132770	0.132770
2.500000	1233.95000	0.069929	0.638579	0.008428	0.141532	0.141532
2.600000	1252.38800	0.032634	0.659787	0.007466	0.150056	0.150056
2.636000	1259.03000	0.030045	0.662166	0.007357	0.150216	0.150216

considering the heating rates of 184.38 & 250 K/s respectively. As the heating rate is increased from 184.38 to 250 K/s, the decrease in concentration of biomass is more for 250 K/s up to certain time (2.2 s). The maximum concentration of $(char)_1$ is obtained in

1.1 s for heating rate of 250 K/s as compared to 1.3 s for 184.38 K/s. So after 1.1 s the concentration of $(char)_1$ decreases, and hence the consumption of biomass also decreases for heating rate of 250 K/s. It is also observed that after 2.2 s, the decrease in concentration of biomass is less for 250 K/s as compared to 184.38 K/s, because the $(char)_1$ left is less for 250 K/s as compared to 184.38 K/s. So the pyrolysis time to reach the desired final concentration of the biomass increases though the heating rate is more.

Table-3.7. Simulated results with the heating rate = 250 K/s for pyrolysis under non-isothermal condition (n_1=0; n_2=n_3=1.5)

t	T	C_B	C_{G_1}	C_{C_1}	C_{G_2}	C_{C_2}
0.000000	773.000000	1.000000	0.000000	0.000000	0.000000	0.000000
0.100000	798.000000	0.981188	0.016199	0.002613	0.000000	0.000000
0.200000	823.000000	0.958363	0.035876	0.005759	0.000001	0.000001
0.300000	848.000000	0.931603	0.058943	0.009444	0.000005	0.000005
0.400000	873.000000	0.901140	0.085162	0.013648	0.000025	0.000025
0.500000	898.000000	0.867328	0.114163	0.018316	0.000097	0.000097
0.600000	923.000000	0.830609	0.145446	0.023328	0.000309	0.000309
0.700000	948.000000	0.791477	0.178369	0.028459	0.000848	0.000848
0.800000	973.000000	0.750444	0.212122	0.033323	0.002056	0.002056
0.900000	998.000000	0.708017	0.245715	0.037342	0.004463	0.004463
1.000000	1023.00000	0.664678	0.278062	0.039815	0.008723	0.008723
1.100000	1048.00000	0.620869	0.308218	0.040139	0.015387	0.015387
1.200000	1073.00000	0.576985	0.335706	0.038138	0.024586	0.024586
1.300000	1098.00000	0.533368	0.360703	0.034239	0.035845	0.035845
1.400000	1123.00000	0.490310	0.383869	0.029312	0.048255	0.048255
1.500000	1148.00000	0.448051	0.405957	0.024269	0.060862	0.060862
1.600000	1173.00000	0.406783	0.427485	0.019749	0.072991	0.072991
1.700000	1198.00000	0.366658	0.448643	0.016031	0.084334	0.084334
1.800000	1223.00000	0.327788	0.469379	0.013120	0.094857	0.094857
1.900000	1248.00000	0.290252	0.489536	0.010886	0.104663	0.104663
2.000000	1273.00000	0.254102	0.508946	0.009170	0.113891	0.113891
2.100000	1298.00000	0.219366	0.527483	0.007837	0.122657	0.122657
2.200000	1323.00000	0.186053	0.545070	0.006787	0.131045	0.131045
2.300000	1348.00000	0.154154	0.561675	0.005956	0.139107	0.139107
2.400000	1373.00000	0.123650	0.577299	0.005301	0.146875	0.146875
2.500000	1398.00000	0.094511	0.591961	0.004794	0.154367	0.154367
2.600000	1423.00000	0.066698	0.605672	0.004396	0.161616	0.161616
2.759000	1462.75000	0.030076	0.624421	0.003358	0.171073	0.171073

The final concentrations of (volatile & gases)$_1$, (char)$_1$ and (volatile & gases)$_2$ or (char)$_2$ are plotted against heating rates as shown in Figs. 3.10-3.12. As the heating rate

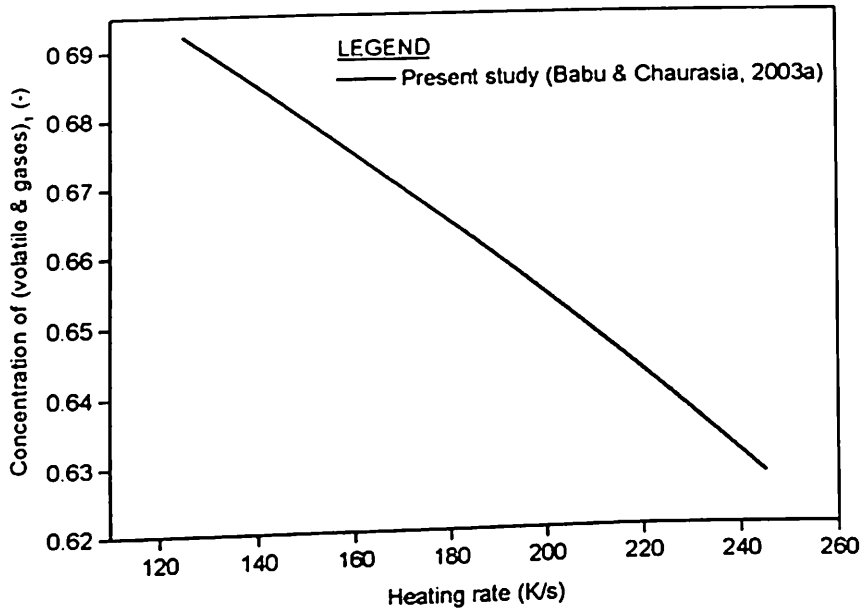

Fig. 3.10. Concentration of (volatile & gases)$_1$ as a function of heating rate for pyrolysis under non-isothermal condition (n_1=0, n_2=n_3=1.5).

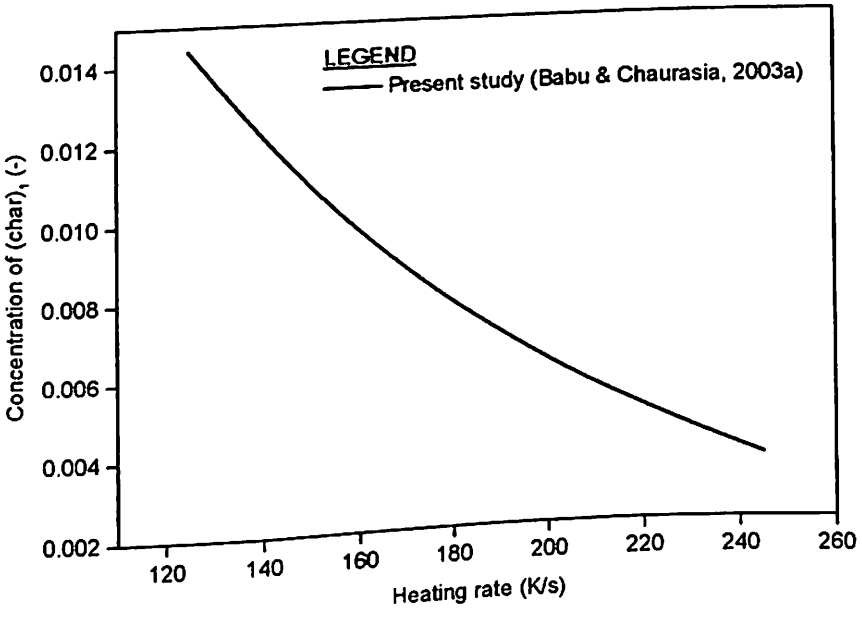

Fig. 3.11. Concentration of (char)$_1$ as a function of heating rate for pyrolysis under non-isothermal condition (n_1=0, n_2=n_3=1.5).

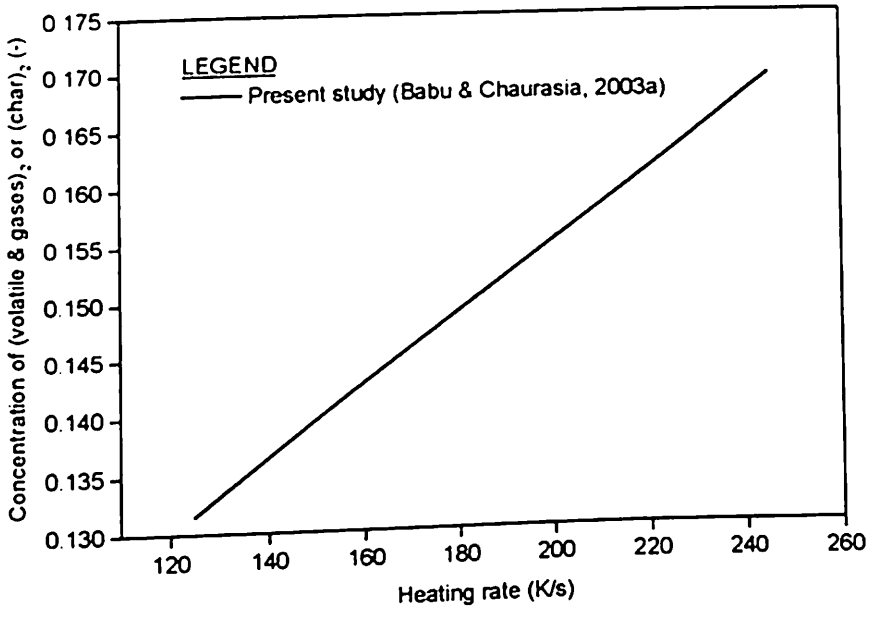

Fig. 3.12. Concentration of (volatile & gases)$_2$ or (char)$_2$ as a function of heating rate for pyrolysis under non-isothermal condition (n_1=0, n_2=n_3=1.5).

increases, the concentrations of (volatile & gases)$_2$ or (char)$_2$ increase, while the concentrations of (volatile & gases)$_1$ and (char)$_1$ decrease as explained earlier. The optimum values of the parameters for the above orders of reactions are given in Table-3.4. From Table-3.4, it is observed that the pyrolysis is much faster (optimum pyrolysis time = 2.636 s) for the case of (n_1=0; n_2=n_3=1.5), because in this case the model equations (3.1–3.3) become independent of the initial biomass concentration. However, the optimum pyrolysis time is much more (9.53 s) for the case of (n_1=1; n_2=n_3=1.5) than the earlier case, because for this case the model equations (3.1–3.3) depend on the initial biomass concentration. The optimum temperature for both the orders of reactions are found to be same i.e. 1259.03 K as it is independent of the orders of reactions.

3.6.2 Isothermal conditions

The concentration profiles for isothermal conditions with orders of reactions of n_1 =1

and $n_2 = n_3 = 1.5$ for the isothermal temperatures of 873 K and 1023 K are shown in Figs 3.13 and 3.14. The obtained trends are same as reported by Srivastava, Sushil, &

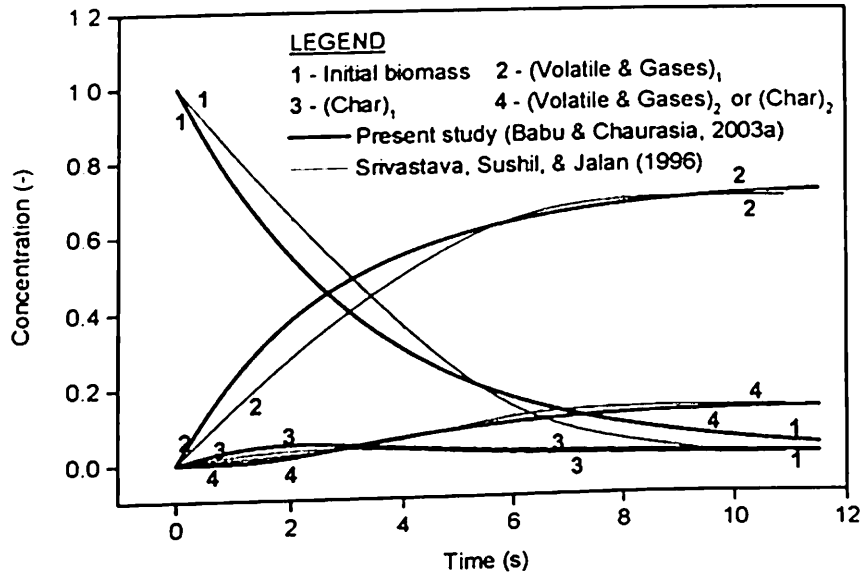

Fig. 3.13. Concentration profile as a function of time for pyrolysis under isothermal condition (T=873, n_1=1, n_2=n_3=1.5).

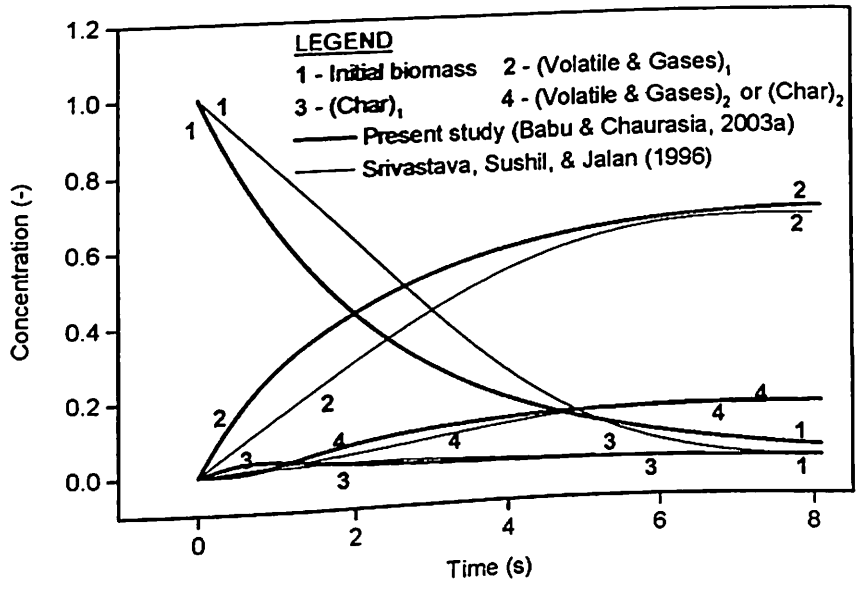

Fig. 3.14. Concentration profile as a function of time pyrolysis under isothermal condition (T=1023 K, n_1=1, n_2=n_3=1.5).

Jalan (1996). The results obtained for 773 K, 973 K and 1073 K are compared with those reported (Srivastava, Sushil, & Jalan, 1996) as shown in Table-3.8. The trend in the final pyrolysis time is same as that reported by Srivastava, Sushil, & Jalan (1996). But when the model is simulated for a wide range of temperatures ranging from 773 K to 1773 K, it is found that the optimum value of final pyrolysis time is 7.987 s at a temperature of 1066 K as shown in Fig. 3.15. This can be explained as above by means of data shown in Tables 3.9 and 3.10 for temperatures of 1066 K and 1373 K. The trends in Figs. 3.16, 3.17 and 3.18 are same as obtained for non-isothermal conditions and can be explained with similar logic using the kinetics. The optimum values for the above orders of reactions are given in Table-3.11. It may be noted that Srivastava, Sushil, & Jalan (1996) simulated results only in a small temperature range between 773 K to 1073 K with a step size of 100 K from 773 K to 973 K and subsequently a step size of 50 K from 973 K to 1073 K, because of which they missed out this decreasing and

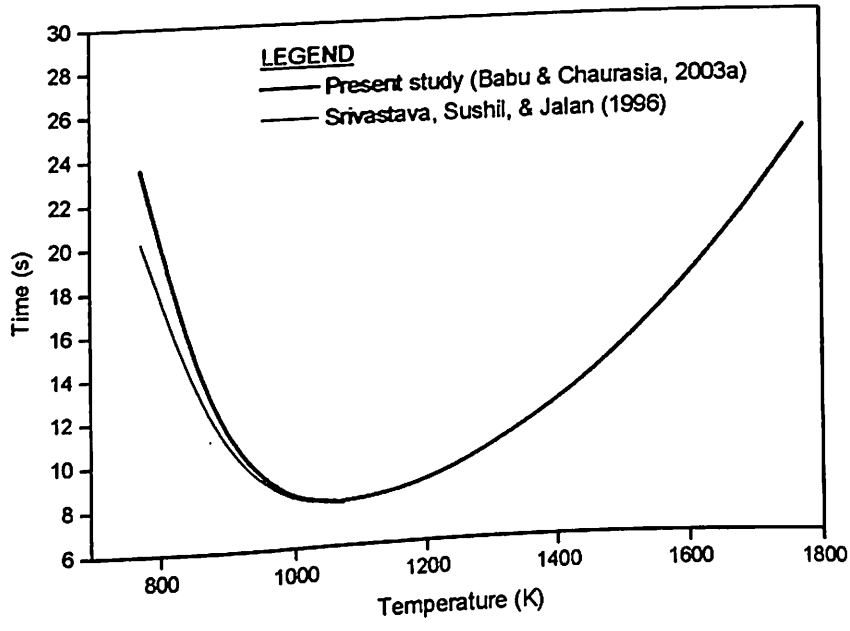

Fig. 3.15. Time as a function of temperature for pyrolysis under isothermal condition (n_1=1, n_2=n_3=1.5).

Table-3.8. Comparison of the simulated results obtained for Pyrolysis under isothermal condition in the present study (Babu & Chaurasia, 2003a) with those reported in literature (Srivastava, Sushil, & Jalan, 1996) (n_1=1; n_2=n_3=1.5)

Final	773 K		973 K		1073 K	
	P	R	P	R	P	R
t	23.54	20.22	8.545	8.38	7.99	7.88
C_B	0.030003	0	0.030008	0	0.030006	0
C_{C_1}	0.013130	0.012	0.003234	0.001	0.001832	0
C_{G_1}	0.709398	0.690	0.686146	0.658	0.653198	0.625
C_{C_2}	0.123735	0.122	0.140306	0.140	0.157257	0.158
C_{G_2}	0.123735	0.122	0.140306	0.140	0.157257	0.158

P – Present study (Babu & Chaurasia, 2003a). R – Srivastava, Sushil, & Jalan (1996)

Table-3.9. Simulated results with the optimum temperature (1066 K) for pyrolysis under isothermal condition (n_1=1; n_2=n_3=1.5)

t	T	C_B	C_{G_1}	C_{C_1}	C_{G_2}	C_{C_2}
0.000000	1066.000000	1.000000	0.000000	0.000000	0.000000	0.000000
0.100000	1066.000000	0.957050	0.035955	0.006983	0.000006	0.000006
0.200000	1066.000000	0.915944	0.070285	0.013585	0.000093	0.000093
0.300000	1066.000000	0.876604	0.102875	0.019639	0.000441	0.000441
0.400000	1066.000000	0.838954	0.133553	0.024920	0.001287	0.001287
0.500000	1066.000000	0.802920	0.162151	0.029212	0.002858	0.002858
0.600000	1066.000000	0.768435	0.188572	0.032370	0.005311	0.005311
0.800000	1066.000000	0.703843	0.235038	0.035267	0.012926	0.012926
0.900000	1066.000000	0.673613	0.255410	0.035247	0.017865	0.017865
1.000000	1066.000000	0.644681	0.274188	0.034508	0.023311	0.023311
2.000000	1066.000000	0.415614	0.413014	0.018818	0.076277	0.076277
3.000000	1066.000000	0.267938	0.504527	0.010717	0.108409	0.108409
4.000000	1066.000000	0.172735	0.564983	0.006953	0.127664	0.127664
5.000000	1066.000000	0.111359	0.604252	0.004820	0.139784	0.139784
6.000000	1066.000000	0.071791	0.629585	0.003463	0.147580	0.147580
7.000000	1066.000000	0.046282	0.645871	0.002543	0.152652	0.152652
7.100000	1066.000000	0.044294	0.647137	0.002467	0.153051	0.153051
7.200000	1066.000000	0.042392	0.648347	0.002395	0.153433	0.153433
7.400000	1066.000000	0.038829	0.650613	0.002256	0.154151	0.154151
7.500000	1066.000000	0.037161	0.651672	0.002191	0.154488	0.154488
7.600000	1066.000000	0.035565	0.652685	0.002127	0.154811	0.154811
7.700000	1066.000000	0.034037	0.653654	0.002066	0.155121	0.155121
7.800000	1066.000000	0.032575	0.654581	0.002006	0.155419	0.155419
7.900000	1066.000000	0.031176	0.655467	0.001949	0.155704	0.155704
7.987000	1066.000000	0.030008	0.656206	0.001900	0.155943	0.155943

Table-3.10. Simulated results with the temperature = 1373 K for pyrolysis under isothermal condition (n_1=1; n_2=n_3=1.5)

t	T	C_B	C_{G_1}	C_{C_1}	C_{G_2}	C_{C_2}
0.000000	1373.000000	1.000000	0.000000	0.000000	0.000000	0.000000
0.100000	1373.000000	0.969956	0.023014	0.006981	0.000024	0.000024
0.200000	1373.000000	0.940816	0.045019	0.013434	0.000366	0.000366
0.300000	1373.000000	0.912550	0.065386	0.018717	0.001674	0.001674
0.400000	1373.000000	0.885134	0.083523	0.022223	0.004560	0.004560
0.500000	1373.000000	0.858541	0.099283	0.023792	0.009192	0.009192
0.600000	1373.000000	0.832748	0.113015	0.023759	0.015239	0.015239
0.700000	1373.000000	0.807729	0.125291	0.022684	0.022148	0.022148
0.800000	1373.000000	0.783462	0.136641	0.021083	0.029407	0.029407
0.900000	1373.000000	0.759924	0.147434	0.019315	0.036663	0.036663
1.000000	1373.000000	0.737093	0.157891	0.017587	0.043714	0.043714
2.000000	1373.000000	0.543307	0.251811	0.008091	0.098396	0.098396
3.000000	1373.000000	0.400468	0.324907	0.004959	0.134833	0.134833
4.000000	1373.000000	0.295182	0.379561	0.003425	0.160916	0.160916
5.000000	1373.000000	0.217577	0.420064	0.002513	0.179923	0.179923
6.000000	1373.000000	0.160374	0.449988	0.001911	0.193863	0.193863
7.000000	1373.000000	0.118211	0.472064	0.001485	0.204120	0.204120
8.000000	1373.000000	0.087133	0.488336	0.001172	0.211680	0.211680
9.000000	1373.000000	0.064225	0.500324	0.000935	0.217258	0.217258
10.00000	1373.000000	0.047340	0.509151	0.000751	0.221379	0.221379
11.00000	1373.000000	0.034894	0.515648	0.000606	0.224426	0.224426
11.49500	1373.000000	0.030003	0.518198	0.000546	0.225626	0.225626

Table-3.11. Optimum Parametric values for different orders of reactions for pyrolysis under isothermal condition

Optimum Parameters	n_1=1; n_2=n_3=1.5	n_1=0; n_2=n_3=1.5
Final pyrolysis time (s)	7.987	2.209
Final pyrolysis temperature (K)	1066	1066
Final concentration of initial biomass (-)	0.030008	0.030250
Final concentration of $(char)_1$ (-)	0.001900	0.017863
Final concentration of $(volatile\ \&\ gases)_1$ (-)	0.656206	0.672005
Final concentration of $(char)_2$ (-)	0.155943	0.139941
Final concentration of $(volatile\ \&\ gases)_2$ (-)	0.155943	0.139941

increasing trend.

Similarly, the concentration profiles for the orders of reactions of $n_1 = 0$ and $n_2 = n_3 = 1.5$ are shown in Figs. 3.19 and 3.20 for isothermal temperatures of 873 K

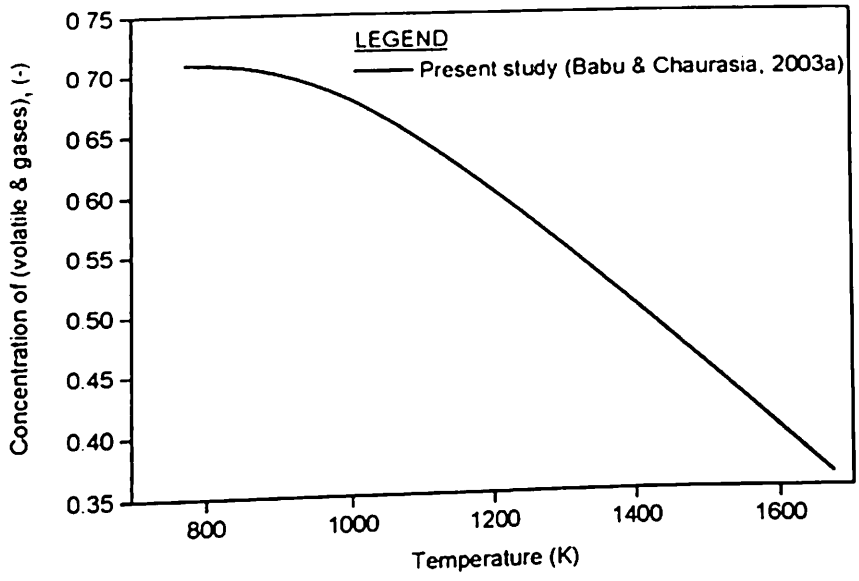

Fig. 3.16. Concentration of (volatile & gases) as a function of temperature for pyrolysis under isothermal condition (n_1=1, n_2=n_3=1.5).

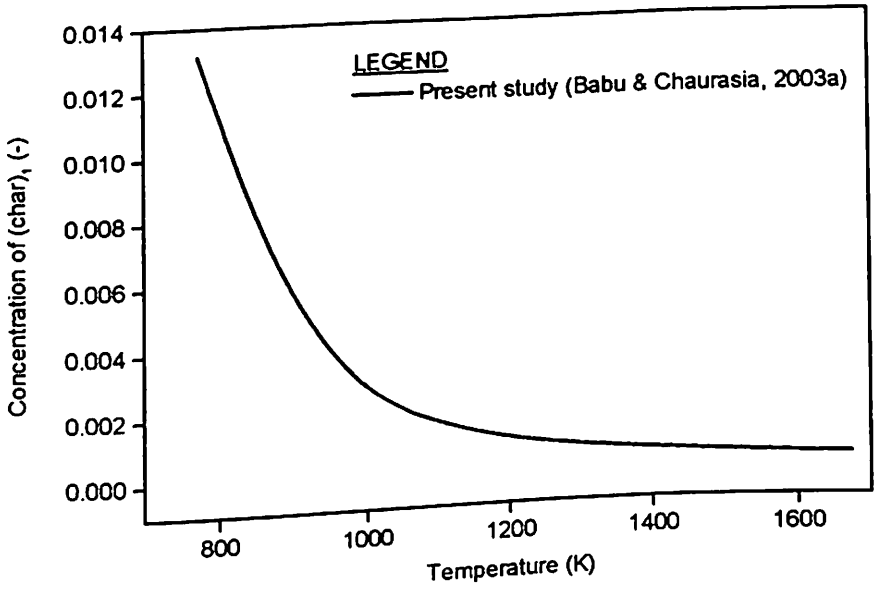

Fig. 3.17. Concentration of (char)$_1$ as a function of temperature for pyrolysis under isothermal condition (n_1=1, n_2=n_3=1.5).

and 1023 K. The results obtained for 773 K, 973 K and 1073 K are compared with those reported in literature (Srivastava, Sushil, & Jalan, 1996) as given in Table-3.12. The

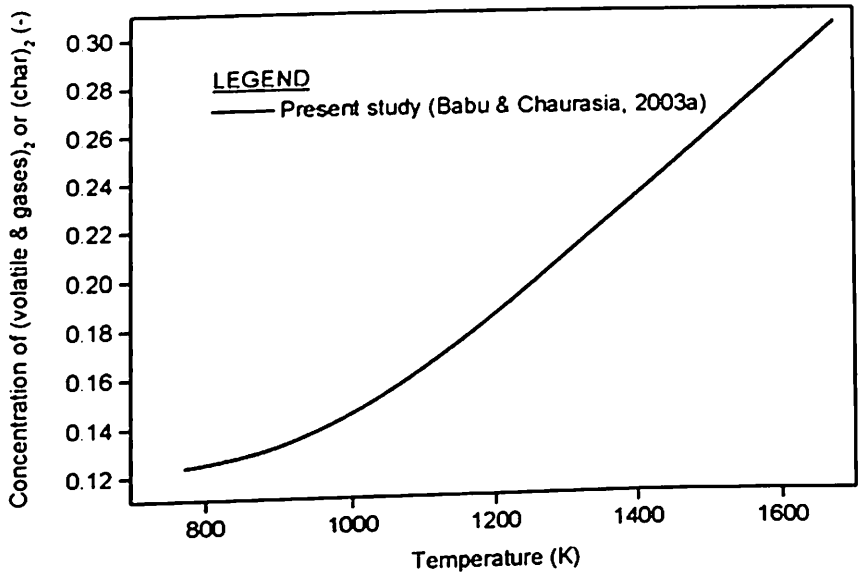

Fig. 3.18. Concentration of (volatile & gases)$_2$ or (char)$_2$ as a function of temperature for pyrolysis under isothermal condition (n_1=1, n_2=n_3=1.5).

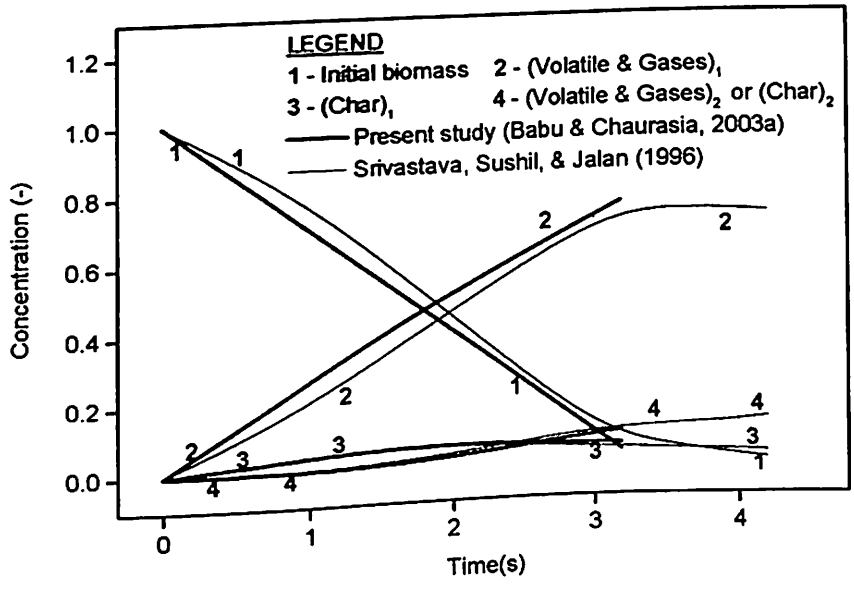

Fig. 3.19. Concentration profile as a function of time for pyrolysis under isothermal condition (T=873 K, n_1=0, n_2=n_3=1.5).

trends are same as reported by Srivastava, Sushil, & Jalan (1996). As shown in Fig. 3.21, the optimum value of final pyrolysis time for the above orders of reactions is found

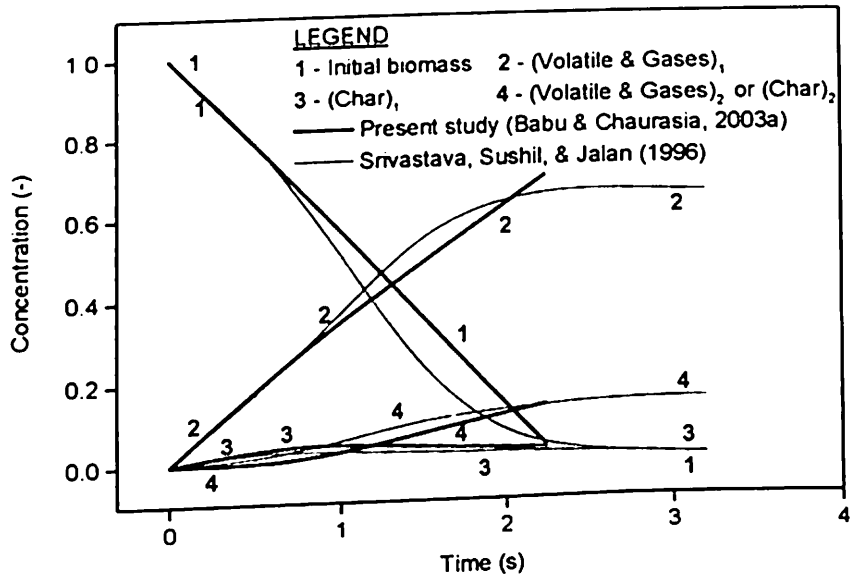

Fig. 3.20. Concentration profile as a function of time for pyrolysis under isothermal condition (T=1023 K, n_1=0, n_2=n_3=1.5).

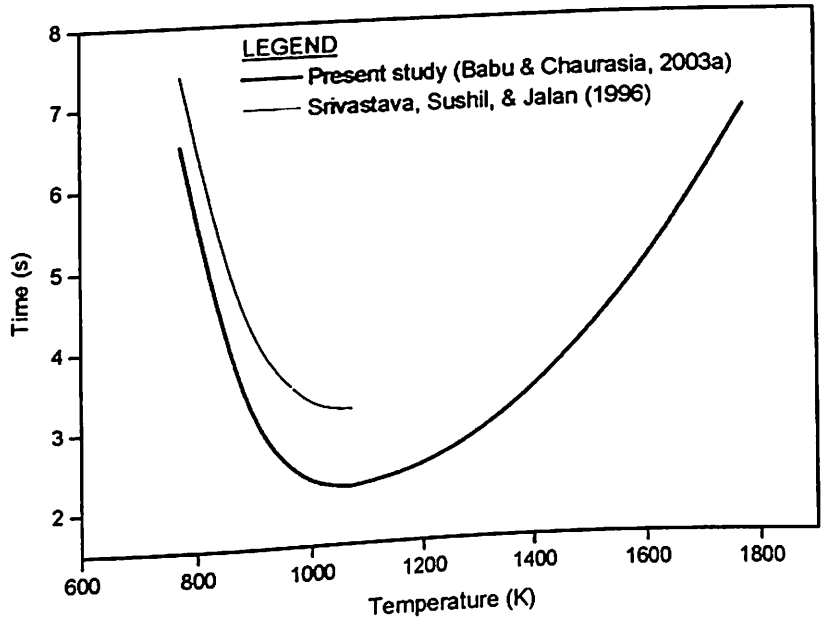

Fig. 3.21. Time as a function of temperature for pyrolysis under isothermal condition (n_1=0, n_2=n_3=1.5).

to be 2.209 s at a temperature of 1066 K. The data given in Tables 3.13 and 3.14 for

Table-3.12. Comparison of the simulated results obtained for Pyrolysis under isothermal condition in the present study (Babu & Chaurasia, 2003a) with those reported in Srivastava, Sushil, & Jalan, 1996) (n_1=0; n_2=n_3=1.5)

Final	773 K		973 K		1073 K	
	P	R	P	R	P	R
t	6.511	7.38	2.363	3.38	2.21	3.18
C_B	0.030139	0	0.030387	0	0.030159	0
C_{C_1}	0.072930	0.417	0.028736	0.003	0.017271	0.002
C_{G_1}	0.769100	0.725	0.711381	0.693	0.668985	0.658
C_{C_2}	0.063916	0.095	0.114748	0.152	0.141793	0.151
C_{G_2}	0.063916	0.095	0.114748	0.152	0.141793	0.151

P – Present study (Babu & Chaurasia, 2003a); R – Srivastava, Sushil, & Jalan (1996)

Table-3.13. Simulated results with the optimum temperature (1066 K) for pyrolysis under isothermal condition (n_1=0; n_2=n_3=1.5)

t	T	C_B	C_{G_1}	C_{C_1}	C_{G_2}	C_{C_2}
0.000000	1066.000000	1.000000	0.000000	0.000000	0.000000	0.000000
0.100000	1066.000000	0.956100	0.036750	0.007137	0.000007	0.000007
0.200000	1066.000000	0.912200	0.073409	0.014184	0.000103	0.000103
0.300000	1066.000000	0.868300	0.109755	0.020917	0.000514	0.000514
0.400000	1066.000000	0.824400	0.145453	0.027002	0.001573	0.001573
0.500000	1066.000000	0.780500	0.180137	0.032074	0.003644	0.003644
0.600000	1066.000000	0.736600	0.213514	0.035838	0.007024	0.007024
0.700000	1066.000000	0.692700	0.245444	0.038156	0.011850	0.011850
0.800000	1066.000000	0.648800	0.275982	0.039081	0.018068	0.018068
0.900000	1066.000000	0.604901	0.305337	0.038823	0.025470	0.025470
1.000000	1066.000000	0.561001	0.333803	0.037676	0.033760	0.033760
1.100000	1066.000000	0.517101	0.361686	0.035947	0.042634	0.042634
1.200000	1066.000000	0.473201	0.389251	0.033900	0.051824	0.051824
1.300000	1066.000000	0.429301	0.416705	0.031740	0.061127	0.061127
1.400000	1066.000000	0.385401	0.444185	0.029609	0.070402	0.070402
1.500000	1066.000000	0.341501	0.471780	0.027591	0.079564	0.079564
1.600000	1066.000000	0.297601	0.499533	0.025731	0.088567	0.088567
1.700000	1066.000000	0.253701	0.527461	0.024047	0.097395	0.097395
1.800000	1066.000000	0.209801	0.555563	0.022535	0.106050	0.106050
1.900000	1066.000000	0.165901	0.583826	0.021186	0.114543	0.114543
2.000000	1066.000000	0.122001	0.612235	0.019983	0.122890	0.122890
2.100000	1066.000000	0.078101	0.640773	0.018908	0.131109	0.131109
2.200000	1066.000000	0.034201	0.669423	0.017945	0.139215	0.139215
2.209000	1066.000000	0.030250	0.672005	0.017863	0.139941	0.139941

Table-3.14. Simulated results with the temperature = 1373 K for pyrolysis under isothermal condition (n_1=0; n_2=n_3=1.5)

t	T	C_B	C_{G_1}	C_{C_1}	C_{G_2}	C_{C_2}
0.000000	1373.000000	1.000000	0.000000	0.000000	0.000000	0.000000
0.100000	1373.000000	0.969496	0.023366	0.007087	0.000025	0.000025
0.200000	1373.000000	0.938992	0.046390	0.013832	0.000393	0.000393
0.300000	1373.000000	0.908488	0.068320	0.019483	0.001855	0.001855
0.400000	1373.000000	0.877984	0.088383	0.023268	0.005183	0.005183
0.500000	1373.000000	0.847480	0.106316	0.024921	0.010642	0.010642
0.600000	1373.000000	0.816976	0.122473	0.024800	0.017876	0.017876
0.700000	1373.000000	0.786472	0.137506	0.023553	0.026235	0.026235
0.800000	1373.000000	0.755968	0.152011	0.021780	0.035120	0.035120
0.900000	1373.000000	0.725463	0.166393	0.019883	0.044130	0.044130
1.000000	1373.000000	0.694959	0.180869	0.018080	0.053046	0.053046
1.100000	1373.000000	0.664455	0.195532	0.016464	0.061774	0.061774
1.200000	1373.000000	0.633951	0.210403	0.015057	0.070294	0.070294
1.300000	1373.000000	0.603447	0.225471	0.013845	0.078618	0.078618
1.400000	1373.000000	0.572943	0.240708	0.012804	0.086772	0.086772
1.500000	1373.000000	0.542439	0.256089	0.011906	0.094783	0.094783
1.600000	1373.000000	0.511935	0.271588	0.011125	0.102676	0.102676
1.700000	1373.000000	0.481431	0.287183	0.010442	0.110472	0.110472
1.800000	1373.000000	0.450927	0.302859	0.009839	0.118187	0.118187
1.900000	1373.000000	0.420423	0.318602	0.009303	0.125836	0.125836
2.000000	1373.000000	0.389919	0.334402	0.008824	0.133428	0.133428
2.100000	1373.000000	0.359415	0.350249	0.008392	0.140972	0.140972
2.200000	1373.000000	0.328911	0.366136	0.008001	0.148476	0.148476
2.300000	1373.000000	0.298407	0.382059	0.007645	0.155945	0.155945
2.400000	1373.000000	0.267903	0.398013	0.007320	0.163382	0.163382
2.500000	1373.000000	0.237399	0.413994	0.007021	0.170793	0.170793
2.600000	1373.000000	0.206894	0.429998	0.006746	0.178181	0.178181
2.700000	1373.000000	0.176390	0.446023	0.006492	0.185547	0.185547
2.800000	1373.000000	0.145886	0.462066	0.006257	0.192895	0.192895
2.900000	1373.000000	0.115382	0.478127	0.006038	0.200226	0.200226
3.000000	1373.000000	0.084878	0.494202	0.005835	0.207543	0.207543
3.100000	1373.000000	0.054374	0.510290	0.005644	0.214846	0.214846
3.179000	1373.000000	0.030276	0.523007	0.005501	0.220608	0.220608

temperatures of 1066 K and 1373 K respectively can be used to explain the above trend in similar lines as that of non-isothermal case. The optimum values of the parameters are given in Table-3.11. The optimum temperature for both the orders of reactions are found to be same i.e. 1066 K as in the previous case, because it is independent of orders

of reactions. Figures 3.22, 3.23 and 3.24 show the concentration profiles for (volatile & gases)$_1$, (char)$_1$ and (volatile & gases)$_2$ or (char)$_2$. The trends are same as discussed earlier. It may be noted that in the present study (Babu & Chaurasia, 2003a), a wide range of temperatures are used for simulating the model equations ranging from 773 K to 1773 K with a maximum step size of 100 K initially to a very small step size of 0.1 K to ensure not to miss out the optimum parametric values. However, Srivastava, Sushil, & Jalan (1996) simulated results only in a small temperature range between 773 K to 1073 K with a step size of 100 K from 773 K to 973 K and subsequently a step size of 50 K from 973 K to 1073 K, because of which they missed out this decreasing and increasing trend which is observed in the present study (Babu & Chaurasia, 2003a).

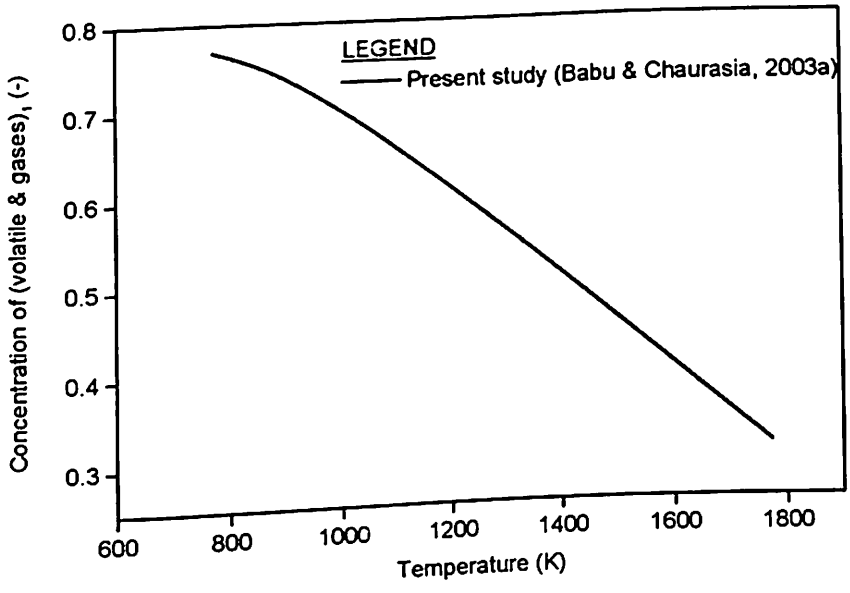

Fig. 3.22. Concentration of (volatile & gases)$_1$ as a function of temperature for pyrolysis under isothermal condition (n_1=0, n_2=n_3=1.5).

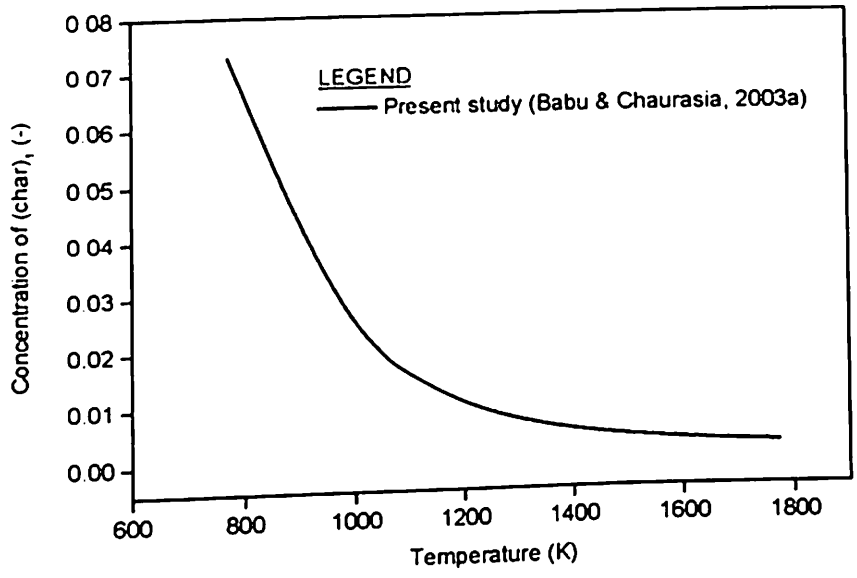

Fig. 3.23. Concentration of $(char)_1$ as a function of temperature for pyrolysis under isothermal condition (n_1=0, n_2=n_3=1.5).

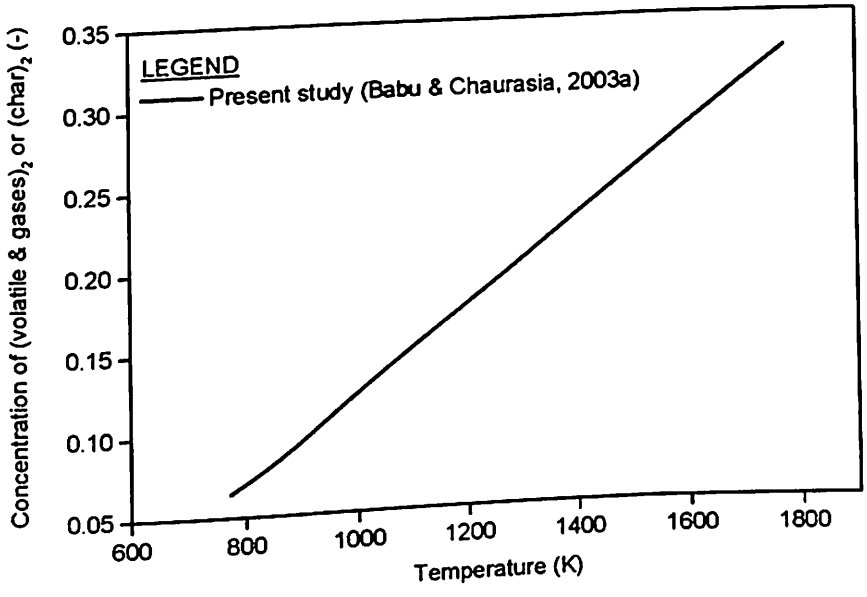

Fig. 3.24. Concentration of $(volatile\ \&\ gases)_2$ or $(char)_2$ as a function of temperature for pyrolysis under isothermal condition (n_1=0, n_2=n_3=1.5).

3.7. Conclusions

- Based on the importance and promising nature of the pyrolysis of biomass process, the modeling and simulation has been carried out for finding out the optimum parameters of the pyrolysis process.
- The qualitative trends obtained for concentrations of initial biomass, (volatile & gases)$_1$, (char)$_1$ and (volatile & gases)$_2$ or (char)$_2$ are found to be same as those reported by earlier investigators. The small quantitative differences are attributed to the numerical methods used and the assumptions made.
- A wide range of heating rate and temperature are used to simulate the model equations with small step sizes for both the isothermal and non-isothermal Pyrolysis process conditions with different orders of reactions.
- Some interesting trends have been obtained, especially with respect to effect of net heating rate and temperature on the final pyrolysis time. The reported literature results indicate a decrease in final pyrolysis time as the net heating rate or temperature is increased. The range of operating conditions used for simulating the model equations is small in the case of earlier investigators' work. But the results obtained using a wide range of operating conditions in the present study (Babu & Chaurasia, 2003a) show that the final pyrolysis time initially decreases and then increases as the net heating rate or temperature is increased, giving an optimum final pyrolysis time corresponding to net heat rate or temperature.
- The above interesting trends are observed for both isothermal and non-isothermal conditions and also with different orders of reactions.

- These interesting trends that are not reported earlier could be well explained from the kinetics by systematically generating huge data upon simulating the model equations.
- For non-isothermal conditions with the orders of reactions of n_1=1; n_2=n_3=1.5 and n_1=0; n_2=n_3=1.5, the optimum value of final pyrolysis time is found to be 9.53 s and 2.636 s respectively, while the optimum value of heating rate is found to be 51 K/s and 184.38 K/s respectively. The optimum value of temperature is same (1259.03 K) for both the orders of reactions.
- For isothermal conditions with the orders of reactions of n_1=1; n_2=n_3=1.5 and n_1=0; n_2=n_3=1.5, the optimum value of final pyrolysis time is found to be 7.987 s & 2.209 s respectively. The optimum value of temperature is same (1066 K) for the both the orders of reactions.
- The work carried out in the present study (Babu & Chaurasia, 2003a) is important and useful for optimal design of the biomass gasifiers, reactors, etc.
- Further work could be extended to determine the optimum parameters for single biomass particles of different shapes by incorporating the heat and mass transfer effects.

CHAPTER 4

MODELING FOR PYROLYSIS OF SOLID PARTICLE: KINETICS AND HEAT TRANSFER EFFECTS

4.1. Introduction

During the last decade, various factors have promoted renewal of interest in the thermochemical processing of solids such as urban wastes, coal and biomass, as potential sources of energy and the chemical feedstocks. In order to develop a pyrolysis process and properly design the necessary equipment for its realization, it is important to provide the models describing the kinetics and the governing mechanisms. This task takes increasing importance as the pyrolysis is studied not only as an independent process, but also as a first step in gasification or combustion processes as well.

The phenomena governing the pyrolysis of a single solid particle of biomass are both chemical and physical. Depending on the operation conditions, the process may be controlled either by the chemical or the physical phenomena or by both. As a consequence, the modeling on the behavior of a single solid particle of biomass under

pyrolysis conditions requires the development of the models describing both the chemical and physical mechanisms and their interactions.

4.2. Background

The pyrolysis process has a great future in the world (Srivastava & Jalan, 1994). Although a large number of studies following the above mentioned approaches exist, there is a lack of models suitable for application to conventional pyrolysis conditions. Fan, Fan, Miyanami, Chen, & Walawender (1977) developed a model for pyrolysis process, which includes the aspects of heat and mass transfer in the particle. The reaction is considered to be of first order with respect to initial particle concentration. Also product concentrations cannot be analyzed from the above model as the secondary reactions are not considered. Miyanami, Fan, Fan, & Walawender (1977) incorporated the effect of heat of reaction in the above model. The various modeling reported appearing in the literature present different versions or enrichment of the model suggested by Bamford, Crank, & Malan (1946). According to this model, the equation for heat conduction in a pyrolyzing solid is combined with those for heat generation, assuming first order kinetics. However, the heat transfer equation does not consider the effect of change of density as a function of time. This model is used by several researchers (Roberts & Clough, 1963; Tinney, 1965; Weatherford & Sheppard, 1965; Matsumoto, Fujiwara, & Kondo, 1969) and is modified by Kung (1972) in order to incorporate the effects of internal convection and variable transport properties. However, no specific kinetic mechanism is suggested to predict the concentration of the various components produced during pyrolysis. Kansa, Perlee, & Chaiken (1977)

included the momentum equation for the motion of pyrolysis gases within the solid. A suitable kinetic mechanism has not been utilized and the solution to the heat and momentum balance equation is based on arbitrary boundary conditions.

Studies have been carried out on pyrolysis of biomass and other substances by several researchers (Anthony & Howard, 1976; Shafizadeh, 1982; Koufopanos, Ramana Rao, Plehiers, & Froment, 1988; Koufopanos, Maschio, & Lucchesi, 1989; Do, & Bell, 1991; Yang, Tanguy, & Roy, 1995; Srivastava, Sushil, & Jalan, 1996; Di Blasi, 1998; Donskoi, & McElwain, 1999; Jai, Galea, & Patel, 1999; Klose & Wiest, 1999; Ruggiero & Manfrida, 1999; Violi, Anna, & Alessio, 1999; Larfeldt, Leckner, & Melaaen, 2000; Li, Kennedy, & Dlugogorski, 2000; Mousquès, Dirion, & Grouset, 2001; Boutin, Ferrer, & Lédé, 2002; Bryden, Ragland, & Rutland, 2002; Demirbaş, 2002b; Mastral, Esperanza, Garcia, & Juste, 2002), but many of them have not included the secondary reactions in pyrolysis kinetics. Kansa, Perlee, & Chaiken (1977) pointed out that secondary reactions are essential to match fully the experimental observations.

In the earlier work as given in chapter 3 (Babu & Chaurasia, 2003a), a linear relationship between the temperature and time has been utilized. In the present work (Babu & Chaurasia, 2002a, 2002b, 2003b; Chaurasia, Babu, Kaur, & Thiruchitrambalam, 2003), temperature profile is predicted by the proposed heat transfer equation utilizing the boundary conditions developed by Pyle & Zaror (1984) and Koufopanos, Papayannakos, Maschio, & Lucchesi (1991). Pyle & Zaror (1984) used the model of Bamford, Crank, & Malan (1946) and dimensionless groups to define the relative importance of internal and external heat transfer and of the intrinsic pyrolysis kinetics. The temperature profiles obtained in the proposed model are compared with (1)

those predicted by Pyle & Zaror (1984) in which they utilized model of Bamford, Crank, & Malan (1946), (2) their experimental data, and (3) the temperature profile predicted by Jalan & Srivastava (1999), for different operating conditions.

Pyle & Zaror (1984) utilized kinetic model assuming first order kinetics, based on the density of initial biomass. The concentration and the final yield of gaseous and volatile products are not predicted by the kinetic model of Koufopanos, Papayannakos, Maschio, & Lucchesi (1991). The effect of change in density as a function of time of the single biomass particle is not considered by Koufopanos, Papayannakos, Maschio, & Lucchesi (1991) and Pyle & Zaror (1984) while solving heat transfer equation. Jalan & Srivastava (1999) have solved the heat transfer equation by neglecting the effect of specific heat and thermal conductivity of char, which are the functions of temperature as reported by Koufopanos, Papayannakos, Maschio, & Lucchesi (1991). The convective heat transfer coefficient is a function of Reynolds number and Prandtl number and is given by $h = 0.322(k_g/l)\mathrm{Pr}^{1/3}\,\mathrm{Re}^{0.5}$ W/m^2 K, as reported by Koufopanos, Papayannakos, Maschio, & Lucchesi (1991), but Jalan & Srivastava (1999) have considered a constant value of $h = 0.322$ W/m^2 K, neglecting the effect of the other parameters. In the present study (Babu & Chaurasia, 2003b), the above anomaly has been rectified. The earlier investigators (Pyle & Zaror, 1984; Koufopanos, Papayannakos, Maschio, & Lucchesi, 1991; Jalan & Srivastava, 1999) considered the temperature range of 300-900 K and pellet diameters 0.002-0.022 m only. In the present study (Babu & Chaurasia, 2003b) a wide range of temperature (303-2700 K) and pellet diameters (0.0005-0.026 m) are considered.

Keeping the above drawbacks of the existing models in view, the kinetic model as

given chapter 3 (Babu & Chaurasia, 2003a) is proposed in the modeling of pyrolysis of a single biomass particle. The model being developed considered the effect of specific heat and the thermal conductivity of char as a function of temperature. Pyle & Zaror (1984) considered the mean value of convective heat transfer coefficient (h) as a function of Reynolds and Prandtl numbers taken from the experimental data reported by them is used throughout in the present study. The model would enable the prediction of yields of both char and gaseous & volatile products. This model also enables the study on the effect of different geometries (slab, cylinder, and sphere) on various parameters of interest.

4.3. Motivation

The pyrolysis rate, in most of the above studies, is represented by the first order kinetics, which is not adequate to describe the pyrolysis rate over a wide range of temperature. Besides, most of the above studies do not consider the role of the secondary reactions between gaseous and carbonaceous products inside the biomass particles during pyrolysis. The wide range of temperature and pellet diameter is not considered in the earlier studies. In order to establish better reactor design techniques, it is necessary to develop the model for the pyrolysis of a single biomass particle. The objectives include the understanding of the interactions between heat transfer and pyrolysis kinetics and the quantitative determination of the pyrolysis reaction's thermal effects. The model being developed would enable the prediction of the yields of both char and gaseous & volatile products. The effect of particle size, constant wall temperature and the boundary condition has been analyzed. The effect of particle size on

the temperature profile, the variation of temperature with radial distance and time during the pyrolysis process for a wide range of temperatures is presented. The above analysis would throw more insight into the complex process of pyrolysis.

4.4. Theory

Most biomass materials are chemically and physically heterogeneous and their components have different reactivities and yield different products. The overall process of pyrolysis can be classified into primary and secondary stages. When a solid particle of biomass is heated in an inert atmosphere, the following phenomena occur. Heat is first transferred to the particle surface by radiation and/or convection and then to the inside of the particle. The temperature inside the particle increases causing, (1) the removal of moisture that is present in the biomass particle and (2) the pre-pyrolysis and main pyrolysis reaction to take place as discussed in chapter 3 (Babu & Chaurasia, 2003a). The heat changes due to the chemical reactions and phase changes contribute to non-linear variations in temperature as a function of time. Volatiles and gaseous products flow through the pores of particle and participate in the heat transfer process. The pyrolysis reactions proceed with a rate depending upon the local temperature.

During the pyrolysis process the pores of the solid are enlarged, and the solid particle merely becomes more porous because biomass converts into gases as discussed by Curtis & Miller (1988). According to Anthony & Howard (1976), the enlarged pores of the pyrolyzing solid offer many reaction sites to the volatile and gaseous products of pyrolysis and favor their interaction with the hot solid.

Inside the pyrolyzing particle, heat is transmitted by the following mechanisms: (a) conduction inside the solid particle, (b) convection inside the particle pore, (c) convection and radiation from the surface of the pellet. For simplicity, it is assumed that heat is transmitted inside the solid by conduction only. The heat transfer coefficient represents the overall effect of the above mechanisms.

4.5. Modeling

The pyrolysis reactions can be described by means of the following scheme as given in chapter 3 (section 3.4) proposed by Babu & Chaurasia (2003a). Adding equations (3.1), (3.3) and (3.5) gives,

$$\frac{\partial \overline{C}_B}{\partial t} + \frac{\partial \overline{C}_{C_1}}{\partial t} + \frac{\partial \overline{C}_{C_2}}{\partial t} = -k_1 \overline{C}_B{}^{n_1} \tag{4.1}$$

which is same as,

$$\frac{\partial C_B}{\partial t} + \frac{\partial C_{C_1}}{\partial t} + \frac{\partial C_{C_2}}{\partial t} = -k_1 C_B{}^{n_1} \text{ as } \overline{C}_B = C_B/C_{B0}, \overline{C}_{G1} = C_{G1}/C_{B0}, \overline{C}_{C1} = C_{C1}/C_{B0}$$

which is equal to $\partial\rho/\partial t$. Hence,

$$\frac{\partial \rho}{\partial t} = -k_1 C_B{}^{n_1} \tag{4.2}$$

Consider a cylinder of radius R, length l and radial thickness dr. Assume the length of the cylinder to be so large that heat transfer takes place in the radial direction only. It is assumed that heat flows in one dimension and that heat transfer inside the particle occurs by conduction only. Based on the above assumptions, the equation representing the energy balance is given by

$$\frac{\partial}{\partial t}\left(C_p \rho T\right) = k\left(\frac{b-1}{r}\frac{\partial T}{\partial r} + \frac{\partial^2 T}{\partial r^2}\right) + \left(-\Delta H\right)\left(-\frac{\partial \rho}{\partial t}\right) \tag{4.3}$$

As ρ and T are functions of t, equation (4.3) can be simplified as:

$$\rho C_p \frac{\partial T}{\partial t} = k\left(\frac{b-1}{r}\frac{\partial T}{\partial r} + \frac{\partial^2 T}{\partial r^2}\right) + \left[\left(-\Delta H\right) + C_p T\right]\left(-\frac{\partial \rho}{\partial t}\right) \tag{4.4}$$

The initial and boundary conditions for equation (4.4) are:

Initial condition:

$$t = 0; \quad C_B = C_{B0}, C_{G1} = C_{C1} = C_{G2} = C_{C2} = 0, T(r,0) = T_0 \tag{4.5}$$

Boundary conditions:

$$t > 0; \quad r = 0, \quad \left(\frac{\partial T}{\partial r}\right)_{r=0} = 0 \tag{4.6}$$

$$t > 0; \quad r = R, \quad k\left(\frac{\partial T}{\partial r}\right)_{r=R} = h\left(T_f - T\right) + \sigma\varepsilon\left(T_f{}^4 - T^4\right) \tag{4.7}$$

In equation (4.7), external heat transfer is considered to occur by a combination of conductive and radiative mechanism.

The dimensionless form of equation (4.4) is given by

$$\frac{\partial \theta}{\partial \tau} = \frac{b-1}{x}\frac{\partial \theta}{\partial x} + \frac{\partial^2 \theta}{\partial x^2} + Q\left(-\frac{\partial \rho}{\partial \tau}\right) \tag{4.8}$$

The initial and boundary conditions in dimensionless forms are:

Initial condition:

$$\tau = 0; \quad \theta(x,0) = 1 \tag{4.9}$$

Boundary conditions:

$$\tau > 0; \quad x = 0, \qquad \frac{\partial \theta}{\partial x} = 0 \tag{4.10}$$

$$\tau > 0; \quad x = 1, \qquad \frac{\partial \theta}{\partial x} = -\theta H \tag{4.11}$$

The following groups are introduced to obtain equations (4.8)-(4.11).

$$\alpha = \frac{k}{\rho C_p} \tag{4.12}$$

$$x = \frac{r}{R} \tag{4.13}$$

$$\tau = \frac{\alpha t}{R^2} \tag{4.14}$$

$$\theta = \frac{T_f - T}{T_f - T_0} \tag{4.15}$$

$$H = \left(\frac{R}{k}\right)\left[h + \varepsilon\sigma\left(T^3 + T^2 T_f + T_f{}^2 T + T_f{}^3\right)\right] \tag{4.16}$$

$$Q = \frac{(-\Delta H) + C_p T}{\rho C_p (T_0 - T_f)} \tag{4.17}$$

However, in order to solve equation (4.8), it is essential to obtain the value of $(-\partial\rho/\partial\tau)$ from chemical kinetics model discussed above. From equation (4.14), we have,

$t = \frac{\tau R^2}{\alpha}$ Hence,

$$\partial t = \frac{R^2 d\tau}{\alpha}$$

Substituting this value in equation (4.2), it becomes

$$-\frac{\partial \rho}{\partial \tau} = \frac{k_1 R^2 (C_B)^n}{\alpha} \tag{4.18}$$

Introducing equation (4.18) in equation (4.8) gives,

$$\frac{\partial \theta}{\partial \tau} = \frac{b-1}{x}\frac{\partial \theta}{\partial x} + \frac{\partial^2 \theta}{\partial x^2} + \frac{QR^2 k_1 (C_B)^n}{\alpha} \tag{4.19}$$

4.5.1. Treatment of condition at the centre, i.e., at x=0

A close look at equation (4.19) reveals that at the centre, i.e., at x=0, the first term on right hand side will become infinity which is physically not possible and so not acceptable. However, this difficulty can be alleviated by making the use of *L' Hospital's rule* (Ghoshdastidar, 1998) according to which

If $\lim f(x)_{x\to a} = \lim g(x)_{x\to a} = 0$ (4.20a)

And $\lim\left[\frac{g'(x)}{f'(x)}\right]_{x\to a} = L$ (4.20b)

Then $\lim\left[\frac{g(x)}{f(x)}\right]_{x\to a} = L$ (4.20c)

Therefore, invoking *L' Hospital's rule* to the centre condition, we obtain,

$$\lim_{x\to 0} \frac{1}{x}\frac{\partial \theta}{\partial x} = \frac{\partial^2 \theta}{\partial x^2} \tag{4.21}$$

Hence, at x=0, equation (4.19) becomes,

$$\frac{\partial \theta}{\partial \tau} = b\frac{\partial^2 \theta}{\partial x^2} + \frac{QR^2 k_1 (C_B)^n}{\alpha} \tag{4.22}$$

Now, equation (4.19) can be solved easily by using the initial and boundary conditions given by equations (4.9)-(4.11).

4.6. Method of solution

The equation (4.19) along with initial and boundary conditions given by equations (4.9)-(4.11) are solved by finite difference method using pure implicit scheme (Appendix-B). Pure implicit scheme is an unconditionally stable scheme, that is, there is no restriction on time-step in sharp contrast with Euler and Crank-Nicholson method as discussed by Ghoshdastidar (1998). The finite difference form of equations (4.22), (4.19) and the equation obtained by using boundary condition i.e. equation (4.11) is as follows:

$$\frac{\theta_1^{p+1}-\theta_1^{p}}{\Delta\tau}=\frac{2b}{(\Delta x)^2}(\theta_2^{p+1}-\theta_1^{p+1})+\frac{QR^2k_1C_B^{n_1}}{\alpha} \tag{4.23}$$

$$\frac{\theta_i^{p+1}-\theta_i^{p}}{\Delta\tau}=\frac{\theta_{i+1}^{p+1}-2\theta_i^{p+1}+\theta_{i-1}^{p+1}}{(\Delta x)^2}+\frac{b-1}{x_i}\frac{\theta_{i+1}^{p+1}-\theta_{i-1}^{p+1}}{2\Delta x}+\frac{QR^2k_1C_B^{n_1}}{\alpha} \tag{4.24}$$

$$\frac{\theta_N^{p+1}-\theta_N^{p}}{\Delta\tau}=\frac{2\Delta xH(-\theta_N^{p+1})-2\theta_N^{p+1}+2\theta_{N-1}^{p+1}}{(\Delta x)^2}-(b-1)\theta_N^{p+1}H+\frac{QR^2k_1C_B^{n_1}}{\alpha} \tag{4.25}$$

Rearranging equations (4.23)-(4.25) will give the following sets of equations, which would facilitate numerical solution.

$$\left(\frac{2b\Delta\tau}{(\Delta x)^2}+1\right)\theta_1^{p+1}+\left(-\frac{2b\Delta\tau}{(\Delta x)^2}\right)\theta_2^{p+1}=\theta_1^{p}+\left(\frac{\Delta\tau QR^2k_1C_B^{n_1}}{\alpha}\right) \tag{4.26}$$

$$\left(\frac{\Delta\tau(b-1)}{2(\Delta x)x_i}-\frac{\Delta\tau}{(\Delta x)^2}\right)\theta_{i-1}^{p+1}+\left(\frac{2\Delta\tau}{(\Delta x)^2}+1\right)\theta_i^{p+1}+\left(-\frac{\Delta\tau(b-1)}{2(\Delta x)x_i}-\frac{\Delta\tau}{(\Delta x)^2}\right)\theta_{i+1}^{p+1}=\theta_i^p+\left(\frac{\Delta\tau QR^2k_1C_B^n}{\alpha}\right) \tag{4.27}$$

$$\left(-\frac{2\Delta\tau}{(\Delta x)^2}\right)\theta_{N-1}^{p+1}+\left(\frac{2\Delta\tau}{(\Delta x)^2}+1+\frac{2\Delta\tau}{\Delta x}H+(b-1)\Delta\tau H\right)\theta_N^{p+1}=\theta_N^p+\left(\frac{\Delta\tau QR^2k_1C_B^n}{\alpha}\right) \tag{4.28}$$

Hence, we have a set of N linear simultaneous algebraic equations and N unknowns, which can be easily solved by standard numerical methods. In the present study (Babu & Chaurasia, 2003b) Tri-Diagonal Matrix Algorithm (TDMA) also known as Thomas Algorithm (Appendix-B) is used to solve the set of equations (4.26)-(4.28). In order to fix the values of $\Delta\tau$ and Δx, the results are obtained for various values of N ranging from 26 to 176. For value of N=151 and N=176, the results are found to be the same. So in order to save the computer time N=151 i.e. ($\Delta x = 1/N$) is used in the present study (Babu & Chaurasia, 2003b).

The temperature profiles obtained from the heat transfer model based on initial conditions serve as an input to the chemical kinetics model. The equations (3.1)-(3.5) are solved by Runge-Kutta fourth order method (Appendix-A) and Runge-Kutta variable step-size method. It is found that Runge-Kutta variable step-size is faster than Runge-Kutta fourth order method as discussed by Babu, Angira, & Nilekar (2002). But Runge-Kutta variable step-size method does not give the solution for a particular and fixed interval of time. Hence, to obtain the solution at a particular interval of time, which is required to compare the results of present study (Babu & Chaurasia, 2003b) with those

reported in literature, Runge-Kutta fourth order method (Appendix-A) with fixed step size is used in the present study (Babu & Chaurasia, 2003b). The Computer Codes in C++ for both constant wall temperature and varying wall temperature are given in Appendix-B. The values of various parameters employed in the present study (Babu & Chaurasia, 2003b) are given in Appendix-C. It may be noted that thermal diffusivity is taken to be a constant and based on initial temperature of wood, which is a representative value in pyrolysis. When separate values for wood at different temperatures are tried in the simulation, it is found that for the same iteration the pyrolysis time is different for different radial positions. The pyrolysis time cannot be different in a given iteration and hence a representative constant value corresponding to initial condition of biomass is used as given in the Appendix-C taken from Jalan & Srivastava (1999). The model equation is solved for cylindrical pellets, spheres, and slab geometries of equivalent radius ranging from 0.00025-0.013 m, and temperature ranging from 303-2700 K.

4.7. Results and discussion

4.7.1. Model Simulation

The set of equations (3.1)-(3.5) and (4.26)-(4.28) are solved numerically subject to the initial and boundary conditions and the results are presented and discussed. Figs. 4.1, 4.2 and 4.3 show the temperature profile as a function of radial distance at the time of completion of pyrolysis (i.e. when biomass concentration=0) for the orders of reactions of $n_1 = 1; n_2 = n_3 = 1.5$ for the particle radii of 0.00025 m, 0.005 m and 0.011 m respectively. It is observed that as the particle dimension increases, the time required for completion of pyrolysis also increase (40 s for 0.00025 m, 188 s for 0.005 m and 589 s

for 0.011 m particle dimension). For the particle radius of 0.00025 m, the temperature is same (1000 K) at all the radial positions at the time of completion of pyrolysis while for

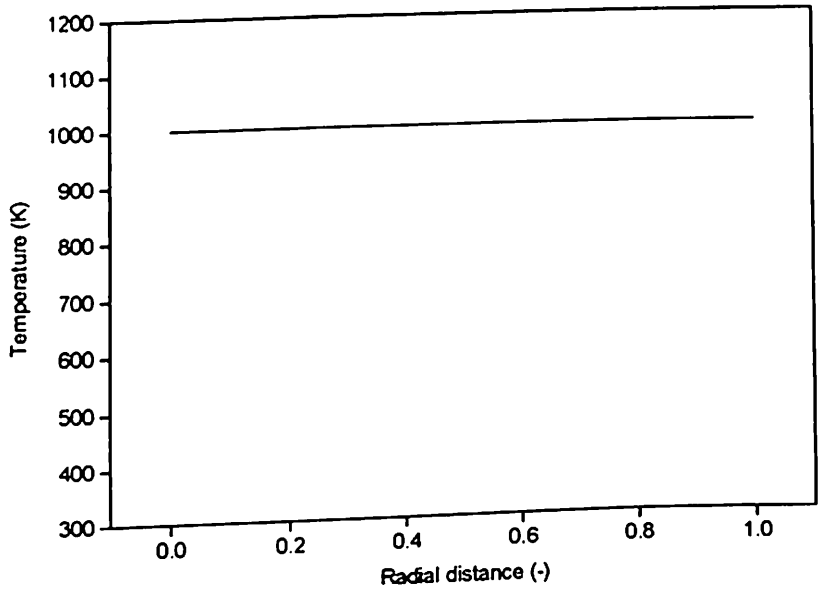

Fig. 4.1. Temperature profile as a function of radial distance at the time of completion of pyrolysis (n_1=1, n_2=n_3=1.5, R=0.00025 m, T_0=303 K, T_f=1000 K, t=40 s).

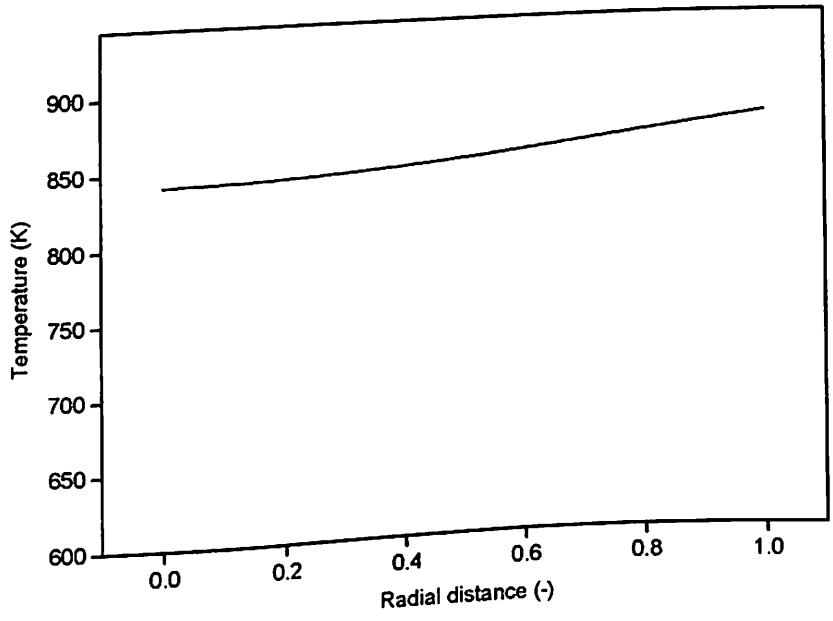

Fig. 4.2. Temperature profile as a function of radial distance at the time of completion of pyrolysis (n_1=1, n_2=n_3=1.5, R=0.005 m, T_0=303 K, T_f=900 K, t=188 s).

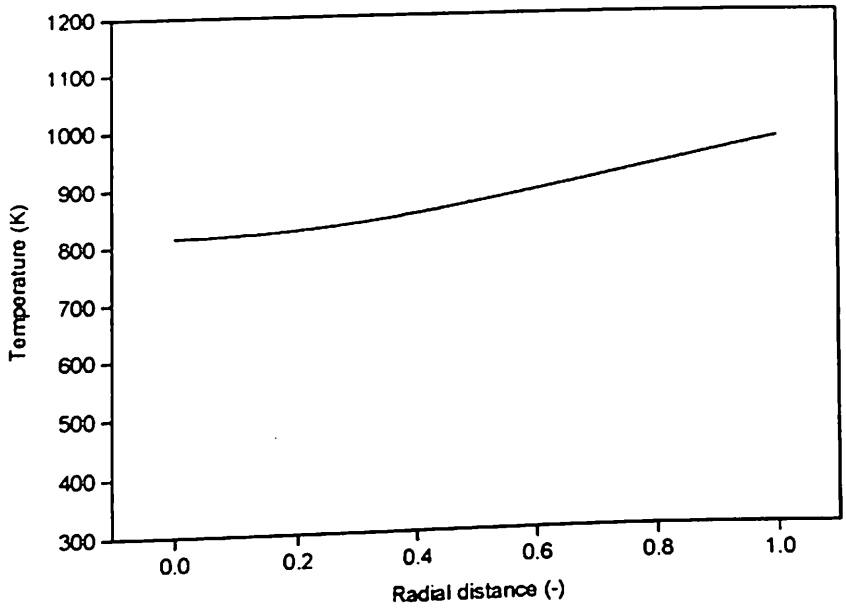

Fig. 4.3. Temperature profile as a function of radial distance at the time of completion of pyrolysis (n_1=1, n_2=n_3=1.5, R=0.011 m, T_0=303 K, T_f=1000 K, t=589 s).

the particle radius of 0.005 m and 0.011 m, the temperature increases from centre to the wall and it is maximum at the wall. Similar trends are obtained for the orders of reactions of $n_1 = 0; n_2 = n_3 = 1.5$ also as shown in Figs. 4.4, 4.5 & 4.6. The simulations are carried out for seeing the effect of particle size on radial temperature profile with different particle radii ranging from 0.00025 m to 0.013 m with a step of 0.00025 m and for all radii and similar trends as mentioned above are obtained. It can be concluded that for a particle radii of 0.0015 m or less, the temperature profile is flat and it changes to increasing trend for higher particle radii greater than 0.0015 m. It is observed that the time for completion of pyrolysis is very less (i.e. pyrolysis is significantly faster) for the case of $n_1 = 0; n_2 = n_3 = 1.5$ when comparisons are made between Figs. 4.1, 4.2 & 4.3 and Figs. 4.4, 4.5 & 4.6, because in this case the model equations (3.1)-(3.3) become

independent of initial biomass concentration as discussed in chapter 3.

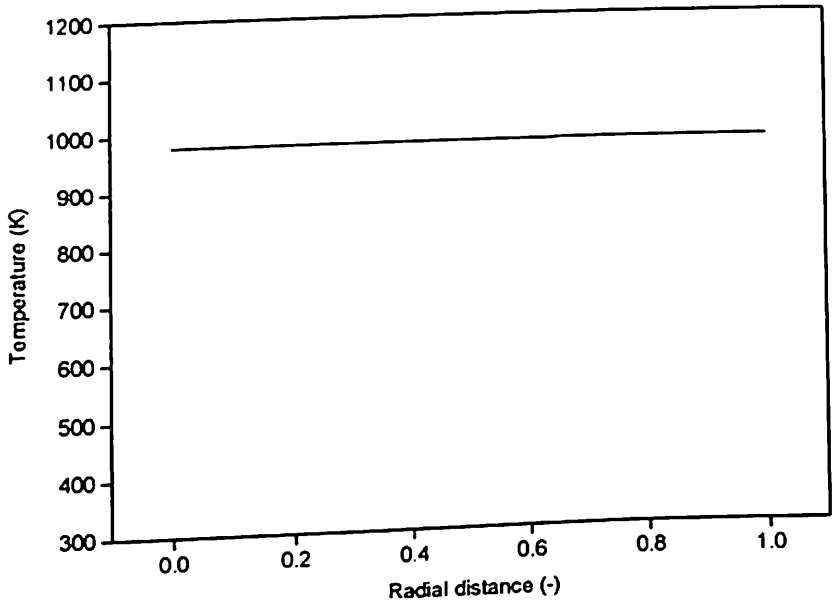

Fig. 4.4. Temperature profile as a function of radial distance at the time of completion of pyrolysis (n_1=0, n_2=n_3=1.5, R=0.00025 m, T_0=303 K, T_f=1000 K, t=6 s).

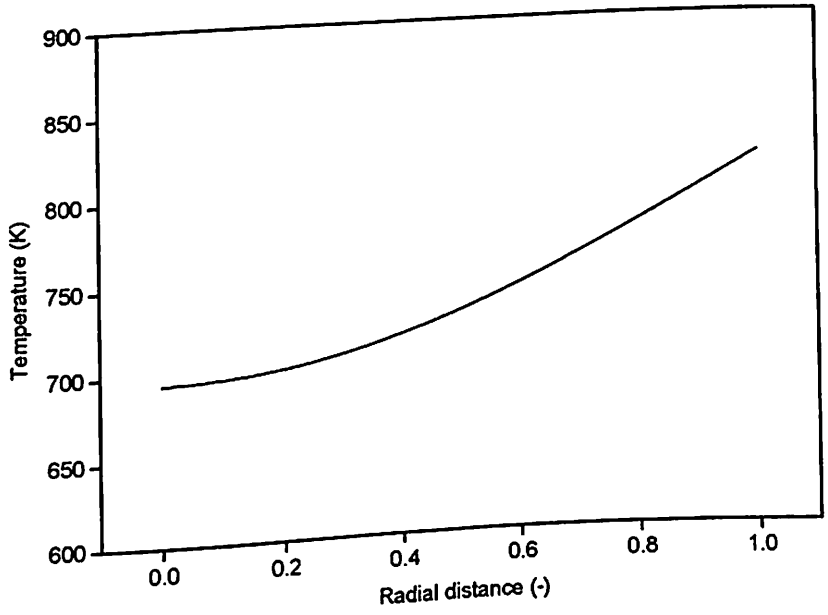

Fig. 4.5. Temperature profile as a function of radial distance at the time of completion of pyrolysis (n_1=0, n_2=n_3=1.5, R=0.005 m, T_0=303 K, T_f=900 K, t=70 s).

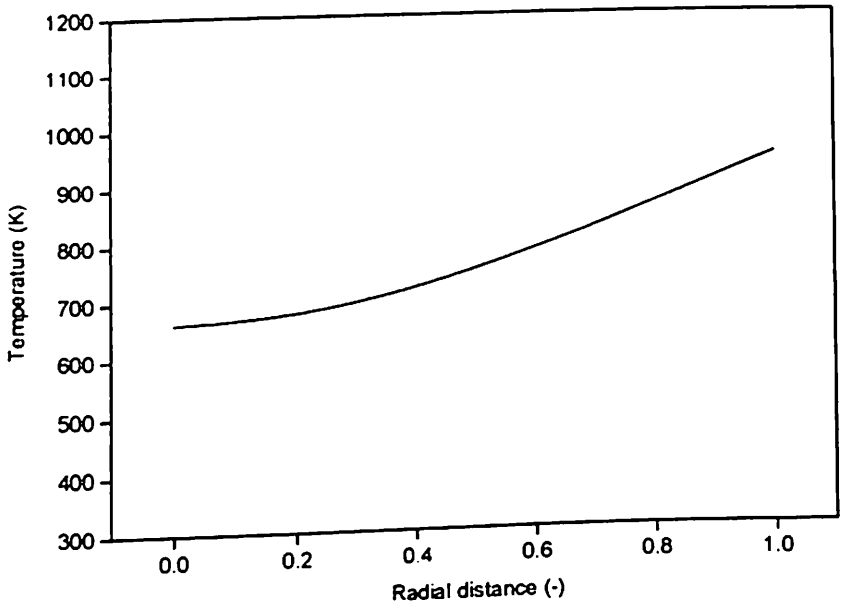

Fig 4.6. Temperature profile as a function of radial distance at the time of completion of pyrolysis (n_1=0, n_2=n_3=1.5, R=0.011 m, T_0=303 K, T_f=1000 K, t=247 s).

Fig. 4.7 shows the temperature profile as a function of radial distance for cylindrical pellet of various radii at 900 K at the time of completion of pyrolysis for orders of reactions of $n_1 = 1, n_2 = n_3 = 1.5$. It is found that as the particle radius increases, the time for completion of pyrolysis also increases. Time required for completion of pyrolysis for the particle of radius 0.00025 m is the least (53 s), while it is maximum for the particle radius of 0.013 m (717 s). For the smaller particle of radii 0.00025 m and 0.001 m, there is no change in temperature along the radial position, while for the other particle radii it is minimum at the centre and maximum at wall. Fig. 4.8 shows the temperature profile as function of radial distance for final temperature of 1200 K. It is seen that as the temperature increases, the pyrolysis completes faster. The trends obtained are same as those shown in Fig. 4.7 and same explanation holds good for this case also. Fig. 4.9 shows the temperature profile as a function of radial distance at 900 K at the time of

completion of pyrolysis for the orders of reactions of $n_1 = 0, n_2 = n_3 = 1.5$. The trends obtained are same as discussed earlier. When comparison is made between Figs. 4.7 and

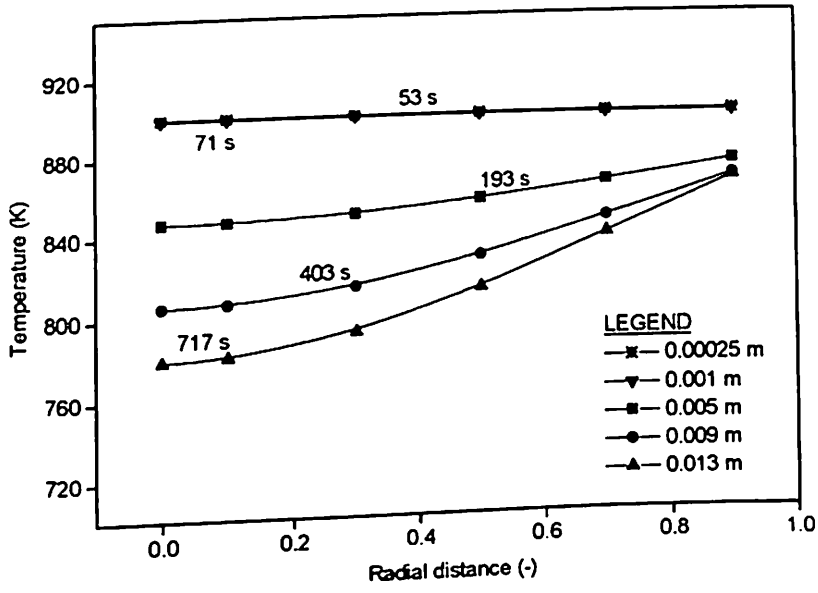

Fig. 4.7. Temperature profile as a function of radial distance for various particle radii at 900 K at the time of completion of pyrolysis (n_1=1, n_2=n_3=1.5, T_0=303 K, T_f=900 K).

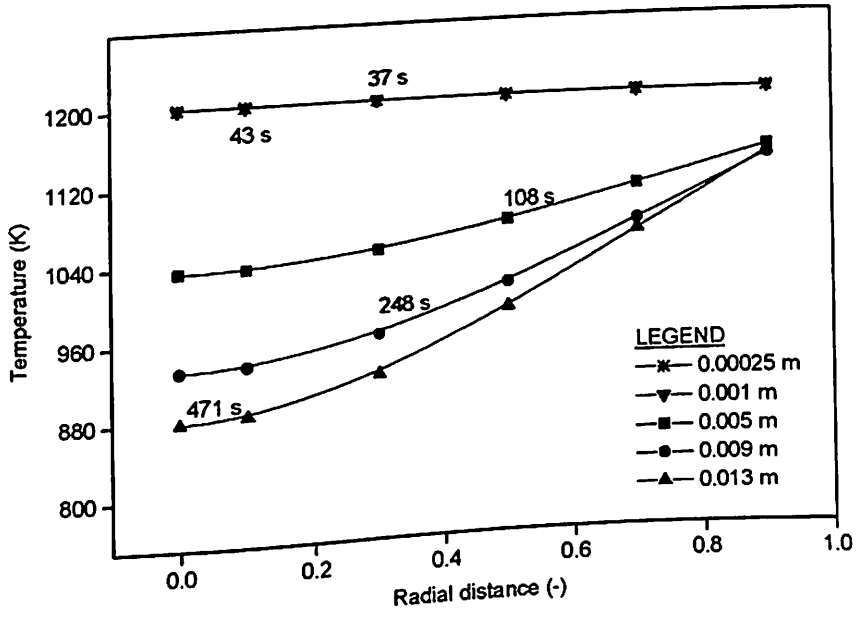

Fig. 4.8. Temperature profile as a function of radial distance for various particle radii at 1200 K at the time of completion of pyrolysis (n_1=1, n_2=n_3=1.5, T_0=303 K, T_f=1200 K).

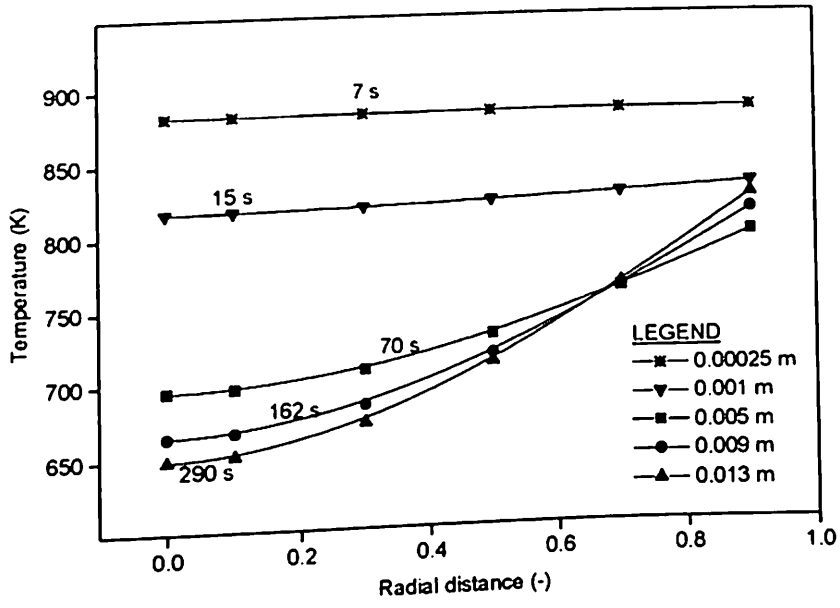

Fig. 4.9. Temperature profile as a function of radial distance for various particle radii at 900 K at the time of completion of pyrolysis (n_1=0, n_2=n_3=1.5, T_0=303 K, T_f=900 K).

4.9, it is found that the time of completion of pyrolysis is less for orders of reactions of $n_1 = 0, n_2 = n_3 = 1.5$ as compared to $n_1 = 1, n_2 = n_3 = 1.5$ for all particle radii. This is due to the fact that for orders of reactions of $n_1 = 0, n_2 = n_3 = 1.5$, the model equations (3.1)-(3.3) become independent of the initial biomass concentration as discussed above.

Based on the observation made in Figs. 4.7, 4.8 and 4.9 above (i.e., the pyrolysis completes faster at higher values of temperature), the model is simulated for wide range of temperatures ranging from 300 K to 2700 K and the particle radii ranging from 0.00025 m to 0.013 m. The results are presented in Figs. 4.10, 4.11 and 4.12 for particle radii of 0.005m and 0.00025 m for cylinder and for particle radius of 0.005 m for sphere. Interestingly, it is found that as the temperature increases, time of completion of pyrolysis decreases up to certain extent giving the optimum pyrolysis time and then goes on increasing with further increase in the temperature. For the particle radius of 0.005m,

the optimum time of completion of pyrolysis is found to be 88 s for final furnace temperature of 1645 K as shown in Fig. 4.10. This can be well explained by the

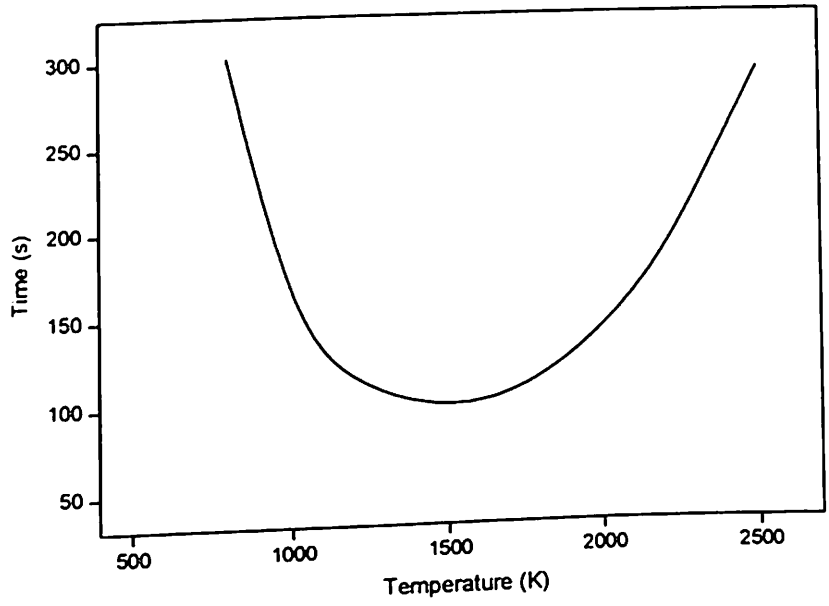

Fig. 4.10. Time of completion of pyrolysis as a function of temperature for particle radius of 0.005 m (n_1=1, n_2=n_3=1.5, T_0=303 K).

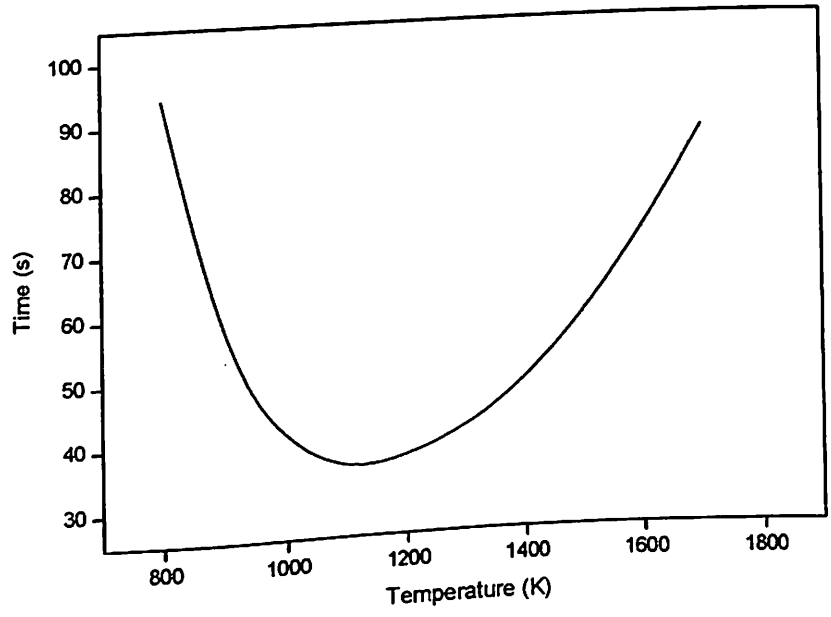

Fig. 4.11. Time of completion of pyrolysis as a function of temperature for particle radius of 0.00025 m (n_1=1, n_2=n_3=1.5, T_0=303 K).

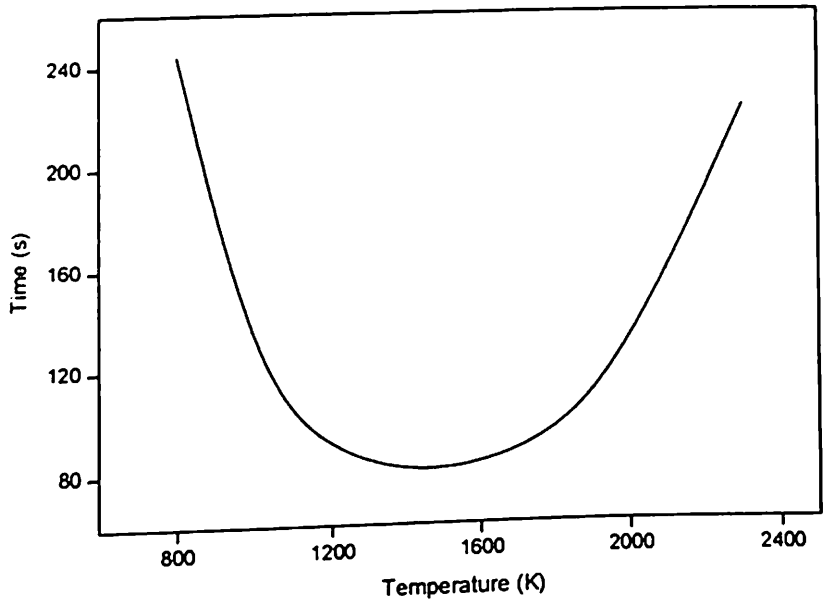

Fig. 4.12. Time of completion of pyrolysis as a function of temperature for spherical particle of radius 0.005 m (n_1=1, n_2=n_3=1.5, T_0=303 K).

pyrolysis kinetics with the help of data presented in Tables 4.1 and 4.2 for optimum final furnace temperature of 1645 K and 2100 K respectively. As the final furnace temperature is increased from 1645 to 2100 K, the decrease in concentration of biomass is more for 2100 K up to certain time (74 s). The maximum concentration of $(char)_1$ is obtained in 38 s for final furnace temperature of 2100 K as compared to 46 s for 1645 K. So after 38 s the concentration of $(char)_1$ decreases, and hence the consumption of biomass also decreases for final furnace temperature of 2100 K. It is also observed that after 74 s, the decrease in concentration of biomass is less for 2100 K as compared to 1645 K, because the $(char)_1$ left is less for 2100 K as compared to 1645 K. So the time of completion of pyrolysis to reach the desired final concentration of biomass (i.e. zero) increases though the final furnace temperature is more. Similar explanation could be given for the results shown in Figs. 4.11 and 4.12 also. The optimum values of the

parameters are given in Table-4.3. From the Table-4.3, it is observed that the final pyrolysis time and final pyrolysis temperature are less for the sphere as compared to the cylinder-II for the same radius of 0.005 m.

Table-4.1. Simulated results with the optimum temperature (1645 K) for pyrolysis of cylindrical pellet of radius 0.005 m (n_1=1; n_2=n_3=1.5)

t	T	C_B	C_{G_1}	C_{C_1}	C_{G_2}	C_{C_2}
1.0	303.041416	650.000000	0.000000	0.000000	0.000000	0.000000
15.0	421.921449	649.965228	0.000003	0.034769	0.000000	0.000000
30.0	620.145975	535.048255	14.281696	99.831749	0.419150	0.419150
38.0	657.662178	385.407963	44.324157	179.732538	20.267671	20.267671
39.0	662.221267	366.467356	46.767841	184.470246	26.147278	26.147278
46.0	703.340007	230.944809	57.246921	184.793708	88.507281	88.507281
47.0	711.305786	210.836541	58.023858	180.265779	100.436911	100.436911
48.0	720.086499	190.575671	58.567103	174.558063	113.149581	113.149581
73.0	1220.206339	0.038576	2.747890	21.643747	312.784893	312.784893
74.0	1234.605217	0.026305	2.364912	21.253188	313.177797	313.177797
75.0	1248.412790	0.018079	2.043245	20.926480	313.506098	313.506098
76.0	1261.670650	0.012521	1.771999	20.651856	313.781812	313.781812
88.0	1387.710904	0.000253	0.414538	19.287125	315.149042	315.149042

Table-4.2. Simulated results with temperature = 2100 K for pyrolysis of cylindrical pellet of radius 0.005 m (n_1=1; n_2=n_3=1.5)

t	T	C_B	C_{G_1}	C_{C_1}	C_{G_2}	C_{C_2}
1.0	303.073899	650.000000	0.000000	0.000000	0.000000	0.000000
15.0	462.544327	649.857429	0.000469	0.142102	0.000000	0.000000
30.0	650.049746	504.244613	45.436203	96.004217	2.157483	2.157483
38.0	695.304910	36.019862	104.855115	131.66940	38.727808	38.727808
39.0	703.247479	311.758513	111.097880	129.60329	48.770158	48.770158
46.0	800.150481	120.676965	141.162004	65.012529	161.574251	161.574251
47.0	825.229412	93.974519	142.913731	50.361562	181.375094	181.375094
48.0	855.242754	69.844726	144.101093	36.229038	199.912571	199.912571
73.0	1636.091153	0.030624	153.513662	0.003811	248.225952	248.225952
74.0	1652.552961	0.025688	153.515172	0.003240	248.227950	248.227950
75.0	1668.394619	0.021661	153.516367	0.002772	248.229600	248.229600
76.0	1683.645462	0.018355	153.517318	0.002386	248.230971	248.230971
88.0	1828.787031	0.003332	153.521042	0.000549	248.237539	248.237539
89.0	1838.269943	0.002941	153.521113	0.000496	248.237725	248.237725
152.0	2072.129027	0.000007	153.521442	0.000009	248.239271	248.239271

Table-4.3. Optimum Parametric values for different particle radii and geometries at the centre (n_1=1; n_2=n_3=1.5)

Optimum Parameters	Cylinder-I	Cylinder-II	Sphere
Particle radii (m)	0.00025	0.005	0.005
Final pyrolysis time (s)	35.0	88.0	78
Final temperature of furnace (K)	1100	1645	1455
Final pyrolysis temperature (K)	1099.99	1387.751	1350.09
Final concentration of initial biomass (kg/m^3)	0	0	0
Final concentration of Char 1 (kg/m^3)	0.00715	19.3174	64.3383
Final concentration of Volatile 1 (kg/m^3)	366.985	0.41275	0.0299
Final concentration of Char 2 (kg/m^3)	141.504	315.135	292.816
Final concentration of Volatile 2 (kg/m^3)	141.504	315.135	292.816

Figs. 4.13 and 4.14 show the temperature profiles as a function of radial distance at various times of progression of pyrolysis for the particle radius of 0.0075 m and 0.005 m respectively, considering both convection and radiation on the wall (surface of the particle). It is observed that as pyrolysis time increases, temperature increases at a given radial position. The rate of increase is high at the radial position close to the wall compared to that at the centre of the particle. In the initial stages of pyrolysis, the temperature profile is very steep near the wall (refer the temperature profile corresponding to 2 s in Fig. 4.13), and as the time progresses the steepness in the temperature profile near the wall decreases. This can be explained with the fact that when the heat transfer takes place by both the mechanisms of convection and radiation from the wall surface, the resistance offered for heat transfer near the wall at initial stages of pyrolysis is very high. On the contrary when heat transfer from wall surface takes place only by convection and with no radiation, the resistance offered for heat transfer near the wall is not as much high as in the above case which is clearly demonstrated by plotting the simulation results as shown in Figs. 4.15 and 4.16. It is also observed that the increase in temperature at various radial positions at different

times of progression of pyrolysis is not significant which is obvious due to the reasons mentioned above.

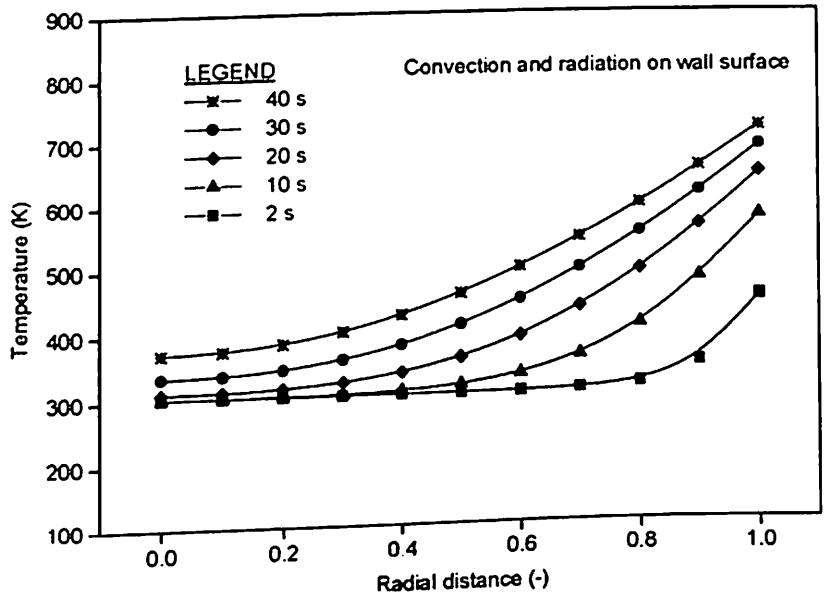

Fig. 4.13. Temperature profile as a function of radial distance considering both convection and radiation on the wall (R=0.0075 m, T_0=303 K, T_f=900 K).

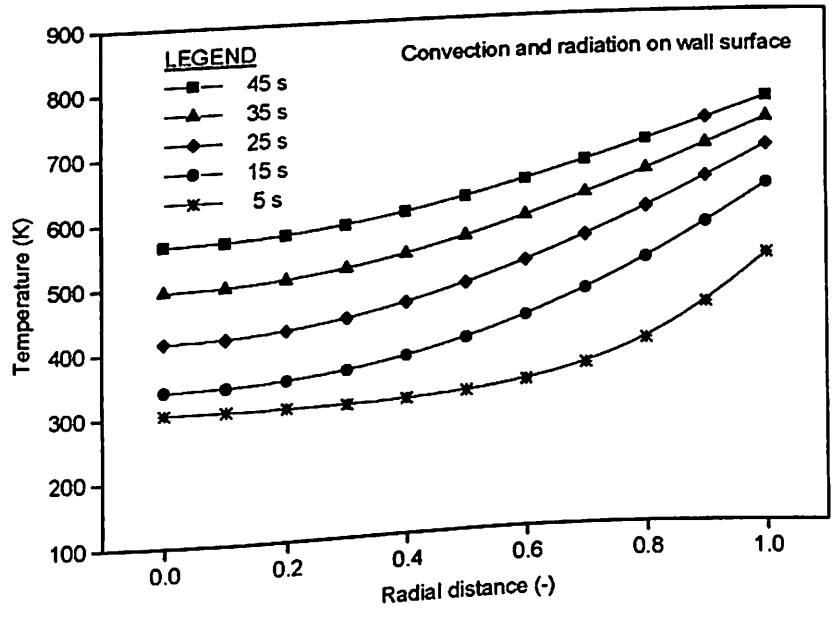

Fig. 4.14. Temperature profile as a function of radial distance considering both convection and radiation on wall surface (R=0.005 m, T_0=303 K, T_f=900 K).

Interestingly, to see the extent of effect of convection on temperature profile, simulations are carried out for a case where there is no radiation at the wall surface, but

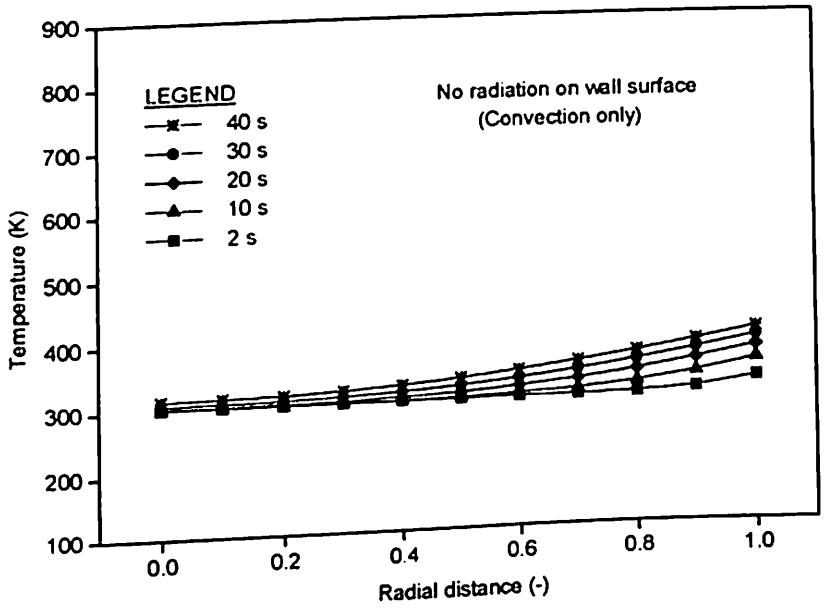

Fig. 4.15. Temperature profile as a function of radial distance considering convection only with no radiation on the wall (R=0.0075 m, T_0=303 K, T_f=900 K).

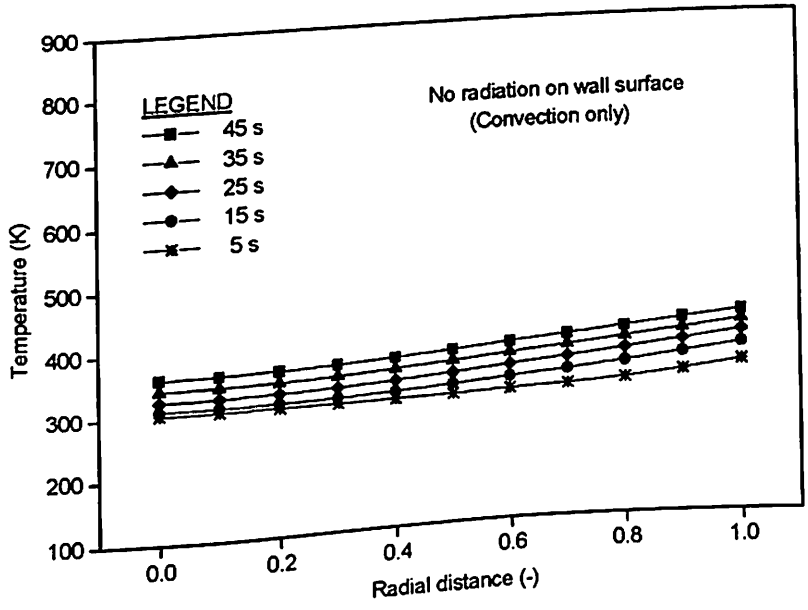

Fig. 4.16. Temperature profile as a function of radial distance considering convection only with no radiation on wall surface (R=0.005 m, T_0=303 K, T_f=900 K).

having ten times of convective heat transfer. The results are plotted in Figs. 4.17 and 4.18 for various times of pyrolysis progression. As expected, the results obtained are almost similar to those corresponding to combined convection and radiation case of Figs. 4.13 and 4.14. This consolidates the explanation given above in terms of resistances offered by various heat transfer mechanisms. It means that more the resistance offered for heat transfer near the wall of the particle (either by combined convection and radiation, or by convection alone but at higher convective rate) the more will be the difference (increase) in temperature profiles. In the present case the total net resistance offered by convection and radiation is approximately equal to ten times of convective resistance with no radiation at the wall of the particle.

The above results shown in Figs. 4.13-4.18 and the justifiable and logical explanation given therein have a lot of practical importance and physical significance in industrial pyrolysis applications. The results obtained consolidate the fact that it is possible to get the same extent of conversion of biomass and with lesser pyrolysis time under controlled conditions by increasing convective heat transfer at much lower operating temperatures which are much safer than at higher operating temperatures leading to combined convective and radiative heat transfer mechanisms which are not safe.

In pyrolysis process, the reactions that take place at low conversions, which practically means the temperature below 573 K, are endothermic in nature and the reactions that take place at high conversions are exothermic as discussed by Koufopanos, Papayannakos, Maschio, & Lucchesi (1991). As the reactions are exothermic at higher conversions, it becomes important to remove the excess heat liberated due to exothermicity of the pyrolysis reactions, which can be considered as waste heat recovery

that can be utilized to cater to the needs of utility requirements such as steam etc. This situation corresponds to isothermal operating conditions. Keeping this in view, the

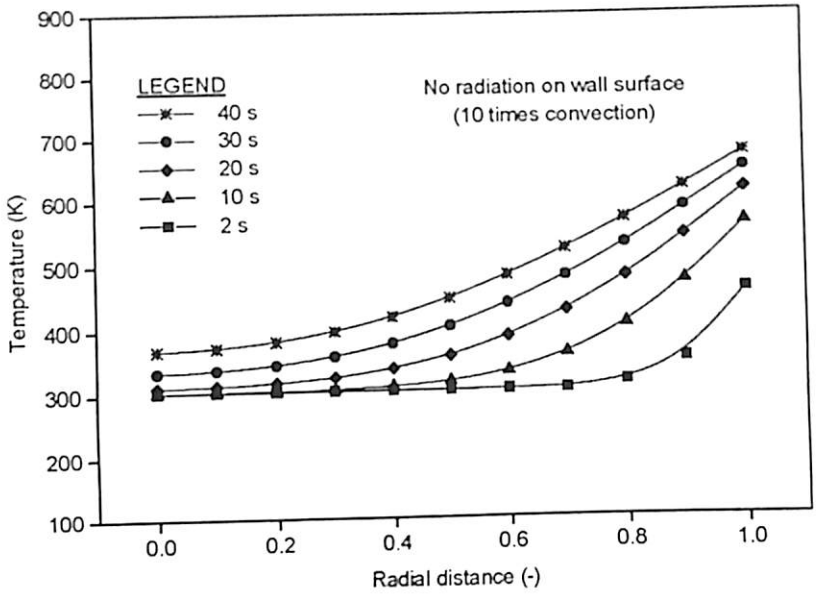

Fig. 4.17. Temperature profile as a function of radial distance considering ten times convection with no radiation on the wall (R=0.0075 m, T_0=303 K, T_f=900 K).

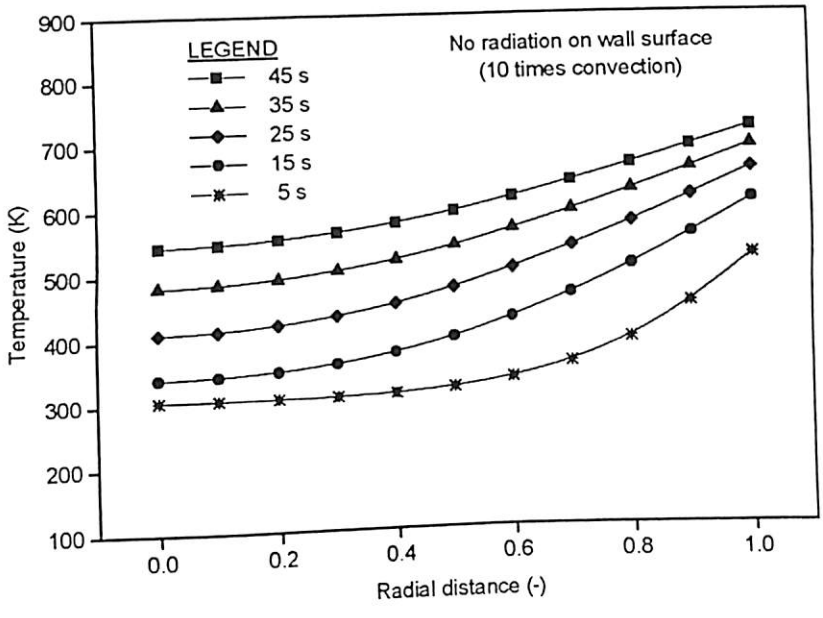

Fig. 4.18. Temperature profile as a function of radial distance considering ten times convection with no radiation on wall surface (R=0.005 m, T_0=303 K, T_f=900 K).

simulations are carried out for the pyrolysis under isothermal condition corresponding to a constant wall temperature and the results are presented in Figs. 4.19 and 4.20 for

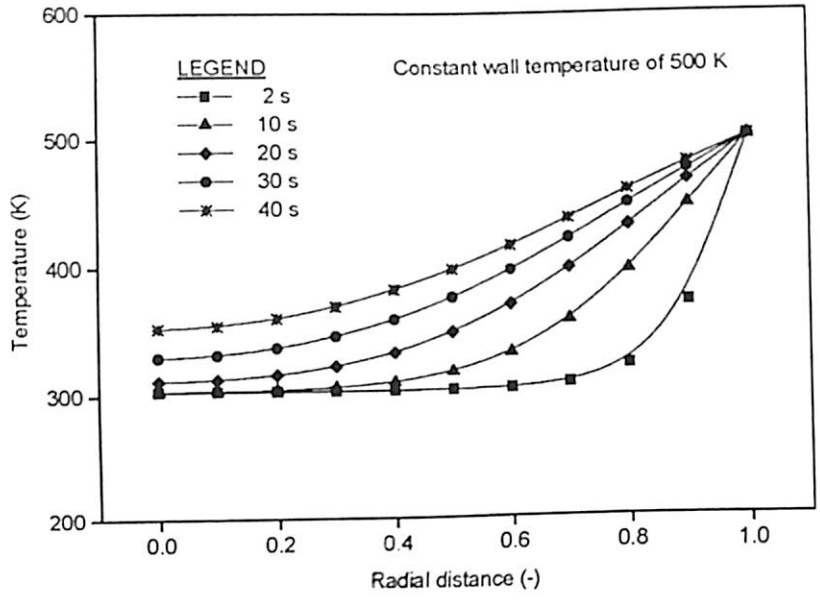

Fig. 4.19. Temperature profile as a function of radial distance considering constant wall temperature of 500 K (R=0.0075 m, T_0=303 K, T_f=500 K).

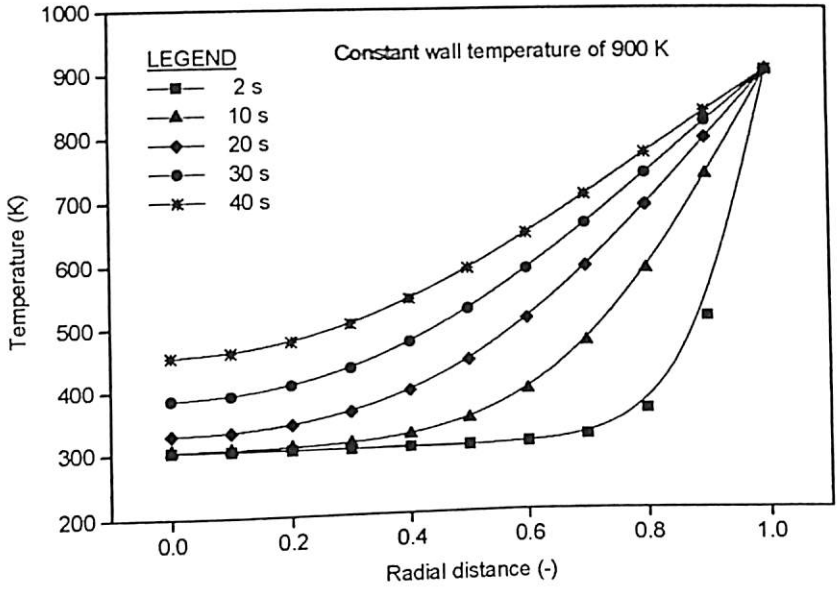

Fig. 4.20. Temperature profile as a function of radial distance considering constant wall temperature of 900 K (R=0.0075 m, T_0=303 K, T_f=900 K).

constant wall temperature of 500 K and 900K. Here again in both cases, the trends in the results obtained are almost similar to the earlier cases, the only difference being the wall temperature is constant. It is seen that, pyrolysis is much faster for 900 K as compared to 500 K, because higher the temperature faster will be the pyrolysis rate.

Fig. 4.21 shows the temperature profiles for different geometries (slab, cylinder and sphere). The radii of cylinder and sphere are taken as half the thickness of slab. It is found that pyrolysis is faster in case of sphere and slowest for the slab, while the trend in temperature profiles obtained for all the three geometries being same. Geometrically, the sphere has got a more heat absorbing capacity as compared to cylinder and slab and it is the least for slab. Mathematically it is reflected in the value of parameter b (b=1, 2 and 3 for slab, cylinder and sphere respectively) in the model equation (4.19) and hence the observed trends in temperature profile. Similar profiles are obtained for particle radius of 0.0005 m as shown in Fig. 4.22.

4.7.2. Model Validation and Comparison

The simultaneous kinetic and heat transfer model developed in the present study (Babu & Chaurasia, 2003b) is compared with the experimental data reported by Pyle & Zaror (1984), model of Bamford, Crank, & Malan (1946) used by Pyle & Zaror (1984) and the model developed by Jalan & Srivastava (1999). Pyle & Zaror (1984) carried out the studies on the course of pyrolysis of cylindrical samples of wood. The experiments are performed in an inert constant temperature environment. Independent measurements of the instantaneous sample weight and the radial temperature are made. A mean value of 8.4 W/m^2 K (includes the dependence on Reynolds number and Prandtl number) is

used throughout for convective heat transfer coefficient, as its value is insensitive to temperature under the experimental conditions as discussed by Pyle & Zaror (1984). It

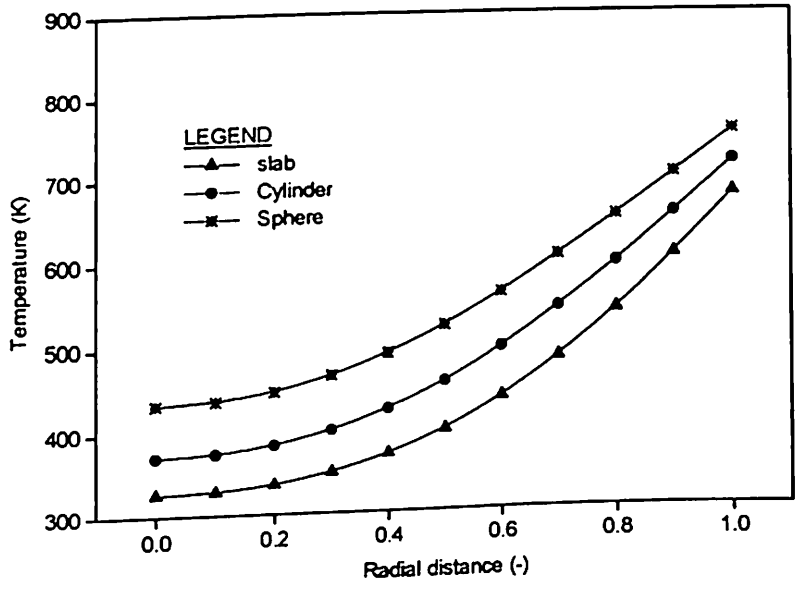

Fig. 4.21. Temperature profile as a function of radial distance for different geometries (R=0.0075 m, T_0=303 K, T_f=900 K, t=40 s).

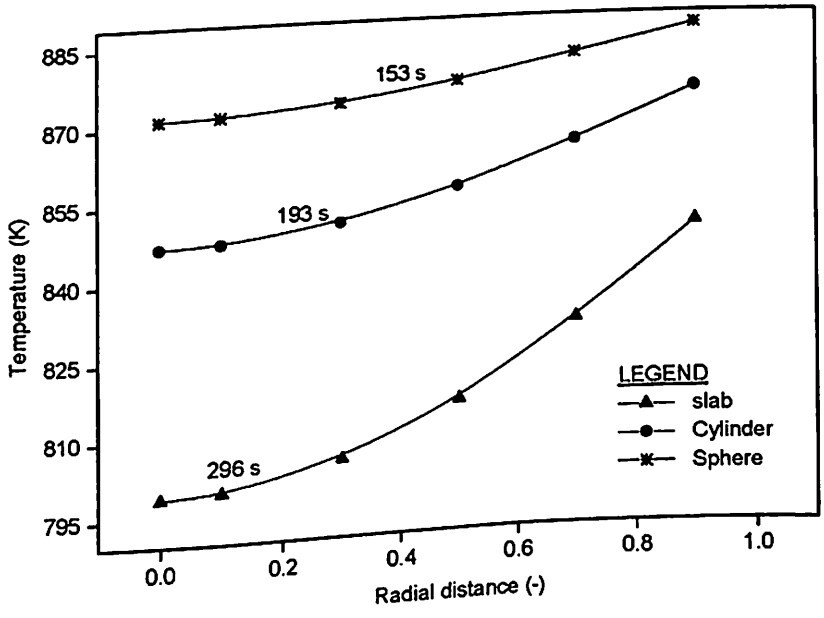

Fig. 4.22. Temperature profile as a function of radial distance for different geometries at the time of completion of pyrolysis (n_1=1, n_2=n_3=1.5, R=0.005 m, T_0=303 K, T_f=900 K).

may be noted that, all the parameters used to test the present model (Babu & Chaurasia, 2003b) are either independently and directly estimated or are taken from the literature.

Fig. 4.23 shows the temperature profile as a function of time at the centre (i.e. x=0) of the cylindrical pellet of radius 0.003 m. This is compared with the profiles obtained by Jalan & Srivastava (1999) and the experimental data obtained by Pyle & Zaror (1984) at the centre of cylindrical pellet. It is found that the model developed in the present study (Babu & Chaurasia, 2003b) is in excellent agreement with the experimental data better than the agreement with the model of Jalan & Srivastava (1999). Keeping the particle size constant when the final temperature is increased from 643 K to 780 K (refer Fig. 4.24), it is observed that there a is deviation in the temperature profile from experimental data at higher values of time. However, this deviation is less for the present model (Babu & Chaurasia, 2003b) when compared to the model of Jalan & Srivastava (1999). As discussed by Jalan & Srivastava (1999), this variation from the experimental data at higher temperatures is due to the fact that, at higher temperatures the cellulose polymers begin to decompose rapidly, suggesting that secondary pyrolysis reactions and convective effects are important. In the present model (Babu & Chaurasia, 2003b), the secondary pyrolysis reactions are being considered. In addition, heat transfer coefficient is considered as a function of Reynolds number and Prandtl number in the present study (Babu & Chaurasia, 2003b) as against a constant value considered by Jalan & Srivastava (1999). Hence, there is a significant improvement in the model predictions close to the experimental data compared to the model of Jalan & Srivastava (1999).

Figs. 4.25 and 4.26 show the temperature profiles for the particle radius of 0.0075 m and final temperatures of 660 K and 773 K respectively. Though the particle radius is

increased from 0.003 m to 0.0075 m, the observations from Figs. 4.25 and 4.26 are same as those from Figs. 4.23 and 4.24. The values used in Figs. (4.23)-(4.26) are given in

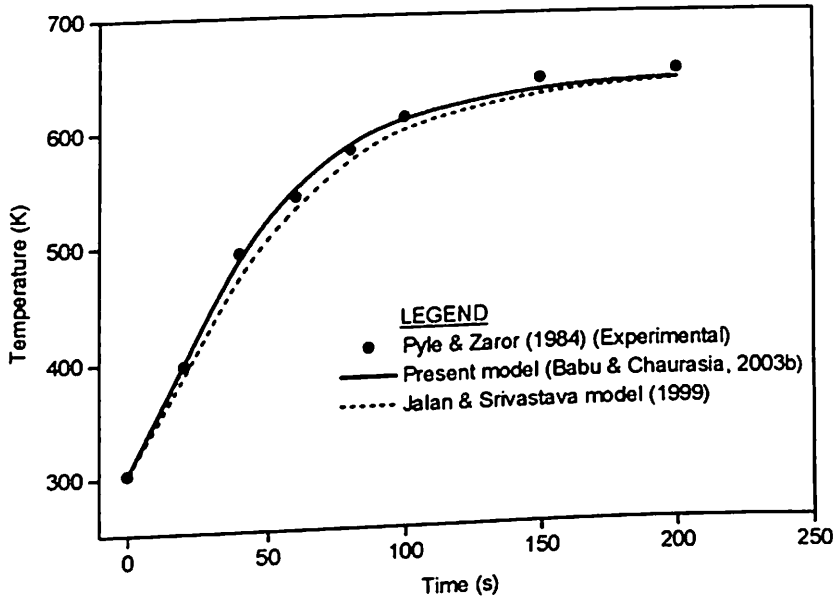

Fig. 4.23. Temperature profile as a function of time at the centre of the cylindrical pellet (R=0.003 m, T_0=303 K, T_f=643 K, x=0).

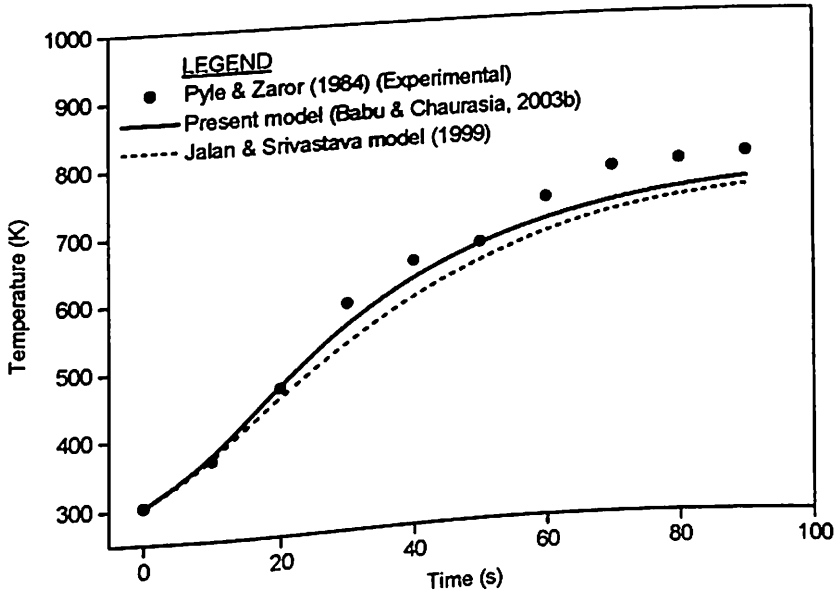

Fig. 4.24. Temperature profile as a function of time at the centre of the cylindrical pellet (R=0.003 m, T_0=303 K, T_f=780 K, x=0).

Tables 4.4-4.7 for quantitative comparison among the present model (Babu & Chaurasia, 2003b), the model of Jalan & Srivastava (1999), and experimental data of Pyle & Zaror

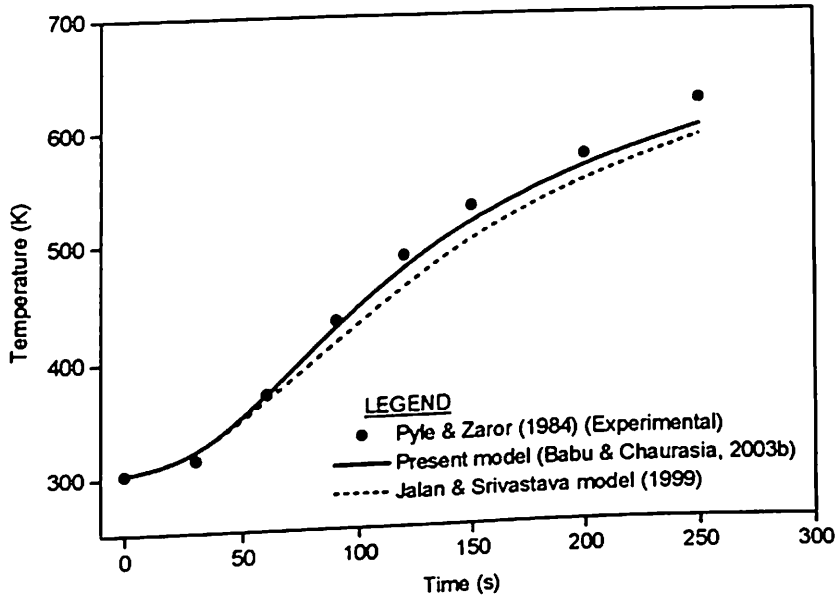

Fig. 4.25. Temperature profile as a function of time at the centre of the cylindrical pellet (R=0.0075 m, T_0=303 K, T_f=660 K, x=0).

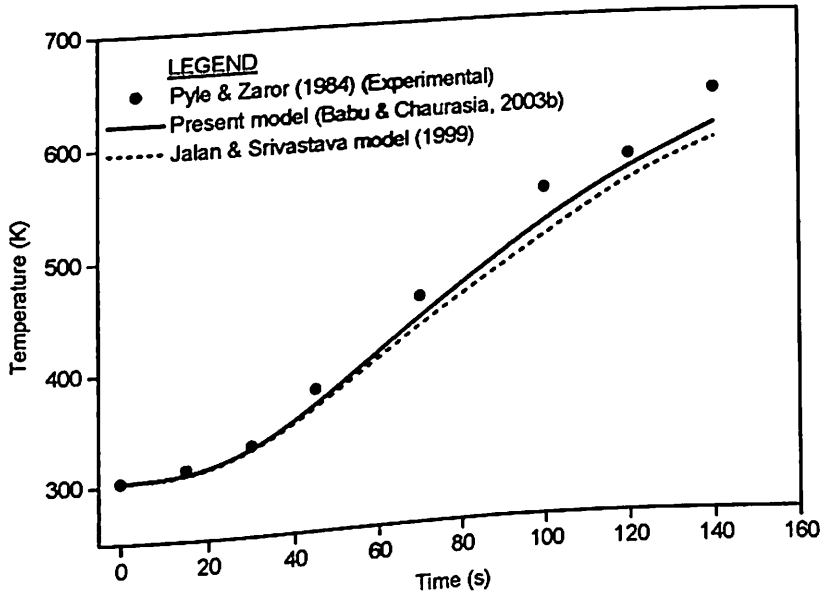

Fig. 4.26. Temperature profile as a function of time at the centre of the cylindrical pellet (R=0.0075 m, T_0=303 K, T_f=773 K, x=0).

Table-4.4. Comparison of present model results with those of earlier models for various stages of pyrolysis (time) at the centre of cylindrical pellet (R = 0.003 m, T_0 = 303 K, T_f = 643 K)

Time(s)	Temperature		
	PZ	P	JS
0	303	303	303
20	397	400	387
40	493	493	478
60	541	552	533
80	581	588	574
100	609	610	602
150	641	634	630
200	648	640	639
Average Percentage Error		**0.75**	**1.56**
Standard deviation		**0.0106**	**0.0189**

PZ=Pyle & Zaror (1984) (Experimental); P=Present study (Babu & Chaurasia, 2003b); JS=Jalan & Srivastava model (1999)

Table-4.5. Comparison of present model results with those of earlier models for various stages of pyrolysis (time) at the centre of cylindrical pellet (R = 0.003 m, T_0 = 303 K, T_f = 780 K)

Time (s)	Temperature		
	PZ	P	JS
0	303	303	303
10	365	366	362
20	466	473	459
30	585	557	539
40	642	619	598
50	664	664	648
60	726	696	679
70	769	719	704
80	777	736	723
90	786	748	736
Average Percentage Error		**3.09**	**4.77**
Standard deviation		**0.0406**	**0.0596**

PZ=Pyle & Zaror (1984) (Experimental); P=Present model (Babu & Chaurasia, 2003b); JS=Jalan & Srivastava model (1999)

(1984). The average percentage error and standard deviation are also calculated. If Y_{exp} is the experimental value of a quantity, Y_{cal} is the value obtained from the modeling equation, and N_p is the number of experimental points used in the calculation, then

average percentage error E_{pa} is defined as follows:

$$E_{pa} = \frac{\sum_{i=1}^{N_p}\left[(Y_{exp} - Y_{cal})/(Y_{exp})\right] * 100}{N_p} \tag{4.29}$$

The standard deviation (SD) is calculated by the following formula,

$$SD = \sqrt{\frac{\sum_{i=1}^{N_p}\left[(Y_{exp} - Y_{cal})/(Y_{exp})\right]^2}{N_p - 1}} \tag{4.30}$$

Table-4.6. Comparison of present model results with those of earlier models for various stages of pyrolysis (time) at the centre of cylindrical pellet (R = 0.0075 m, T_0 = 303 K, T_f = 660 K)

Time (s)	Temperature		
	PZ	P	JS
0	303	303	303
30	315	316	317
60	371	370	366
90	432	428	414
120	486	477	460
150	528	516	501
200	572	565	552
250	621	597	588
Average Percentage Error		**1.34**	**3.20**
Standard deviation		**0.0193**	**0.0405**

PZ=Pyle & Zaror (1984) (Experimental); P=Present model (Babu & Chaurasia, 2003b); JS=Jalan & Srivastava model (1999)

Table-4.7. Comparison of present model results with those of earlier models for various stages of pyrolysis (time) at the centre of cylindrical pellet (R = 0.0075 m, T_0 = 303 K, T_f = 773 K)

Time (s)	Temperature		
	PZ	P	JS
0	303	303	303
15	312	305	304
30	330	324	323
45	377	362	359
70	454	437	430
100	545	518	503
120	572	562	553
140	629	598	584
Average Percentage Error		**2.89**	**4.06**
Standard deviation		**0.0359**	**0.0511**

PZ=Pyle & Zaror (1984) (Experimental); P=Present model (Babu & Chaurasia, 2003b); JS=Jalan & Srivastava model (1999)

In all the cases it is found that the average percentage error and standard deviation from experimental data are significantly less in the present model (Babu & Chaurasia, 2003b) predictions as compared to the predictions of the model by Jalan & Srivastava (1999). Here again, the difference is slightly more at higher value of the final temperature.

Figs. 4.27, 4.28, 4.29 and 4.30 show the temperature profiles as a function of dimensional radial distance at various times for the final temperature of 643 K. The temperature profiles obtained in the present study (Babu & Chaurasia, 2003b) are in much better agreement with the experimental data of Pyle & Zaror (1984) when compared to the other two models. The values of temperatures at different radial positions for Figs. (4.27) - (4.30) are shown in Tables 4.8-4.11 also for quantitative comparison of the present model (Babu & Chaurasia, 2003b) with the earlier models and the literature data.

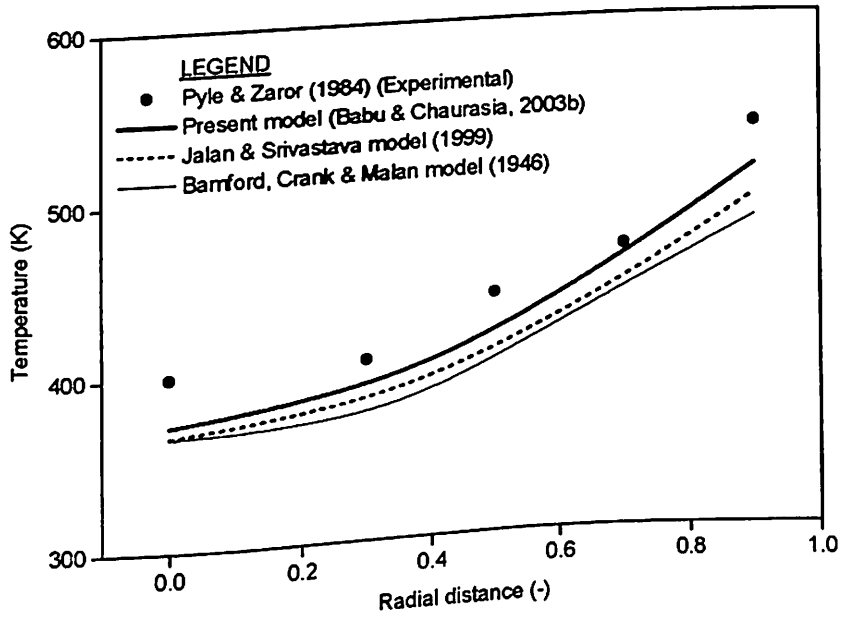

Fig. 4.27. Temperature profile as a function of radial distance (R=0.011 m, T_0=303 K, T_f=643 K, t=2 min).

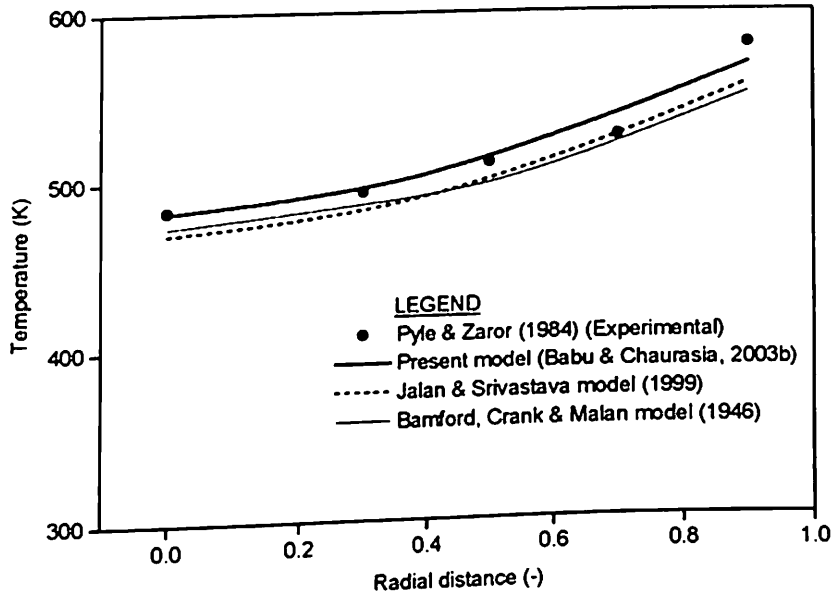

Fig. 4.28. Temperature profile as a function of radial distance (R=0.011 m, T_0=303 K, T_f=643 K, t=4 min).

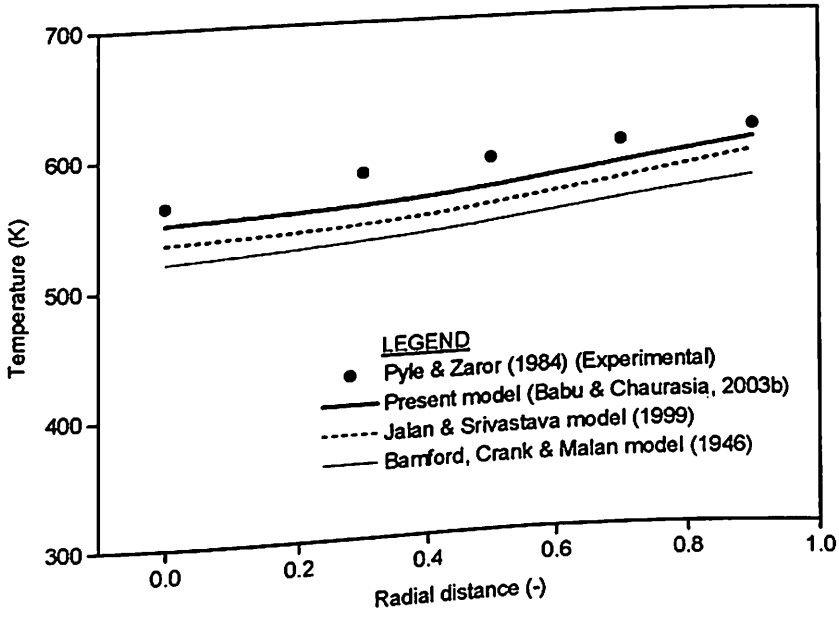

Fig. 4.29. Temperature profile as a function of radial distance (R=0.011 m, T_0=303 K, T_f=643 K, t=6 min).

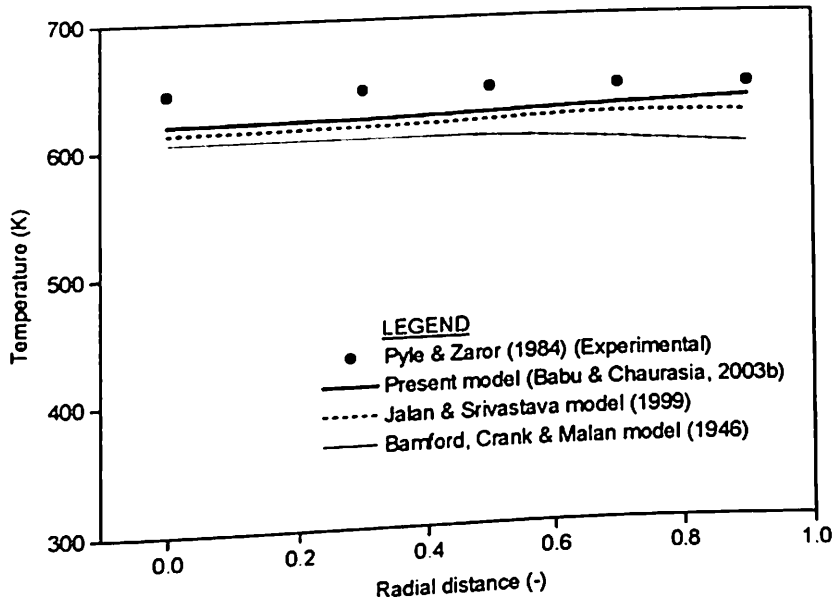

Fig. 4.30. Temperature profile as a function of radial distance (R=0.011 m, T_0=303 K, T_f=643 K, t=11 min).

Table-4.8. Comparison of present model results with those of earlier models for pyrolysis time = 2 min (R = 0.011 m, T_0 = 303 K, T_f = 643 K)

x	Temperature			
	PZ	P	JS	BCM
0	400	372	366	365
0.3	405	388	380	370
0.5	440	416	406	400
0.7	465	458	444	440
0.9	535	510	493	480
Average Percentage Error		**4.57**	**6.95**	**8.43**
Standard deviation		**0.0548**	**0.0794**	**0.0959**

PZ=Pyle & Zaror (1984) (Experimental); P=Present model (Babu & Chaurasia, 2003b);
JS=Jalan & Srivastava model (1999); BCM= Bamford, Crank & Malan model (1946)

Figs. 4.31 and 4.32 show the temperature profiles when the temperature is increased from 643 K to 753 K as a function of radial distance for 2 min and 3 min respectively. In this case also, the temperature profiles obtained in the present study (Babu & Chaurasia, 2003b) are in close agreement with the experimental data of Pyle & Zaror (1984), as shown in Tables 4.12 and 4.13. The average percentage error and standard

Table-4.9. Comparison of present model results with those of earlier models for pyrolysis time = 4 min (R = 0.011 m, T_0 = 303 K, T_f = 643 K)

x	Temperature			
	PZ	P	JS	BCM
0	483	482	469	473
0.3	493	493	480	485
0.5	510	512	499	495
0.7	525	537	524	520
0.9	580	568	556	550
Average Percentage Error		**0.94**	**2.40**	**2.55**
Standard deviation		**0.0156**	**0.0305**	**0.0329**

PZ=Pyle & Zaror (1984) (Experimental); P=Present model (Babu & Chaurasia, 2003b);
JS=Jalan & Srivastava model (1999); BCM= Bamford, Crank & Malan model (1946)

Table-4.10. Comparison of present model results with those of earlier models for pyrolysis time = 6 min (R = 0.011 m, T_0 = 303 K, T_f = 643 K)

x	Temperature			
	PZ	P	JS	BCM
0	563	550	535	520
0.3	583	557	542	530
0.5	590	567	554	540
0.7	600	583	570	555
0.9	610	600	590	570
Average Percentage Error		**3.03**	**5.28**	**7.85**
Standard deviation		**0.0358**	**0.0607**	**0.0883**

PZ=Pyle & Zaror (1984) (Experimental); P=Present model (Babu & Chaurasia, 2003b);
JS=Jalan & Srivastava model (1999); BCM= Bamford, Crank & Malan model (1946)

Table-4.11. Comparison of present model results with those of earlier models for pyrolysis time = 11 min (R = 0.011 m, T_0 = 303 K, T_f = 643 K)

x	Temperature			
	PZ	P	JS	BCM
0	643	619	612	605
0.3	643	620	614	605
0.5	643	623	617	605
0.7	643	627	622	600
0.9	643	632	620	595
Average Percentage Error		**2.92**	**4.04**	**6.38**
Standard deviation		**0.0337**	**0.0457**	**0.0716**

PZ=Pyle & Zaror (1984) (Experimental); P=Present model (Babu & Chaurasia, 2003b);
JS=Jalan & Srivastava model (1999); BCM= Bamford, Crank & Malan model (1946)

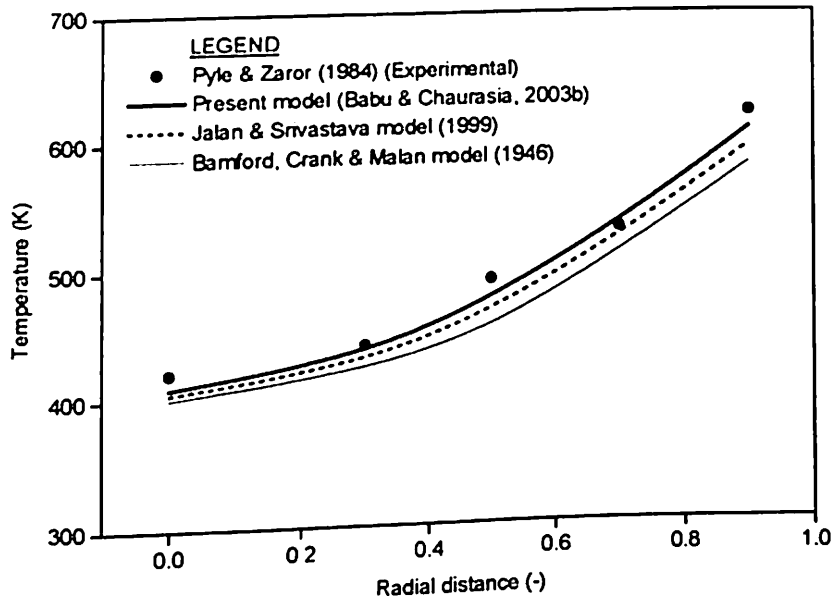

Fig. 4.31. Temperature profile as a function of radial distance (R=0.011 m, T_0=303 K, T_f=753 K, t=2 min).

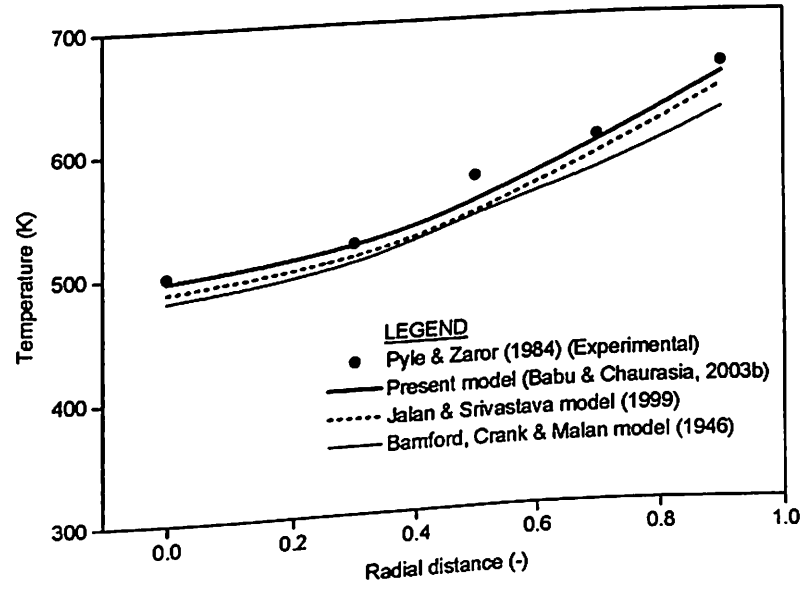

Fig. 4.32. Temperature profile as a function of radial distance (R=0.011 m, T_0=303 K, T_f=753 K, t=3 min).

deviation from the experimental data is less in present the model (Babu & Chaurasia, 2003b) as is evident from Tables 4.4-4.13. Thus, the experimental results of Pyle & Zaror (1984) are in agreement with the predictions of the model presented here.

Table-4.12. Comparison of present model results with those of earlier models for pyrolysis time = 2min (R = 0.011 m, T_0 = 303 K, T_f = 753 K)

x	Temperature			
	PZ	P	JS	BCM
0	420	408	404	400
0.3	440	432	426	420
0.5	490	474	464	450
0.7	530	533	522	510
0.9	620	607	594	580
Average Percentage Error		**2.12**	**3.60**	**5.54**
Standard deviation		**0.0259**	**0.0426**	**0.0644**

PZ=Pyle & Zaror (1984) (Experimental); P=Present model (Babu & Chaurasia, 2003b); JS=Jalan & Srivastava model (1999); BCM= Bamford, Crank & Malan model (1946)

Table-4.13. Comparison of present model results with those of earlier models for pyrolysis time = 3min (R = 0.011 m, T_0 = 303 K, T_f =753 K)

x	Temperature			
	PZ	P	JS	BCM
0	500	496	487	480
0.3	520	515	506	500
0.5	570	548	539	540
0.7	600	594	584	570
0.9	658	649	639	620
Average Percentage Error		**1.60**	**3.26**	**4.78**
Standard deviation		**0.0220**	**0.0384**	**0.0540**

PZ=Pyle & Zaror (1984) (Experimental); P=Present model (Babu & Chaurasia, 2003b); JS=Jalan & Srivastava model (1999); BCM= Bamford, Crank & Malan model (1946)

4.8. Conclusions

- The simulated results obtained from the model developed in the present study (Babu & Chaurasia, 2003b) are in excellent agreement with the experimental data of Pyle & Zaror (1984), in comparison with the mathematical model of Jalan & Srivastava

(1999) and model of Bamford, Crank, & Malan (1946) used by Pyle & Zaror (1984), as is clear from Figs. (4.27)-(4.32) and Tables (4.8)-(4.13).

- The limitation of the model of Pyle & Zaror (1984) is, it assumes first order kinetics for the rate equation and does not consider the secondary reactions.
- The main conclusion resulting from this study concerns the possibility of modeling the pyrolysis of a single biomass particle by coupling the heat transfer equation with the pyrolysis chemical kinetics equation.
- The pyrolysis rate has been simulated by two parallel primary reactions and a third secondary reaction between the volatile and gaseous products and char. The secondary reactions are responsible for carbon enrichment of the final residual.
- The model developed in the present study (Babu & Chaurasia, 2003b) is used for a wide range of temperature from 303-2700 K and of particle radius from 0.00025-0.013 m.
- As the particle size increases, there is an increase in the time required for completion of pyrolysis at a certain pyrolysis temperature and hence the impact of secondary reactions.
- The pyrolysis is fast for zeroth order as compared to first order of reaction 1, as the rates are independent of initial biomass concentration for zeroth order.
- As the constant wall temperature is increased, the pyrolysis is completed faster.
- A simple model as developed in the present study (Babu & Chaurasia, 2003b) with very few realistic and restrictive assumptions combined with the thermal properties variation with temperature, can describe the overall progress of a set of processes of great complexity such as pyrolysis.

- The model developed can be utilized to predict the temperature and concentration profiles for different types of biomass for a wide range of particle dimensions and temperatures.
- As the model is simple and accurate, it is very useful in the design of industrial pyrolysis units.
- Biomass gasification and pyrolysis are the most important areas in renewable energy on which the government in general, and MNES (Ministry of Non-Conventional Energy Sources) in particular are very much focused and lot of policy decisions have been made to encourage the use of these form of energy.

CHAPTER 5

PYROLYSIS OF BIOMASS: IMPROVED MODELS FOR SIMULTANEOUS KINETICS AND TRANSPORT OF HEAT, MASS, AND MOMENTUM

5.1. Introduction

For the last two decades, there is a growing interest exists in the energy sources which can be renewed. The driving force for this development is the increasing concern about the environmental impact of the use of fossil and nuclear sources of energy, besides the increasing consciousness about the limited fossil fuel resources. Biomass is a renewable resource which is a part of the flow of resources occurring naturally and repeatedly in the environment. Biomass can be considered as a relatively clean fuel as it decreases or even eliminates net CO_2 emission and has a low sulphur and NO_x content. Also, the particulate emissions are lower in biomass than in fossil fuels.

The strong interaction between chemical and physical processes in the thermal degradation of biomass samples makes the understanding of conversion dynamics very difficult. The knowledge on kinetics of the pyrolysis of biomass is very significant in designing a fluid-solid gasifier. In spite of these many advantages, little work has been

reported in literature on the mechanistic modeling of such kinetics. This may be attributed to the extreme complexity of pyrolysis process due to the presence of homogeneous and heterogeneous reactions consecutively along with heat, mass, and momentum transfer operations occurring simultaneously during the process. Mathematical and numerical modeling could be very useful tools to assess the role played by different mechanisms.

5.2. Background

A general mathematical model of the pyrolysis process is not only difficult to formulate but also tedious to solve. The complication, as pointed out by Roberts (1970), comes from the formulation of mathematical models correctly accounting for physical and chemical processes and from the acquisition of reliable data to be used for simulations than from computational requirements. Most of the mathematical models published to date use simplifying assumptions for the description of both transport phenomena and chemical processes. Many of the researchers neglected the convective and diffusive transport of volatiles and gases (Anthony & Howard, 1976; Shafizadeh, 1982; Liliedahl & Sjöström, 1998; Beis, Onay, & KoçKar, 2002; Boutin, Ferrer, & Lédé, 2002). In most cases, chemical processes have been modeled according to a one-step, first order, Arrhenius reaction mechanism as mentioned in chapter 4. It is well known that they neither describe the dependence of the char yield on reaction conditions nor the competition between the formation of tars and gases. Consequently, even though they have been widely used to understand fire initiation and growth, they are scarcely useful to optimize reactor design for thermochemical conversion of renewable fuels, where

accurate predictions of product distribution are required. On the other hand, in some cases, the one-step kinetic scheme has been coupled with a rather detailed description of physical processes (Kung, 1972; Kansa, Perlee, & Chaiken, 1977; Villermaux, Antoine, Lede, & Soulignac, 1986; Alves & Figueiredo, 1989; Janse, Westerhout, & Prins, 2000). Non-constant char yield, multistep reaction schemes in conjunction with the models of transport phenomena have also been recently developed (Chan, Kelbon, & Krieger, 1985; Curtis & Miller, 1988; Hastaoglu & Berruti, 1989; Di Blasi, 1993b, 1994a,1994b).

In order to understand the role played by assumptions, usually made in the mathematical description of large sample pyrolysis, models of different complexity are compared in the present study (Babu & Chaurasia, 2003c, 2004a; Chaurasia & Babu, 2003a, 2003b). A generalized mathematical model for pyrolysis of biomass has been developed. Subsequently two simplified models are obtained by making simplified assumptions applicable for practical situations. These models are validated with the experimental data reported in literature. The model being developed considered the effect of specific heat capacity and thermal conductivity of char as a function of temperature. The mean value of convective heat transfer coefficient taken from the data reported in the literature (Pyle & Zaror, 1984; Di Blasi, 1997) is used throughout for low and high values of final temperature respectively, in which the functional dependency on Reynolds & Prandtl numbers is incorporated. The model would enable the prediction of product yields and can be used for different geometries (slab, cylinder and sphere).

5.3. Motivation

Unfortunately, the mathematical complications involved in the numerical solution of

some of the more sophisticated models make them unsuitable for design and prediction purposes, particularly given the difficulties of establishing and incorporating the basic physical and chemical phenomena. Also, the lack of reliable experimental data on the dynamics of biomass pyrolysis under conditions relevant to carbonization (relatively low temperatures and heating rates) makes it difficult to select the appropriately simplified models. It is useful for formulating effective and less expensive computer models, since the numerical solution of general, non-simplified models can be rather time consuming. So in the present study (Babu & Chaurasia, 2004a), taking the practical situations in pyrolysis of biomass into account, two simplified models are proposed from the generalized model by introducing specific assumptions for each of them.

5.4. Description of mathematical model

Using the kinetic scheme as given in chapter 3, three models are proposed in the present study (Babu & Chaurasia, 2004a) under two categories namely, (1) Generalized reference model (Model-I), and (2) Simplified models (Model-II & Model-III).

5.4.1. Generalized reference model (Model-I)

The generalized model incorporated all the possible effects of kinetics, heat transfer, mass transfer, and momentum transfer. The assumptions made in developing this model are as follows:

(1) The thermal and transport properties (porosity, thermal conductivity, specific heat, mass diffusivity) vary with the conversion level.

(2) Heat transfer occurs by all the three modes (i.e., conduction, convection and

radiation).

(3) Gas-phase processes occur under unsteady-state conditions.

(4) Transport of mass takes place by convection and diffusion of volatile species.

(5) Pressure and velocity vary along the porous sample.

(6) Local thermal equilibrium exists between solid matrix and the flowing gases.

(7) The system is one-dimensional.

(8) No moisture content and no particle shrinkage.

Utilizing the kinetic scheme as described in chapter 3 and with the assumptions as stated above, the generalized model (Model-I) is obtained and reported in dimensionless form in Table-5.1. The equations shown in Table-5.1 are obtained with the help of dimensionless groups given in Appendix-C (equations C.1-C.20).

This generalized model, consisting of equations (5.1)-(5.17), which is the most comprehensive one, is named as Model-I (generalized reference model). However, under specific conditions, some of the assumptions made in this generalized model are to be relaxed. Taking the practical situations in pyrolysis of biomass into account, two simplified models are proposed by introducing specific assumptions for each of them. The simulations obtained through this model are used as reference and compared with the simulations obtained using the simplified models. Simplifications are introduced only in the description of the physical processes.

5.4.2. Simplified models

These simplified models include additional assumptions other than those in the generalized reference model (Model-I). Many a times, in practical situations, the generalized model may not give good predictions. In such cases, there is a need to relax

Table-5.1. Mathematical model

Particle model

Mass conservation for biomass, (gases and volatiles)$_1$, (char)$_1$, (gases and volatiles)$_2$ and (char)$_2$:

$$\frac{\partial \overline{C}_B}{\partial t} = -k_1 \overline{C}_B^{n_1} - k_2 \overline{C}_B^{n_1} \tag{5.1}$$

$$\varepsilon'' \frac{\partial \overline{C}_{G1}}{\partial \tau} + \frac{uR}{\alpha}\frac{\partial \overline{C}_{G1}}{\partial x} = \frac{\overline{D}_{G1}}{Le}\left(\frac{b-1}{x}\frac{\partial \overline{C}_{G1}}{\partial x} + \frac{\partial^2 \overline{C}_{G1}}{\partial x^2}\right) + \frac{R^2 k_1 \overline{C}_B^{n_1}}{\alpha} - \frac{\varepsilon'' R^2 k_3 \overline{C}_{G1}^{n_2} \overline{C}_{C1}^{n_3}}{\alpha} \tag{5.2}$$

$$\frac{\partial \overline{C}_{C1}}{\partial t} = k_2 \overline{C}_B^{n_1} - k_3 \overline{C}_{G1}^{n_2} \overline{C}_{C1}^{n_3} \tag{5.3}$$

$$\frac{\partial \overline{C}_{G2}}{\partial t} = k_3 \overline{C}_{G1}^{n_2} \overline{C}_{C1}^{n_3} \tag{5.4}$$

$$\frac{\partial \overline{C}_{C2}}{\partial t} = k_3 \overline{C}_{G1}^{n_2} \overline{C}_{C1}^{n_3} \tag{5.5}$$

Enthalpy:

$$\frac{\partial \theta}{\partial \tau} = \frac{b-1}{x}\frac{\partial \theta}{\partial x} + \frac{\partial^2 \theta}{\partial x^2} + \frac{Q'' R^2 k_1}{\alpha} + \frac{1}{Le}\left(\overline{D}_{G1}\frac{\partial \overline{C}_{G1}}{\partial x}\right)\overline{C}_{pG1}\overline{C}_{B0}\frac{\partial \theta}{\partial x} \tag{5.6}$$

Initial conditions:

$$\tau = 0; \quad \overline{C}_B = 1,\ \overline{C}_{G1} = \overline{C}_{C1} = \overline{C}_{G2} = \overline{C}_{C2} = 0,\ \theta(x,0) = 1 \tag{5.7}$$

Particle boundary conditions:

$$\tau > 0; \quad x = 0, \quad \frac{\partial \overline{C}_{G1}}{\partial x} = 0,\ \frac{\partial \theta}{\partial x} = 0 \tag{5.8)-(5.9}$$

$$\tau > 0; \quad x = 1, \quad \overline{D}_{G1}\left(\frac{\partial \overline{C}_{G1}}{\partial x}\right) = Sh(\overline{C}_{G10} - \overline{C}_{G1}) \tag{5.10}$$

$$\tau > 0; \quad x = 1, \quad \frac{\partial \theta}{\partial x} = -\theta\, Bi_M \tag{5.11}$$

Koufopanos et al. (1991) correlation:

$$h = 0.322(k/l)Pr^{1/3}Re^{0.5} \tag{5.12}$$

Darcy law and state equation:

$$u = -\frac{\phi}{\mu}\frac{\partial p}{\partial x} \tag{5.13}$$

$$p = C_{G1} R_c T / W_m \tag{5.14}$$

Other relations:

$$\varepsilon'' = \varepsilon_0'' + \gamma(1 - \overline{C}_B),\ \phi = \eta\phi_B + (1-\eta)\phi_{C1},\ \eta = C_B / C_{B0} \tag{5.15)-(5.17}$$

Conversion of biomass:

$$X = \frac{\overline{C}_{B_0} - \left[\left(\sum_{i=1}^{N} \overline{C}_B\right)\Big/(N+1)\right]}{\overline{C}_{B_0}} \tag{5.18}$$

some of the assumptions made in the generalized model. Starting from the generalized model, the following two simplified models are proposed in the present study (Babu & Chaurasia, 2004a) for specific cases.

5.4.2.1. First Simplified Model (Model-II)

In most of the practical situations of industrial pyrolysis reactions, the contributions of the bulk motion of gases inside the pores of the particle are insignificant. Because the resistance offered by the pores in the solid particle is so high, that the transport of these gases would take place essentially by diffusion mechanism but not by bulk motion (i.e. convection). Taking this situation into consideration, the first simplified model (Model-II) is proposed by making an additional assumption that there is no bulk motion contribution (i.e. convective transport is neglected) to the temperature profile and product yield predictions. In this treatment, a conservation equation for the mass concentration of (gases and volatiles)$_1$ [equation (5.2)] is modified by neglecting the second term on left hand side. Hence, the first simplified model (Model-II) consists of equations (5.1)-(5.12) and (5.15).

5.4.2.2. Second Simplified Model (Model-III)

Analogous to the above momentum transport, the corresponding convective part in heat transport of the gases within the particle also does not contribute significantly for the reasons explained above. As the temperatures are also not too high so as to have the radiation effects, even the radiative heat transfer of gases within the particles could also be neglected. In addition, as dense particles and various kinds of hard wood are generally used in pyrolysis of biomass gasification, the effect of porosity of the solid pellet is insignificant. And hence the second simplified model (Model-III) is proposed

based on the following two assumptions concerning the practical applications: (1) The basic mode of transfer inside the solid particle in the process of pyrolysis takes place by conduction heat transfer only. (2) The effect of porosity of the solid particle is negligible. Based on these assumptions, conservation equation for mass concentration of (gases and volatiles)$_1$ [equation (5.2)] and heat transfer model [equation (5.6)] respectively become:

$$\frac{\partial \overline{C}_{G1}}{\partial t} = k_1 \overline{C}_B^{n_1} - k_3 \overline{C}_{G1}^{n_2} \overline{C}_{C1}^{n_3} \tag{5.19}$$

$$\frac{\partial \theta}{\partial \tau} = \frac{b-1}{x}\frac{\partial \theta}{\partial x} + \frac{\partial^2 \theta}{\partial x^2} + \frac{Q'' R^2 k_1}{\alpha} \tag{5.20}$$

So the second simplified model (Model-III) consists of equations (5.1), (5.19), (5.3)-(5.5), (5.20), (5.7), (5.9), (5.11), and (5.12). Interestingly, this is similar to the model proposed (Babu & Chaurasia, 2003b) as given in chapter 4, which means that the generalized reference model reduced to the model proposed under specific conditions.

Simulations are carried out considering different particle geometries (slab, cylinder and sphere) of equivalent radius ranging from 0.0001-0.017 m, and temperature ranging from 303-2800 K. The values of various parameters employed in the present study (Babu & Chaurasia, 2004a) are given in Appendix-C. The Computer Codes in C ++ for Model-I and Model-II are given in Appendix-D while for Model-III in Appendix-B.

5.5. Results and discussion

5.5.1. Model validation and comparison

The simultaneous kinetic, mass, heat, and momentum transfer model developed in the present study (Babu & Chaurasia, 2004a) is compared with the experimental data

reported by Pyle & Zaror (1984), model of Bamford, Crank, & Malan (1946) used by Pyle & Zaror (1984) and the model developed by Jalan & Srivastava (1999). Pyle & Zaror (1984) carried out the experimental studies on the course of pyrolysis of cylindrical samples of wood. They performed the experiments in an inert constant temperature environment, and measured the instantaneous sample weight and radial temperature profile.

The major constituents of wood are cellulose, hemi-cellulose and lignin. There is some variation in the relative abundance of these constituents in different species of wood but as an approximate guideline, cellulose is taken to be 50% and the other two 25% each by dry weight. Shafizadeh (1982) has studied the pyrolysis of cellulose at various temperatures. At temperature less than or equal to 673 K, the dominant process is the reduction in degree of polymerization and diffusion and convection effects are negligible. In the second step, at temperatures above 673 K, there is formation of char, tar, and gaseous products and diffusion & convection effects are predominant. Hence, a mean value of 8.4 W m^{-2} K^{-1} (Pyle & Zaror, 1984) [in which the dependence on Reynolds number and Prandtl number is incorporated and estimated employing equation (5.12)] is used throughout for convective heat transfer coefficient at the final temperature less than or equal to 673 K. Similarly, a mean value of 20.0 W m^{-2} K^{-1} (Di Blasi, 1997) [again employing equation (5.12)] is used throughout for convective heat transfer coefficient at the final temperature greater than 673 K. It may be noted that, all the parameters used to test the present models are either independently and directly estimated or are taken from the literature.

Fig. 5.1 shows the temperature profile as a function of time at the centre (i.e. x=0) of

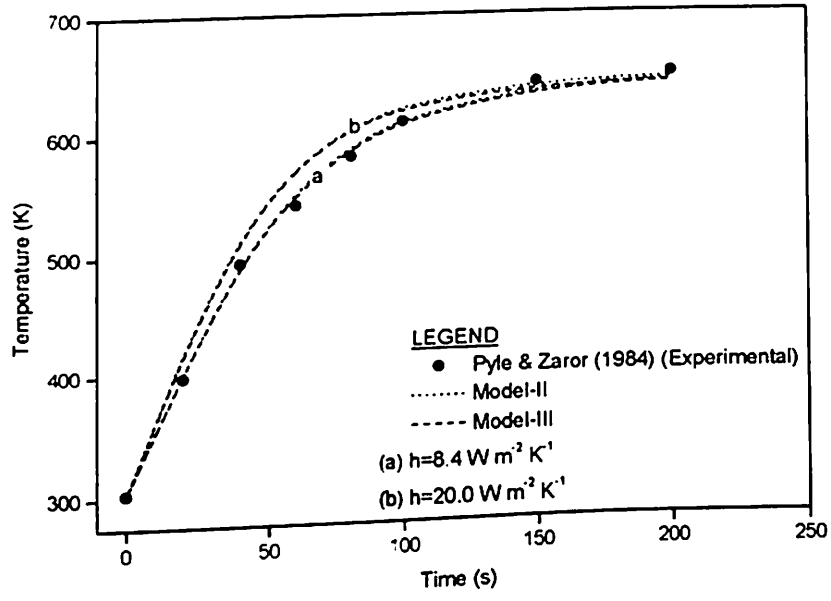

Fig. 5.1. Temperature profile as a function of time at the centre of the cylindrical pellet for different values of h (R=0.003 m, T_0=303 K, T_f=643 K, x=0)

the cylindrical pellet of radius 0.003 m. It is found that both the simplified models (Model-II and Model-III) are in good agreement with the experimental data for lower value of h (8.4 W m^{-2} K^{-1}) as the final temperature is less than 673 K. This is compared with the profiles obtained by Jalan & Srivastava (1999) and the experimental data obtained by Pyle & Zaror (1984) at the centre of the cylindrical pellet as shown in Fig. 5.2. It is found that all the models (Model-I, II & III) developed in the present study (Babu & Chaurasia, 2004a) are in excellent agreement with the experimental data better than the agreement with the model of Jalan & Srivastava (1999).

The temperature profile as a function of time for the cylindrical pellet of radius 0.0075 m is shown in Fig. 5.3. It is found that both the models (Model II and Model III) are in good agreement with the experimental data for higher value of h (20.0 W m^{-2} K^{-1}) as the final temperature is greater than 673 K. Fig. 5.4 shows the comparison of

experimental data of Pyle & Zaror (1984) with the results of temperature as a function of time for cylindrical pellet of radius 0.0075 m using Models-I, II, III and the model

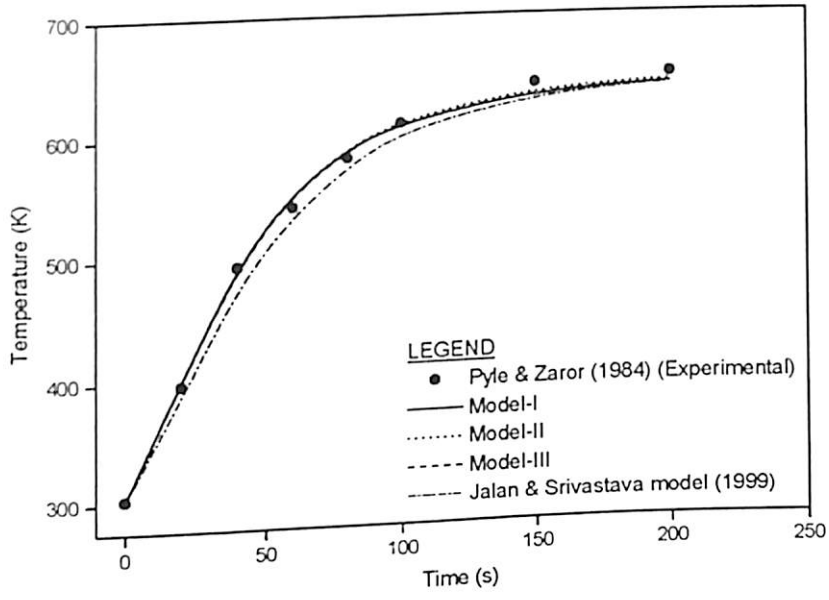

Fig. 5.2. Temperature profile as a function of time at the centre of the cylindrical pellet (R=0.003 m, T_0=303 K, T_f=643 K, x=0, h=8.4 W m^{-2} K^{-1}).

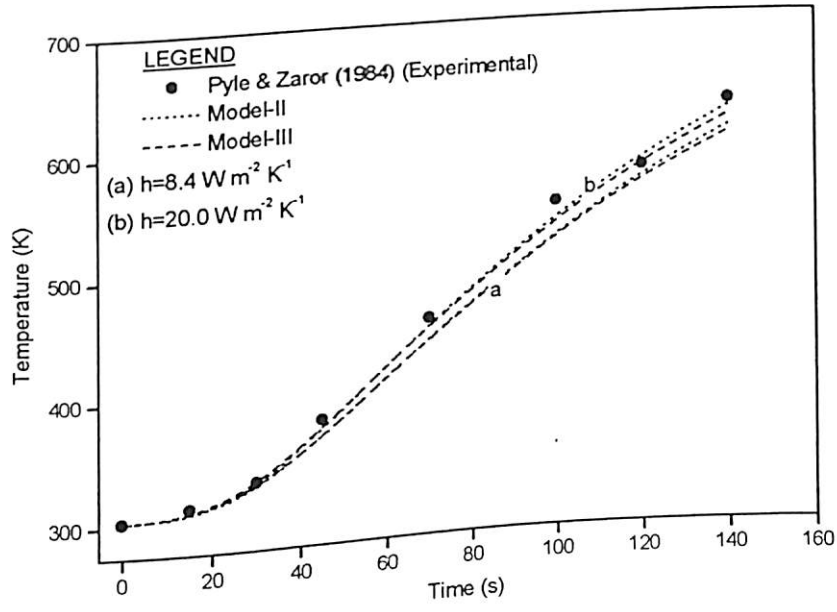

Fig. 5.3. Temperature profile as a function of time at the centre of the cylindrical pellet for different values of h (R=0.0075 m, T_0=303 K, T_f=773 K, x=0).

of Jalan & Srivastava (1999). Here also it is found that the models developed in the present study (Babu & Chaurasia, 2004a) are in good agreement with the experimental data better than the agreement with the model of Jalan & Srivastava (1999). It may be noted that there is a deviation from the experimental data and Model-I predictions at higher values of temperature and pyrolysis time. In fact, Model-I under-predicts the experimental data. This is due to the fact that at higher values of temperature and pyrolysis time, cellulose polymers begin to decompose rapidly, suggesting that secondary pyrolysis reactions are important (Jalan & Srivastava, 1999). As the pyrolysis progresses, the temperature inside the particle and also the velocity of the gases that are formed will increase. So it escapes the cellulose matrix faster and secondary reactions of the volatiles produced by primary reactions cannot take place as the residence time is very less. In Model-I, both convection and diffusion effects are considered and hence the under-prediction of particle temperature at higher values of pyrolysis time. So there is a deviation at higher value of temperature and pyrolysis time from the experimental data using Model-I. However, in Model-II it is assumed that there is no bulk motion contribution and in Model III it is assumed that heat transfer takes place by conduction only, both of which lead to the prediction of an increase in temperature of particle in the simulated results at higher value of pyrolysis time. In fact, volatiles and gases that are formed by primary reaction get sufficient time to undergo secondary pyrolysis reaction resulting in the formation of volatiles and gases of different composition and this leads to an increase in temperature at higher values of pyrolysis time. This is the reason why Model-II and Model-III predict the results well even at high pyrolysis time matching with the experimental data.

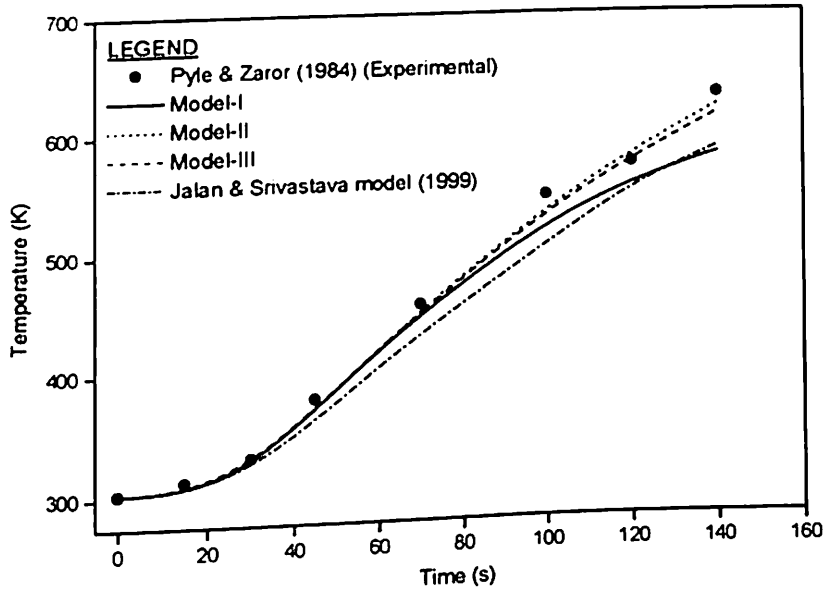

Fig. 5.4. Temperature profile as a function of time at the centre of the cylindrical pellet (R=0.0075 m, T_0=303 K, T_f=773 K, x=0, h=20.0 W m^{-2} K^{-1}).

The simulated results used in Figs. 5.2 and 5.4 are given in Table-5.2 and Table-5.3 respectively for quantitative comparison of present models with the model of Jalan & Srivastava (1999) and experimental data of Pyle & Zaror (1984). In all the cases, it is found that the average percentage error and standard deviation from experimental data are significantly less in the prediction of present models as compared to the predictions of the model of Jalan & Srivastava (1999). It may be noted from Table-5.3 that though the *SD* for Model-I (=0.0392) is slightly higher than that for Model-II and III (=0.0186 and 0.0194 respectively), it is still much less when compared to *SD* (=0.0511) of the model of Jalan & Srivastava (1999).

Fig. 5.5 shows the temperature profile as a function of dimensionless radial distance for the final temperature of 643 K at the pyrolysis time of 4 min for particle radius of 0.011 m. In this case also it is observed that the predictions of present models are in

Table-5.2 Comparison of present models results with those of earlier models for various stages of pyrolysis (time) at the centre of cylindrical pellet (R = 0.003 m, T_0 = 303 K, T_f = 643 K)

Time (s)	Temperature (K)				
	PZ	Model-I	Model-II	Model-III	JS
0	303	303	303	303	303
20	397	401	401	400	387
40	493	495	495	493	478
60	541	553	554	552	533
80	581	589	590	588	574
100	609	609	612	610	602
150	641	633	636	634	630
200	648	640	642	640	639
Epa		**0.93**	**0.93**	**0.75**	**1.56**
SD		**0.0125**	**0.0125**	**0.0106**	**0.0189**

PZ=Pyle & Zaror (1984) (Experimental); JS=Jalan & Srivastava model (1999)

Table-5.3. Comparison of present models results with those of earlier models for various stages of pyrolysis (time) at the centre of cylindrical pellet (R = 0.0075 m, T_0 = 303 K, T_f = 773 K)

Time (s)	Temperature (K)				
	PZ	Model-I	Model-II	Model-III	JS
0	303	303	303	303	303
15	312	304	304	305	304
30	330	325	325	327	323
45	377	368	368	369	359
70	454	447	449	448	430
100	545	521	534	531	503
120	572	556	580	575	553
140	629	579	619	612	584
Epa		**2.89**	**1.56**	**1.66**	**4.06**
SD		**0.0392**	**0.0186**	**0.0194**	**0.0511**

PZ=Pyle & Zaror (1984) (Experimental); JS=Jalan & Srivastava model (1999)

better agreement with experimental data (Pyle & Zaror, 1984) at low value of h (8.4 W m^{-2} K^{-1}) as the final temperature is less than 673 K. The temperature profiles obtained in the present study (Babu & Chaurasia, 2004a) are in much better agreement with the experimental data (Pyle & Zaror, 1984) when compared to the other models (Bamford, Crank, & Malan, 1946; Jalan & Srivastava, 1999) as shown in Fig. 5.6. The temperature profile at t =11 min keeping the same particle size of 0.011 m is shown in Fig. 5.7. At

this high value of pyrolysis time, it is found that the first simplified model (Model-II) predictions are in excellent agreement with the experimental data (Pyle & Zaror, 1984)

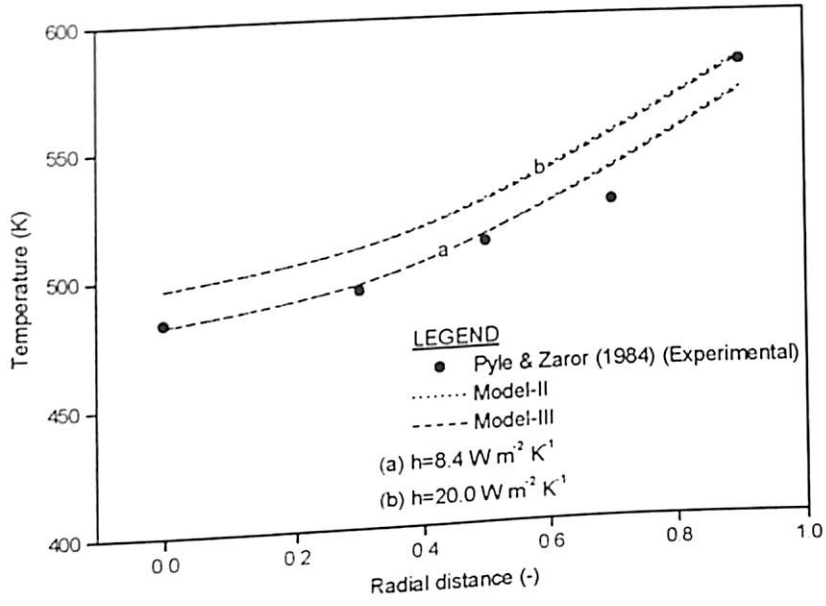

Fig. 5.5. Temperature profile as a function of radial distance for different values of h (R=0.011 m, T_0=303 K, T_f=643 K, t=4 min).

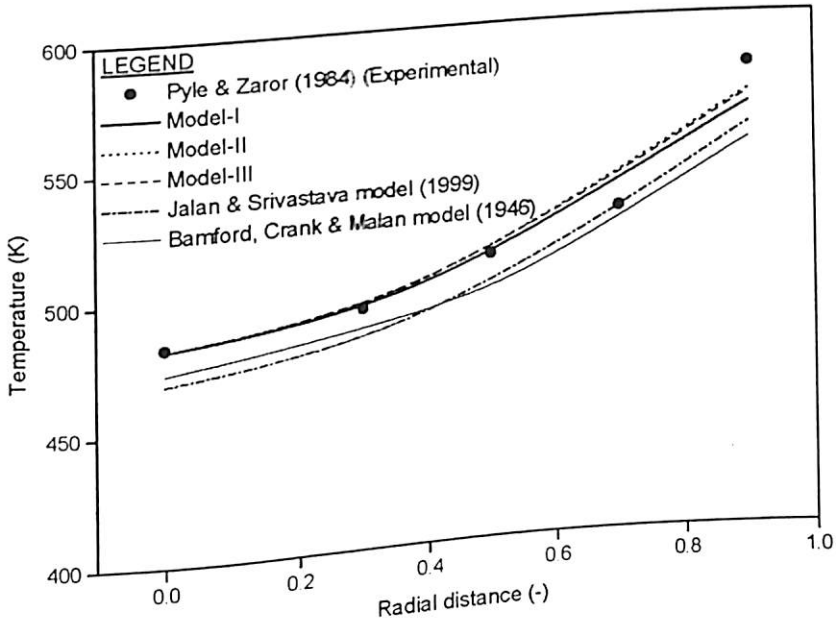

Fig. 5.6. Temperature profile as a function of radial distance (R=0.011 m, T_0=303 K, T_f=643 K, t=4 min, h=8.4 W m^{-2} K^{-1}).

as compared to the predictions with other models for the reasons mentioned above. The simulated results at different radial positions for Figs. 5.6 and 5.7 are shown in Table-5.4 and Table-5.5 respectively for quantitative comparison of the present model with the earlier models and the literature data, which substantiates the better predictions using the present models. However, it may be noted both from Fig. 5.7 & Table-5.5 that Model-I

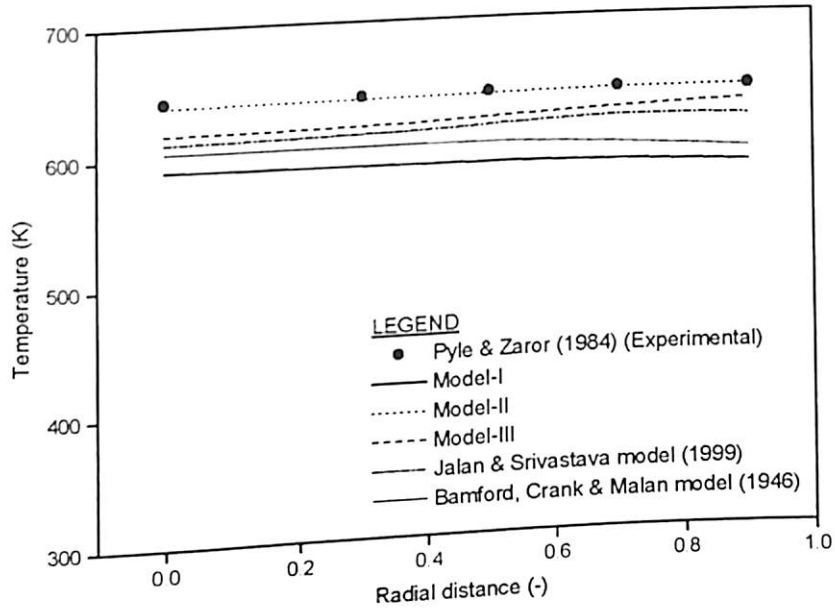

Fig. 5.7. Temperature profile as a function of radial distance (R=0.011 m, T_0=303 K, T_f=643 K, t=11 min, h=8.4 W m^{-2} K^{-1}).

Table-5.4. Comparison of present models results with those of earlier models for pyrolysis time = 4 min (R = 0.011 m, T_0 = 303 K, T_f = 643 K)

x	Temperature (K)					
	PZ	Model-I	Model-II	Model-III	JS	BCM
0	483	482	482	482	469	473
0.3	493	492	493	493	480	485
0.5	510	510	512	512	499	495
0.7	525	535	538	537	524	520
0.9	580	564	569	568	556	550
Epa		**1.01**	**0.94**	**0.94**	**2.40**	**2.55**
SD		**0.0168**	**0.0156**	**0.0156**	**0.0305**	**0.0329**

PZ=Pyle & Zaror (1984) (Experimental); **JS**=Jalan & Srivastava model (1999);
BCM= Bamford, Crank & Malan model (1946)

under-predicts the experimental data for the reasons explained earlier as this correspond to a condition of higher value of pyrolysis time. Figs. 5.8 and 5.9 show the temperature profiles when the temperature is increased from 643 K to 753 K as a function of radial distance for a time period of 2 min. In this case also, the temperature profiles obtained in the present models are in better agreement with the experimental data (Pyle & Zaror,

Table-5.5. Comparison of present models results with those of earlier models for pyrolysis time = 11 min (R = 0.011 m, T_0 = 303 K, T_f = 643 K)

x	Temperature (K)					
	PZ	Model-I	Model-II	Model-III	JS	BCM
0	643	591	640	619	612	605
0.3	643	590	641	620	614	605
0.5	643	589	641	623	617	605
0.7	643	587	642	627	622	600
0.9	643	584	643	632	620	595
Epa		**8.52**	**0.247**	**2.92**	**4.04**	**6.38**
SD		**0.0953**	**0.0033**	**0.0337**	**0.0457**	**0.0716**

PZ=Pyle & Zaror (1984) (Experimental); JS=Jalan & Srivastava model (1999);
BCM= Bamford, Crank & Malan model (1946)

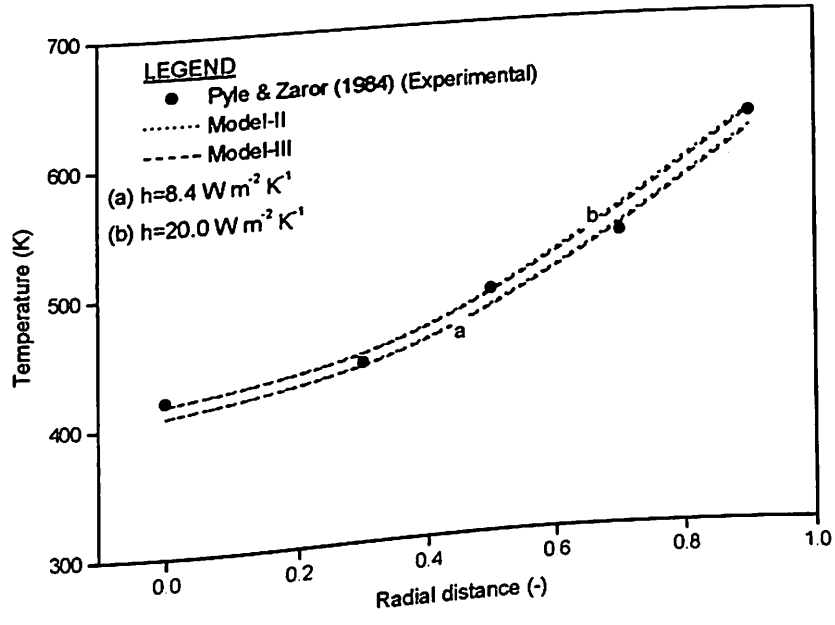

Fig. 5.8. Temperature profile as a function of radial distance for different values of h (R=0.011 m, T_0=303 K, T_f=753 K, t=2 min).

1984), which is also substantiated by the E_{pa} and SD (as given by equations 4.29 and 4.30) values in Table-5.6. Fig. 5.10 shows the conversion profile as a function of

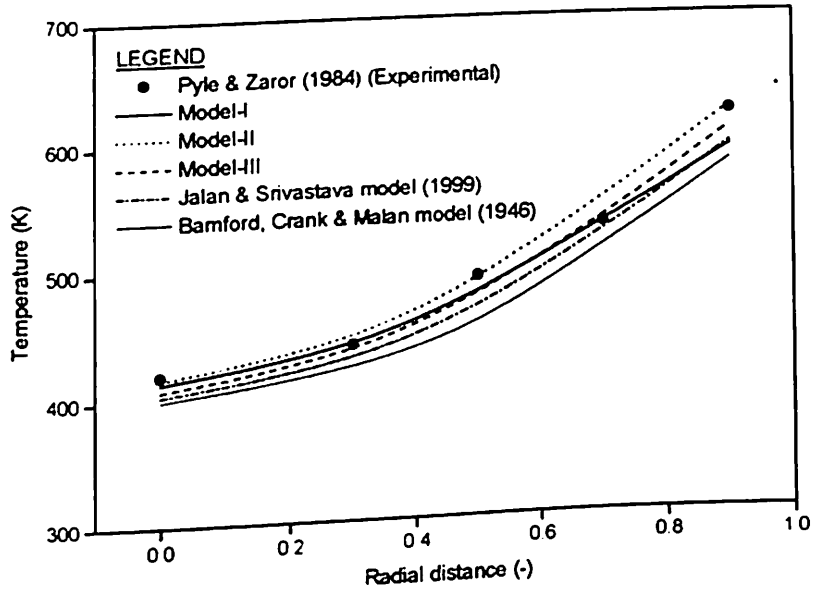

Fig. 5.9. Temperature profile as a function of radial distance (R=0.011 m, T_0=303 K, T_f=753 K. t=2 min, h=20.0 W m^{-2} K^{-1}).

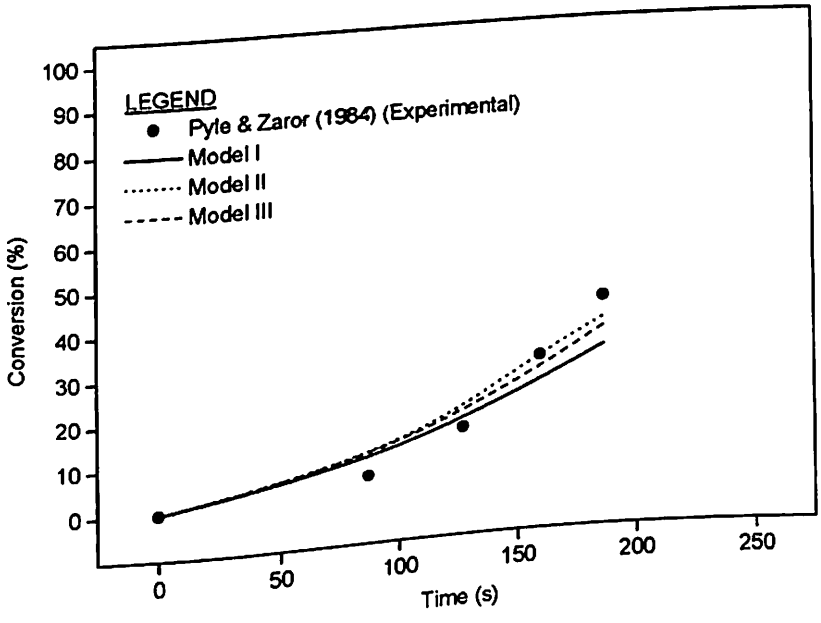

Fig. 5.10. Conversion profile as a function of time with cylindrical pellet (R=0.011 m, T_0=303 K, T_f=753 K).

time with the cylindrical pellet of radius 0.011 m and final temperature of 753 K. As can be seen from the figure, the models developed are in better agreement with the experimental data for conversion profile also. The average percentage error and standard deviation from experimental data is less in the simplified models (Model-II and Model-III) as seen from Tables 5.2-5.6 also. Though all the three models proposed in the present study (Babu & Chaurasia, 2004a) performed well under varied conditions, it is observed that the predictions of simplified models (Model-II and Model-III) are in excellent agreement with the experimental data as compared to Model-I predictions in all the situations.

Table-5.6. Comparison of present models results with those of earlier models for pyrolysis time = 2min (R = 0.011 m, T_0 = 303 K, T_f = 753 K)

x	Temperature (K)					
	PZ	Model-I	Model-II	Model-III	JS	BCM
0	420	414	417	408	404	400
0.3	440	437	442	432	426	420
0.5	490	476	486	474	464	450
0.7	530	530	549	533	522	510
0.9	620	591	623	607	594	580
Epa		**1.93**	**1.59**	**2.12**	**3.60**	**5.54**
SD		**0.0285**	**0.0190**	**0.0259**	**0.0429**	**0.0644**

PZ=Pyle & Zaror (1984) (Experimental); JS=Jalan & Srivastava model (1999);
BCM= Bamford, Crank & Malan model (1946

5.5.2. Simulation results

The improved validated model, which is best suited for wide range of operating conditions, is utilized to investigate the influence of particle size & particle shape on the time to reach 100 % conversion and product distribution. The effect of temperature on particle size and conversion time is studied by considering wide ranges of particle radii and temperatures. As the pyrolysis reactions are exothermic and/or endothermic in different operating range of temperatures, the understanding on the effect of heat of

reaction in the reactor is equally important. So, extensive simulations are also carried out to examine the effect of heat of reaction number on the biomass conversion, concentration and temperature profiles considering both the exothermic and endothermic reactions. Simulations are also carried out to study the effect of density of biomass.

5.5.2.1. Effect of particle size and shape on conversion time and product yields

Fig. 5.11 shows the time to reach 100% conversion for the three different particle shapes when a surface temperature of 643 K has been imposed. The spherical particle has a shortest conversion time as can be expected based on higher surface to volume ratio. Geometrically the sphere has got a more heat absorbing capacity as compared to cylinder and slab and it is the least for slab. Mathematically it is reflected in the value of

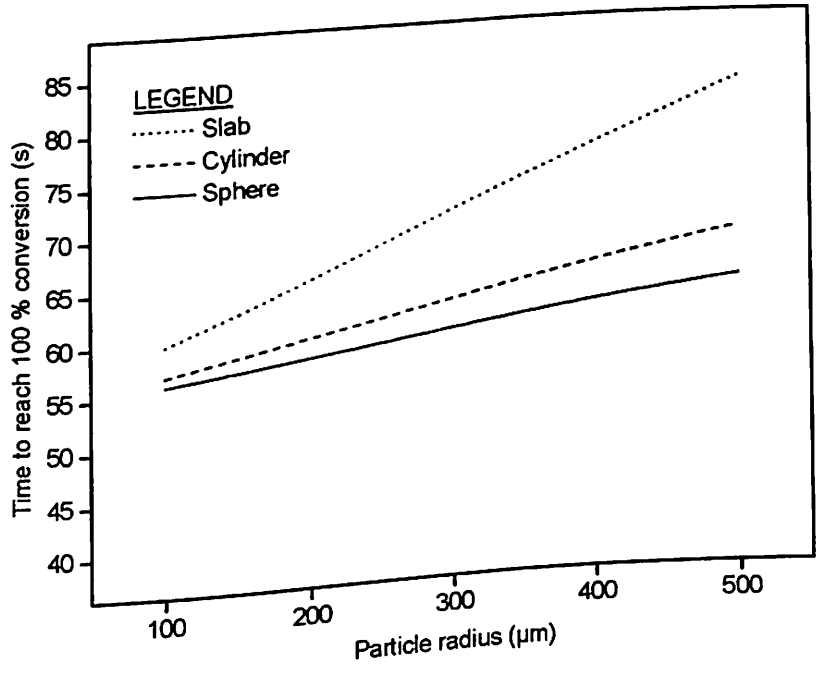

Fig. 5.11. Time to reach 100 % conversion as a function of particle for different geometries (T_0=303 K, T_f=643 K).

parameter b (b=1, 2 and 3 for slab, cylinder and sphere respectively) in the model equations (5.2) and (5.6) and hence resulted in the observed trends. A significant increase in conversion time is observed for slab as compared to cylinder and sphere.

Figs. 5.12-5.14 are concerned with the product distribution corresponding to the final temperature of 643 K. They show a decrease in the yield of (volatiles & gases)$_1$, with an increase in the yield of (char)$_1$ and (volatiles & gases)$_2$ or (char)$_2$ as particle radius is increased. The yield of (volatiles & gases)$_1$ is maximum for sphere and is the least for slab while the yield of (char)$_1$ and (volatiles & gases)$_2$ or (char)$_2$ is more for slab and is the least for sphere. This is due to the decrease in average particle temperature at various radial positions as the particle radius is increased. This decrease in temperature will be different for various shapes as a result of different heat of penetration and will be more for slab & least for sphere due to higher surface/volume ratio as mentioned above.

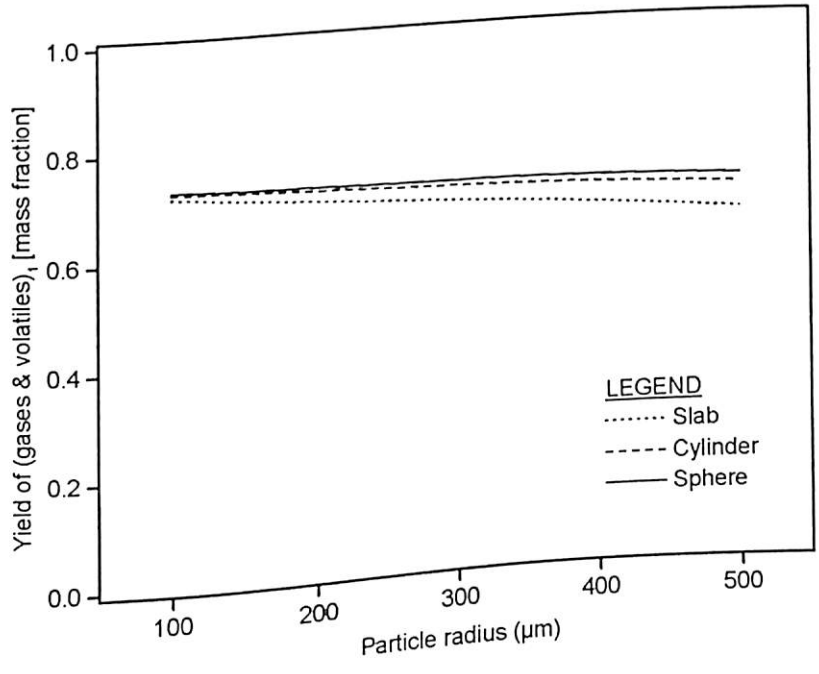

Fig. 5.12. Yield of (gases & volatiles)$_1$ as a function of particle radius for different geometries (T_0=303 K, T_f=643 K).

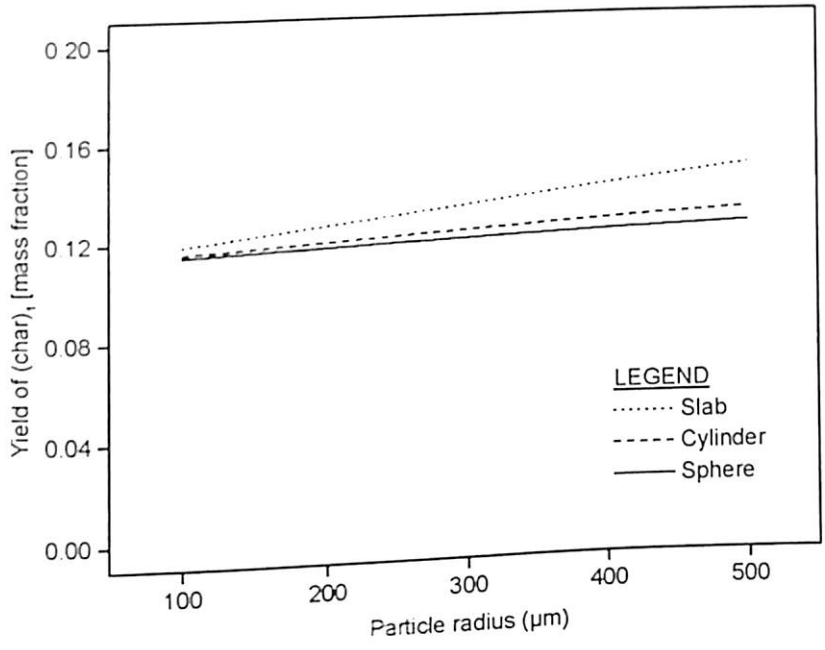

Fig. 5.13. Yield of $(char)_1$ as a function of particle radius for different geometries (T_0=303 K, T_f=643 K).

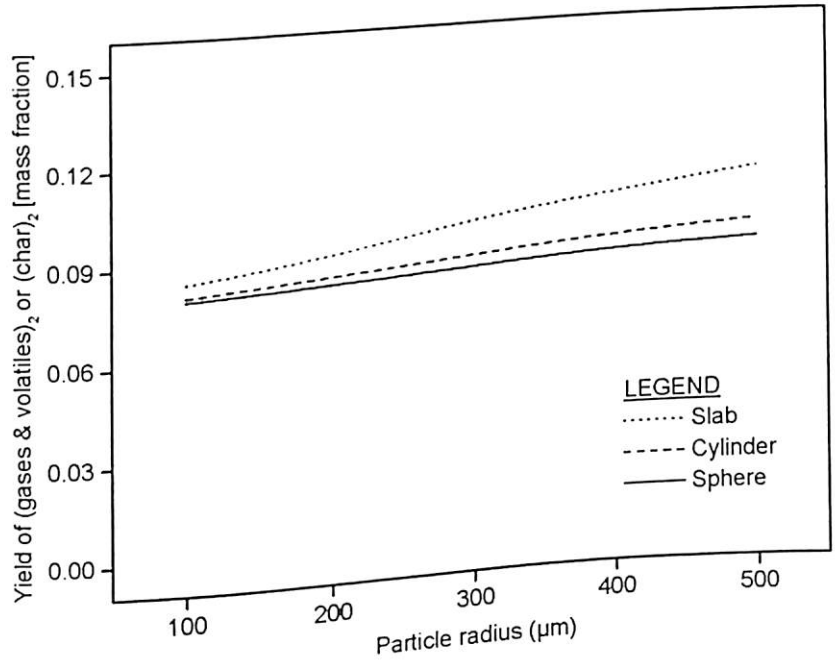

Fig. 5.14. Yield of $(gases\ \&\ volatiles)_2$ or $(char)_2$ as a function of particle radius for different geometries (T_0=303 K, T_f=643 K).

The decrease in temperature favors the char yield as mentioned by Shafizadeh (1982). As the decrease in temperature is more for slab, the yield of $(char)_1$ and $(volatiles \& gases)_2$ or $(char)_2$ (Figs. 5.13 & 5.14) is more for slab as compared to other geometries.

The effect of particle radius on pyrolysis products is shown in Fig. 5.15. Extensive simulations are carried out for particle radius ranging from 0.0001 - 0.02 m for final temperature of 900 K. The formation of $(char)_1$ and $(volatiles \& gases)_2$ or $(char)_2$ are favored at the expense of decrease in $(volatiles \& gases)_1$ formation as the particle radius is increased. This is due to the high residence time of volatiles & gases within the particle, thicker char layer and slow rates of formation of pyrolysis products. The yield of $(volatiles \& gases)_1$ decreases up to a particle radius of 0.015 m and then again increases at the expense of decrease in $(char)_1$ formation. This is a consequence of successively higher temperatures at the surface due to increase in the pyrolysis time as particle size is increased. On the whole, the increase in particle radius favors the attainment of larger yields of $(char)_1$ at the expense of decrease in the formation of other two products.

Similar trends are observed with slab and sphere geometries shown along with cylinder geometry in Fig. 5.16. A significant increase in pyrolysis time is observed as the particle size is increased. A spherical particle has the shortest conversion time, as can be expected based on the higher surface-to-volume ratio. However, at small particle radius (typically less than 1 mm), the rate of reaction becomes dominant and the different particle shapes show nearly equal conversion times. A comparison of concentration of the products of primary and secondary pyrolysis reactions indicates that the activity of the primary reactions is significant as compared to the activity of secondary reactions.

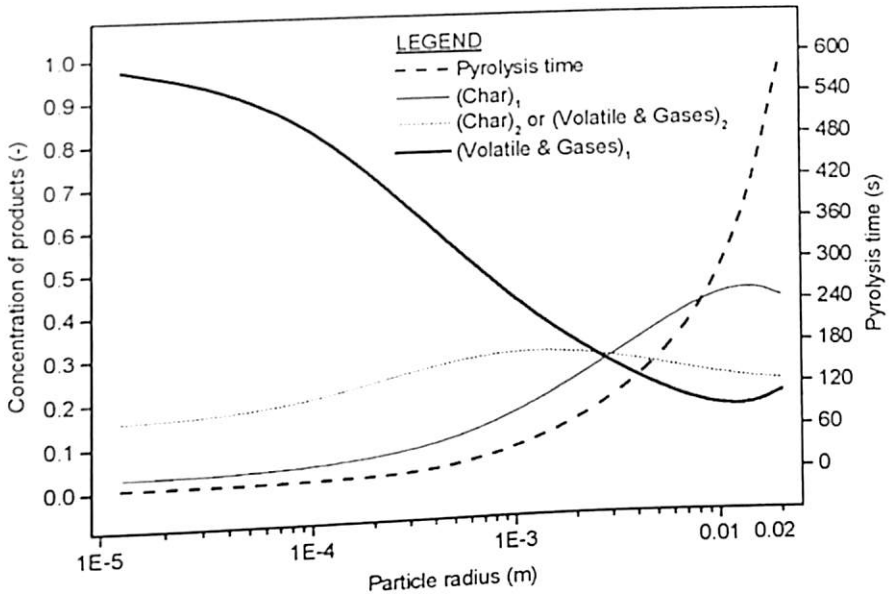

Fig. 5.15. Average concentration of products and pyrolysis time as functions of particle radius with cylindrical pellet (T_0=303 K, T_f=900 K).

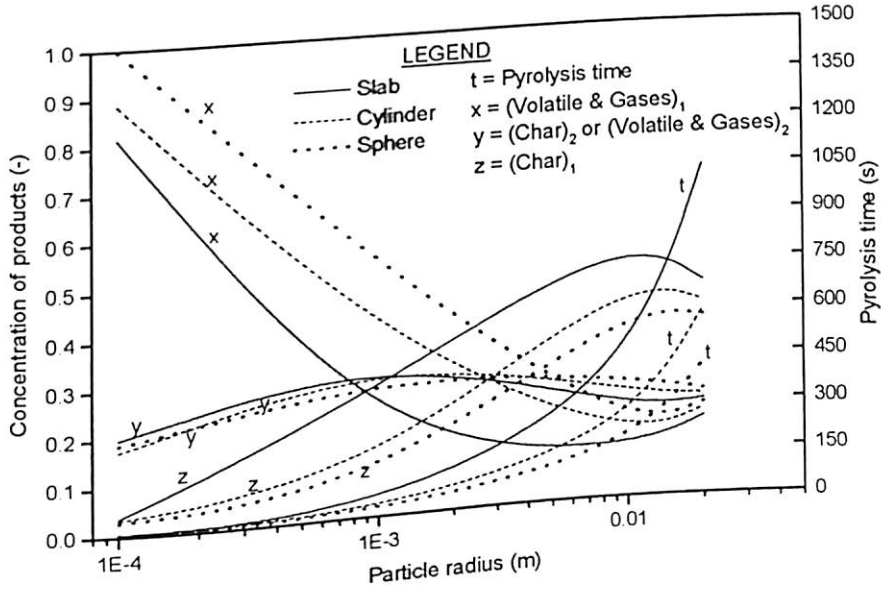

Fig. 5.16. Average concentration of products and pyrolysis time as functions of particle radius (R) with slab, cylinder and sphere (T_0=303 K, T_f=900 K).

5.5.2.2. Effect of Heat of reaction number on biomass conversion

The effect of Q'' on the progress of pyrolysis of biomass is shown in Fig. 5.17 for R=0.003 m, where the biomass conversion is plotted against the pyrolysis time for different values of Q''. A negative value stands for exothermic reaction while positive value represents endothermic reaction. It is observed from the figure that the biomass conversion is more sensitive to the variation of Q'' when it is negative than when it is positive. The biomass conversion increases with pyrolysis time for a given value of Q''.

The biomass conversion at the early stages (up to about 40 s) of the pyrolysis reaction does not appear to be profoundly affected by different values of Q''. However, the effect

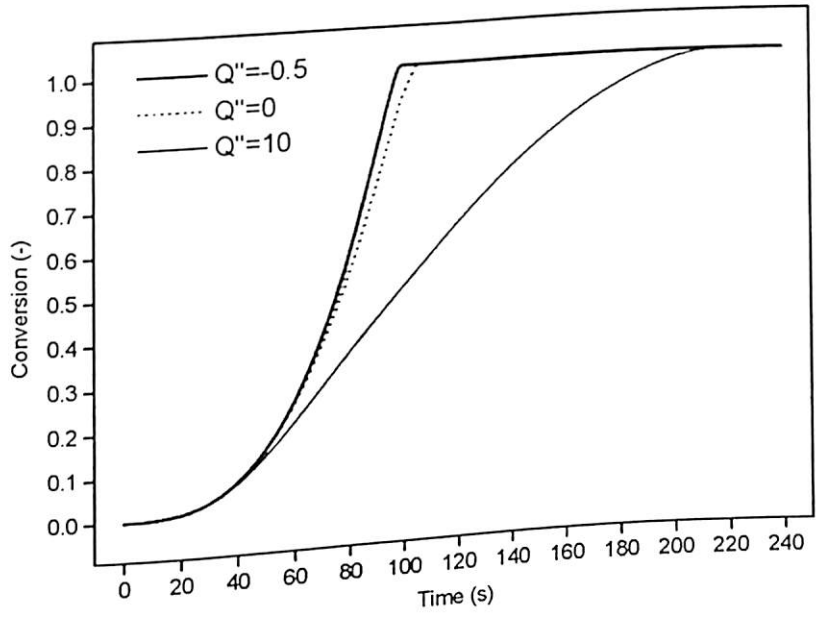

Fig. 5.17. Effect of Q" on conversion of biomass (R=0.003 m, T_0=303 K, T_f=643 K).

of Q'' on biomass conversion becomes significant at a later stage. For Q'' = -0.5, the slope of the curve is very steep representing a very abrupt and fast increase in conversion with pyrolysis time. This is due to the fact that the progress of the pyrolysis reaction is

accelerated not only by heat conduction, convection, and radiation from the surrounding environment, but also by the heat generated inside the particle from the exothermic reaction. For endothermic reaction (Q''=10), the sensible heat content of the particle is consumed as the heat of reaction. Therefore, heating of particle from the surrounding environment would not be as effective as the exothermic reaction in raising the temperature of the particle. Thus, the rate of increase in the conversion is relatively low at any given reaction time. The conversion of biomass is almost complete at t =97.63 s for Q''=-0.5 and after this time the conversion reaches its asymptotic value and becomes constant then on, but for Q''=10, the conversion is only 48 % even at t= 97.63 s, completes (100%) at 213.65 s, and constant then onwards. The value of Q''=0 (i.e., zero heat of reaction initially) does not imply an isothermal process, since heat transfer from the surrounding environment would still significantly affect the rate of pyrolysis reaction, and hence the steep increase in conversion with increase in pyrolysis time. Similar trends are observed for particle radius of 0.0025 m also as shown in Fig. 5.18.

5.5.2.3. Effect of Heat of reaction number on temperature profile

The temperature profiles in the solid particle of biomass for the cases of Q''=10 and Q''=-0.5 at various stages of pyrolysis are shown in Figs. 5.19 and 5.20 respectively for R=0.003 m. It is seen that for the case of Q''=10, the temperature increases with radial distance. The temperature is minimum at the centre and maximum at the wall of the particle. Note that the temperature gradient, $d\theta/dx$, is consistently positive or equal to zero. In other words, the particle temperature never exceeds the final temperature of 643 K. This situation is termed as '*heat-transfer-controlled reaction*' (Miyanami, Fan,

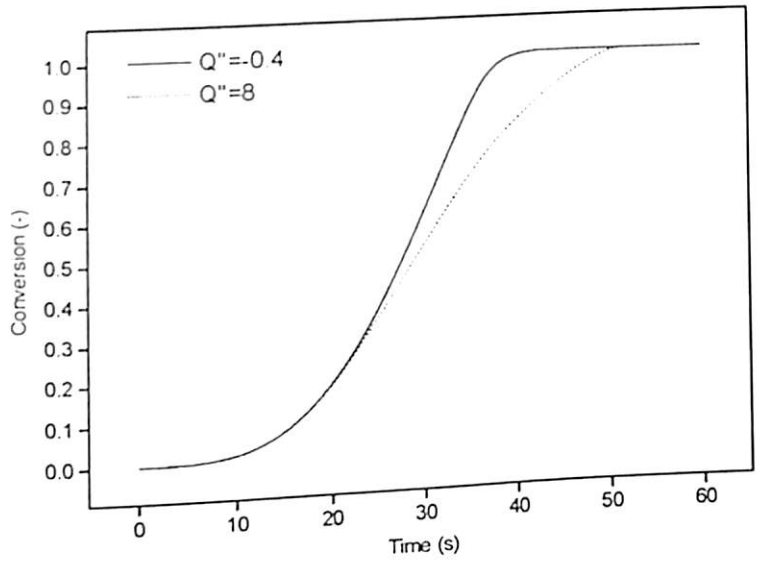

Fig. 5.18. Effect of Q'' on conversion of biomass (R=0.0025 m, T_0=303 K, T_f=753 K).

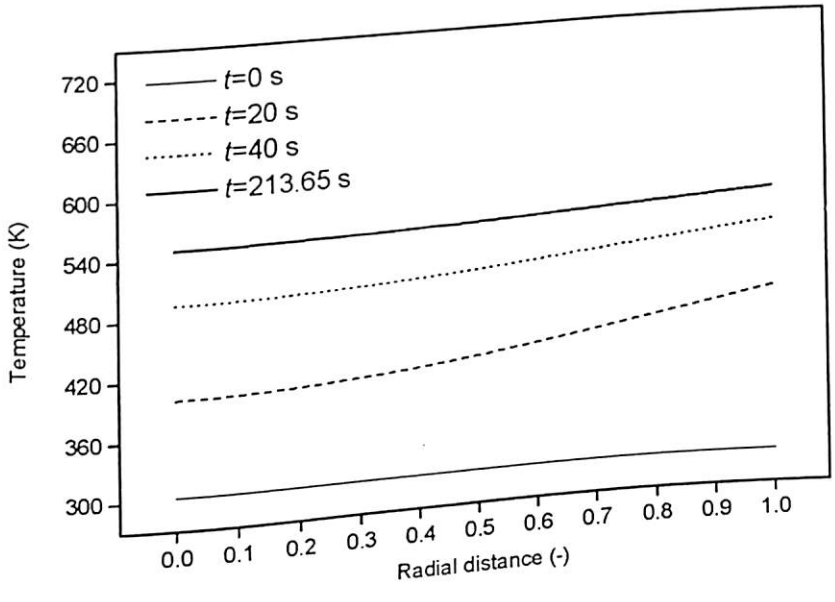

Fig. 5.19. Temperature profile as a function of radial distance for different values of t (Q''=10, R=0.003 m, T_0=303 K, T_f=643 K).

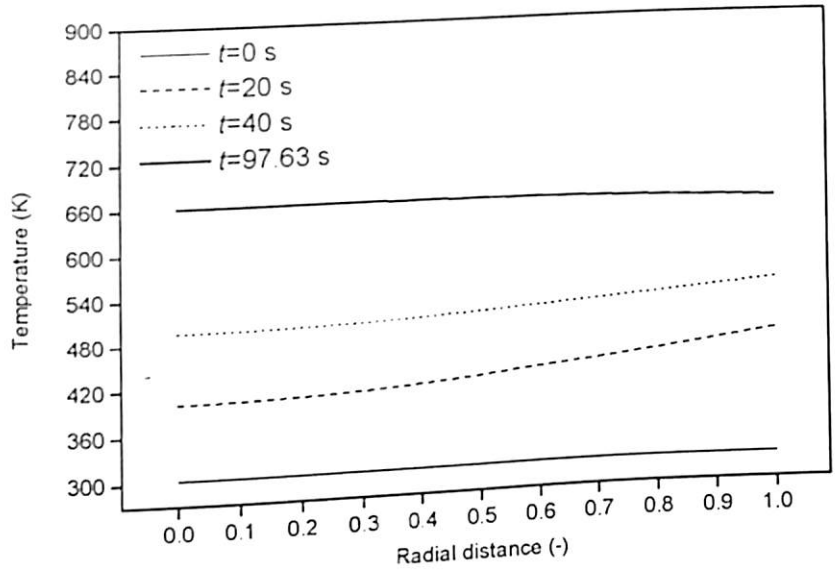

Fig. 5.20. Temperature profile as a function of radial distance for different values of t (Q''=-0.5, R=0.003 m, T_0=303 K, T_f=643 K).

Fan, & Walawender, 1977). For Q''=-0.5, however, the situation becomes different in that the temperature in the particle appears to increase beyond the surface temperature of 643 K when conversion of biomass is close to completion (Refer temperature profile for 97.63 s in Fig. 5.20). In the case when the particle temperature exceeds the surface temperature, the temperature gradient, $d\theta / dx$, at the surface becomes negative; thus the heat conduction is towards the surroundings. Obviously, the heat source from the surrounding environment, which is utilized to initiate the pyrolysis reaction, is no longer required. The heat source could be viewed simply as a trigger for the early stages of the reaction. This situation is termed the '*self-sustaining reaction*' (Miyanami, Fan, Fan, & Walawender, 1977).

From both the figures (Fig. 5.19 and Fig. 5.20), it is evident that initially at t=0 the temperature profile is flat as no pyrolysis reaction begun. As the time progresses (at

t=20 s), there exists the temperature gradient across the radial distance of the particle. As the time progresses further (at t=40 s), the temperature gradient decreases, and finally at t=97.63 s for Q''=-0.5 and t=213.65 s for Q''=10 the temperature profile becomes almost flat indicating that the pyrolysis is close to completion. This effect can be visualized from Fig. 5.17 also for Q''=-0.5 and Q''=10 for which at t=97.63 s and t=213.65 s respectively, the conversion is almost complete. The trends in Figs. 5.19 & 5.20 are also observed for particle radius of 0.0025 m as shown in Figs. 5.21 & 5.22.

5.5.2.4. Effect of Heat of reaction number on biomass concentration profile

The concentration profiles of biomass are shown in Figs. 5.23 and 5.24 for the cases of Q''=10 and Q''=-0.5 respectively. It is seen that the concentration is more at the centre than at the surface as the pyrolysis progresses. This may be attributed to the combined effects of the rate of heat transfer as well as the rate of chemical reaction

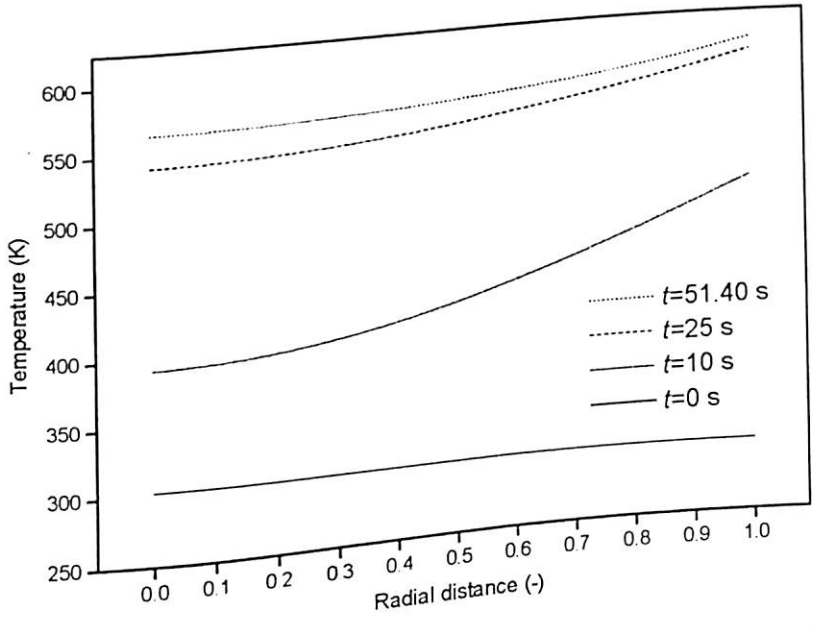

Fig. 5.21. Temperature profile as a function of radial distance for different values of t (Q''=8, R=0.0025 m, T_0=303 K, T_f=753 K).

during the process. In the early stages of the reaction (up to about 40 s), the decrease in concentration of biomass is nearly same for both the cases. At a given radial position

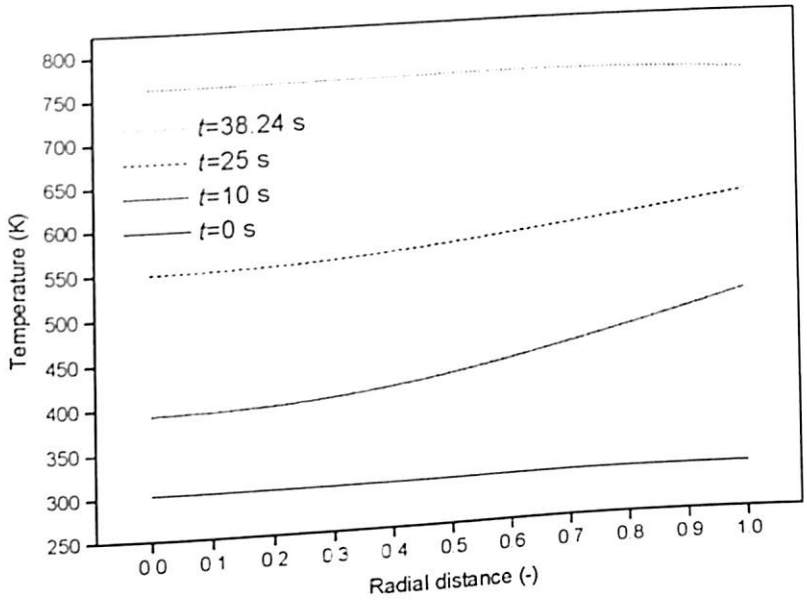

Fig. 5.22. Temperature profile as a function of radial distance for different values of t (Q''=-0.4 R=0.0025 m, T_0=303 K, T_f=753 K).

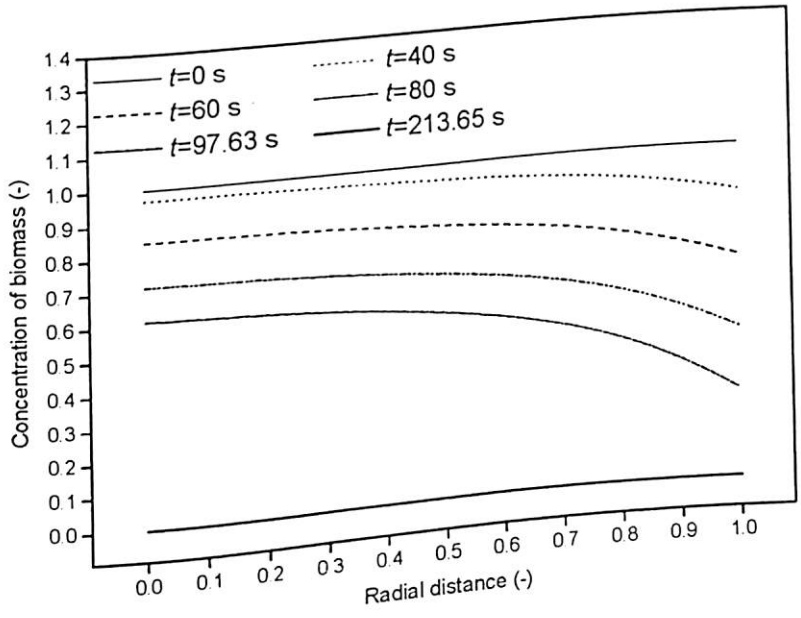

Fig. 5.23. Concentration profile as a function of radial distance for different values of t (Q''=10, R=0.003 m, T_0=303 K, T_f=643 K).

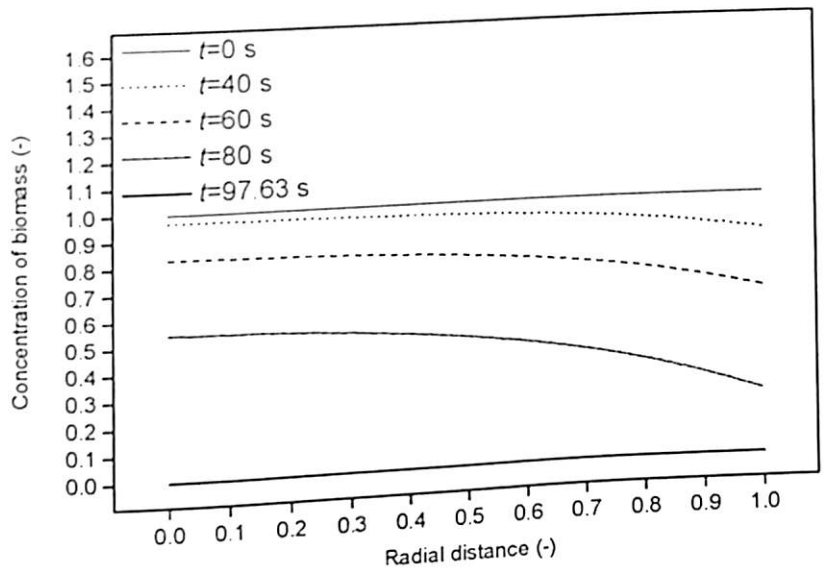

Fig. 5.24. Concentration profile as a function of radial distance for different values of t (Q''=-0.5, R=0.003 m, T_0=303 K, T_f=643 K).

after pyrolysis time of 40 s, the decrease in concentration of biomass for the case of Q''=-0.5 is much larger than that for the case of Q''=10. The pyrolysis is nearly complete at t=97.63 s for Q''=-0.5, but it is only 48 % for Q''=10 at t=97.63 s as can be visualized from Fig. 5.17 also, and the time of completion of pyrolysis is higher for Q''=10 (213.65 s). This is because the temperature in the particle for Q''=-0.5 is higher than that for Q''=10 at any given time. Consequently, the effective mass diffusivity of the volatiles and gases through the particle is greater for the former case than for the latter case. It may also be noted that starting from a concentration profile at t=0, the concentration gradient increases as time progresses, and ultimately the concentration profiles become flat again when reaching the near complete conversion stage. These results are in conjunction with the results shown in Figs. 5.19 & 5.20 of the temperature profiles. For

particle radius of 0.0025 m also, similar trends as shown in Figs. 5.23 and 5.24 are observed as shown in Figs. 5.25 and 5.26.

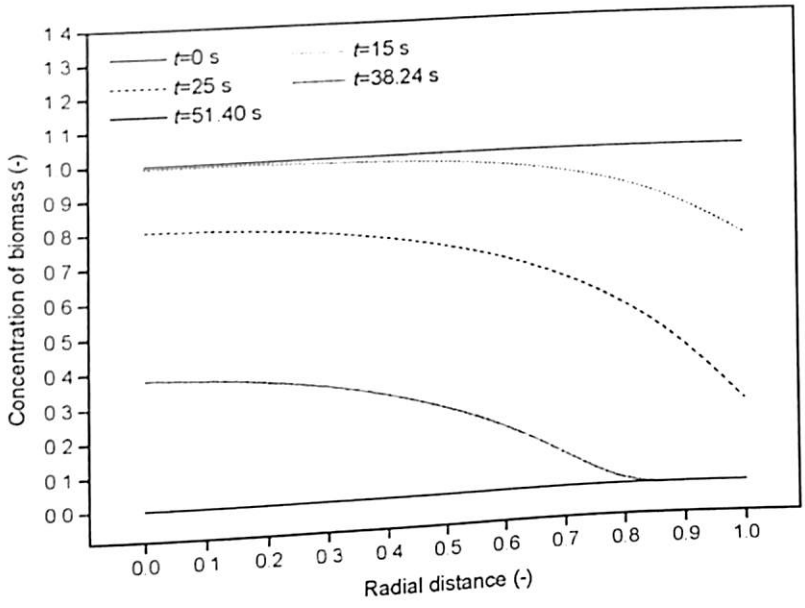

Fig. 5.25. Concentration profile as a function of radial distance for different values of t (Q''=8, R=0.0025 m, T_0=303 K, T_f=753 K).

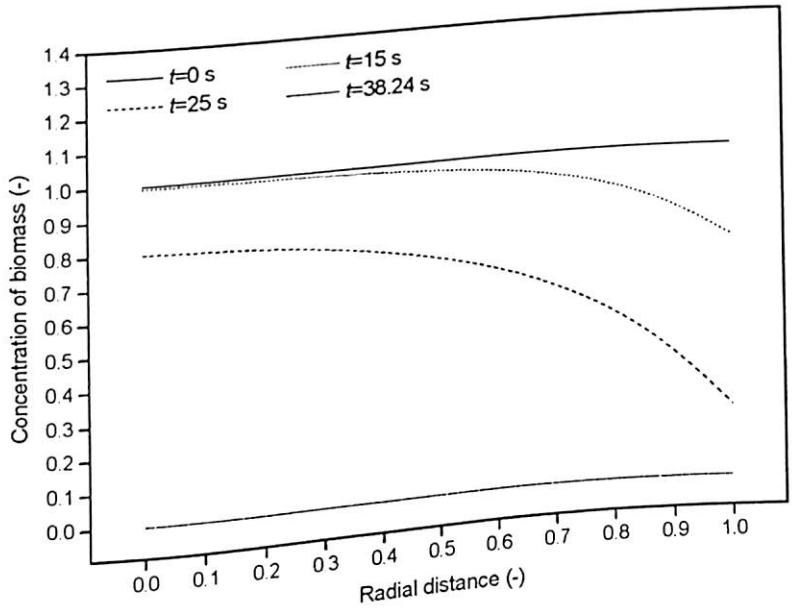

Fig. 5.26. Concentration profile as a function of radial distance for different values of t (Q''=-0.4, R=0.0025 m, T_0=303 K, T_f=753 K).

5.5.2.5. Effect of density of biomass on concentration of products and pyrolysis time

Biomass density has been varied in the range of values between 400-1600 kg/m^3. However, no dependence of this parameter on concentration of products has been observed. Fig. 5.27 shows the concentration of products and conversion time as functions of the biomass density for R=0.009 m with cylindrical geometry. No effect of density on both the primary and secondary reaction products is observed. The primary solid degradation rate, and thus the volatile release rate, depends on the both the temperature and solid density. Although on one hand, the temperature of primary degradation becomes lower leading to slower heating rates of volatile release, on the other hand, the increased solid density makes the primary degradation rate faster. The two effects counteract with each other, resulting in an almost constant release rate of volatiles and char, as the density of biomass is increased. The conversion time does not depend on the density of biomass and is nearly constant (161 s).

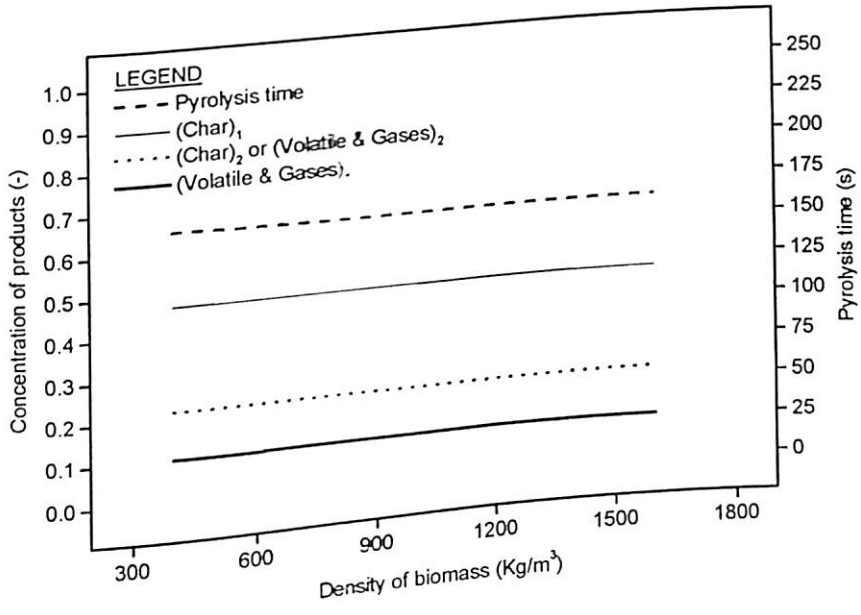

Fig. 5.27. Average concentration of products and pyrolysis time as functions of density of biomass (ρ) with cylindrical pellet (R=0.009 m, T_0=303 K, T_f=900 K).

5.6. Conclusions

Simulations are carried out using the models developed in the present study (Babu & Chaurasia, 2004a) for different geometries (slab, cylinder and sphere) for temperature ranging from 303-2800 K and the equivalent particle radius ranging from 0.0001-0.017 m.

- The simulated results obtained from all the three models (Models I, II, and III) developed in the present study (Babu & Chaurasia, 2004a) are in excellent agreement with the experimental data of Pyle & Zaror (1984), when compared to the mathematical model of Jalan & Srivastava (1999) and model of Bamford, Crank & Malan (1946) used by Pyle & Zaror (1984).
- Model-I is a generalized reference model, which gives good prediction of the temperature profiles for lower temperature and lower times of pyrolysis. However, the two improved simplified models (Model-II and Model-III) predict well in the entire range of temperature and pyrolysis time.
- Model-III is in excellent agreement with the experimental data (Pyle & Zaror, 1984) as compared to the other developed models (Model-I and Model-II) and the models reported in literature (Jalan & Srivastava, 1999; Bamford, Crank, & Malan, 1946) for wide range of operating conditions.
- The spherical particle has a shortest conversion time as compared to slab and cylinder.
- The yield of $(\text{volatiles \& gases})_1$ is maximum for sphere and is least for slab while the yield of $(\text{char})_1$ and $(\text{volatiles \& gases})_2$ or $(\text{char})_2$ is more for slab and is least for sphere.

- As the temperature increases, the pyrolysis completes faster.
- Pyrolysis is faster in case of sphere (pyrolysis time=95 s) and slowest for slab (pyrolysis time=185 s), while the trend in temperature profiles obtained for all the three geometries being same.
- The concentration of $(char)_1$ increases while the concentration of $(volatile\ \&\ gases)_1$ decreases as the particle thickness is increased for all the three geometries (slab, cylinder, and sphere).
- Two typical pyrolysis reactions, namely, *heat-transfer-controlled reaction* and *self-sustaining reaction*, are considered. The former is characterized by positive value of heat of reaction number Q'', e.g. 10, and the latter is characterized by negative value, e.g., -0.5.
- For the value of $Q''=10$ (endothermic reaction), the temperature profile increases monotonically to that of the steady state, and the rate of decrease in concentration of biomass is very less.
- When Q'' is -0.5 (exothermic reaction), the temperature in the particle rapidly overshoots the surface temperature after a certain concentration of biomass, and the rate of decrease in concentration of biomass is very fast.
- In the early stages (up to about 40 s) of the reaction, the biomass conversion does not appear to be significantly affected by different values of Q''. Also, the decrease in concentration of biomass is nearly same for heat of reaction number of 10 and -0.5 in the early stages of pyrolysis.
- The completion time for pyrolysis is less (=97.63 s) for exothermic reaction (Q'' = -0.5) as against a higher value (=213.65 s) for endothermic reaction (Q'' =10).

- The variation in temperature profile and concentration profile for exothermic and endothermic pyrolysis reaction could be well explained by using heat of reaction number.
- There is no effect of density of biomass on both the primary and secondary reaction products. The conversion time does not depend on density of biomass and is nearly constant for complete conversion.

CHAPTER

6

DOMINANT DESIGN VARIABLES IN PYROLYSIS OF BIOMASS PARTICLES OF DIFFERENT GEOMETRIES IN THERMALLY THICK REGIME

6.1. Introduction

Biomass, mainly in the form of wood, is the oldest form of energy used by human being. An understanding of the chemical processes and transport mechanisms of biomass pyrolysis is important for many applications including optimization of boilers and large scale furnaces, determining forest fire behavior, and predicting the resistance of buildings to fire.

In relation to the devolatilization (pyrolysis) stage, the effects of particle size have been extensively examined by both experiment (Chan, Kelbon, & Krieger, 1988) and comprehensive theories (Di Blasi, 1996c). Physico-chemical properties of biomass depend widely on the type of feedstock. For example, density may vary (Kanury, & Blackshear, 1970) from 100 kg/m^3 (balsa, bagasse, straw) to 1200 kg/m^3 (lignum vitae). It is expected that effective thermal and physical properties of char should reflect those

of virgin biomass (Lee, Chaiken, & Singer, 1976) and thus show significant variation with the feedstock. In the present work (Babu & Chaurasia, 2004b, 2004c), the variations associated the widely variable properties (thermal conductivity, heat transfer coefficient, emissivity, heat of reaction number and reactor temperature) affecting the pyrolysis of biomass is examined, through a detailed mathematical model including all the main chemical and physical processes of biomass pyrolysis. The effect of these properties on average concentration of products is studied for three different geometries (slab, cylinder, and sphere). To establish the extent to which each property is important in terms of average concentration of products and pyrolysis time (conversion time), sensitivity analysis is carried out. The highest sensitivity is associated with reactor temperature and emissivity. Applications of these findings in reactor design and operation are discussed. The pyrolysis process is considered because it is not only an independent process for biomass conversion but it also represents a fundamental stage in gasification and combustion (Matsui, Kojima, Kunii, & Furusawa, 1987; Narvaez, Orio, Aznar, & Corella, 1996; Di Blasi, 1997, 2000a, 2000b; Demirbaş, 2002c).

6.2. Background

Thermal processes are often considered as the most valuable methods of upgrading the energy of biomass (Lede, Panagopoulos, Li, & Villermaux, 1985; Bilbao, Millera, & Murillo, 1993; Di Blasi, 1998; Arena, & Mastellone, 2000; Demirbaş, 2002d). Convection and radiation of the solid is the indirect external heating mode of thermal degradation. The heating rate of solid is the most important factor in particle dynamics and product distribution. Indirect heating (Di Blasi, 1994a; 1996b) is associated with

purely kinetic control (very small particle sizes and/or very slow external heat transfer rates) or with heat transfer control. If the particle size is sufficiently small (< 2 mm), intra-particle activity of secondary reactions is negligible even at high reaction temperatures (Di Blasi, 1996c). Since the main objective of the present study (Babu & Chaurasia, 2004b, 2004c) is to understand the role played by thermal and thermodynamic properties, only the case of heat-transfer-controlled conversion (thermally thick regime) is considered.

The strong interaction between chemical and physical processes in the thermal degradation of large biomass samples makes the understanding of conversion dynamics very difficult. Mathematical and numerical modeling could by very useful tools to assess the role played by the different mechanisms. However, theoretical analyses of biomass fuel pyrolysis and combustion are rather complicated. The complication as pointed (Roberts, 1970), comes more from the formulation of mathematical models correctly accounting for physical and chemical processes and from the acquisition of reliable data to be used for simulations than from computational requirements. Most of the models (Bamford, Crank, & Malan, 1946; Fan, Fan, Miyanami, Chen, & Walawender, 1977; Kansa, Perlee, & Chaiken, 1977; Miyanami, Fan, Fan, & Walawender, 1977; Jalan & Srivastava, 1999) published to date have not considered secondary reactions in pyrolysis kinetics, no specific kinetic mechanism is suggested to predict the concentration of the various components produced during pyrolysis and did not consider specific heat & thermal conductivity of char as a function of temperature. Model-III (as discussed in Chapter 5) which is in excellent agreement with the experimental data (Pyle & Zaror, 1984) as compared to the other developed models

(Model-I and Model-II) and the models reported in literature (Jalan & Srivastava, 1999; Bamford, Crank, & Malan, 1946) for wide range of operating conditions is used in the present study (Babu & Chaurasia, 2004b, 2004c).

6.3. Motivation

There has been an increasing interest for thermochemical conversion of biomass and urban wastes for upgrading energy in terms of more easily handled fuels, namely gases, liquids, and charcoal in the past decade (Antal, 1982, 1985; Bridgwater & Evans, 1993). Each product can be commercially interesting depending upon the type of application. Thermal and thermodynamic properties such as thermal conductivity, heat transfer coefficient, emissivity, heat of reaction number, and reactor temperature affect the pyrolysis of biomass in several ways. Hence, it is very important to know how the product distribution depends on the feedstock properties, process conditions, and different geometries such as slab, cylinder, and sphere.

6.4. Results and discussion

6.4.1. Model validation and comparison

As discussed in chapter 5, the simulated results obtained from all the three models (Models I, II, and III) are in excellent agreement with the experimental data of Pyle & Zaror (1984), when compared to the mathematical model of Jalan & Srivastava (1999) and the model of Bamford, Crank, & Malan (1946) used by Pyle & Zaror (1984). It is observed that, Model-I gives good prediction of the temperature profiles for lower temperature and lower times of pyrolysis. However, the two improved simplified

models (Model-II and Model-III) predict well in the entire range of temperature and pyrolysis time. Model-III is in excellent agreement with the experimental data (Pyle & Zaror, 1984) as compared to the other developed models (Model-I and Model-II) and the models reported in literature (Bamford, Crank, & Malan, 1946; Jalan & Srivastava, 1999) for wide range of operating conditions. This model is utilized in the present study (Babu & Chaurasia, 2004b, 2004c). Some more results of model validation (not given in chapters 4 and 5) are given in Figs. 6.1-6.4.

The Model-III utilized in the present study (Babu & Chaurasia, 2004b, 2004c) is compared with the model of Liliedahl & Sjöström (1998) as shown in Figs. 6.1-6.3. Fig. 6.1 shows the conversion profile as a function of time with cylindrical pellet of radius 0.011 m and final temperature of 753 K. The model used is in better agreement as compared to the model of Liliedahl & Sjöström (1998), while the latter underpredicts

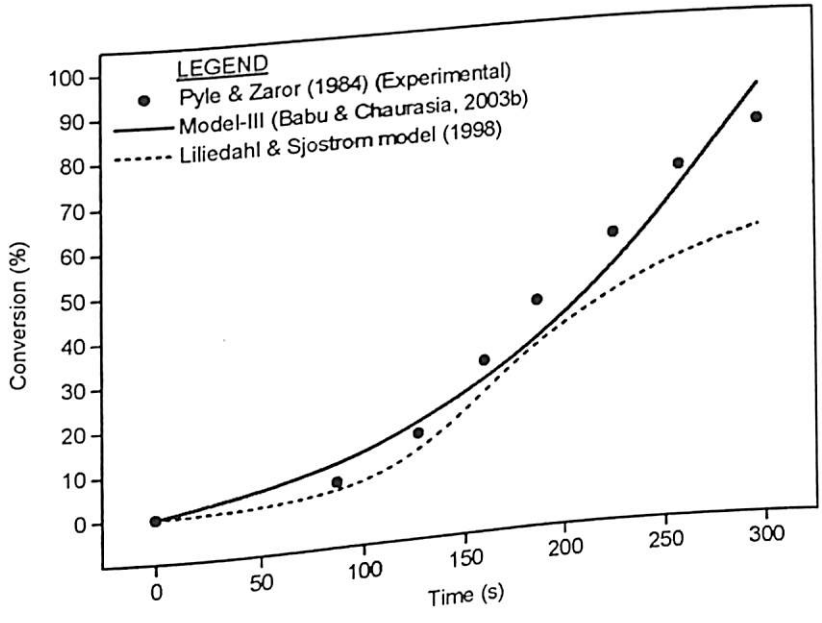

Fig. 6.1. Conversion profile as a function of time with cylindrical pellet (R=0.011 m, T_0=303 K, T_f=753 K).

the conversion at higher values of pyrolysis time. This may be due to the fact that while developing the model, Liliedahl & Sjöström (1998) did not consider the variation of thermal conductivity and specific heat capacity of biomass with temperature. In order to test the validity of the model which is used in the present study (Babu & Chaurasia, 2004b, 2004c) for wide range of particle sizes and temperatures, it is also compared with the experimental data of Alves & Figueiredo (1989) as shown in Figs. 6.2 and 6.3. In this case also, the better agreement of the model as compared to the model reported in the literature (Liliedahl & Sjöström, 1998) is found. At lower values of final temperature the model of Liliedahl & Sjöström (1998) overpredicts the data, and at higher values of final temperature it underpredicts, while the present model predicts well for a wide range of final temperatures.

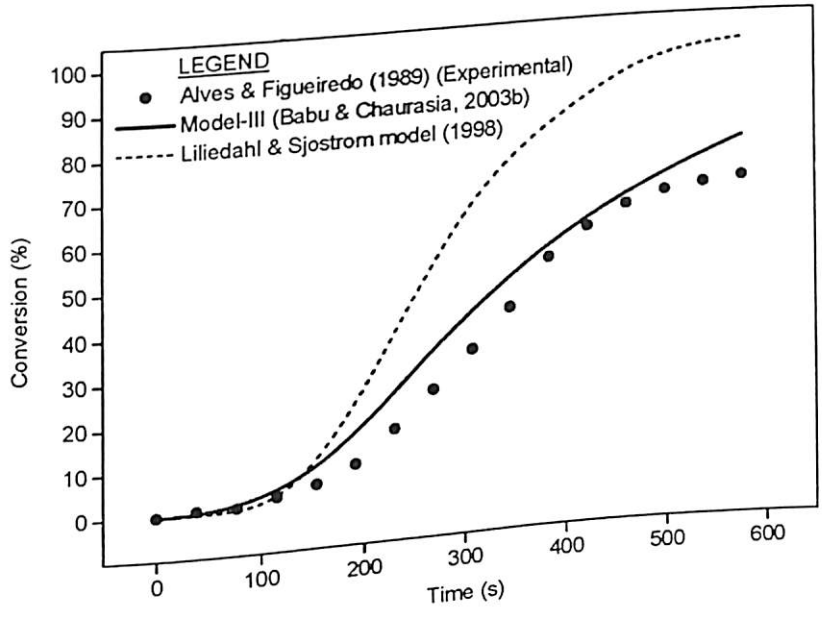

Fig. 6.2. Conversion profile as a function of time with cylindrical pellet (R=0.00915 m, T_0=303 K, T_f=679 K).

Measurements of product distributions for different sized single cellulose particles are not available to make quantitative comparisons with model predictions. However, cellulose pyrolysis in fluid-bed and entrained-flow reactors (Scott, Piskorz, Bergougnou, Graham, & Overend, 1988) and in low-temperature vacuum tube furnace (Shafizadeh, Furneaux, Cochran, Scholl, & Sakai, 1979) can be considered for comparison and some conclusions can be drawn. To this end, the experimental data have been replotted together with the simulation results, obtained for particle half-thickness of 0.0000125 m (thermally thin regime) as shown in Fig. 6.4. Since in both experiments very thin particles (powder) by Shafizadeh, Furneaux, Cochran, Scholl, & Sakai (1979) and particle sizes of about 100 μm by Scott, Piskorz, Bergougnou, Graham, & Overend (1988) are used, it can be guessed that intraparticle resistance to heat transfer is negligible. As shown, the match between the model and experimental data is very good.

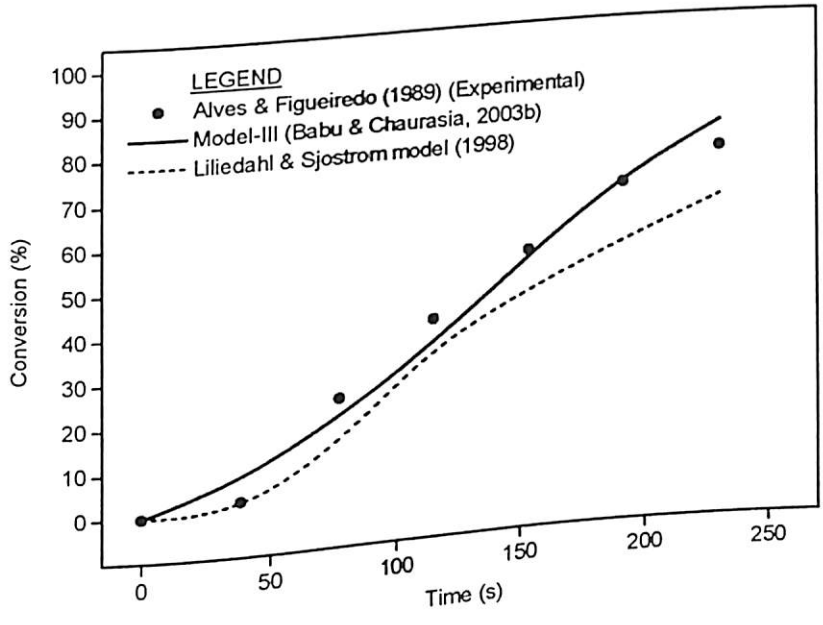

Fig. 6.3. Conversion profile as a function of time with cylindrical pellet (R=0.00925 m, T_0=303 K, T_f=873 K).

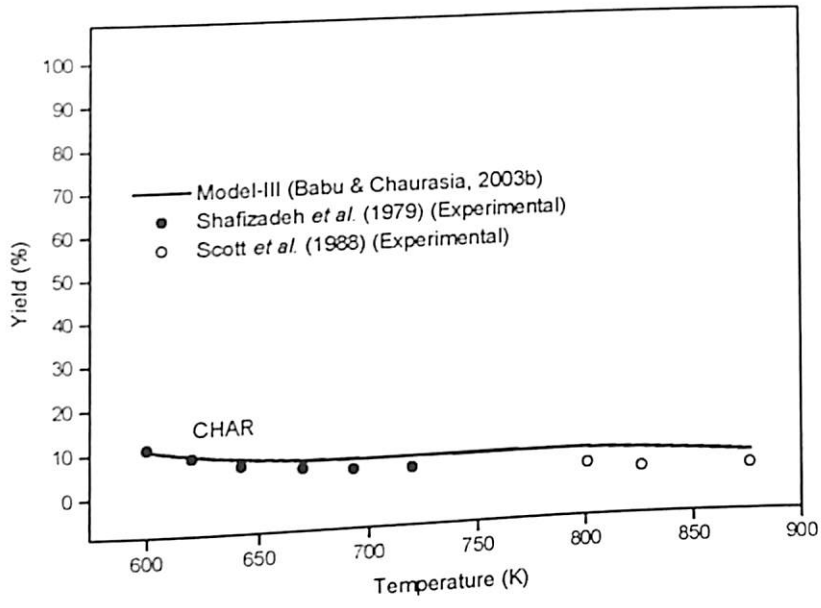

Fig. 6.4. Average char yield as a function of temperature for particle half-thickness of 0.0000125 m.

6.4.2. Simulation results

Excellent agreement between the present model predictions and experimental data reported in literature consolidates the model validity for wide range of operating conditions. Hence, extensive simulations have been carried out for the slab, cylindrical, and spherical geometries of the biomass particles of radius R=0.011 m (thermally thick regime), by varying heat of reaction number (Q"), thermal conductivity of biomass (k), convective heat transfer coefficient (h), emissivity (ε) and reactor temperature T_f. The Computer Codes in C++ for heat of reaction number (Q") and thermal conductivity of biomass (k) are given in Appendix-E while the Computer codes for other properties is same as the Computer code in C++ of Model-III given in Appendix-B.

6.4.2.1. Effect of heat of reaction number (Q")

6.4.2.1.1. Exothermic reactions

Average concentration of products and pyrolysis time as functions of heat of reaction number (Q"), for R=0.011 m (thermally thick regime) are shown in Fig. 6.5 for cylindrical geometry. The negative value of Q" stands for exothermic reaction. The degree of exothermicity is the negative of heat of reaction number. As the heat of reaction number decreases, the degree of exothermicity of the reaction increases. Concentration of products of both primary and secondary pyrolysis reactions is shown. It is observed that average concentration of (volatile & gases)$_1$ increases at the expense of (char)$_1$, while the concentration of (volatile & gases)$_2$ is almost constant, as degree of exothermicity increases (i.e. Q" decreases). It may be noted that the kinetic expression for (char)$_2$ and (volatile & gases)$_2$ are same, and hence the concentration profiles for these two products are same as shown in Fig. 6.5. A significant reduction in pyrolysis time is predicted. A comparison in concentration of products of primary and secondary pyrolysis reactions indicates that variations in Q" mainly affect the extent of primary reactions. Indeed, only a barely discernible decrease in (volatile & gases)$_2$ is predicted as Q" decreases (for all the cases, the activity of primary reactions is significant, given the large particle size).

Temperature profile reported in Fig. 6.6 for different values of heat of reaction number ranging from -0.7 to -0.1 can be used to explain the simulated variations in the product distributions that are shown in Fig. 6.5. As degree of exothermicity increases, the temperature at a particular radial position increases. The particle temperature rapidly overshoots and then again decreases along the radial position. It is observed that the

maxima in the temperature occurs at a radial position of 0.7 irrespective of the value of Q''. When particle temperature exceeds the surface temperature, the temperature

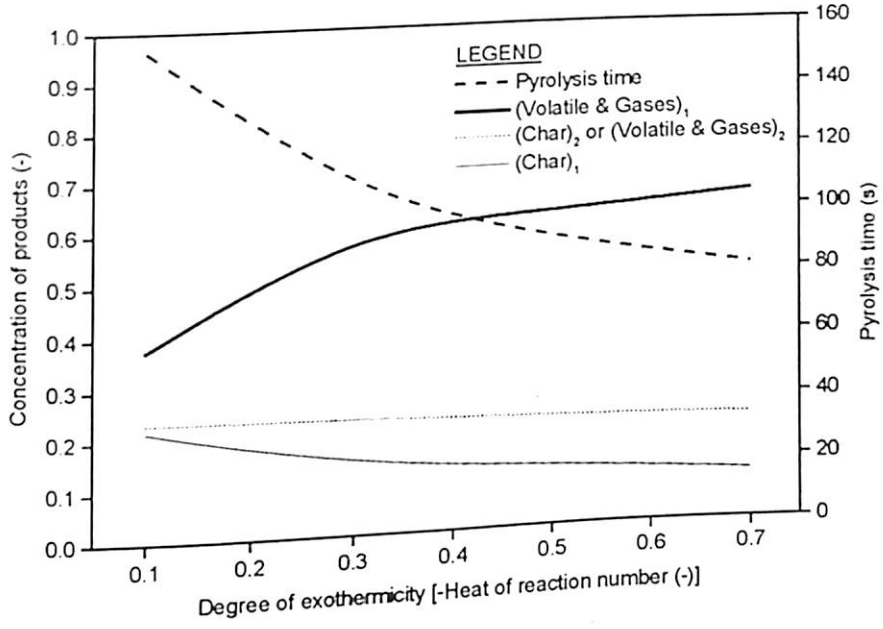

Fig. 6.5. Average concentration of products and pyrolysis time as functions of heat of reaction number (Q'') for exothermic reaction with cylindrical pellet (R=0.011 m, T_0=303 K, T_f=900 K).

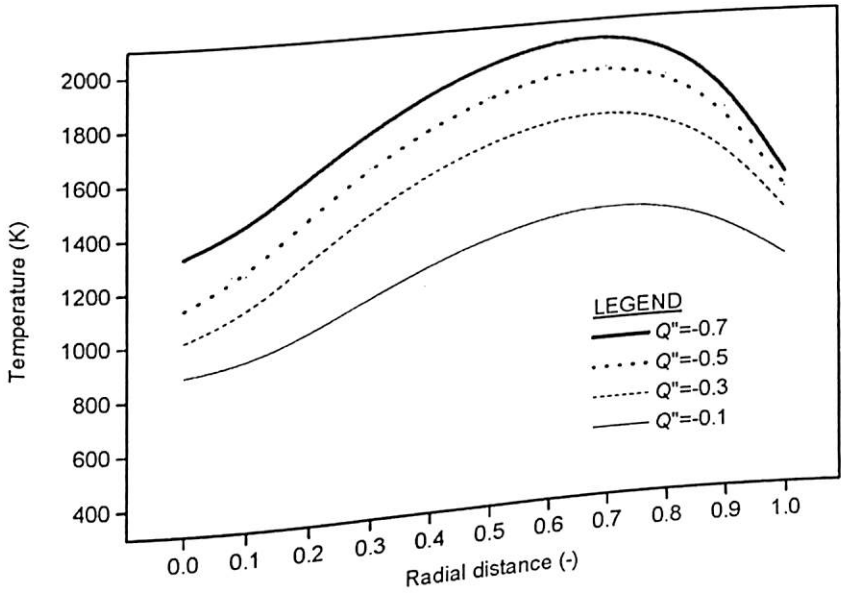

Fig. 6.6. Temperature profile as a function of radial distance for different values of heat of reaction number (Q'') for exothermic reaction with cylindrical pellet (R=0.011 m, T_0=303 K, T_f=900 K).

gradient, $d\theta/dx$, at the surface becomes negative; thus the conduction is towards the surroundings. Obviously, the heat source from the environment is no longer required. The heat source can be viewed simply as a trigger for the early stage of the pyrolysis reaction. This situation is termed as *'self-sustaining reaction'* (Miyanami, Fan, Fan, & Walawender, 1977). This is the major advantage of pyrolysis process. The trends in temperature profile are in qualitative agreement with the data reported by Pyle & Zaror (1984) and Koufopanos, Papayannakos, Maschio, & Lucchesi (1991). The increased rate of heat transfer towards the interior of the particle, by decreasing Q'', shortens the pyrolysis time and also affects the total amount of volatiles released and the flow velocity. The increased temperature, increases the flow velocity and greatly reduces intra-particle volatile residence times, with a consequent reduction in the activity of secondary reactions and an increase in the (volatile & gases)$_1$ at the expense of (char)$_1$ as shown in Fig. 6.5.

Average concentration of products and pyrolysis time as functions of heat of reaction number for the slab, cylinder, and sphere are shown together in Fig. 6.7. The trends observed for slab and sphere geometries are similar as those shown for cylinder in Fig. 6.5. The increase in concentration of (volatile & gases)$_1$ is the highest for slab geometry and is least for the sphere. This is at the expense of decrease in concentration of (char)$_1$ which is more for sphere and least for slab. It is found that pyrolysis is faster (less pyrolysis time) in case of sphere and slowest for slab. Geometrically, the sphere has got a more heat absorbing capacity as compared to cylinder and slab and it is the least for slab. Mathematically it is reflected in the value of parameter b (b=1, 2 and 3 for slab, cylinder, and sphere respectively) in the model equation and hence the observed trends in the

profile for pyrolysis time. These results are in qualitative agreement with the simulation results of Liliedahl & Sjöström (1998). The simulated variations in the product distributions for slab and spherical geometry can be explained similarly as the explanation given for cylindrical geometry in Fig. 6.5.

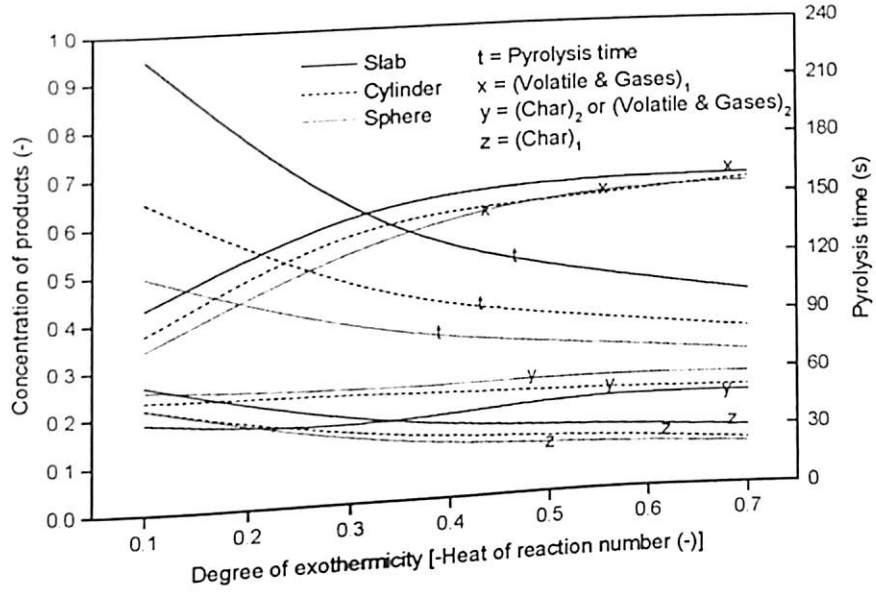

Fig. 6.7. Average concentration of products and pyrolysis time as functions of heat of reaction number (Q'') for exothermic reaction with slab, cylinder and sphere (R=0.011 m, T_0=303 K, T_f=900 K).

6.4.2.1.2. Endothermic reactions

Average concentration of products and pyrolysis time as functions of heat of reaction number (Q'') for endothermic reaction is shown in Fig. 6.8 for cylindrical geometry. In this case, the value of Q'' is positive which indicates endothermic reaction. The degree of endothermicity is representative of heat of reaction number. As the heat of reaction number increases, the degree of endothermicity of the reaction also increases. It is observed that average concentration of $(char)_1$ increases at the expense of (volatile &

gases)$_1$ and (volatile & gases)$_2$ as value of Q'' increases. The final conversion time for pyrolysis is found to increase with increase in value of Q''. Here concentration of products of primary and secondary pyrolysis reactions indicate that variations in Q'' affect activities of both the reactions.

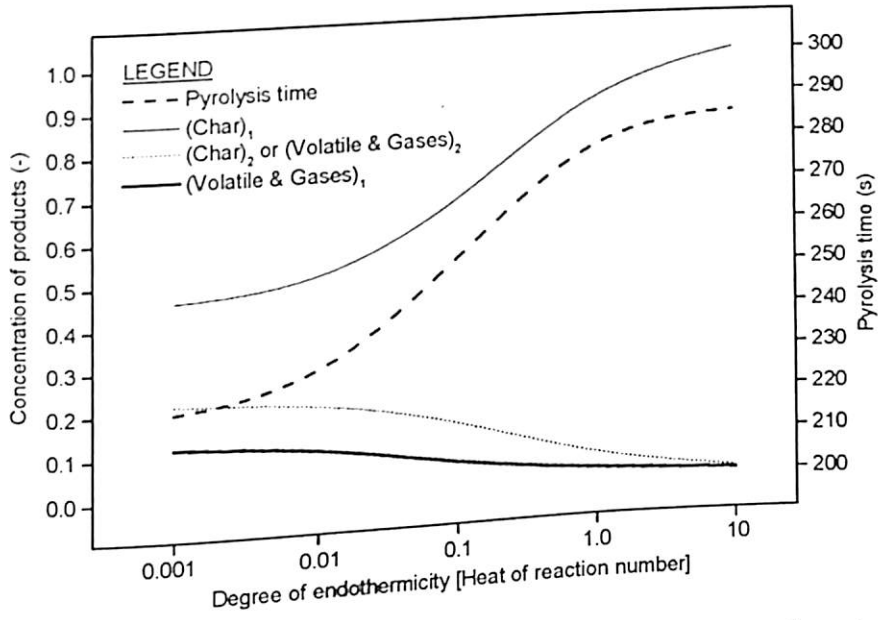

Fig. 6.8. Average concentration of products and pyrolysis time as functions of heat of reaction number (Q'') for endothermic reaction with cylindrical pellet (R=0.011 m, T_0=303 K, T_f=900 K).

Fig. 6.9 shows the temperature profile for different values of Q'' ranging from 0.001 to 1.0, which can be used to explain the simulated variations in product distribution that are shown in Fig. 6.8. The temperature is minimum at the centre and maximum at the wall of the particle. At any particular radial position, the temperature is found to decrease with increase in the value of Q'' as endothermicity of the reaction increases. It may be noted that the temperature gradient, $d\theta/dx$, is consistently positive or equal to zero. In other words, the particle temperature never exceeds the final temperature of 900 K. This situation is termed as '*heat-transfer-controlled reaction*' (Miyanami, Fan, Fan,

& Walawender, 1977). By increasing Q'', the rate of heat transfer decreases, and hence the pyrolysis time increases and affects the product distribution. Due to decrease in

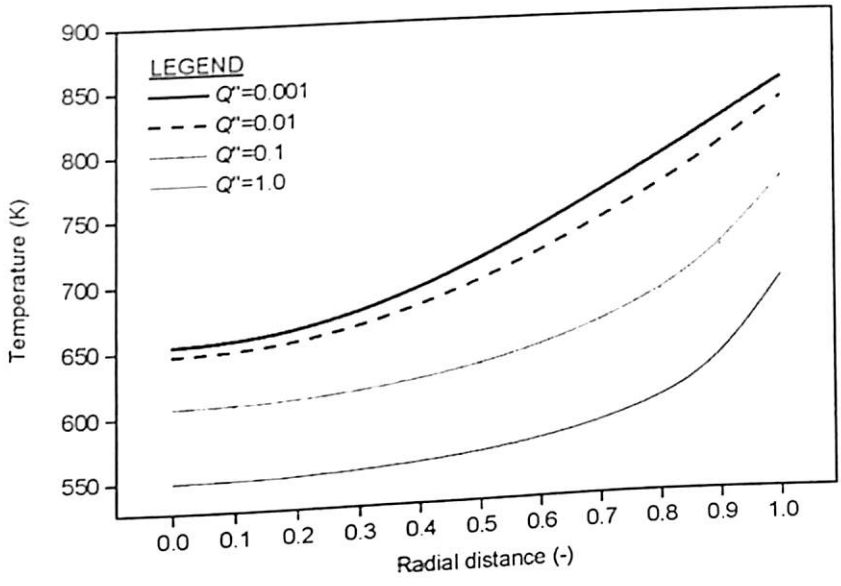

Fig. 6.9. Temperature profile as a function of radial distance for different values of heat of reaction number (Q'') for endothermic reaction with cylindrical pellet (R=0.011 m, T_0=303 K, T_f=900 K).

temperature, there is a reduction in activity of secondary reactions, and an increase in the concentration of $(char)_1$ at the expense of decrease in the concentration of (volatile & $gases)_1$ as shown in Fig. 6.8. It may be noted that endothermic reaction favors the production of $(char)_1$ while exothermic reaction favors the production of (volatile & $gases)_1$. The pyrolysis progresses faster (less pyrolysis time) as degree of exothermicity increases while pyrolysis slows down as the degree of endothermicity increases. The variations in concentration of products for different geometries along with cylinder again are shown in Fig. 6.10. The trends obtained are similar to those reported in Fig. 6.8. The concentration of $(char)_1$ is the highest for slab and is least for sphere. This is due to the decrease in concentrations of (volatile & $gases)_1$ and (volatile & $gases)_2$ which is least for

slab as compared to cylindrical and spherical geometries. The trends observed in Fig. 6.10 for slab and sphere can be explained in similar manner by the temperature profiles as given for cylindrical geometry in Fig. 6.9. Here also the time of completion of pyrolysis is least for sphere as compared to slab and cylinder at any particular value of heat of reaction number as explained above.

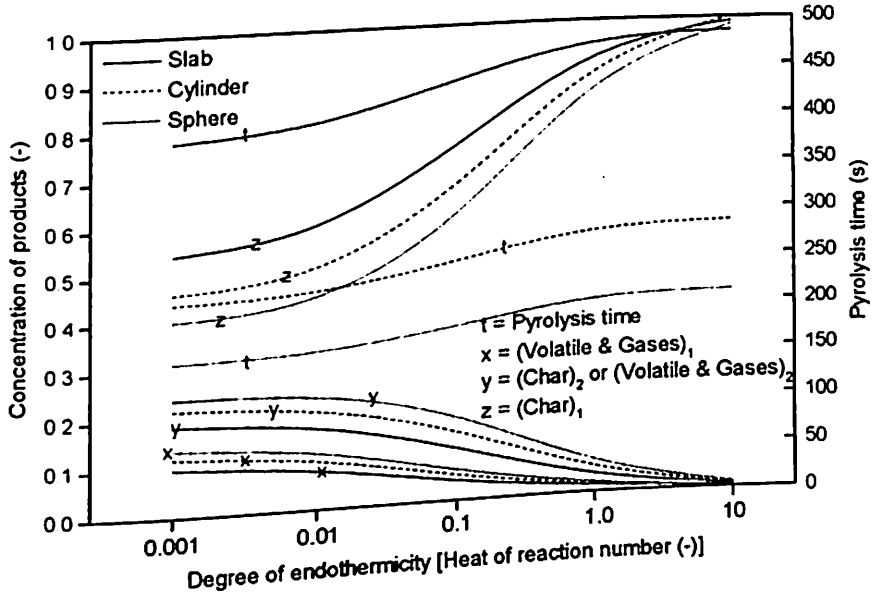

Fig. 6.10. Average concentration of products and pyrolysis time as functions of heat of reaction number (Q'') for endothermic reaction with slab, cylinder and sphere (R=0.011 m, T_0=303 K, T_f=900 K).

6.4.2.2. Effect of thermal conductivity of biomass (k)

Biomass thermal conductivities are reported (Kanury & Blackshear, 1970) to vary in the range of $3\times10^{-2} - 40\times10^{-2}$ W/mK. The effect of this parameter on average concentration of products and conversion time with cylindrical pellet are shown in Fig. 6.11 for R=0.011 m. It is found that, the average concentration of products of $(char)_1$ increases while the concentration of $(volatile\ \&\ gases)_1$ decreases as thermal conductivity

increases. The concentration of (volatile & gases)$_2$ increases up to $k = 0.175$ W/mK and then decreases as k is further increased. This is due to the fact that for the value of $k = 0.175$ W/mK, the concentrations of primary products are equal and thereafter the concentration of (char)$_1$ increases at the expense of (volatile & gases)$_1$ showing the trade-off between these two concentrations. Hence, the lower values of thermal conductivity leads to the formation of a good quality gas having higher concentration of (volatile & gases)$_1$ and lowest possible value of (char)$_1$. A significant increase in pyrolysis time is observed as k is increased. A comparison of the concentration of products during primary and secondary pyrolysis indicates that the activity of the primary reactions is significant as compared to the activity of secondary reactions.

Fig. 6.12 shows the temperature profile as a function of radial distance simulated for different values of k, which can be used to explain the simulated variations in the

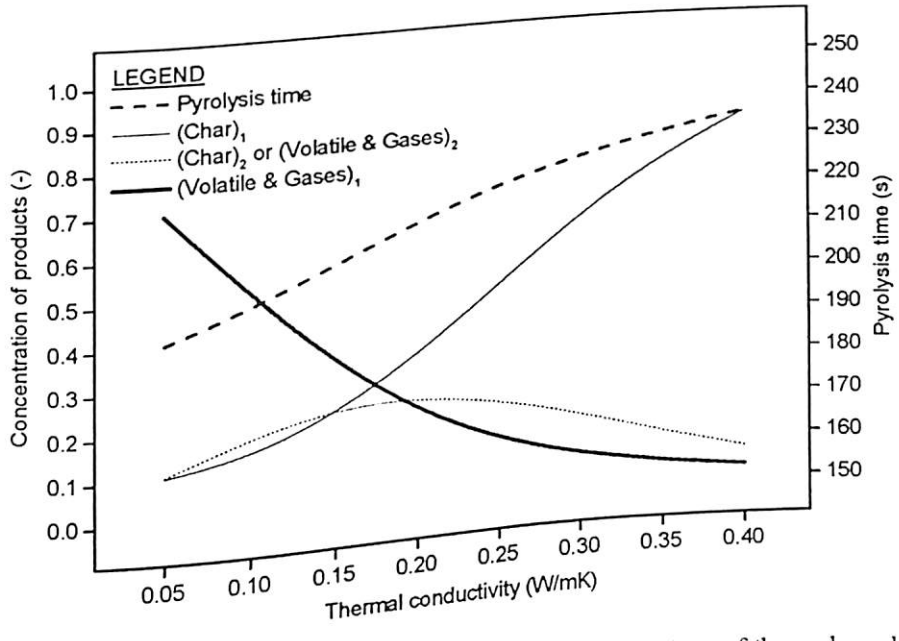

Fig. 6.11. Average concentration of products and pyrolysis time as functions of thermal conductivity with cylindrical pellet (R=0.011 m, T_0=303 K, T_f=900 K).

product distribution shown in Fig. 6.11. In Fig. 6.11, we have seen that concentration of $(char)_1$ increases while the concentration of $(volatile\ \&\ gases)_1$ decreases as k is increased. This is a consequence of decrease in temperature at any radial position with respect to increase in k value. Therefore the charring reactions (favoring the char formation) are successively favoured to a large extent. The pyrolysis time increases linearly with k, given slower particle heating rate successively. The results shown in Fig. 6.11 are in accordance with those reported by Shafizadeh (1979). He also reported increase in char concentration and decrease in the concentration of volatile & gases as temperature is decreased (i.e. heating rate is slow). The concentration of products and pyrolysis time for slab and sphere along with cylinder are shown in Fig. 6.13. The trends are same as those reported in Fig. 6.11 for cylinder. The increase in concentration of $(char)_1$ is the highest for slab at the expense of decrease in concentration of (volatile &

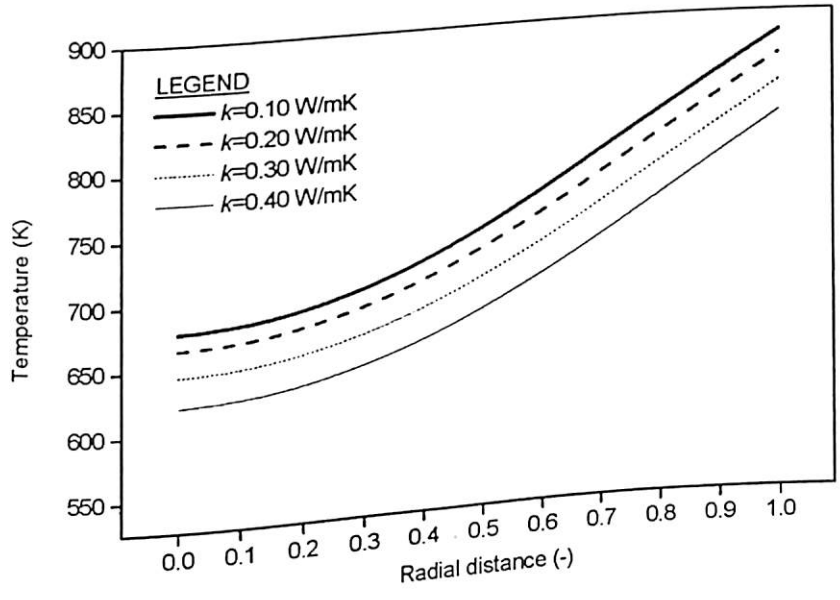

Fig. 6.12. Temperature profile as a function of radial distance for different values of thermal conductivity with cylindrical pellet (R=0.011 m, T_0=303 K, T_f=900 K).

gases)$_1$, which is the least for slab as compared to other geometries. As explained above, the pyrolysis reactions progresses faster in sphere as compared to slab and cylinder.

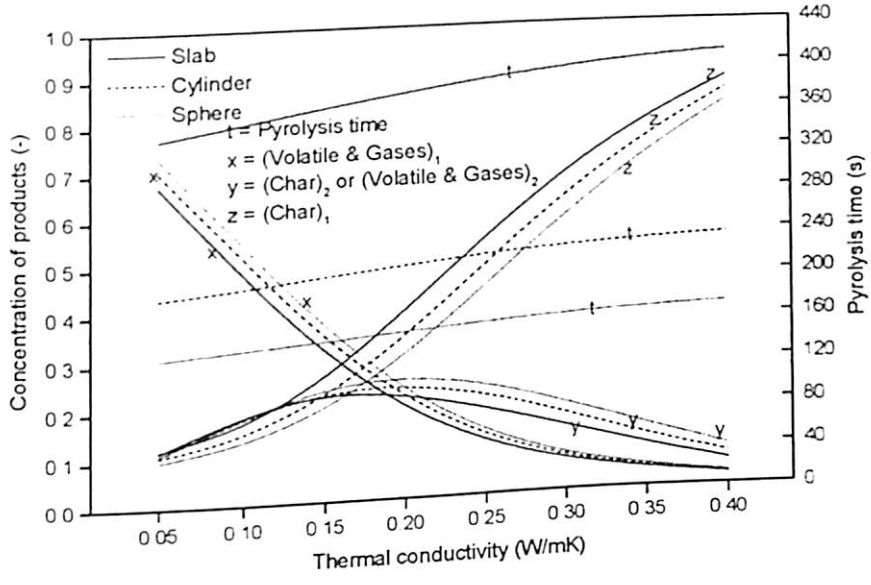

Fig. 6.13. Average concentration of products and pyrolysis time as functions of thermal conductivity with slab, cylinder and sphere (R=0.011 m, T_0=303 K, T_f=900 K).

6.4.2.3. Effect of convective heat transfer coefficient (h)

Simulations are carried out to study the effect of convective heat transfer coefficient on pyrolysis for cylinder, slab, and sphere geometries. The dependence of concentration of products and pyrolysis time on heat transfer coefficient with cylindrical pellet is shown in Fig. 6.14 for R=0.011 m. The effect of h on concentration of the products during the secondary pyrolysis is not very significant. It increases with increase in value of h, maximum for h=80 W/m^{2}K, and thereafter decreases as h is further increased. The concentration of (volatile & gases)$_1$ increases at the expense of concentration of (char)$_1$ with an increase in the value of h. The concentration of primary products become equal at h=80 W/m^{2}K at which the concentration of secondary products is

maximum and thereafter it decreases as h is further increased. These results again substantiate the existence of trade-off between the concentrations of (volatile & gases)$_1$ and (char)$_1$ as discussed earlier.

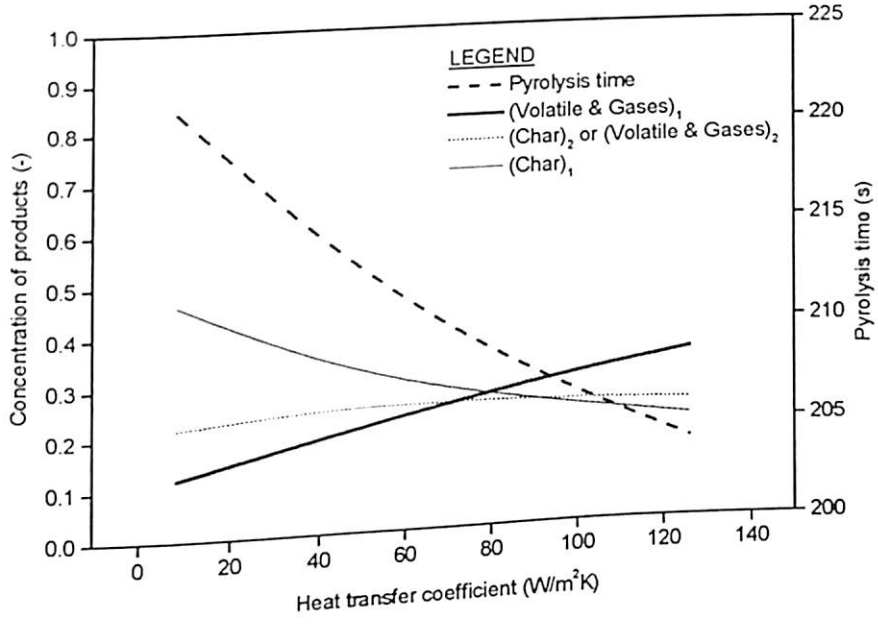

Fig. 6.14. Average concentration of products and pyrolysis time as functions of convective heat transfer coefficient with cylindrical pellet (R=0.011 m, T_0=303 K, T_f=900 K).

The results obtained in Fig. 6.14 can be well explained with the help of temperature profile shown in Fig. 6.15 for different values of h. The pyrolysis time shows a decreasing trend with increasing value of h ranging from 8.4-126.0 W/m^{2}K. This is understandable because with an increase in h, temperature at any radial position increases and thus the pyrolysis time decreases. As the pyrolysis time decreases, activity of secondary reactions are of less importance and only the activity of primary reactions appear to be significantly influenced by the heat transfer coefficient. Also, as the temperature is increased with increase in the value of h, the heat transfer rate increases

and hence the concentration of (volatile & gases)$_1$ increases at the expense of (char)$_1$, the trends of which are in agreement with those reported by Shafizadeh (1979). Fig. 6.16

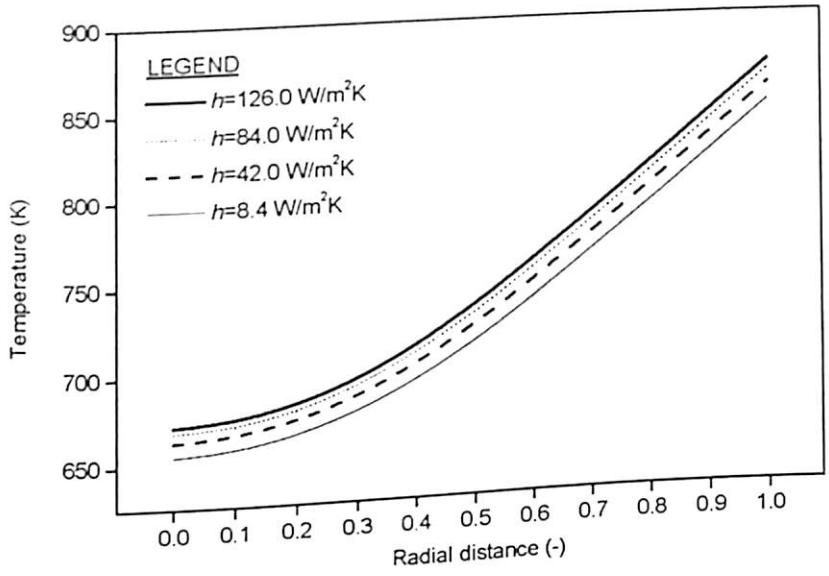

Fig. 6.15. Temperature profile as a function of radial distance for different values of convective heat transfer coefficient with cylindrical pellet (R=0.011 m, T_0=303 K, T_f=900 K).

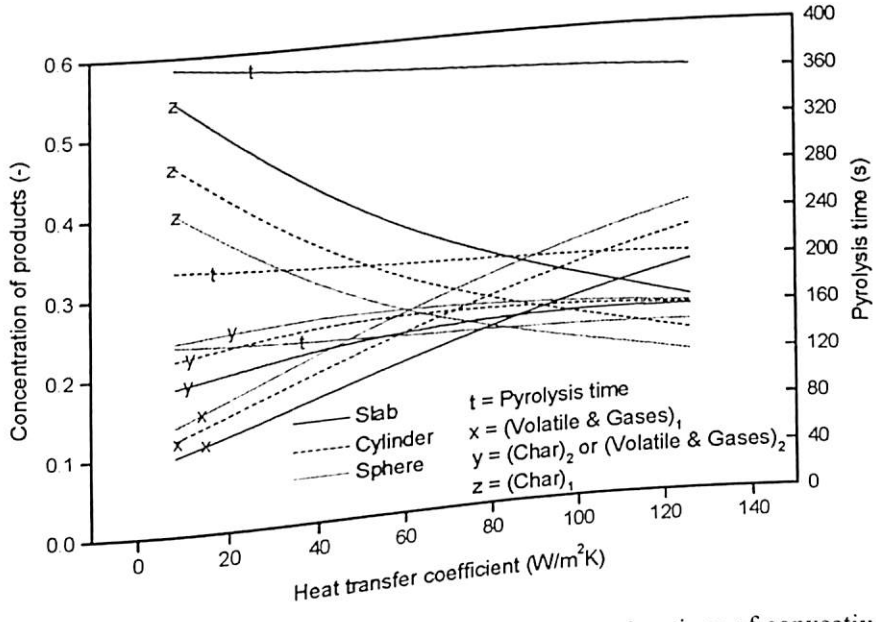

Fig. 6.16. Average concentration of products and pyrolysis time as functions of convective heat transfer coefficient with slab, cylinder and sphere (R=0.011 m, T_0=303 K, T_f=900 K).

shows the concentration of products for slab and sphere along with cylinder. The increase in concentration of (volatile & gases)$_1$ is maximum for the sphere and is least for the slab. The time required for completion of pyrolysis reaction is more for the slab as compared to the cylinder and sphere. The variation in concentration of products for slab and sphere can be explained in similar fashion as above based on temperature profiles.

The results shown in Figs. 6.14 and 6.16 and the corresponding explanation given above have a lot of practical importance and physical significance in the industrial pyrolysis applications. The results obtained consolidate the fact that it is possible to increase the concentration of (volatile & gases)$_1$ with lesser pyrolysis time under the controlled conditions by increasing convective heat transfer at much lower operating temperatures. Higher operating temperatures may lead to combined convective and radiative heat transfer mechanisms, which are not safe and hence lower operating temperatures are preferable.

6.4.2.4. Effect of emissivity (ε)

The emissivity is varied in the entire possible range from 0 to 1 in order to study the effect of this parameter on concentration of products and pyrolysis time. The dependence of this parameter on concentration of products and pyrolysis time with cylindrical pellet is shown in Fig. 6.17 for R=0.011 m. The concentration of (volatile & gases)$_1$ and (char)$_2$ or (volatile & gases)$_2$ is found to increase at the expense of (char)$_1$. When heat transfer from wall surface takes place only by convection and with no radiation (i.e. ε=0.0), the resistance offered for heat transfer near the wall is not very high. It is observed that the increase in temperature at various radial positions is not significant for ε=0.0 as shown in Fig. 6.18. Therefore, the product contains only the

$(char)_1$ at ε=0.0 as shown in Fig. 6.17. Average concentration of products does not appear to be profoundly affected for values of ε up to 0.2 as shown in Fig. 6.17.

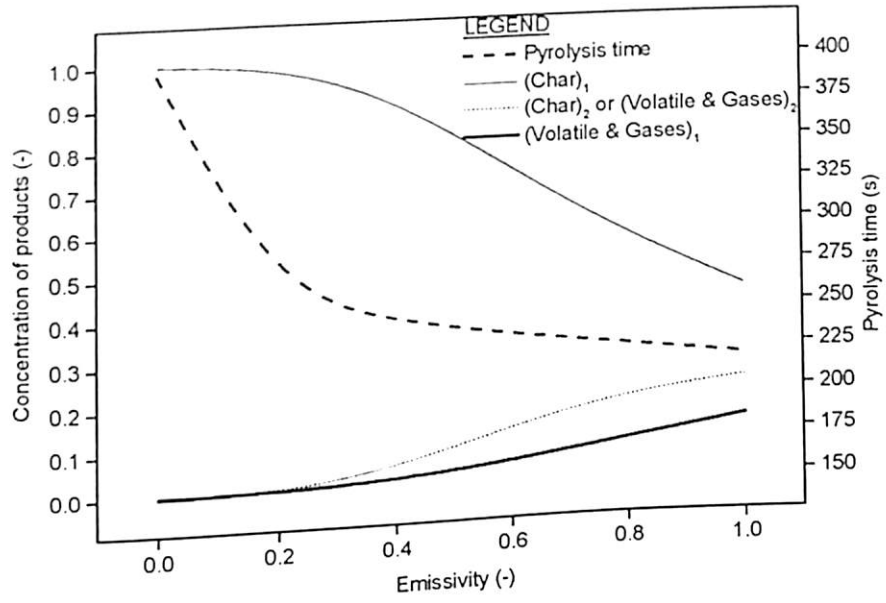

Fig. 6.17. Average concentration of products and pyrolysis time as functions of emissivity with cylindrical pellet (R=0.011 m, T_0=303 K, T_f=900 K).

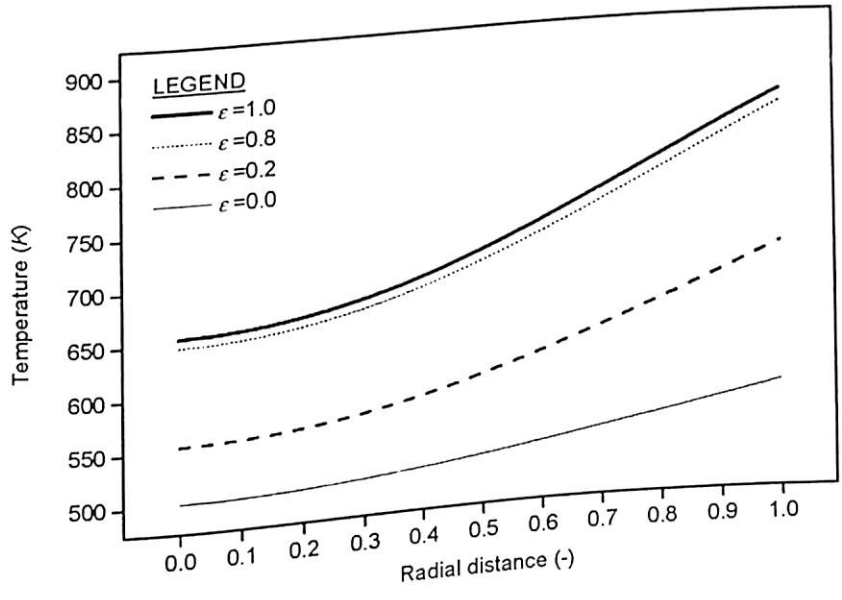

Fig. 6.18. Temperature profile as a function of radial distance for different values of emissivity with cylindrical pellet (R=0.011 m, T_0=303 K, T_f=900 K).

However, pyrolysis time shows a rapid decrease for ε=0.2 due to an increase in the temperature at different radial positions as shown in Fig. 6.18. The effect of ε on concentration of products becomes significant at higher values of ε, and it is found that the activities of both primary and secondary pyrolysis reactions are changing significantly. Same trends as reported in Fig. 6.17 are observed for concentration of products and pyrolysis time for slab and sphere also as shown in Fig. 6.19. The time of completion of pyrolysis is the least for sphere as compared to that for the slab and cylinder.

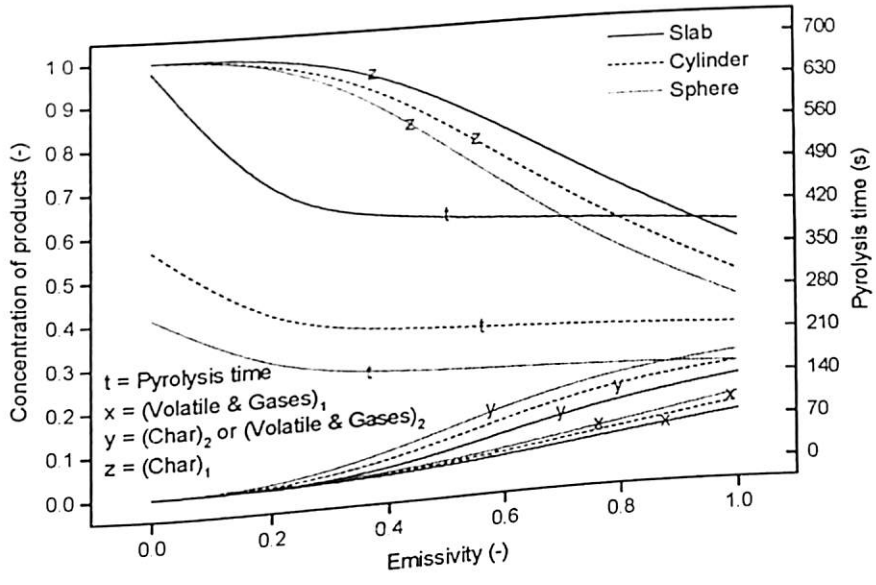

Fig. 6.19. Average concentration of products and pyrolysis time as functions of emissivity with slab, cylinder and sphere (R=0.011 m, T_0=303 K, T_f=900 K).

6.4.2.5. Effect of temperature (T_f)

The effect of final temperature on concentration of products and pyrolysis time is shown in Fig. 6.20 with cylindrical pellet for R=0.011 m. It is observed that at low temperature (below 900 K) the yield of $(char)_1$ is favoured while high temperature

(above 1100 K) is characterized by high gas production i.e. (volatile & gases)$_1$ at the expense of (char)$_1$. At 1250 K, the concentration of (char)$_1$ and (volatile & gases)$_1$ are equal at which the concentration of (char)$_2$ or (volatile & gases)$_2$ is maximum. Above this temperature, the concentration of (char)$_1$ decreases while the concentration of (volatile & gases)$_1$ increases i.e. there is a trade-off between these concentrations. Buekens & Schoeters (1980) also found that pyrolysis at lower temperatures favors production of char; whereas at higher temperatures results in the fission, dehydration, disproportionation, decarboxylation, and decarbonylation reactions, which favors gas production. The same trends are observed for slab and sphere as shown in Fig. 6.21. The time of completion of pyrolysis reactions is more for slab and is least for sphere.

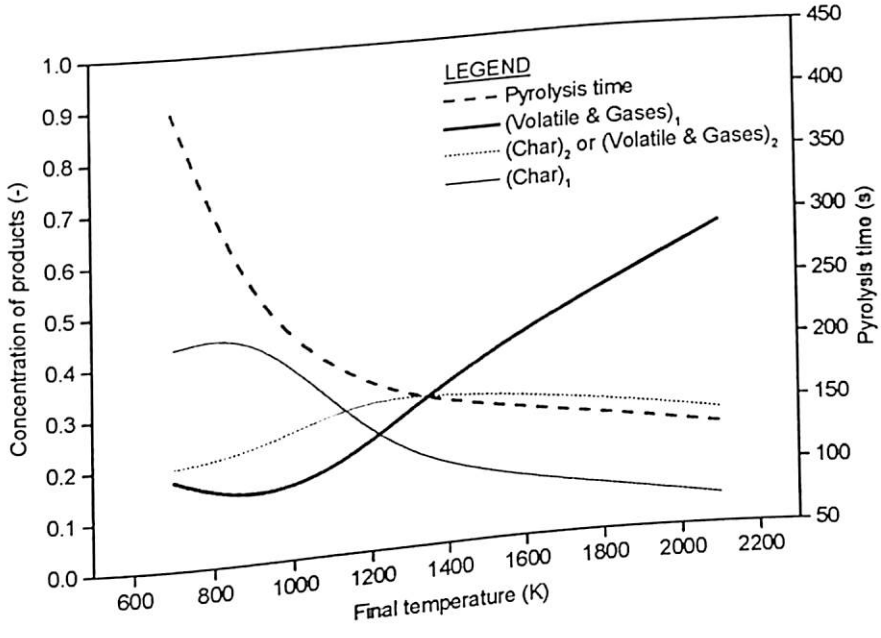

Fig. 6.20. Average concentration of products and pyrolysis time as functions of final temperature with cylindrical pellet (R=0.011 m, T_0=303 K).

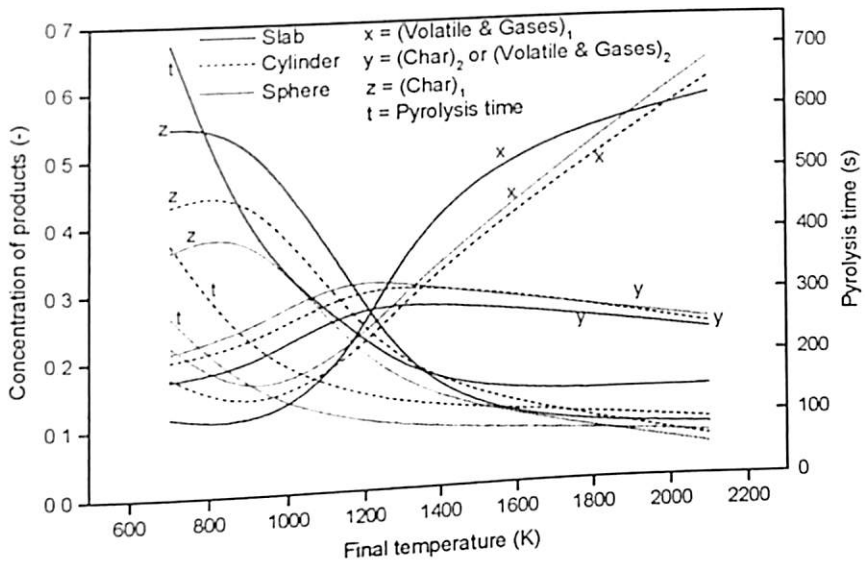

Fig. 6.21. Average concentration of products and pyrolysis time as functions of final temperature with slab, cylinder and sphere (R=0.011 m, T_0=303 K).

6.5. Sensitivity Analysis

A further set of simulations are carried out for different geometries to establish the extent to which each of the properties examined is important in terms of the average concentration of products and the pyrolysis time (conversion time). For each property, a deviation of 50 % (positive and negative) with respect to the reference value shown in Table-6.1 is considered. Tables 6.2-6.4 summarize the results obtained in the present study (Babu & Chaurasia, 2004b, 2004c) for the slab, cylinder, and sphere respectively in terms of the sensitivity parameter. Sensitivity is defined as the ratio of the percentage change of the outputs to the percentage change of the inputs, with respect to their reference values (Pyle & Zaror, 1984; Di Blasi, 1997). Inputs are the properties and outputs are the average concentration of products and the conversion time.

Table-6.1. Reference values for the properties used in sensitivity analysis

Property	Values
Heat of reaction number (exothermic reaction)	$Q^{*}_{exo} = -0.2$
Heat of reaction number (endothermic reaction)	$Q^{*}_{endo} = 0.1$
Wood thermal conductivity	$k = 0.2$ W/m K
Convective heat transfer coefficient	$h = 8.4$ W/m^2 K
Emissivity coefficient	$\varepsilon = 0.6$
Final temperature	$T_f = 1400$ K

The negative sign against a particular concentration of products and conversion time indicates a decrease in their value with an increase in the value of the properties (or vice versa). Highest sensitivity is found for the final reactor temperature (T_f) with $(char)_1$ and the conversion time for all the geometries. Therefore, the reactor temperature is the most significant and hence an important variable for the production of $(char)_1$. Large variations in the concentration of $(volatile\ \&\ gases)_1$ are associated with emissivity (ε) and thermal conductivity (k) of biomass. For an increase in the concentration of $(char)_2$ or $(volatile\ \&\ gases)_2$ also, the emissivity is found to be the most important variable. Finally, certain influence in the conversion time is associated with the heat of reaction number for the exothermic reaction (Q_{exo}), whereas the effects are not very significant with the change in the remaining variable (h). The least sensitive parameter is the convective heat transfer coefficient (h) for the concentration of the products and the conversion time. Thus, in order to maximize the concentration (yield) of a particular product, there are specific parameters, which are to be controlled. The sensitivity for all the parameters is found to be the highest for the slab geometry and is least for the spherical geometry.

Table-6.2. Sensitivity analysis for pyrolysis with ±50% variation to reference values of properties with cylindrical geometry

Properties	(Volatile & Gases)$_1$	(Char)$_1$	(Char)$_2$ or (Volatile & Gases)$_2$	Conversion time
$\dot{Q}_{exo}(+)$	0.4212	-0.3989	0.1675	-0.2602
$\dot{Q}_{exo}(-)$	0.4853	-0.4590	-0.1860	-0.5366
$\dot{Q}_{endo}(+)$	-0.4359	0.1739	-0.2848	0.0553
$\dot{Q}_{endo}(-)$	-0.8283	0.2429	-0.4095	0.0949
$k(+)$	-1.3336	1.7170	-0.6265	0.1121
$k(-)$	-2.9073	1.1496	0.4508	0.1495
$h(+)$	0.0491	-0.0849	0.0556	0.0090
$h(-)$	0.1595	-0.1039	0.0573	-0.0090
ε (+)	2.9942	-0.6511	1.4102	-0.1026
ε (-)	1.6056	-0.6490	1.7293	-0.1624
$T_f(+)$	1.6001	-1.1242	-0.4808	-0.5366
$T_f(-)$	0.9584	-4.4741	0.6702	-4.52

Table-6.3. Sensitivity analysis for pyrolysis with ±50% variation to reference values of properties with slab

Properties	(Volatile & Gases)$_1$	(Char)$_1$	(Char)$_2$ or (Volatile & Gases)$_2$	Conversion time
$\dot{Q}_{exo}(+)$	0.3107	-0.3241	-0.3006	-0.3214
$\dot{Q}_{exo}(-)$	0.4263	-0.6093	-0.0668	-0.7024
$\dot{Q}_{endo}(+)$	-0.4167	0.1284	-0.3458	0.0451
$\dot{Q}_{endo}(-)$	-0.8206	0.1986	-0.5394	0.0767
$k(+)$	-1.3252	1.4615	-0.7510	0.1061
$k(-)$	-3.0710	1.1604	0.2639	0.1326
$h(+)$	0.1591	-0.0818	0.0816	-0.0051
$h(-)$	0.1574	-0.0795	0.0845	-0.0103
ε (+)	3.1010	-0.5706	1.9532	-0.0876
ε (-)	1.6520	-0.4559	1.8205	-0.1313
$T_f(+)$	0.4146	-0.3379	-0.3887	0.0576
$T_f(-)$	1.5139	-9.8295	0.7526	-8.3597

Table-6.4. Sensitivity analysis for pyrolysis with ±50% variation to reference values of properties with sphere

Properties	(Volatile & Gases)$_1$	(Char)$_1$	(Char)$_2$ or (Volatile & Gases)$_2$	Conversion time
$\dot{Q}_{exo}(+)$	0.1976	-0.3058	-0.1121	-0.2222
$\dot{Q}_{exo}(-)$	0.6310	-0.8691	-0.0308	-0.4040
$\dot{Q}_{endo}(+)$	-0.4443	0.2015	-0.2798	0.0659
$\dot{Q}_{endo}(-)$	-0.8092	0.2759	-0.2859	0.1099
$k(+)$	-1.3321	1.9039	-0.5501	0.1307
$k(-)$	-2.8098	1.1370	0.5518	0.1438
$h(+)$	0.1553	-0.0979	0.0362	-0.0127
$h(-)$	0.1564	-0.1106	0.0368	-0.0127
ε (+)	2.8799	-0.7028	1.0589	-0.1071
ε (−)	1.5740	-0.8457	1.6319	-0.1905
$T_f(+)$	1.6986	-1.1787	-0.3753	-0.5055
$T_f(-)$	0.7039	-4.3719	0.5438	-4.2637

6.6. Conclusions

Simulations are carried out in the present study (Babu & Chaurasia, 2004b, 2004c) using the Model-III (chapter 5) for the temperature ranging between 303-2100 K and the equivalent particle radius ranging between 0.0000125-0.011 m. The pyrolysis rate is obtained by considering two parallel primary reactions and a third secondary reaction between the volatile & gaseous products and char. The secondary reactions are responsible for carbon enrichment of the final residual. The effects of the parameters such as heat of reaction number, thermal conductivity, heat transfer coefficient, emissivity, and reactor temperature have been analyzed. Based on the results obtained using above simulations, the following conclusions are drawn.

- The results obtained from the model are in good agreement with quite a few experimental results reported in literature (Shafizadeh, Furneaux, Cochran, Scholl, &

Sakai, 1979; Pyle & Zaror, 1984; Scott, Piskorz, Bergougnou, Graham, & Overend, 1988; Alves & Figueiredo, 1989) as compared to the models developed by the earlier researchers (Bamford, Crank, & Malan, 1946; Liliedahl & Sjöström, 1998; Jalan & Srivastava, 1999).

- Two typical pyrolysis reactions, namely, '*heat-transfer-controlled reaction*' and '*self-sustaining reaction*', are considered. The former is characterized by positive value of heat of reaction number Q^*, e.g. 10, and the latter is characterized by negative value, e.g., -0.5.
- In case of '*self-sustaining reaction*', the heat source from the surrounding environment which is utilized to initiate the pyrolysis reaction is not required at the later stage as the reaction is exothermic. This is the major advantage of pyrolysis process.
- The production of $(char)_1$ is favoured by the endothermic reactions while the production of $(volatile\ \&\ gases)_1$ is favoured by the exothermic reactions.
- The results of the parametric study to predict the dependence of the average concentration of products and the conversion time on thermal and physical properties during convective/radiant pyrolysis are applicable to both the gasification (devolatilization stage) and pyrolysis units.
- Thermal and physical properties are important mainly for large particles (thermally thick regime).
- The conversion time becomes successively longer as the thermal conductivity of biomass increases and/or emissivity decreases, thus affecting the reactor throughput.

- Gas quality (low char content), for a fixed particle size, is better for feedstocks with low thermal conductivity.
- In many cases the desired product is char. High char concentration is associated with the lower values of reactor final temperature.
- Activity of the primary reactions is greatly affected by the biomass thermal properties (emissivity and thermal conductivity). Secondary reactions are also found to be affected by emissivity.
- The two most significant variables are emissivity and reactor temperature.
- The least sensitive parameter is the convective heat transfer coefficient.
- The sensitivity for all the parameters is highest for the slab geometry and is lowest for the spherical geometry.

CHAPTER 7

HEAT TRANSFER AND KINETICS IN THE PYROLYSIS OF SHRINKING BIOMASS PARTICLE

7.1. Introduction

Biomass fuels represent a promising route for the production of charcoal, medium heating value gases and condensable organic components (tars), through pyrolytic conversion. The understanding of the interaction between chemical and physical mechanisms during solid pyrolysis is of fundamental importance, for the optimal design of chemical pyrolysis reactors and combustors. Several mathematical models are available for pyrolysis, which consider conservation of mass, momentum, energy, multiple two-step reaction mechanism, and flow of volatiles and gases within the particle. But, many of these models do not consider shrinkage or swelling of the particle as the pyrolysis proceeds. The shrinking of the solid particle affects the pyrolysis in several ways. The medium properties (porosity, permeability, density, mass diffusivity, specific heat capacity and thermal conductivity), volume occupied by the volatiles (gas and tar), volume occupied by the solid (wood and char), and consequently the total

volume of the particle also change continuously. As a result of the chemical restructuring during pyrolysis, the density of char increases. The temperature profile of the particle changes due to increased density and decreased distance across the pyrolysis region. A sharper temperature gradient causes heat to reach the interior of the particle more quickly, and the thinner and hotter char layer also affects the product yield. In the present work (Babu & Chaurasia, 2003e, 2004d), the impact of shrinkage on pyrolysis of biomass particles is studied employing a kinetic model coupled with heat transfer model utilizing a practically significant kinetic scheme consisting of physically measurable parameters.

7.2. Background

Several researchers have developed models for biomass pyrolysis (Bamford, Crank & Malan, 1946; Broido & Nelson, 1975; Park & Levenspiel, 1975; Fan, Fan, Miyanami, Chen, & Walawender, 1977; Miyanami, Fan, Fan, & Walawender, 1977; Chan, Kelbon & Krieger, 1985; Ragland, Boerger & Baker, 1988; Alves & Figueiredo, 1989; Boroson, Howard, Longwell, & Peters, 1989; Saastamoinen, 1993; Antal & Varhegyi, 1995; Di Blasi, 1995, 1996b; Melaaen & Grønli, 1997; Sato, Aoki, Miura, & Patrick, 1997; Şensöz, Angin & Yorgun, 2000; Bryden, Ragland & Rutland, 2002; Dong & De Pater, 2002; Hagge & Bryden, 2002). Many of these models do not include the impact of shrinkage in the pyrolysis process. It is based on the assumption that the total volume of the particle does not change during thermal degradation. On the other hand, experiments conducted for large biomass particles (Lee, Chaiken & Singer, 1976; Chan, Kelbon & Krieger, 1988) have shown significant shrinkage of the char layer as the pyrolysis front

propagates through the solid. Morel, Amundson & Park (1990) have modeled the changes in the particle size, due to disintegration of the solid structure at some critical conversion during char gasification. Villermaux, Antoine, Lede, & Soulignac, (1986) described the shrinkage effects assuming that the solid density remains constant as degradation occurs, but they considered very simplified one-step reaction model and the secondary reactions are not considered.

The actual reaction scheme of pyrolysis of biomass is extremely complex because of formation of over a hundreds of intermediate products. Pyrolysis of biomass is, therefore, generally modeled on the basis of apparent kinetics. Different kinetic schemes are used by various researchers as given in chapter 2.

Di Blasi (1996b) and Hagge & Bryden (2002) utilized the kinetic scheme (Shafizadeh & Chin, 1977; Thurner and Mann, 1981; Chan, Kelbon & Krieger, 1985; Font, Marcilla, Verdu, & Devesa, 1990) as given by equation (2.7) while studying the impact of shrinkage on the pyrolysis of biomass. But, the main drawback of this kinetic model as pointed out by Di Blasi (2000b) is that it is based on the assumption of a constant ratio between the yields of solid char and volatile products. Therefore, it is not applicable for fast pyrolysis and to predict product distribution. Consequently, it cannot predict the dependence of product yields on the reactor temperature and the heating rate, which is of fundamental importance in reactor design and operation. The kinetic constants k_1, k_2, and k_3 of primary reactions and k_4 & k_5 of secondary reactions should correspond to the same wood sample. However, Di Blasi (1996b) and Hagge & Bryden (2002) in their studies took the kinetic constants of primary reactions (k_1, k_2, k_3) from Thurner & Mann (1981), Chan, Kelbon & Krieger (1985) & Font, Marcilla, Verdu, & Devesa (1990), and

kinetic constants for secondary reactions, k_4 and k_5 from Liden, Berruti & Scott (1988) and Di Blasi (1993b) respectively. In fact, the wood samples used for the above primary & secondary reactions in the above references are not of same type.

A recent re-examination (Varhegyi, Jakab & Antal, 1994) of the Broido-Shafizadeh scheme as given by equation (2.8) of cellulose pyrolysis (with kinetic constants k_1, k_2, and k_3 as in Bradbury, Sakai & Shafizadeh, 1979), extended to include secondary reactions with kinetic constant k_4 (Liden, Berruti & Scott, 1988) has raised some questions about the importance of the initiation reaction leading to the formation of "active" cellulose intermediate. More precisely, new kinetic measurements seem to indicate that such a reaction is superfluous in the temperature range 523-643 K. Even rough estimations of kinetic data for the formation of an intermediate "active" wood are not available.

Keeping the drawbacks of the above schemes, the kinetic scheme given by equation (2.3) proposed by Koufopanos, Papayannakos, Maschio, & Lucchesi (1991) and also utilized successfully as discussed in chapters 3, 4, 5, & 6 is used in the present study (Babu & Chaurasia, 2004d) also. Koufopanos, Papayannakos, Maschio, & Lucchesi (1991) have determined both primary and secondary reaction rate constants and heat of pyrolysis by matching the models with measured mass loss and temperature profile data. This approach is to be favoured since it enhances the reliability of the model validation.

7.3. Motivation

Shrinkage occurs in the char layer during the pyrolysis reactions because of a rearrangement of chemical bonds and the coalescence of graphite nuclei within the

biomass particle. The amount of char shrinkage is a function of wood species, heat flux, and temperature. Varying compositions of lignin, cellulose & hemicellulose and other organic & inorganic materials result in different amounts of shrinkage for different species. Char shrinkage increases as the temperature increases and also increases with the amount of time at a given temperature. The inclusion of shrinkage reduces the pyrolysis time and affects the product yield. The modeling of pyrolysis of biomass incorporating shrinkage can be used to gain an understanding of how it can affect the pyrolysis process, and to understand what pyrolysis or combustion conditions must be considered. This can provide an improved qualitative understanding of pyrolysis and guide further research into modeling of biomass pyrolysis and combustion.

7.4. Description of mathematical model

In the present study (Babu & Chaurasia, 2004d), a biomass particle of cylindrical shape of radius R, length l, and radial thickness dr is considered. The length/diameter ratio of 5 is considered to be high enough to assume that the cylinders approximate bodies with an infinite axial length (Tye, 1969), so that heat transfer takes place in radial direction only. It is assumed that heat flows in one dimension and heat transfer inside the particle occurs by conduction only. The heat transfer coefficient represents the overall effect of the above mechanisms. The chemical kinetics and heat transfer model equations (7.1)-(7.9) along with initial & boundary conditions are given in Table-7.1. The dimensionless forms are given by equations (7.10)-(7.18) with the dimensionless groups as given in Appendix-C (equations C.1-C.20).

The time evolution for V_S, V_g and V are described by equations (7.19)-(7.23). As the pyrolysis progresses, the volume occupied by the solid is assumed to decrease linearly with the wood mass and to increase with the char mass, by a chosen shrinkage

Table-7.1. Mathematical model

Koufopanos et al. (1991) mechanism

Virgin biomass B (n_1 order decay)

Reaction 1 Reaction 2

(Volatile + Gases)$_1$ + (Char)$_1$ —Reaction 3→ (Volatile + Gases)$_2$ + (Char)$_2$

(n_2 order decay) (n_3 order decay)

Particle model

Conservation of biomass, (gases and volatiles)$_1$ (char)$_1$, (gases and volatiles)$_2$ & (char)$_2$:

$$\frac{\partial(C_B V)}{\partial t} = -(k_1 + k_2) C_B^{n_1} V \tag{7.1}$$

$$\frac{\partial(C_{G1} V_g)}{\partial t} = k_1 C_B^{n_1} V - k_3 C_{G1}^{n_2} V_g C_{C1}^{n_3} V \tag{7.2}$$

$$\frac{\partial(C_{C1} V)}{\partial t} = k_2 C_B^{n_1} V - k_3 C_{G1}^{n_2} V_g C_{C1}^{n_3} V \tag{7.3}$$

$$\frac{\partial(C_{G2} V_g)}{\partial t} = k_3 C_{G1}^{n_2} V_g C_{C1}^{n_3} V \tag{7.4}$$

$$\frac{\partial(C_{C2} V)}{\partial t} = k_3 C_{G1}^{n_2} V_g C_{C1}^{n_3} V \tag{7.5}$$

Enthalpy:

$$\frac{\partial}{\partial t}\left(C_p \rho T\right) = k\left(\frac{b-1}{r}\frac{\partial T}{\partial r} + \frac{\partial^2 T}{\partial r^2}\right) + (-\Delta H)\left(-\frac{\partial \rho}{\partial t}\right) \tag{7.6}$$

Initial conditions:

$$t = 0; \quad C_B = C_{B0},\ C_{G1} = C_{C1} = C_{G2} = C_{C2} = 0,\ V = V_{B0},\ V_g = 0.5 V_{B0},\ T(r,0) = T_0 \tag{7.7}$$

Particle boundary conditions:

$$t > 0; \quad r = 0, \quad \left(\frac{\partial T}{\partial r}\right)_{r=0} = 0 \tag{7.8}$$

$$t > 0; \quad r = R, \quad k_{eff}\left(\frac{\partial T}{\partial r}\right)_{r=R} = h\left(T_f - T\right) + \sigma\varepsilon\left(T_f^4 - T^4\right) \tag{7.9}$$

Table-7.1. Mathematical model (Continued)

Dimensionless forms of equations (7.1)-(7.9):

$$\frac{\partial(\overline{C}_B\overline{V})}{\partial t} = -(k_1 + k_2)\overline{C}_B^{n_1}\overline{V} \tag{7.10}$$

$$\frac{\partial(\overline{C}_{G1}\overline{V}_g)}{\partial t} = k_1\overline{C}_B^{n_1}\overline{V} - k_3\overline{C}_{G1}^{n_2}\overline{V}_g\overline{C}_{C1}^{n_3}\overline{V} \tag{7.11}$$

$$\frac{\partial(\overline{C}_{C1}\overline{V})}{\partial t} = k_2\overline{C}_B^{n_1}\overline{V} - k_3\overline{C}_{G1}^{n_2}\overline{V}_g\overline{C}_{C1}^{n_3}\overline{V} \tag{7.12}$$

$$\frac{\partial(\overline{C}_{G2}\overline{V}_g)}{\partial t} = k_3\overline{C}_{G1}^{n_2}\overline{V}_g\overline{C}_{C1}^{n_3}\overline{V} \tag{7.13}$$

$$\frac{\partial(\overline{C}_{C2}\overline{V})}{\partial t} = k_3\overline{C}_{G1}^{n_2}\overline{V}_g\overline{C}_{C1}^{n_3}\overline{V} \tag{7.14}$$

$$\frac{\partial\theta}{\partial\tau} = \frac{b-1}{x}\frac{\partial\theta}{\partial x} + \frac{\partial^2\theta}{\partial x^2} + \frac{Q''R^2k_1}{\alpha} \tag{7.15}$$

$$\tau = 0; \quad \overline{C}_B = 1,\ \overline{C}_{G1} = \overline{C}_{C1} = \overline{C}_{G2} = \overline{C}_{C2} = 0,\ \overline{V} = 1,\ \overline{V}_g = 0.5,\ \theta(x,0) = 1 \tag{7.16}$$

$$\tau > 0; \quad x = 0, \quad \frac{\partial\theta}{\partial x} = 0 \tag{7.17}$$

$$\tau > 0; \quad x = 1, \quad \frac{\partial\theta}{\partial x} = -\theta H \tag{7.18}$$

Equations describing the time evolution for V_S, V_g and V:

$$\frac{V_S}{V_{S0}} = \frac{M_B}{M_{B0}} + \frac{\alpha' M_C}{M_{B0}} \tag{7.19}$$

$$V_g = V_{g0} + \beta'(V_{S0} - V_S) \tag{7.20}$$

$$V_{g0} = \eta V_{gi} + (1-\eta)V_{gf} \tag{7.21}$$

$$V_{gf} = \gamma' V_{gi} \tag{7.22}$$

$$V = V_g + V_S \tag{7.23}$$

$$\overline{V} = V/V_{S0},\ \overline{V}_g = V_g/V_{S0} \tag{7.24)-(7.25}$$

Koufopanos et al. (1991) correlation:

$$h = 0.322(k/l)Pr^{1/3}Re^{0.5} \tag{7.26}$$

Other relations:

$$\varepsilon'' = V_g/V,\ \eta = M_B/M_{B0} \tag{7.27)-(7.28}$$

Conversion of biomass:

$$X = \frac{\overline{C}_{B_0} - \left[\left(\sum_{i=1}^{N}\overline{C}_B\right)\Big/(N+1)\right]}{\overline{C}_{B_0}} \tag{7.29}$$

factor, α' given by equation (7.19). The volume of volatiles is made up of two contributions. As given by equation (7.20), the first V_{g0} is the initial volume occupied by volatiles, and the second term $\beta'(V_{s0} - V_s)$ is the fraction of volume left by the solid as a consequence of the pyrolysis process. To consider the structural changes that take place during the pyrolysis, V_{g0} may also vary linearly with the composition of the degrading medium, from initial value, V_{gi}, determined by the initial solid porosity, to a final value taken as a fraction, γ', of the initial one as given by equations (7.21) and (7.22). The total particle volume is expressed by equation (7.23). The parameters α', β' and γ' vary from 0 for total disintegration of the particle to 1 for no shrinkage.

7.5. Numerical solution and Simulation

As discussed in chapter 4, finite difference pure implicit scheme utilizing Tri-Diagonal Matrix Algorithm (TDMA) also known as Thomas Algorithm (Carnahan, Luther & James, 1969) is employed for solving heat transfer model equation and Runge-Kutta 4th order method is used for chemical kinetics model equations. Simulations are carried out for cylindrical geometry considering radius ranging from 0.0000125 m to 0.05 m, and temperature ranging from 303 K to 900 K. The values of the parameters α', β' and γ' can be varied from 0.0 which represents total shrinkage to 1.0 which represents no shrinkage of the particle. Extensive simulations have been out carried by varying the values of these parameters between 0.0 and 1.0 with different combinations. It is found that for $\alpha' = 0.2$, $\beta' = 0.0$ and $\gamma' = 0.2$ which nearly represents the total shrinkage of the particle, the model is in excellent agreement with many experimental

results (Shafizadeh, Furneaux, Cochran, Scholl, & Sakai, 1979; Pyle & Zaror, 1984; Scott, Piskorz, Bergougnou, Graham, & Overend, 1988). Hence, same values of the parameters are retained for all the simulations. In the present study (Babu & Chaurasia, 2004d), the choice of lower possible values of shrinkage factor ($\alpha' = 0.2, \beta' = 0.0, \gamma' = 0.2$) is more realistic of incorporating shrinkage effect as against relatively higher values ($\alpha' = 0.5, \beta' = 0.0, \gamma' = 0.5$) as taken by Di Blasi (1996b). It may be noted that Hagge & Bryden (2002) in their study considered the shrinkage due to char only, and they did not consider the shrinkage due to volume occupied by the volatiles as discussed by Di Blasi (1996b). This limitation is also rectified in the present study (Babu & Chaurasia, 2004d). The values of various parameters employed are given in Appendix-C. The Computer Codes in C++ for present model (Babu & Chaurasia, 2004d) with shrinkage is given in Appendix-F while for Model-III (without shrinkage) in Appendix-B.

7.6. Results and discussion

7.6.1. Model validation and comparison

Figs. 7.1 and 7.2 show the temperature profile as a function of time at the centre (i.e. x=0) of the cylindrical pellet of radius 0.003 m for final temperature of 643 K and 780 K respectively. This is compared with profiles obtained by the model of Jalan & Srivastava (1999), Model-III without shrinkage (consists of equations 5.1, 5.19, 5.3-5.5, 5.20, 5.7, 5.9, 5.11, and 5.12) and the experimental data obtained by Pyle & Zaror (1984). It is found that the present model (Babu & Chaurasia, 2004d) with shrinkage is in excellent agreement with the experimental data better than the agreement with the

model of Jalan & Srivastava (1999) and Model-III without shrinkage for both values of final temperatures of 643 K and 780 K. The present model (Babu & Chaurasia, 2004d)

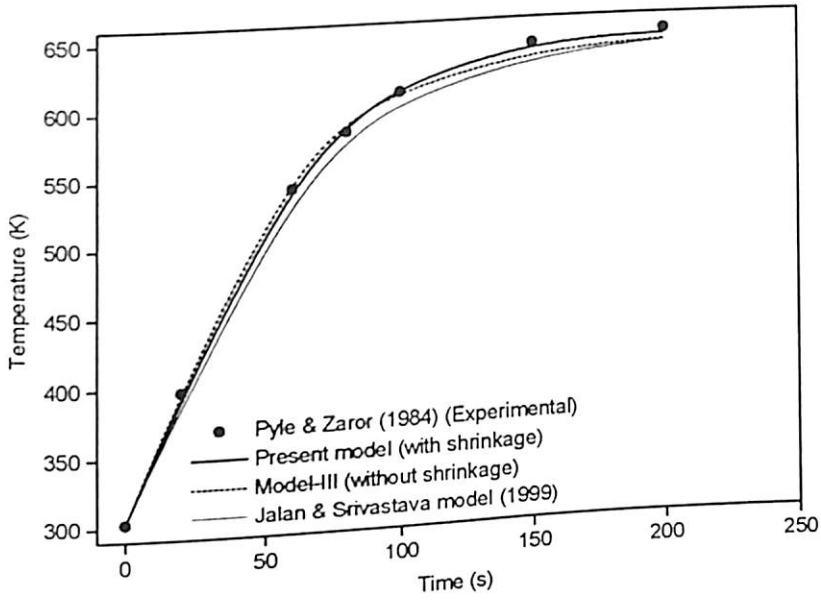

Fig. 7.1. Temperature profile as a function of time at the centre of the cylindrical pellet (R=0.003 m, T_0=303 K, T_f=643 K, x=0).

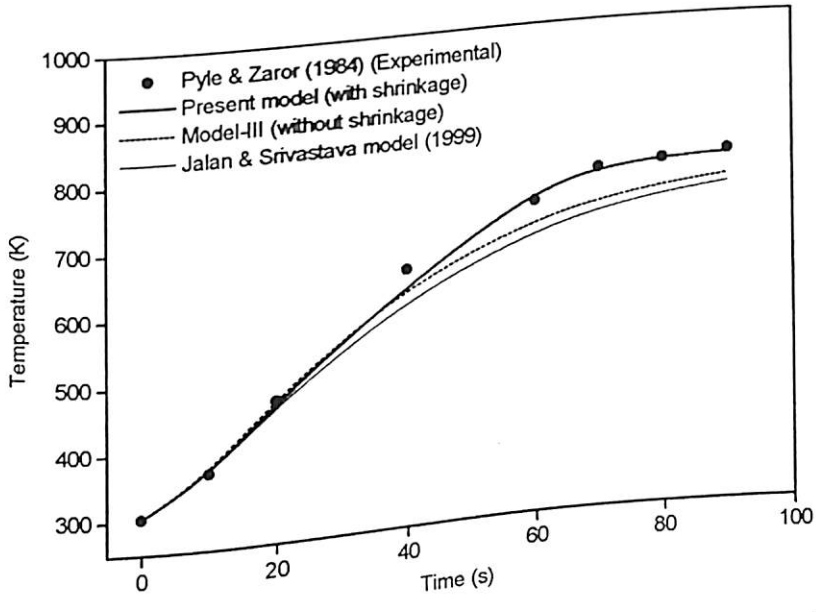

Fig. 7.2. Temperature profile as a function of time at the centre of the cylindrical pellet (R=0.003 m, T_0=303 K, T_f=780 K, x=0).

predicts better even for particle radius of 0.0075 m as compared to the other models as shown in Fig. 7.3. As is evident in general from Figs. 7.1, 7.2 & 7.3, and particularly from Figs. 7.2 & 7.3, the earlier models underpredict the experimental data at higher values of pyrolysis time, while the present model (Babu & Chaurasia, 2004d) predictions match excellently well for the entire duration of pyrolysis time. This explains the importance of shrinkage effect that is being incorporated in the present model (Babu & Chaurasia, 2004d).

Figs. 7.4, 7.5 & 7.6 show the temperature profiles as a function of dimensional radial distance for the final temperature of 643 K after 4 min, 6 min, & 11 min respectively. The temperature profiles obtained using present model (Babu & Chaurasia, 2004d) with shrinkage are in much better agreement with the experimental data of Pyle & Zaror (1984) when compared to the other three models. Here again the present model (Babu &

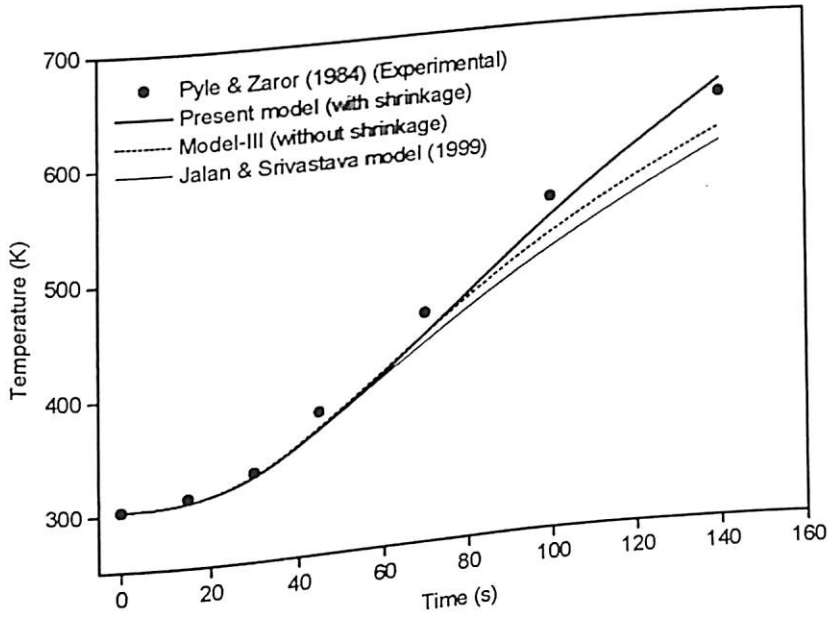

Fig. 7.3. Temperature profile as a function of time at the centre of the cylindrical pellet (R=0.0075 m, T_0=303 K, T_f=773 K, x=0).

Chaurasia, 2004d) predictions are in excellent agreement with experimental data, substantiating the shrinkage effect, for the entire range of dimensionless distance (from

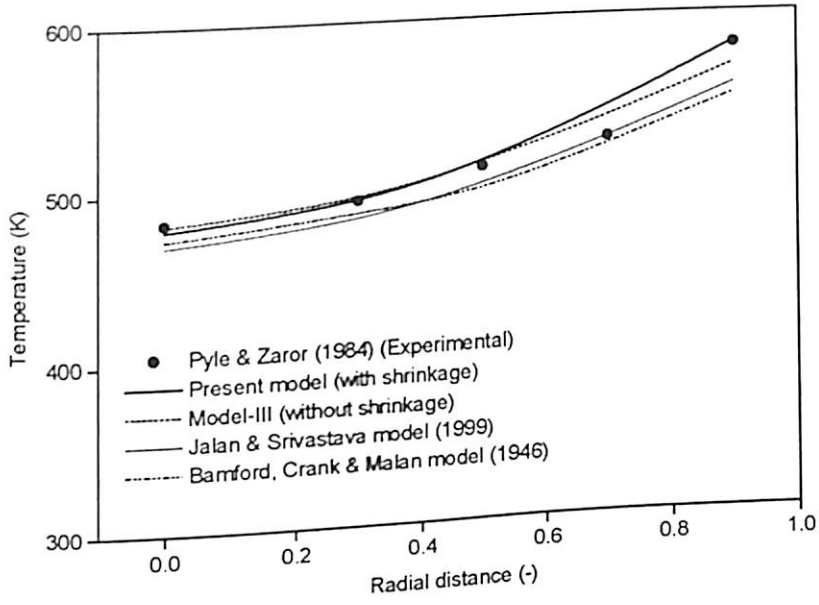

Fig. 7.4. Temperature profile as a function of radial distance with cylindrical pellet (R=0.011 m, T_0=303 K, T_f=643 K, t=4 min).

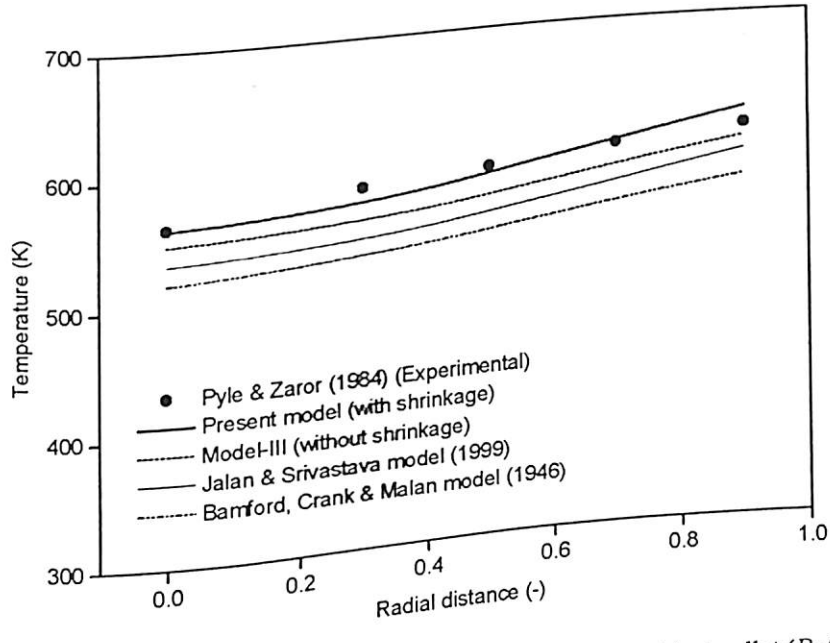

Fig. 7.5. Temperature profile as a function of radial distance with cylindrical pellet (R=0.011 m, T_0=303 K, T_f=643 K, t=6 min).

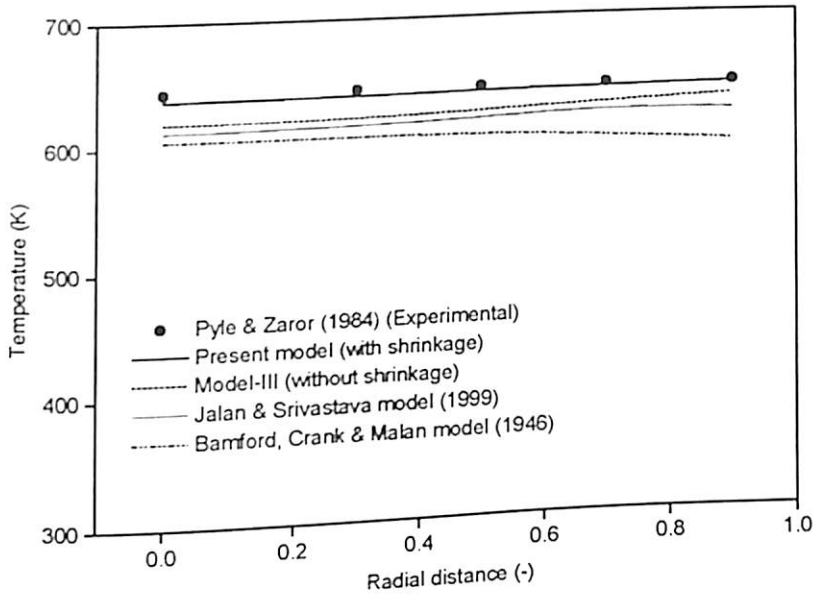

Fig. 7.6. Temperature profile as a function of radial distance with cylindrical pellet (R=0.011 m, T_i=303 K, T_f=643 K, t=11 min).

centre to the surface) of the particle, while the earlier models underpredict all through the distances from centre to surface of the particle. The present model (Babu & Chaurasia, 2004d) is also compared with the model of Liliedahl & Sjöström (1998) as shown in Fig. 7.7. Fig. 7.7 shows the conversion profile as a function of time with cylindrical pellet of radius 0.011 m and final temperature of 753 K. The present model (Babu & Chaurasia, 2004d) is in better agreement as compared to the model of Liliedahl & Sjöström (1998), while the latter underpredicts the conversion at higher values of pyrolysis time. This may be due to the fact that while developing the model, Liliedahl and Sjöström (1998) considered thermal conductivity and specific heat capacity of biomass to be constant, and also did not incorporate the shrinkage effect. The present model (Babu & Chaurasia, 2004d) is in better agreement with the experimental data of Shafizadeh, Furneaux,

Cochran, Scholl, & Sakai (1979) and Scott, Piskorz, Bergougnou, Graham, & Overend (1988) also as shown in Fig. 7.8.

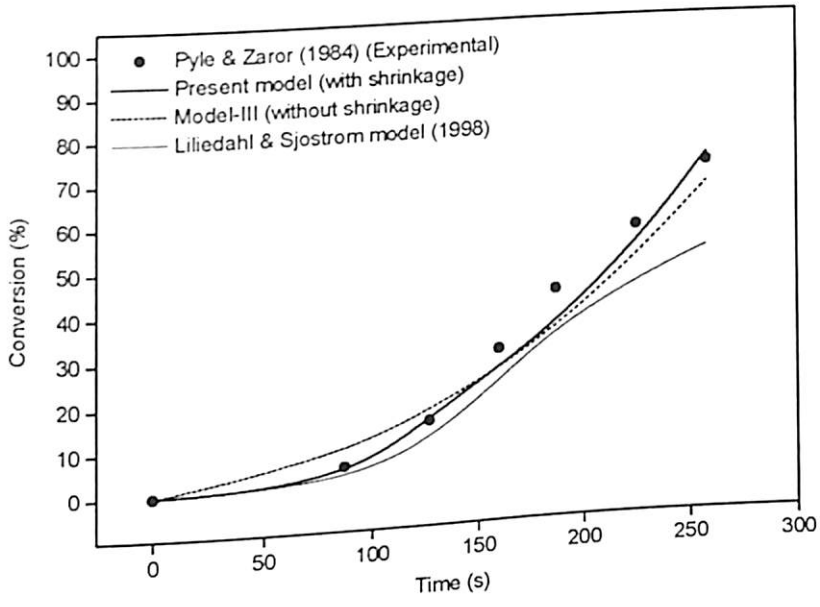

Fig. 7.7. Conversion profile as a function of time with cylindrical pellet (R=0.011 m, T_0=303 K, T_f=753 K).

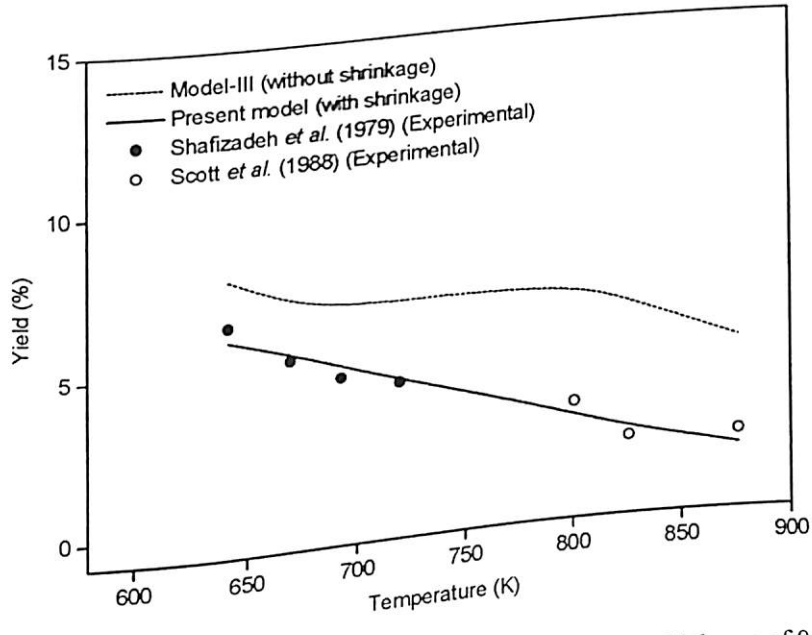

Fig. 7.8. Average char yield as a function of temperature for particle half-thickness of 0.0000125 m.

The values are also given in Tables 7.2-7.8 for quantitative comparison of present model (Babu & Chaurasia, 2004d) with shrinkage with the earlier models and the literature data. The average percentage error and standard deviation are also calculated. In all the cases, it is found that the average percentage error and standard deviation from experimental data are significantly less with the model developed in the present study (Babu & Chaurasia, 2004d) as compared to the other models.

Table-7.2. Comparison of present model results with shrinkage with those of earlier models for various stages of pyrolysis (time) at the centre of cylindrical pellet (R = 0.003 m, T_0 = 303 K, T_f = 643 K)

Time (s)	Temperature (K)			
	PZ	PS	MWS	JS
0	303	303	303	303
20	397	394	400	387
60	541	545	552	533
80	581	585	588	574
100	609	614	610	602
150	641	641	634	630
200	648	644	640	639
Epa		**0.51**	**0.92**	**1.35**
SD		**0.0066**	**0.0122**	**0.0164**

PZ=Pyle & Zaror (1984) (Experimental); PS=Present model (Babu & Chaurasia, 2004d) with shrinkage; MWS=Model-III without shrinkage; JS=Jalan & Srivastava model (1999)

Table-7.3. Comparison of present model results with shrinkage with those of earlier models for various stages of pyrolysis (time) at the centre of cylindrical pellet (R = 0.003 m, T_0 = 303 K, T_f = 780 K)

Time (s)	Temperature (K)			
	PZ	PS	MWS	JS
0	303	303	303	303
10	365	363	366	362
20	466	465	473	459
40	642	618	619	598
60	726	741	696	679
70	769	766	719	704
80	777	777	736	723
90	786	781	748	736
Epa		**0.94**	**3.26**	**4.68**
SD		**0.0165**	**0.0424**	**0.0600**

PZ=Pyle & Zaror (1984) (Experimental); PS=Present model (Babu & Chaurasia, 2004d) with shrinkage; MWS=Model-III without shrinkage; JS=Jalan & Srivastava model (1999)

Table-7.4. Comparison of present model results with shrinkage with those of earlier models for various stages of pyrolysis (time) at the centre of cylindrical pellet (R = 0.0075 m, T_0 = 303 K, T_f = 773 K)

Time (s)	Temperature (K)			
	PZ	PS	MWS	JS
0	303	303	303	303
15	312	305	305	304
30	330	323	324	323
45	377	360	362	359
70	454	434	437	430
100	545	532	518	503
140	629	641	598	585
Epa		2.51	3.10	4.21
SD		0.0313	0.0381	0.0533

PZ=Pyle & Zaror (1984) (Experimental); PS=Present model (Babu & Chaurasia, 2004d) with shrinkage; MWS=Model-III without shrinkage; JS=Jalan & Srivastava model (1999)

Table-7.5. Comparison of present model results with shrinkage with those of earlier models for pyrolysis time = 6 min (R = 0.011 m, T_0 = 303 K, T_f = 643 K)

x	Temperature (K)				
	PZ	PS	MWS	JS	BCM
0	563	562	550	535	520
0.3	583	570	557	542	530
0.5	590	584	567	554	540
0.7	600	602	583	570	555
0.9	610	623	600	590	570
Epa		1.17	3.03	5.28	7.85
SD		0.0163	0.0358	0.0607	0.0883

PZ=Pyle & Zaror (1984) (Experimental); PS=Present model (Babu & Chaurasia, 2004d) with shrinkage; MWS=Model-III without shrinkage; JS=Jalan & Srivastava model (1999); BCM= Bamford, Crank & Malan model (1946)

Table-7.6. Comparison of present model results with shrinkage with those of earlier models for pyrolysis time = 11 min (R = 0.011 m, T_0 = 303 K, T_f = 643 K)

x	Temperature (K)				
	PZ	PS	MWS	JS	BCM
0	643	637	619	612	605
0.3	643	638	620	614	605
0.5	643	639	623	617	605
0.7	643	640	627	622	600
0.9	643	642	632	620	595
Epa		0.59	2.92	4.04	6.38
SD		0.0073	0.0337	0.0457	0.0716

PZ=Pyle & Zaror (1984) (Experimental); PS=Present model (Babu & Chaurasia, 2004d) with shrinkage; MWS=Model-III without shrinkage; JS=Jalan & Srivastava model (1999); BCM= Bamford, Crank & Malan model (1946)

Table-7.7. Comparison of present model results with shrinkage with those of earlier model without shrinkage for char yield obtained by Shafizadeh *et al.* (1979) (R = 0.0000125 m, T_0 = 303 K)

T_f(K)	Char Yield		
	SF	PS	MWS
642	6.43	5.98	7.85
670	5.22	5.42	7.04
693	4.52	4.89	6.78
720	4.17	4.28	6.73
*E*pa		**5.21**	**28.83**
SD		**0.0677**	**0.5155**

SF=Shafizadeh *et al.* (1979) (Experimental); MWS=Model-III without shrinkage
PS=Present model (Babu & Chaurasia, 2004d) with shrinkage

Table-7.8. Comparison of present model results with shrinkage with those of earlier model without shrinkage for char yield obtained by Scott *et al.* (1988) (R = 0.0000125 m, T_0 = 303 K)

T_f(K)	Char Yield		
	SC	PS	MWS
801	2.96	2.56	6.65
826	1.74	2.02	6.03
876	1.74	1.29	4.72
*E*pa		**17.75**	**63.26**
SD		**0.2356**	**2.2985**

SF=Shafizadeh *et al.* (1979) (Experimental); MWS=Model-III without shrinkage
PS=Present model (Babu & Chaurasia, 2004d) with shrinkage

7.6.2. Simulation results

The numerical model is used to examine the impact of shrinkage on particle size, pyrolysis time, product yields, specific heat capacity, and Biot number. The radius of cylinder ranges from 0.0000125 - 0.05 m. The temperatures range from 303 - 900 K.

The excellent agreement between the present model predictions with the experimental data reported in the literature much better than the earlier models as discussed in above section consolidates the model validity for wide range of operating conditions. Hence, extensive simulations have been carried out for cylindrical geometry. In case of kinetically controlled reaction (very small particle sizes) intra-particle activity of

secondary reactions is negligible even at high reaction temperatures. Since the main objective of this study is to understand the impact of shrinkage, only the case of heat-transfer-controlled conversion (thermally thin and thick regimes) is considered.

7.6.2.1. Effect of particle size

Fig. 7.9 shows the temperature profile during pyrolysis of a thermally thin cylindrical particle of radius 0.00025 m exposed to a final temperature of 900 K. The temperature at the centre and the surface of the particle is found to be uniform. As expected, there is a very little difference between the case in which shrinkage is considered and the case in which shrinkage is not considered. In this case there is no char insulating the unreacted core. As a consequence, the shrinkage has a minor impact on pyrolysis time and product yield. The pyrolysis time for both the cases is found to be 5.5 s. In the pyrolysis of thermally thin particle, the resistance to heat transfer within the particle is small compared to the external heat transfer. Thus, there is little residence time in the particle, and the secondary pyrolysis reactions have a little impact on the product yield.

In thermally thick pyrolysis the relative rates of internal and external heat transfer are similar. The particle temperature is not uniform throughout as for the thermally thin regime. The thin pyrolysis region separates the unreacted core, which is surrounded by the char layer. As the pyrolysis progresses, the char layer grows at the expense of the unreacted core. The heat transfer to the unreacted core reduces due to the insulation of the char layer around the particle. Shrinkage of the char layer causes a sharper temperature gradient, increases heat transfer to the interior of the particle and raising pyrolysis temperatures. Fig. 7.10 shows the temperature profile as a function of time for a 0.04 m particle (0.02 m radius) exposed to a final temperature of 900 K for different

radial positions. The temperature of the shrinking particle (present model results) is more than non-shrinking particle (Model-III) at any radial position. The increase in temperature is less near the centre of the particle than at the surface of the particle.

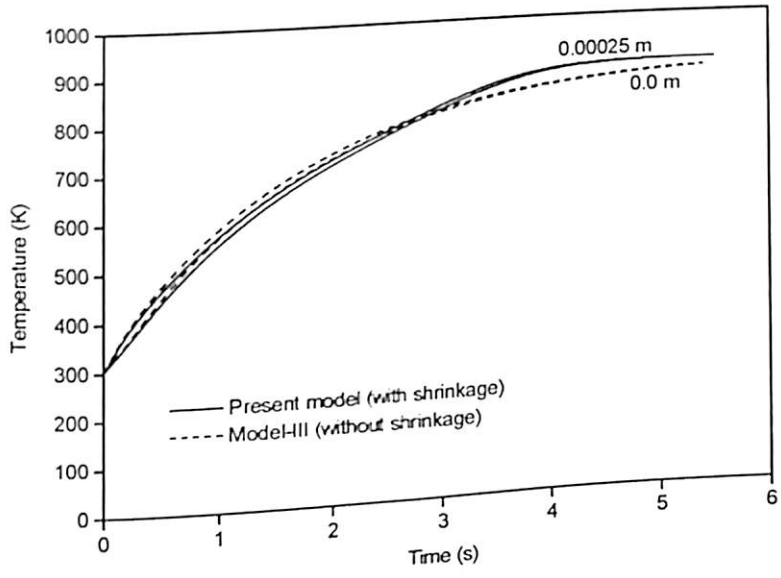

Fig. 7.9. Temperature profile as a function of time with cylindrical pellet for different radial position (R=0.00025 m, T_0=303 K, T_f=900 K).

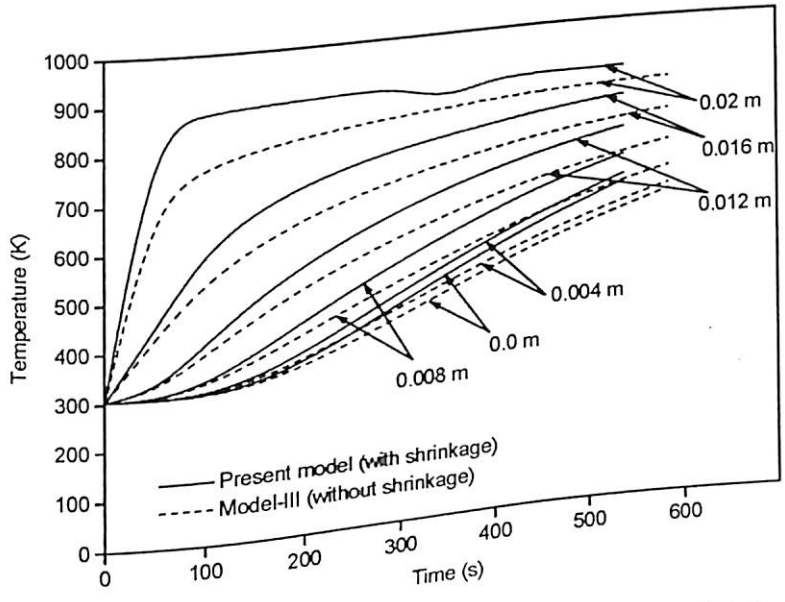

Fig. 7.10. Temperature profile as a function of time with cylindrical pellet for different radial position (R=0.02 m, T_0=303 K, T_f=900 K).

There is difference more than 50 K in temperature between the shrinking and non-shrinking particle at the surface. As the char layer begins to develop, the shrinking char layer allows more rapid internal heat transfer. The increase in the rate of internal heat transfer increases the interior temperature of the particle. The higher temperature values within the shrinking particle increase the rate of primary pyrolysis reactions thus reducing the time for completion of pyrolysis. The pyrolysis conversion time is found to be 538 s for shrinking particle as compared to 585 s for the non-shrinking particle. It is interesting to note from Fig. 7.10 that for the shrinking particle there is a dip (slight decrease and then increase) in temperature for particle at the surface (at the radial position of 0.02 m) at a time of 350 s. the phenomena of which is not observed for any other radial position of the particle from centre to the surface. In order to understand this typical phenomenon, further simulations are carried out at the surface of the particle of different sizes (radii) ranging from 0.00025-0.05 m. Up to a particle radius of 0.014 m, this dip is not observed at the surface of the particle. Typical simulated results are shown in Figs. 7.11-7.13.

Figs. 7.11, 7.12, and 7.13 show the temperature profile as a function of time at the surface for 0.014 m, 0.02 m, and 0.025 m particle radius respectively exposed to a final temperature of 900 K. As can be seen from Fig. 7.11, there is no dip in temperature at the surface of the particle, as also mentioned above. Not having this dip in temperature at the surface of the particle for smaller sizes can also be seen from Fig. 7.9, where the results for a particle radius of 0.00025 m are plotted. But, for a particle radius greater than 0.014 m this dip in temperature (we call it a 'thermal wave') is observed for the shrinking particle as shown in Figs. 7.12 and 7.13. The pyrolysis temperature reaches to

895 K after 300 s, drops to 862 K after 350 s and again increases then on as shown in Fig. 7.12 for the shrinking particle. This occurs because of two factors. First, there is less insulation from the char between the cold unreacted center and the surface. Second,

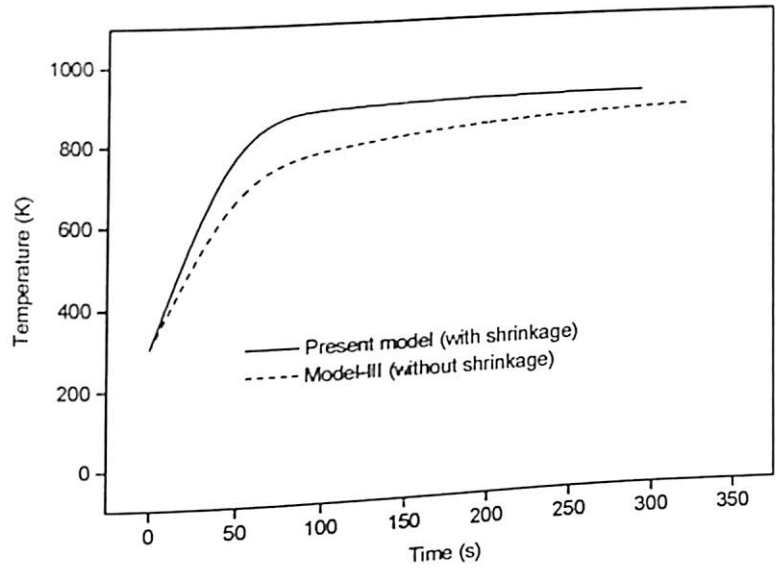

Fig. 7.11. Temperature profile as a function of time with cylindrical pellet at the surface of the particle (R=0.014 m, T_0=303 K, T_f=900 K).

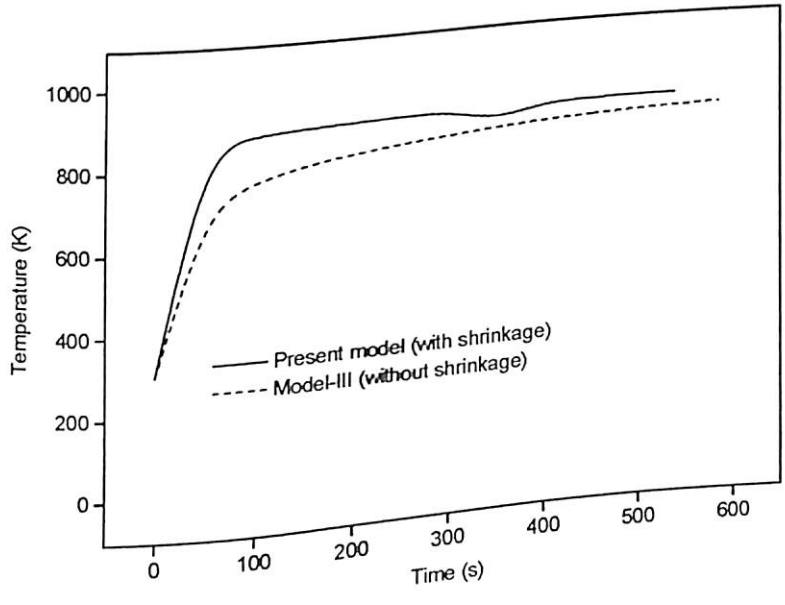

Fig. 7.12. Temperature profile as a function of time with cylindrical pellet at the surface of the particle (R=0.02 m, T_0=303 K, T_f=900 K).

the higher pyrolysis rates result in higher flux rates of pyrolysis products, providing additional cooling for the char layer and reducing the temperature after certain pyrolysis time. The higher pyrolysis rates are due to higher heat transfer rate to the core of the particle, resulting in an increased overall production rate of pyrolysis products in the shrinking particle. As a larger exterior char layer develops in the non-shrinking particle, the char layer insulates the particle. This reduces the heat transfer to the non-shrinking particle relative to the shrinking particle. So rate of production of pyrolysis products is less, and hence no additional cooling for the char layer and hence no 'thermal wave' is observed in the non-shrinking particle. The higher heat transfer rates of the shrinking particle reduce the pyrolysis time from 585 s to 538 s and 850 s to 793 s for particle radius of 0.02 m and 0.025 m respectively. As the particle radius increases (0.025 m) the impact of shrinkage increases, resulting in an increase in the number of thermal waves.

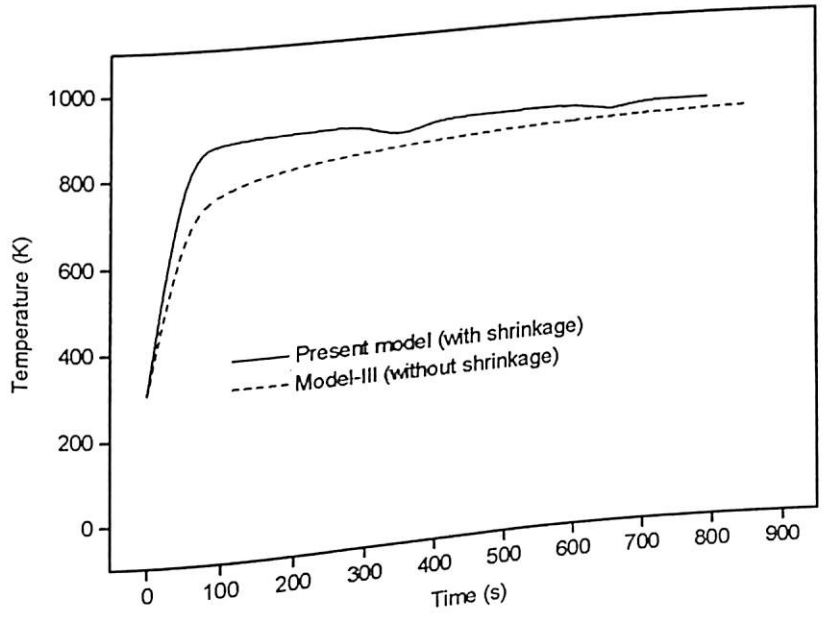

Fig. 7.13. Temperature profile as a function of time with cylindrical pellet at the surface of the particle (R=0.025 m, T_0=303 K, T_f=900 K).

The secondary thermal wave near the end of pyrolysis is a result of the increase in primary pyrolysis production at the centre of the particle, as shown in Fig. 7.13. The number of thermal waves increases further, for larger size particles.

7.6.2.2. Effect of pyrolysis time

Figs. 7.14 and 7.15 summarize the impact of shrinkage on the pyrolysis time. The effects of shrinkage increase with the particle size and the final temperature. The thicker char layer is formed for larger particle sizes. The internal resistance to heat transfer for the unreacted core reduces as a result of shrinkage by reducing the insulating affect of the char. This increases the importance of the char layer and hence the importance of shrinkage. As shown in Fig. 7.14. shrinkage does not have a significant affect on pyrolysis time, as the particle radius is small (0.001 m). The pyrolysis time decreases as the temperature is increased. There is very less difference (< 1 s) in the pyrolysis time

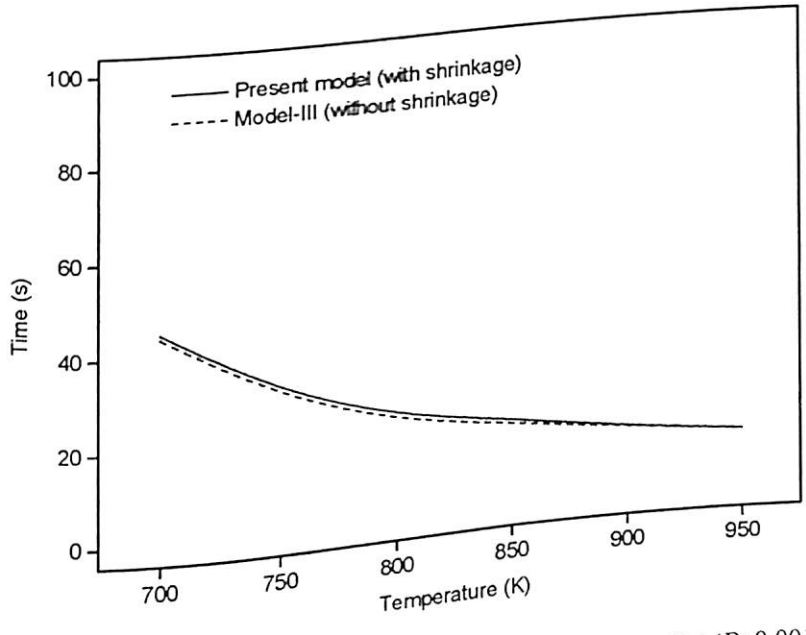

Fig. 7.14. Pyrolysis times as a function of temperature with cylindrical pellet (R=0.001 m, T_0=303 K).

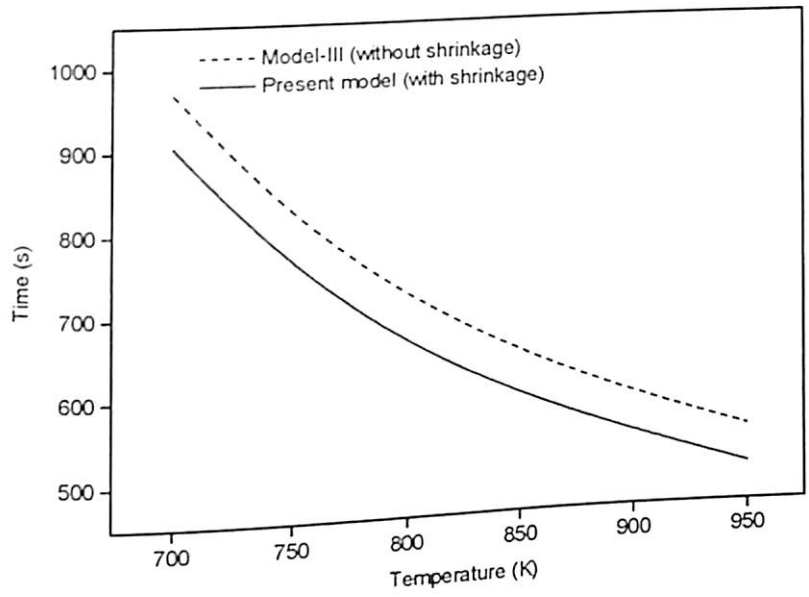

Fig. 7.15. Pyrolysis times as a function of temperature with cylindrical pellet (R=0.02 m, T_0=303 K).

between the shrinking and the non-shrinking particle. As the particle radius increases to 0.02 m, the impact of shrinkage on pyrolysis time is observed as shown in Fig. 7.15. As the shrinkage reduces the insulating affect of the char, the pyrolysis time reduces by more than 50 s for all the external temperatures as compared to the non-shrinking particle. Reduction in pyrolysis time implies the higher pyrolysis rates due to higher heat transfer rate from shrinked surface to the core of the particle. This results in an increased overall production rate of pyrolysis products in the shrinking particle as also mentioned in the previous section.

7.6.2.3. Effect on product yield

The impact of shrinkage on pyrolysis products is shown in Figs. 7.16-7.18. Extensive simulations are carried out for both the shrinking and the non-shrinking particles for particle radius ranging from 0.0001-0.05 m for different final temperatures. Shrinkage

favor high rates of heat transfer from the shrinked surface towards the interior of the solid and large pyrolysis temperatures are attained. The shrinkage affects the pyrolysis in several ways. It includes the reduction of residence time of gases within the particle, cooling of the char layer due to higher mass flux rates of pyrolysis products, and thinning of the pyrolysis reaction region. This effect favors the formation of (volatiles & gases)$_1$ (as in Fig. 7.16) at the expense of the decrease in formation of (char)$_1$ (as in Fig. 7.17) and (volatiles & gases)$_2$ or (char)$_2$ (as in Fig. 7.18). As the surface temperature increases from 600-900 K, the yield of (char)$_1$ (as in Fig. 7.17) decreases while the yield of (volatiles & gases)$_1$ (as in Fig. 7.16) increases. As shown in Fig. 7.17, the production of (char)$_1$ decreases with increase in temperature and increases with particle size. It may be due to a small amount of repolymerization as mentioned by Hagge & Bryden (2002). Secondary reactions occur as volatiles & gases flow through the char layer. Secondary char formation is negligible (as in Fig. 7.18) due to very low reaction rate for the deposition of volatiles & gases onto the char layer. This is due to the fact that the residence time is very less in the shrinking particle.

Non-shrinking particles favor the formation of (char)$_1$ (as in Fig. 7.17) and (volatiles & gases)$_1$ & gases)$_2$ or (char)$_2$ (as in Fig. 7.18) at the expense of decrease in (volatiles & gases)$_1$ formation (as in Fig. 7.16). This is due to the high residence time of volatiles & gases within the particle, thicker char layer and slow rates of formation of pyrolysis products. The yield of (volatiles & gases)$_1$ (as in Fig. 7.16) decreases up to a particle radius of 0.015 m and then again increases at the expense of decrease in (char)$_1$ formation (as in Fig. 7.17) for the final temperature of 750 K and 900 K. This is a consequence of successively higher temperatures at the surface due to increase in the pyrolysis time as

particle size is increased. This trend is not observed for 600 K, as the temperature is less (<673 K). For this case, the reduction in degree of polymerization is dominant, and

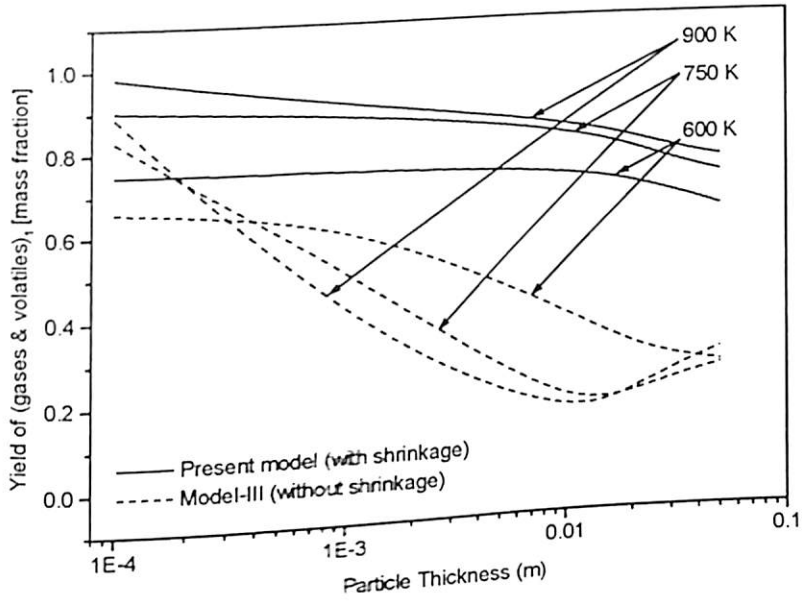

Fig. 7.16. Yield of (gases & volatiles)$_1$ as a function of particle radius with cylindrical pellet for different values of final temperatures (T_0=303 K).

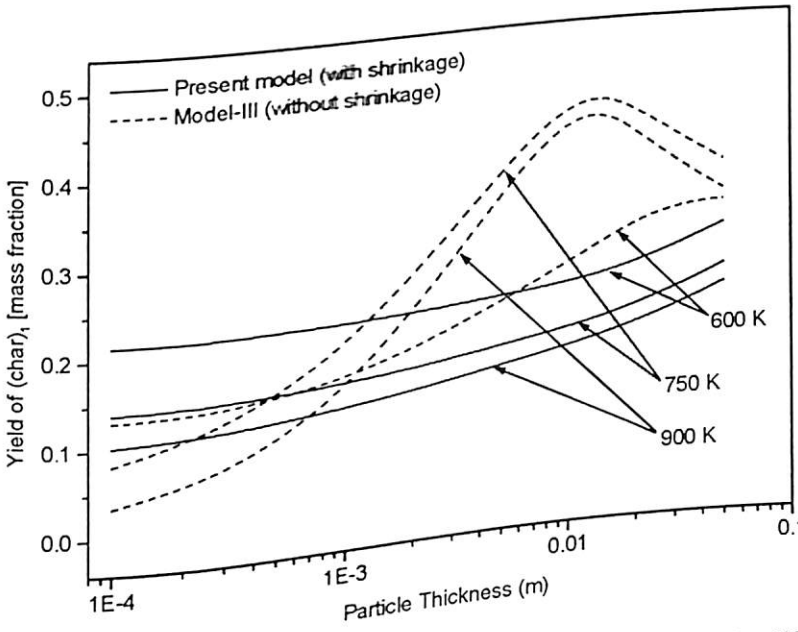

Fig. 7.17. Yield of (char)$_1$ as a function of particle radius with cylindrical pellet for different values of final temperatures (T_0=303 K).

hence diffusion and convection effects are negligible (Shafizadeh, 1982). Also, the temperature at the surface is same as the particle size is increased for the final temperature of 600 K.

From the analysis of the product yield distribution, it appears that the particle shrinkage affects both primary and secondary reaction paths due to different heat transfer conditions interior to the particle and to reduce volatile residence times, respectively. On the whole, the shrinkage of the particle favors the attainment of larger yields of (volatiles & gases)$_1$ (as in Fig. 7.16) at the expense of decrease in the formation of other two products (as in Figs. 7.17 & 7.18).

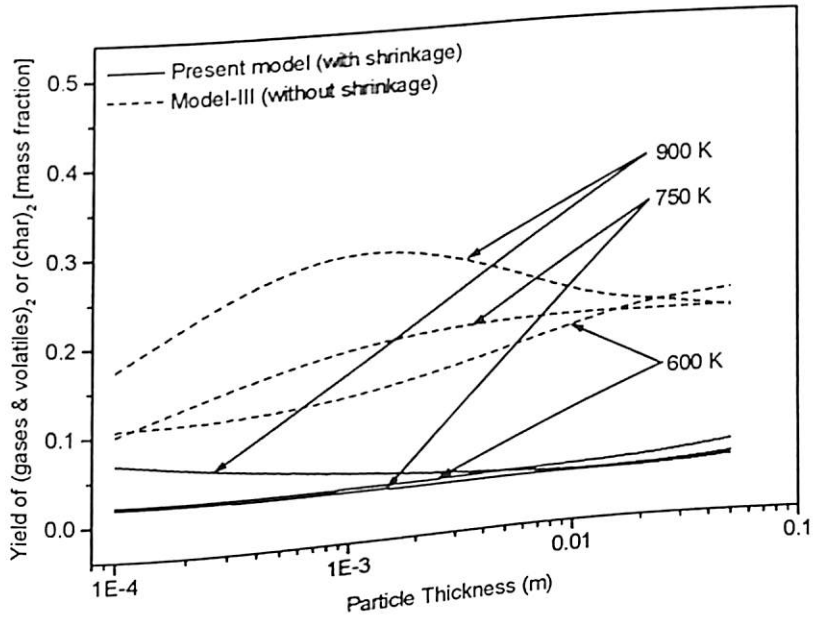

Fig. 7.18. Yield of (gases & volatiles)$_2$ as a function of particle radius with cylindrical pellet for different values of final temperatures (T_0=303 K).

7.6.2.4. Effect of specific heat capacity

Fig. 7.19 shows the dependence of primary & secondary product yields and conversion time on specific heat capacity of biomass for final temperature of 900 K for

R=0.02 m. It can be seen that specific heat capacity do not affect both primary and secondary product yields. Conversion time also does not depend on specific heat

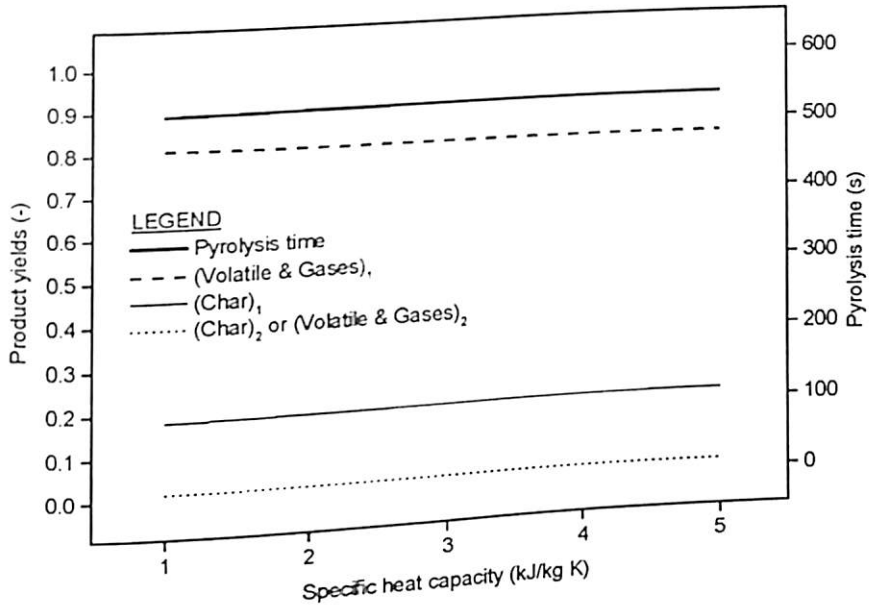

Fig. 7.19. Final product yields and pyrolysis time as functions of specific heat capacity with cylindrical pellet as simulated using present model with shrinkage (R=0.02 m, T_0=303 K, T_f=900 K).

capacity indicating that energetics of secondary reactions are not important. Fig. 7.20 reports the temperature profile as a function of radial distance for different values of specific heat capacity, which can be used to explain the results obtained in Fig. 7.19. It is seen that the temperature profile is nearly same along the radial position for all the values of specific heat capacities considered. Constant product yields are predicted because the flow field results only from the net mass addition from the solid to the gas as specific heat capacity is increased as shown in Fig. 7.19.

7.6.2.5. *Effect of Biot number*

The conversion of biomass with respect to pyrolysis time is shown in Fig. 7.21 for various values of Biot number for R=0.02 m. It can be seen that at any given time, there

is an increase in biomass conversion as the Biot number increases. Since the Biot number is defined by equation (C.7) as given in Appendix-C, for a specified value of R,

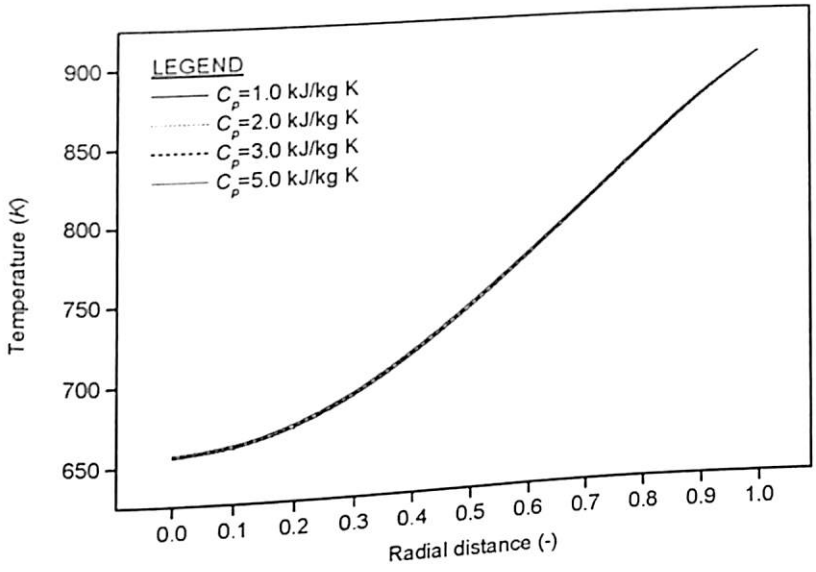

Fig. 7.20. Temperature profile as a function of radial distance for different values of specific heat capacity with cylindrical pellet as simulated using present model with shrinkage (R=0.02 m, T_0=303 K, T_f=900 K).

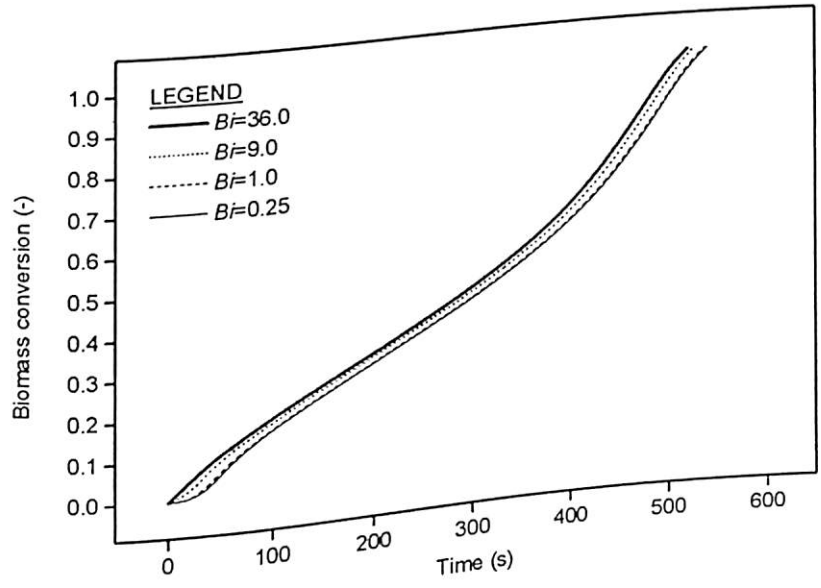

Fig. 7.21. Effect of Biot number on biomass conversion with cylindrical pellet as simulated using present model with shrinkage (R=0.02 m, T_0=303 K, T_f=900 K).

an increase in Biot number is accompanied by an enhancement in the rate of heat transfer, which in turn, accelerates the pyrolysis reaction. Biomass concentration profile as a function of radial distance for the cases of Bi=0.25 (low value) and Bi=36.0 (high value) are given, respectively, in Figs. 7.22 and 7.23. As can be seen from these figures, the concentration variation with respect to radial distance at any given time is nearly same as Biot number, Bi, is increased. The time for completion of pyrolysis for Bi=36.0 is less (520 s) as compared to Bi=0.25 (541 s). This is due to the fact that a smaller value of Bi at any specified value of R corresponds to a smaller heat transfer rate. This consequently gives rise to a predominantly heat-transfer-controlled reaction. Figs. 7.24 and 7.25 show the temperature profile as a function of radial distance with t as a parameter for cases of Bi=0.25 and Bi=36.0 respectively. The temperature gradient is nearly same for both the values of Biot number. The temperature profile is linear after the completion of pyrolysis for both the cases. The pyrolysis conversion time for

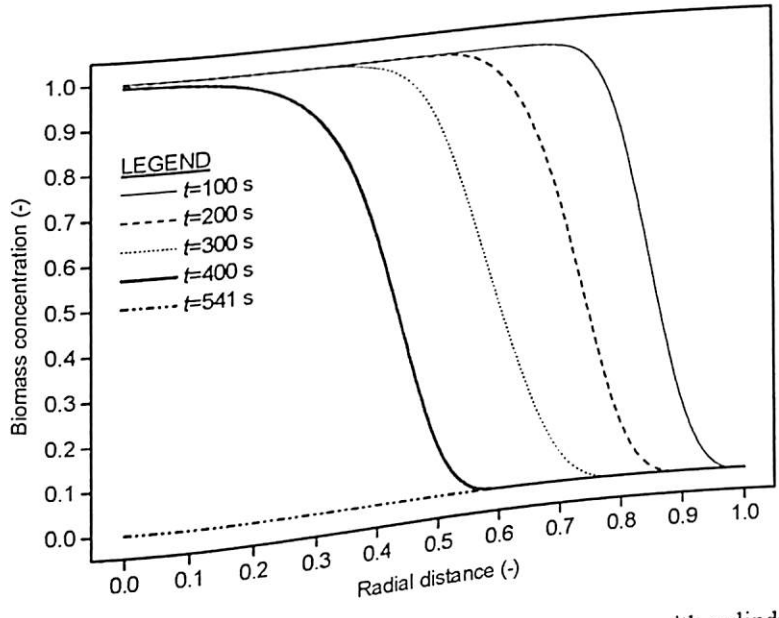

Fig. 7.22. Biomass concentration profile as a function of radial distance with cylindrical pellet at various values of time as simulated using present model with shrinkage (R=0.02 m, T_0=303 K, T_f=900 K, Bi=0.25).

Bi=0.25 is more (541 s) as compared to Bi=36.0 (520 s) i.e. as the Biot number increases rate of completion of pyrolysis is faster. Therefore, it can be stated that the progress of

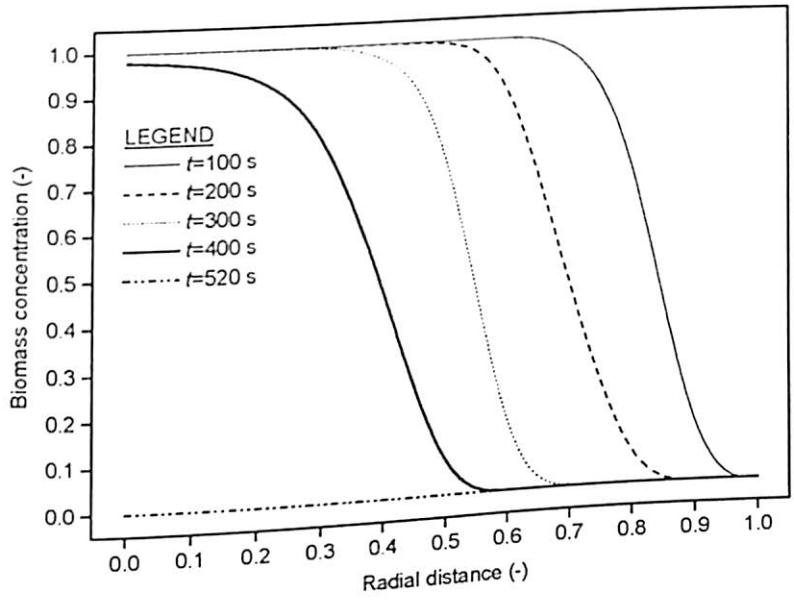

Fig. 7.23. Biomass concentration profile as a function of radial distance with cylindrical pellet at various values of time as simulated using present model with shrinkage (R=0.02 m, T_0=303 K, T_f=900 K, Bi=36.0).

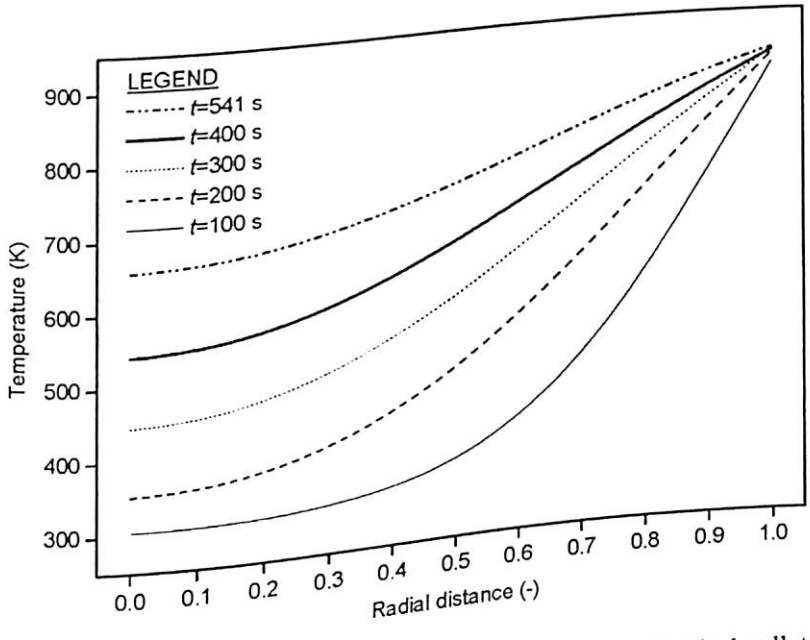

Fig. 7.24. Temperature profile as a function of radial distance with cylindrical pellet at various values of time as simulated using present model with shrinkage (R=0.02 m, T_0=303 K, T_f=900 K, Bi=0.25).

pyrolysis reaction is controlled by the heat transfer rate inside the solid particle for small values of Biot number. However, both rates including the heat transfer and the chemical reaction are important in determining the overall rate of the reaction when the value of Biot number is large.

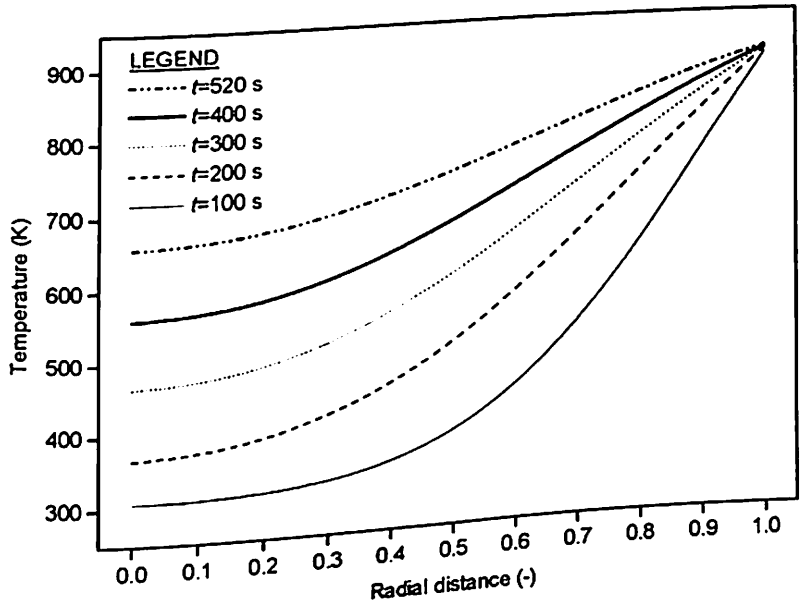

Fig. 7.25. Temperature profile as a function of radial distance with cylindrical pellet at various values of time as simulated using present model with shrinkage (R=0.02 m, T_0=303 K, T_f=900 K, Bi=36.0).

The main objective of the pyrolysis of a solid is usually to obtain product yields. Therefore, it is also important to know the effect of Bi on product yields in the solid particle. Fig. 7.26 shows the final product yields and pyrolysis time as functions of Biot number. There is slight decrease in pyrolysis time as Bi increases. It can be seen that Biot number do not affect both primary and secondary product yields. This can be explained from Figs. 7.24 and 7.25. As stated previously, the temperature is nearly same at any specified time, t, and radial position of the particle, as Bi increases from 0.25 (Fig. 7.24) to 36.0 (Fig. 7.25), so the rate of pyrolysis reaction is same.

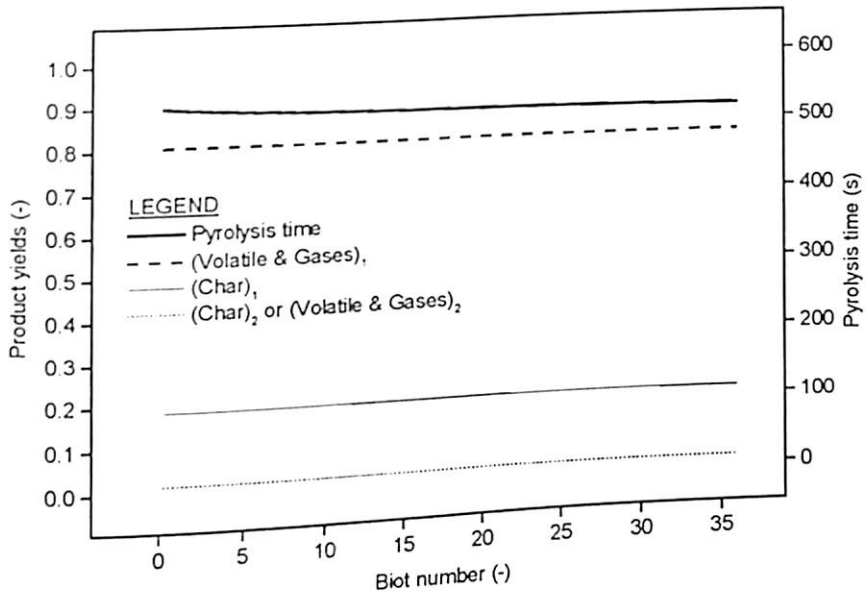

Fig. 7.26. Final product yields and pyrolysis time as functions of Biot number with cylindrical pellet as simulated using present model with shrinkage (R=0.02 m, T_0=303 K, T_f=900 K).

7.7. Conclusions

The impact of shrinkage on pyrolysis of biomass particles is studied employing a kinetic model coupled with heat transfer model using a practically significant kinetic scheme consisting of physically measurable parameters. The shrinkage model has been used to examine the impact of shrinkage on particle size, pyrolysis time, product yields, specific heat capacity, and Biot number. Simulations are carried out for temperatures ranging from 303-900 K, the particle radius ranging from 0.0000125-0.05 m and shrinkage factors ranging from 0.0 to 1.0. Based on the results obtained the following conclusions are drawn:

- The simulated results obtained from the model in the present study (Babu & Chaurasia, 2004d) with shrinkage ($\alpha' = 0.2, \beta' = 0.0, \gamma' = 0.2$) are in excellent agreement with wide range of experimental results reported in literature (Shafizadeh, Furneaux, Cochran, Scholl, & Sakai, 1979; Pyle & Zaror, 1984; Scott, Piskorz, Bergougnou, Graham, & Overend, 1988) as compared to the model developed by earlier researchers (Bamford, Crank, & Malan, 1946; Liliedahl & Sjöström, 1998; Jalan & Srivastava, 1999; Babu & Chaurasia, 2003a).

- The choice of lower possible values of shrinkage factor ($\alpha' = 0.2, \beta' = 0.0, \gamma' = 0.2$) in the study is more realistic of incorporating shrinkage effect, and hence resulted in better model predictions, as against relatively higher values ($\alpha' = 0.5, \beta' = 0.0, \gamma' = 0.5$) as taken by Di Blasi (1996b).

- The impact of shrinkage affects the pyrolysis in several ways. It includes reduction of the residence time of gases within the particle, cooling of the char layer due to higher mass flux rates of pyrolysis products and thinning the pyrolysis reaction region.

- The higher heat transfer rates of the shrinking particle reduce the pyrolysis time.

- Shrinkage has negligible affect on pyrolysis in the thermally thin regime. However, shrinkage affects both the pyrolysis time and the yield of pyrolysis products in thermally thick regime.

- The shrinkage of the particle favors the attainment of larger yields of (volatiles & gases)$_1$ at the expense of other two products.

- Specific heat capacity does not affect the primary and secondary product yields. Conversion time also does not depend on specific heat capacity indicating that energetics of secondary reactions are not important.
- The progress of pyrolysis reaction is controlled by the heat transfer rate inside the solid particle for small values of Biot number. However, both rates including the heat transfer and the chemical reaction are important in determining the overall rate of reaction for the large values of Biot number.
- The model is used to examine the impact of shrinkage, to gain an understanding of how it can affect the pyrolysis process, and to understand what pyrolysis or combustion conditions must be considered. This can provide an improved qualitative understanding of pyrolysis and guide further research into modeling of biomass pyrolysis and combustion.

CHAPTER 8

OPTIMIZATION OF PYROLYSIS OF BIOMASS USING DIFFERENTIAL EVOLUTION APPROACH

8.1. Introduction

To find a function's true global optimum, Differential Evolution (DE) is one of the simple and significantly faster evolutionary optimization techniques. Pyrolysis of biomass is an important and promising chemical process in the area of renewable energy sources. In the present study (Babu & Chaurasia, 2003d), modeling and simulation of the above process is coupled with the optimization of a non-linear function using DE. The objective in this problem is to estimate the optimal time of pyrolysis and heating rate under the restriction on concentration of biomass.

8.2. Background

Differential Evolution (DE) is an evolutionary optimization technique, which is exceptionally simple, significantly faster & robust at numerical optimization and is more

likely to find a function's true global optimum. DE (Price & Storn, 1997) is an improved version of GA (Goldberg, 1989) for faster optimization. Unlike simple GA that uses binary coding for representing problem parameters, DE uses real coding of floating point numbers. Among the DE's advantages are its simple structure, ease of use, speed and robustness. Price & Storn (1997) gave the working principle of DE with single strategy. Later on, they suggested ten different strategies of DE (Price & Storn, 2003). A strategy that works out to be the best for a given problem may not work well when applied for a different problem. Also, the strategy and key parameters to be adopted for a problem are to be determined by trial & error. The key parameters of control are: NP-the population size. CR-the crossover constant, F-the weight applied to random differential (scaling factor). The detailed DE algorithm used in the present study (Babu & Chaurasia, 2003d) is given below:

- Choose a strategy.
- Initialize the value of D (Number of independent parameters), NP, CR, F & gen_max.
- Initialize all the vector population randomly in the given upper & lower bound.

  For I=1 to NP

  {For j=1 to D

  x_{ij} = random Number}
- Evaluate the cost of each vector.
- Find out the vector with the lowest cost.
- Repeat.
- Perform mutation & recombination.

  a) For each vector x_t (target vector), select three distinct vectors x_a, x_b & x_c (select

five, if two vector differences are to be used) randomly from the current population (primary array) other than vector x_t.

b) Perform crossover for each target vector with its noisy vector to create a trial vector.

- After the mutation & recombination, if the bound (i.e. lower & upper limit of a variable) is violated then it can be brought in the bound range (i.e. between lower & upper limit) either by forcing it to lower/upper limit (forced bound) or by randomly assigning a value in the bound range (without forcing).
- Perform selection for each target vector, x_t by comparing its cost with that of the trial vector. Vector with lower cost is selected for next generation.
- Till termination criteria do not meet.
- Print results.

The crucial idea behind DE is a scheme for generating trial parameter vectors. Basically, DE adds the weighted difference between two population vectors to a third vector. Price & Storn (1997) have given some simple rules for choosing key parameters of DE for any given application. DE has been successfully applied in various fields. The various applications of DE are: digital filter design (Storn, 1995), batch fermentation process (Wang & Cheng, 1999; Chiou & Wang, 1999), dynamic optimization of continuous polymer reactor (Lee, Han & Chang, 1999), estimation of heat transfer parameters in trickle bed reactor (Babu & Sastry, 1999), optimal design of heat exchangers (Babu & Munawar, 2000, 2001), synthesis & optimization of heat integrated distillation system (Babu & Singh, 2000), optimization of an alkylation reaction (Babu & Chaturvedi, 2000), scenario-integrated optimization of dynamic systems (Babu &

Gautam, 2001), optimization of non-linear functions (Babu & Angira, 2001a), optimization of thermal cracker operation (Babu & Angira, 2001b), optimization of non-linear chemical processes (Babu & Angira, 2002; Angira & Babu, 2003), optimization of MINLP problems (Babu & Angira, 2003a), optimization of extraction process (Babu & Angira, 2003b), optimal design of gas transmission network (Babu, Angira, Chakole, & Mubeen, 2003; Babu, Chakole, & Mubeen, 2003), multi-objective optimization (Babu & Jehan, 2003). DE can also be applied to optimization of oil shale pyrolysis (Wen & Yen, 1977; Luss, 1978), pyrolysis of porous materials (Kordylewski & Rybak, 1986), pattern recognition analysis of pyrolysis gas chromatographic data (Lavine, Moores, & Helfend, 1999), optimization of coal pyrolysis modeling (Donskoi & Mcelwain, 2000; Li., Grace, Watkinson, Lim, & Ergüdenler, 2001), etc.

8.3. Motivation

As discussed in chapter 3 (Babu & Chaurasia, 2003a), some of the important parameters affecting the process of pyrolysis of biomass are temperature, concentration, time, and heating conditions. The optimum parameters in the pyrolysis of biomass have been estimated as given in chapter 3 (Babu & Chaurasia, 2003a). It is considered that by varying the temperature or heating rate (in an optimal fashion) during the heating process it is possible to increase the yield of the pyrolysis products beyond what is possible with isothermal or non-isothermal heating respectively. Furthermore, it is found that as the temperature or heating rate increase, the pyrolysis time decreases up to certain extent and then start increasing with further increase in temperature or heating rate. This point appears to be rather interesting and provided motivation to examine the problem in

greater detail. The purpose of this work (Babu & Chaurasia, 2003d) is to find the optimum values of these parameters for non-isothermal heating conditions by using DE.

8.4. Problem formulation and method of solution

Problem formulation is same as given in section 3.4 (chapter 3). The goal is to find the minimum value of pyrolysis time and the other optimum parameters corresponding to the optimum value of pyrolysis time. The objective function in dimensionless form is given by:

$$Min\ \tau = 2.4617\overline{HR}^4 - 8.886\overline{HR}^3 + 12.583\overline{HR}^2 - 7.7199\overline{HR} + 3.4088 \tag{8.1}$$

Subject to $0.2 \le \overline{HR} \le 1.2$

Dimensionless groups:

$$\tau = \frac{\alpha\, t}{R^2} \tag{8.2}$$

$$\overline{HR} = \frac{HR \times t}{T_0} \tag{8.3}$$

The optimum values of pyrolysis time and heating rate are found by using the Differential Evolution. It serves as the input to the coupled ordinary differential equations (3.1-3.6) to find the optimum parameters using Runge-Kutta fourth order method. The initial condition is as follows:

At t=0, $\overline{C}_B$=1, $\overline{C}_{G1} = \overline{C}_{C1} = \overline{C}_{G2} = \overline{C}_{C2}$=0.

The final concentration of biomass is assumed to be equal to 0.03, because beyond that concentration, pyrolysis is found to be very slow and of little practical importance. So, the iterations are continued till $C_B \le 0.03$. The optimum values of the parameters are

found using $n_1 = 1$, $n_2 = n_3 = 1.5$ for non-isothermal condition. The problem is solved considering particle radius of $R = 0.001\,\text{m}$ and initial temperature of $T_0 = 773\,\text{K}$. Thermal diffusivity is taken to be a constant ($\alpha = 1.79 \times 10^{-7}\,\text{m}^2/\text{s}$) and based on the initial temperature of wood, which is a representative value in pyrolysis. The Computer Code in C++ for the present problem is given in Appendix-G.

8.5. Results and discussion

The final pyrolysis time vs. heating rates are plotted and shown in Fig. 8.1. It is found that final pyrolysis time first decreases with increasing heating rate, reaches the optimum value and then increases as heating rate is further increased. The key parameters used in Differential Evolution are CR=0.7, F=0.5, NP=10, seed=9, accuracy=0.000001%. For the orders of reactions considered, the optimum values of heating rate & final pyrolysis time are found to be 50.7165 K/s and 9.5268 s respectively

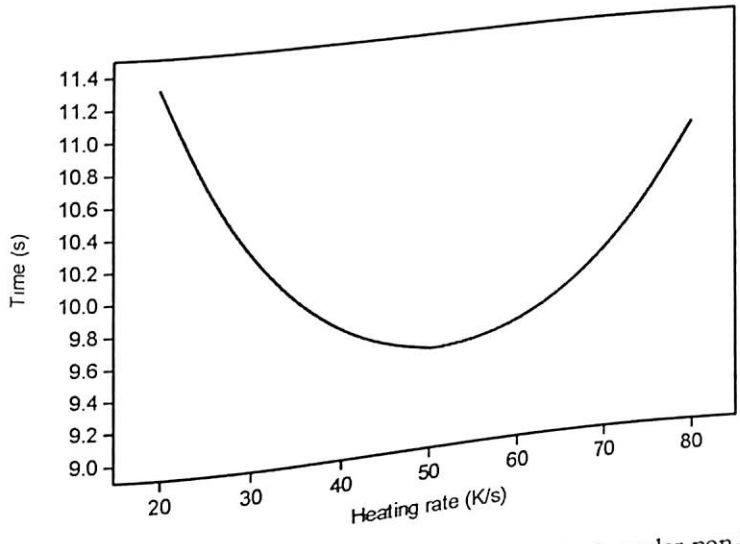

Fig. 8.1. Pyrolysis time as a function of heating rate for pyrolysis under non-isothermal condition (n_1=1, n_2=n_3=1.5).

after eighteen generations.

This interesting decreasing and increasing trend in final pyrolysis time with heating rate can be explained physically by comparing optimum heating rate value (50.7165 K/s) with a value slightly greater than it (say 70 K/s). It is well known that as the pyrolysis proceeds (i) temperature increases, (ii) concentration of biomass decreases and reaches the final value, (iii) concentration of $(volatile)_1$ increases, (iv) concentration of $(char)_1$ increases up to certain value of time and then decreases, and (v) concentrations of $(volatile\ \&\ char)_2$ increase as discussed in chapter 3 (Babu & Chaurasia, 2003a). The rate of decrease in concentration is more for higher value of heating rate as compared to optimum value up to certain value of time. The concentration of $(char)_1$ will reach to its maximum value earlier for higher heating rate. After attaining the maximum value, the concentration of $(char)_1$ starts decreasing for both the heating rates. The rate of decrease in concentration of biomass is less for higher heating rate as compared to optimum heating rate value, because the $(char)_1$ left for higher value of heating rate is less. So the reaction between $(volatile)_1$ and $(char)_1$ slows down for higher value of heating rate as compared to optimum heating rate value, and hence it takes more time to reach the desired final concentration of biomass. Hence the final pyrolysis time is more for high value as compared to optimum value of heating rate.

The optimum values of the parameters are shown in Table-8.1. The maximum concentration is obtained for $(volatile)_1$ as compared to other products. The heating rate influences the reaction pathway and hence, the final products. The char yield is supported at low heating rates whereas the yield of volatiles increases markedly at higher heating rates. At low heating rates, particularly those involving large samples, the

residence time of all primary products within the pyrolysing matrix would dominate, accounting for large char yields.

Table-8.1. Optimum parametric values for pyrolysis under non-isothermal condition

Optimum Parameters	$n_1=1$; $n_2=n_3=1.5$
Heating rate (K/s)	50.7165
Final pyrolysis time (s)	9.5268
Final pyrolysis temperature (K)	1256.1614
Final concentration of initial biomass (-)	0.030047
Final concentration of $(char)_1$ (-)	0.000709
Final concentration of $(volatile)_1$ (-)	0.685714
Final concentration of $(char)_2$ (-)	0.141765
Final concentration of $(volatile)_2$ (-)	0.141765

8.6. Conclusions

- The modeling and simulation of the pyrolysis of biomass process coupled with the optimization of a non-linear function using Differential Evolution (an evolutionary computation method) approach has been presented.
- The best key parameters for the present problem are: NP=10, CR=0.7, F=0.5.
- This successful application of DE indicates that it has great potential and can be applied to advantage in all the highly non-linear & complex engineering problems.

CHAPTER 9

CONCLUDING REMARKS, SUMMARY AND FUTURE SCOPE

9.1. Introduction

Biomass, being a readily available renewable energy source that reduces sulfur dioxide and carbon dioxide emissions, is an attractive option as a fuel for power generation. It has the potential to provide a cost effective and sustainable supply of energy in the future, while at the same time, aiding countries in meeting their greenhouse gas reduction targets. Intensive research has been carried out on thermal conversion techniques for biomass like combustion, gasification, and pyrolysis. There has been an increasing interest for thermochemical conversion of biomass through pyrolysis for upgrading energy in terms of more easily handled fuels, namely gases, liquids, and charcoal. Each product can be commercially interesting depending upon the type of application. The understanding of the interaction between chemical and physical mechanisms during pyrolysis of biomass is of fundamental importance for the optimal design of chemical pyrolysis reactors and combustors. The pyrolysis of biomass has a lot

of practical importance and physical significance in industrial pyrolysis applications. The pyrolysis process has a great future in the world.

The pyrolysis reactions proceed with a rate depending upon the local temperature. During the pyrolysis process the pores of the solid are enlarged, and the solid particle merely becomes more porous because biomass converts into gases. The enlarged pores of the pyrolyzing solid offer many reaction sites to the volatile and gaseous products of pyrolysis and favor their interaction with the hot solid. Inside the pyrolyzing particle, heat is transmitted by the following mechanisms: (a) conduction inside the solid particle, (b) convection inside the particle pore, (c) convection and radiation from the surface of the pellet.

The study of pyrolysis is gaining increasing importance, as it is not only an independent process, but it is also a first step in the gasification or combustion process. The pivotal role of pyrolysis has prompted many researchers to attempt to model this phenomenon mathematically. The primary objectives of these models are to provide a diagnostic tool for evaluating the importance of various system parameters and to identify the system characteristics useful to experimentalists. However, the inherent complexity of the pyrolysis process has posed formidable challenges to modeling attempts. The pyrolytic decomposition of biomass involves a complex series of reactions, and consequently, changes in the experimental heating conditions or sample composition and preparation may affect not only the rate of reaction, but also the actual course of reactions.

Fan, Fan, Miyanami, Chen, & Walawender (1977) developed a model for pyrolysis process, which includes the aspects of heat and mass transfer in the particle. The

reaction is considered to be of first order with respect to initial particle concentration. Also product concentrations cannot be analyzed from the above model as the secondary reactions are not considered. Miyanami, Fan, Fan, & Walawender (1977) incorporated the effect of heat of reaction in the above model. The various modeling reported appearing in the literature present different versions or enrichment of the model suggested by Bamford, Crank, & Malan (1946). According to this model, the equation for heat conduction in a pyrolyzing solid is combined with those for heat generation, assuming first order kinetics. However, the heat transfer equation does not consider the effect of change of density as a function of time. This model is used by several researchers (Roberts & Clough, 1963; Tinney, 1965; Weatherford & Sheppard, 1965; Matsumoto, Fujiwara, & Kondo, 1969) and is modified by Kung (1972) in order to incorporate the effects of internal convection and variable transport properties. However, no specific kinetic mechanism is suggested to predict the concentration of the various components produced during pyrolysis. Kansa, Perlee, & Chaiken (1977) included the momentum equation for the motion of pyrolysis gases within the solid. A suitable kinetic mechanism has not been utilized and the solution to the heat and momentum balance equation is based on arbitrary boundary conditions.

Studies have been carried out on pyrolysis of biomass and other substances by several researchers (Anthony & Howard, 1976; Shafizadeh, 1982; Koufopanos, Ramana Rao, Plehiers, & Froment, 1988; Koufopanos, Maschio, & Lucchesi, 1989; Do, & Bell, 1991; Yang, Tanguy, & Roy, 1995; Srivastava, Sushil, & Jalan, 1996; Di Blasi, 1998; Donskoi, & McElwain, 1999; Jai, Galea, & Patel, 1999; Klose & Wiest, 1999; Ruggiero & Manfrida, 1999; Violi, Anna, & Alessio, 1999; Larfeldt, Leckner, & Melaaen, 2000; Li,

Kennedy, & Dlugogorski, 2000; Mousquès, Dirion, & Grouset, 2001; Boutin, Ferrer, & Lédé, 2002; Bryden, Ragland, & Rutland, 2002; Demirbaş, 2002b; Mastral, Esperanza, Garcia, & Juste, 2002), but many of them have not included the secondary reactions in pyrolysis kinetics. Kansa, Perlee, & Chaiken (1977) pointed out that secondary reactions are essential to match fully the experimental observations.

Pyle & Zaror (1984) utilized kinetic model assuming first order kinetics, based on the density of initial biomass. Jalan & Srivastava (1999) have solved the heat transfer equation by neglecting the effect of specific heat and thermal conductivity of char, which are the functions of temperature as reported by Koufopanos, Papayannakos, Maschio, & Lucchesi (1991). The convective heat transfer coefficient is a function of Reynolds number and Prandtl number and is given by $h = 0.322\left(k_g / l\right)\mathrm{Pr}^{1/3}\,\mathrm{Re}^{0.5}$ W/m^2 K, as reported by Koufopanos, Papayannakos, Maschio, & Lucchesi (1991), but Jalan & Srivastava (1999) have considered a constant value of $h = 0.322$ W/m^2 K, neglecting the effect of the other parameters. The earlier investigators (Pyle & Zaror, 1984; Koufopanos, Papayannakos, Maschio, & Lucchesi, 1991; Jalan & Srivastava, 1999) considered the temperature range of 300-900 K and pellet diameters 0.002-0.022 m only.

9.2. Scope of work

Based on the background work reported in literature with their limitations as discussed above and the importance & useful applications of pyrolysis process the scope of the present work are as follows:

1. To understand the physical aspects of pyrolysis in modeling of biomass gasification.

2. To incorporate the effect of convective heat transfer coefficient as a function of Reynolds number & Prandtl number and specific heat capacity & thermal conductivity of char as functions of temperature.
3. To incorporate autocatalytic secondary pyrolysis reactions and density of char as a function of time.
4. Incorporating the effect of thermal and transport properties such as porosity, thermal conductivity, specific heat and mass diffusivity on pyrolysis.
5. Improvement on the existing models considering residence time effects, shrinkage, particle size distribution, different geometries, changes in material properties, heat of reaction during the course of pyrolysis, etc.
6. Validating the proposed models with the actual experimental data obtained from the literature.

9.3. Studies on optimum parameters

Based on the importance and promising nature of the pyrolysis of biomass process, the modeling and simulation has been carried out in this study for finding out the optimum parameters of the pyrolysis process. Some interesting trends have been obtained, especially with respect to effect of net heating rate and temperature on the final pyrolysis time. The reported literature results indicate a decrease in final pyrolysis time as the net heating rate or temperature is increased. But the results obtained using a wide range of operating conditions in the present study show that the final pyrolysis time initially decreases and then increases as the net heating rate or temperature is increased, giving an optimum final pyrolysis time corresponding to net heating rate or temperature.

9.4. Development of mathematical model

Unfortunately, the mathematical complications involved in the numerical solution of some of the more sophisticated models make them unsuitable for design and prediction purposes, particularly given the difficulties of establishing and incorporating the basic physical and chemical phenomena. Also, the lack of reliable experimental data on the dynamics of biomass pyrolysis under conditions relevant to carbonization (relatively low temperatures and heating rates) makes it difficult to select the appropriately simplified models. It is useful for formulating effective and less expensive computer models, since the numerical solution of general, non-simplified models can be rather time consuming.

In the present study, the description of chemical processes of pyrolysis is coupled to an unsteady-state, one-dimensional, variable property model of transport phenomena including heat transfer (by all the three modes, i.e., convection, conduction & radiation), mass transfer (transport of volatiles & gases by diffusion & convection), and momentum transfer. A generalized reference model (Model-I) incorporating all the above effects is proposed. This is further improved by proposing two simplified models (Model-II & Model-III) incorporating additional assumptions. Finite difference pure implicit scheme utilizing Tri-Diagonal Matrix Algorithm (TDMA) is employed for solving heat transfer and mass transfer model equations. Runge-Kutta 4^{th} order method is used for solving chemical kinetics model equations. Simulations are carried out considering different geometries (slab, cylinder, and sphere) of equivalent radius ranging from 0.0000125 m to 0.05 m, and temperature ranging from 303 K to 2800 K. The results obtained from the model are in good agreement with many experimental results (Shafizadeh, Furneaux, Cochran, Scholl, & Sakai, 1979; Pyle & Zaror, 1984; Scott, Piskorz, Bergougnou,

Graham, & Overend, 1988; Alves & Figueiredo, 1989).

9.5. Studies on heat transfer coefficient, particle size and orders of reactions

By increasing convective heat transfer it is possible to get the same extent of conversion of biomass and with lesser pyrolysis time under controlled conditions at much lower operating temperatures which are much safer than at higher operating temperatures leading to combined convective and radiative heat transfer mechanisms which are not safe. As the particle size increases, there is an increase in the time required for completion of pyrolysis at a certain pyrolysis temperature and hence the impact of secondary reactions increases. The concentration of $(char)_1$ increases while the concentration of $(volatile\ \&\ gases)_1$ decreases as the particle thickness is increased for all the three geometries (slab, cylinder, and sphere). The spherical particle has a shortest conversion time as can be expected based on higher surface/volume ratio. Geometrically, the sphere has got a more heat absorbing capacity as compared to cylinder & slab and it is the least for slab. The pyrolysis is completed faster, as the constant wall temperature is increased. Orders of reactions also affect the pyrolysis process. The pyrolysis is faster for zeroth order as compared to first order reaction, as the rates are independent of initial biomass concentration for zeroth order.

9.6. Studies on heat of reaction

In case of exothermic reaction, the particle temperature exceeds the surface temperature. The temperature gradient at the surface becomes negative and thus the heat conduction is towards the surroundings. The heat source from the surrounding

environment, which is utilized to initiate the pyrolysis reaction, is no longer required. The heat source could be viewed simply as a trigger for the early stages of the reaction. This situation is termed the '*self-sustaining reaction*'. In endothermic reaction, the temperature increases with radial distance. The temperature is minimum at the centre and maximum at the wall of the particle. The temperature gradient is consistently positive or equal to zero. In other words, the particle temperature never exceeds the final temperature. This situation is termed as '*heat-transfer-controlled reaction*'.

9.7. Studies on thermal and thermodynamic properties

Wide ranges of heat transfer coefficient (8.4-126.0 W/m^2K), thermal conductivity (0.03-0.40 W/mK), reactor temperature (303-2800 K), emissivity (0.0-1.0) and heat of reaction number (-0.7 to -0.1 for exothermic reactions and 0.001 to 1.0 for endothermic reactions) are considered. The effect of these properties on average concentration of products is studied for three different geometries (slab, cylinder, and sphere). To establish the extent to which each property is important in terms of average concentration of products and pyrolysis time (conversion time), sensitivity analysis is carried out. Gas quality (low char content), for a fixed particle size, is better for feedstocks with low thermal conductivity. In many cases the desired product is char. High char concentration is associated with the lower values of reactor final temperature. The highest sensitivity is associated with reactor temperature and emissivity. The least sensitive parameter is the convective heat transfer coefficient. The sensitivity for all the parameters is highest for the slab geometry and is lowest for the spherical geometry. Applications of these findings in reactor design and operation are very useful.

9.8. Studies on shrinking of biomass particle

Shrinkage occurs in the char layer during the pyrolysis reactions because of a rearrangement of chemical bonds and the coalescence of graphite nuclei within the biomass particle. The amount of char shrinkage is a function of wood species, heat flux, and temperature. Varying compositions of lignin, cellulose, & hemicellulose and other organic and inorganic materials result in different extents of shrinkage for different species. Char shrinkage increases as the temperature increases and also increases with the amount of time at a given temperature. The inclusion of shrinkage reduces the pyrolysis time and affects the product yield. Shrinkage has negligible affect on pyrolysis in the thermally thin regime. However, shrinkage affects both the pyrolysis time and the yield of pyrolysis products in thermally thick regime. The shrinkage of the particle favors the attainment of larger yields of (volatiles & gases)$_1$ at the expense of (char)$_1$ and (volatiles & gases)$_2$.

The progress of pyrolysis reaction is controlled by the heat transfer rate inside the solid particle for the small values of Biot number. However, both rates including the heat transfer and the chemical reaction are important in determining the overall rate of reaction for higher value of Biot number. The values of shrinkage factor α', β' and γ' can be varied from 0.0 which represents total shrinkage to 1.0 which represents no shrinkage of the particle. The choice of lower possible values of shrinkage factor ($\alpha' = 0.2, \beta' = 0.0, \gamma' = 0.2$) in the present study is more realistic of incorporating shrinkage effect as against relatively higher values as considered by other researchers.

9.9. Studies to find optimal product concentrations using Differential Evolution

Differential Evolution (DE) is an evolutionary optimization technique, which is exceptionally simple, significantly faster & robust at numerical optimization and is more likely to find a function's true global optimum. The improved validated model is coupled with the optimization of a non-linear function using DE. Optimal time of pyrolysis and heating rate under the restriction on concentration of biomass is found. It serves as the input to the coupled ordinary differential equations to find the optimum values of volatiles and char using Runge-Kutta fourth order method.

9.10. Major contributions

1. The proposed models in this study are validated with a wide range of experimental results reported in literature.
2. The model results reported in literature indicate a decrease in final pyrolysis time as the net heating rate or temperature is increased. But the results obtained using a wide range of operating conditions in the present study show that the final pyrolysis time initially decreases and then increases as the net heating rate or temperature is increased. This phenomenon could be well explained both qualitatively and quantitatively by proposing appropriate realistic models and through simulations.
3. Identification of operating conditions (by increasing convective heat transfer under controlled conditions) at which it is possible to get the same extent of conversion of biomass with lesser pyrolysis time that could be obtained when radiation is present at higher temperature ranges.

4. The heat source from the surrounding environment which is utilized to initiate the pyrolysis reaction is not required at the later stage as the reaction is exothermic. This situation is termed the '*self-sustaining reaction*'. This is the major advantage of pyrolysis process.
5. Identification of dominant design variables for pyrolysis process through sensitivity analysis. The highest sensitivity is associated with reactor temperature and emissivity. The least sensitive parameter is the convective heat transfer coefficient. The sensitivity for all the parameters is highest for the slab geometry and is lowest for the spherical geometry.
6. The models on pyrolysis of biomass are corrected, updated, and also new models are proposed by incorporating the shrinkage effect. This resulted in an accurate prediction of yield of a wide range of products obtained during pyrolysis. The earlier models under-predict the product yields.
7. The favoring and attainment of larger yields of $(volatiles \ \& \ gases)_1$ at the expense of $(char)_1$ and $(volatiles \ \& \ gases)_2$ could be well explained by choosing the appropriate kinetic scheme.

9.11. Future scope

The work carried out in the present study can be extended by considering the following objectives:

1. Dominant design variables in pyrolysis of biomass particles of different geometries by incorporating the shrinkage effect.

2. The influence of heat transfer mechanisms on the structure of the pyrolysis front and global characteristics, such as conversion time, mass loss rate and product yields.
3. The intensity of radiative heat flux & its orientation with respect to biomass particle.
4. Single-particle effects in the description of primary pyrolysis and moisture evaporation for a correct prediction of the volatiles & gases and thus for quality of the producer gas.
5. To estimate reliable kinetic data and to investigate the dependence of physical properties on temperature and solid composition by performing the experiments.
6. Coupling of detailed single-particle model of pyrolysis of biomass with a mechanistic external heat transfer model in a fixed bed gasifier in order to evaluate the particle heating rates and to predict the devolatilization characteristics.
7. Determining the effects of most important operational variables such as biomass feed rate and air-to-fuel ratio on process dynamics, composition and quality of the producer gas and overall efficiency of the process.
8. Extensive sensitivity analysis for parameters used in the modeling of fixed bed gasifier, the physico-chemical properties of feedstocks and the plant size.

REFERENCES

Akdeniz, F., & Küçük, M. M. (1998). Liquids from olive husk by using supercritical fluid extraction and thermochemical methods. *Energy Education Science and Technology*, *1*, 17-22.

Alonso, M. J. G., Borrego, A. G., Alvarez, D., & Menéndez, R. (1999). Pyrolysis behavior of pulverized coals at different temperatures. *Fuel*, *78*, 1501-1513.

Alves, S. S., & Figueiredo, J. L. (1989). A model for pyrolysis of wet wood. *Chemical Engineering Science*, *44*, 2861-2869.

Angira, R., & Babu, B. V. (2003). Evolutionary computation for global optimization of non-linear chemical engineering processes. *Proceedings of International symposium on process systems engineering & control (ISPSEC '03)-for productivity enhancement through design and optimization*, IIT-Bombay, Mumbai, India, 87-91. (Also available via Internet as .pdf file at http://bvbabu.50megs.com/custom.html/#56).

Antal, M. J. (1982). Biomass pyrolysis: a review of the literature. Part I-Carbohydrate pyrolysis. *Advances in Solar Energy*; Boer, K. W., & Duffie, J. A., Eds.; American Solar Energy Society: Boulder, CO, *1*, 61-111.

Antal, M. J. (1985). Biomass pyrolysis: a review of the literature. Part II-Lignocellulose pyrolysis. *Advances in Solar Energy*; Boer, K. W., & Duffie, J. A., Eds.; American Solar Energy Society: Boulder, CO, *2*, 175-255.

Antal, M. J., & Varhegyi, G. (1995). Cellulose pyrolysis kinetics: The current state of knowledge. *Industrial & Engineering Chemistry Research*, *34*, 703-717.

Anthony, D. B., & Howard, J. B. (1976). Devolatilization and hydrogasification. *AIChE Journal* , *22*, 625-656.

Arena, U., & Mastellone, M. L. (2000). Defluidization phenomena during the pyrolysis of two plastic wastes. *Chemical Engineering Science*, *55*, 2849-2860.

Babu, B. V., & Angira, R. (2001). Optimization of non-linear functions using evolutionary computation. *Proceedings of 12th ISME conference*, Chennai, India, 153-157. *(Also available via Internet as .pdf file at http://bvbabu.50megs.com/custom.html/#34).*

Babu, B. V., & Angira, R. (2001). Optimization of thermal cracker operation using differential evolution. *Proceedings of International symposium & 54th annual Session of IIChE (CHEMCON-2001)*, Chennai, India. *(Also available via Internet as .pdf file at http://bvbabu.50megs.com/custom.html/#38).*

Babu, B. V., & Angira, R. (2002). Optimization of non-linear chemical processes using evolutionary algorithm. *Proceedings of International symposium & 55th Annual Session of IIChE (CHEMCON-2002)*, Hyderabad, India. *(Also available via Internet as .pdf file at http://bvbabu.50megs.com/custom.html/#54).*

Babu, B. V., & Angira, R. (2003a). A differential evolution approach for global optimization of MINLP problems. *Proceedings of 4th Asia Pacific Conference on Simulated Evolution and Learning (SEAL-2002)*, Singapore, 2, 880-884. (Also available via Internet as .pdf file at *http://bvbabu.50megs.com/custom.html/#46*).

Babu, B. V., & Angira, R. (2003b). New Strategies of Differential Evolution for Optimization of Extraction Process. *Proceedings of International symposium & 56th annual session of IIChE (CHEMCON-2003)*, Bhubhaneswar, India. *(Also available via Internet as .pdf file at http://bvbabu.50megs.com/custom.html/#71).*

Babu, B. V., & Chaturvedi, G. (2000). Evolutionary computation strategy for optimization of an alkylation reaction. *Proceedings of International symposium & 53rd Annual Session of IIChE (CHEMCON-2000)*, Calcutta, India. *(Also available via Internet as .pdf file at http://bvbabu.50megs.com/custom.html/#31).*

Babu, B. V., & Chaurasia, A. S. (2002a). Modeling & simulation of pyrolysis: influence of particle size and temperature. *Proceedings of International conference on multimedia and design*, Mumbai, India, 4, 103-128. *(Also available via Internet as .pdf file at http://bvbabu.50megs.com/custom.html/#51).*

Babu, B. V., & Chaurasia, A. S. (2002b). Modeling & simulation of pyrolysis: effect of convective heat transfer & orders of reactions. *Proceedings of International symposium & 55th annual session of IIChE (CHEMCON-2002)*, OU, Hyderabad, India, 105-106. *(Also available via Internet as .pdf file at http://bvbabu.50megs.com/custom.html/#52).*

Babu, B. V., & Chaurasia, A. S. (2003a). Modeling, simulation, and estimation of optimum parameters in pyrolysis of biomass. *Energy Conversion and Management*, 44, 2135-2158. *(Also available via Internet as .pdf file at http://bvbabu.50megs.com/custom.html/#47).*

Babu, B. V., & Chaurasia, A. S. (2003b). Modeling for pyrolysis of solid particle: kinetics and heat transfer effects. *Energy Conversion and Management*, 44, 2251-2275. *(Also available via Internet as .pdf file at http://bvbabu.50megs.com/custom.html/#50).*

Babu, B. V., & Chaurasia, A. S. (2003c). Modeling & simulation of pyrolysis of biomass: effect of heat of reaction. *Proceedings of International symposium on process systems engineering and control (ISPSEC '03) - for productivity enhancement through design and optimization*, IIT-Bombay, Mumbai, India, 181-186. *(Also available via Internet as .pdf file at http://bvbabu.50megs.com/custom.html/#55).*

Babu, B. V., & Chaurasia, A. S. (2003d). Optimization of pyrolysis of biomass using differential evolution approach. *Proceedings of Second International Conference on Computational Intelligence, Robotics, and Autonomous Systems (CIRAS-2003)*, Singapore. *(Also available via Internet as .pdf file at http://bvbabu.50megs.com/custom.html/#73).*

Babu, B. V., & Chaurasia, A. S. (2003e). Pyrolysis of shrinking cylindrical biomass pellet. *Proceedings of International symposium & 56th annual session of IIChE (CHEMCON-2003)*, Bhubhaneswar, India. *(Also available via Internet as .pdf file at http://bvbabu.50megs.com/custom.html/#70).*

Babu, B. V., & Chaurasia, A. S. (2004a). Pyrolysis of biomass: Improved models for simultaneous kinetics and transport of heat, mass, and momentum. *Energy Conversion and Management*, Accepted (In Press). *(Also available via Internet as .pdf file at http://bvbabu.50megs.com/custom.html/#60).*

Babu, B. V., & Chaurasia, A. S. (2004b). Parametric study of thermal and thermodynamic properties on pyrolysis of biomass in thermally thick regime. *Energy Conversion and Management, 45*, 53-72. *(Also available via Internet as .pdf file at http://bvbabu.50megs.com/custom.html/#62).*

Babu, B. V., & Chaurasia, A. S. (2004c). Dominant design variables in pyrolysis of biomass particles of different geometries in thermally thick regime. *Chemical Engineering Science*, Accepted (In Press). *(Also available via Internet at http://bvbabu.50megs.com/custom.html/#64).*

Babu, B. V., & Chaurasia, A. S. (2004d). Heat transfer and kinetics in the pyrolysis of shrinking biomass particle. Communicated to *Chemical Engineering Science*.

Babu, B. V., & Gautam, K. (2001). Evolutionary computation for scenario-integrated optimization of dynamic systems. *Proceedings of International symposium & 54th annual session of IIChE (CHEMCON-2001)*, Chennai, India. *(Also available via Internet as .pdf file at http://bvbabu.50megs.com/custom.html/#39).*

Babu, B. V., & Jehan, M. M. L. (2003). Differential Evolution for Multi-Objective Optimization. *Accepted and to be presented at International Conference on Evolutionary Computation (CEC-2003), Canberra, Australia. (Also available via Internet as .pdf file at http://bvbabu.50megs.com/custom.html/#78).*

Babu, B. V., & Munawar, S. A. (2000). Differential evolution for the optimal design of heat exchangers. *Proceedings of all-India seminar on chemical engineering progress on resource development: a vision 2010 & beyond*, IE (I), Bhubaneswar, India. *(Also available via Internet as .pdf file at http://bvbabu.50megs.com/custom.html/#28).*

Babu, B. V., & Munawar, S. A. (2001). Optimal design of shell & tube heat exchanger by different strategies of differential evolution, *PreJournal.com–The Faculty Lounge, Article No. 003873, posted on website Journal http://www.prejournal.com.*

Babu, B. V., & Sastry, K. K. N. (1999). Estimation of heat-transfer parameters in a trickle-bed reactor using differential evolution and orthogonal collocation, *Computers & Chemical Engineering, 23*, 327-339. *(Also available via Internet as .pdf file at http://bvbabu.50megs.com/custom.html/#24).*

Babu, B. V., & Singh, R. P. (2000). Synthesis & optimization of heat integrated distillation systems using differential evolution. *Proceedings of all-India seminar on chemical engineering progress on resource development: a vision 2010 & beyond*, IE (I), Bhubaneswar, India.

Babu, B. V., Angira, R., & Nilekar, A. (2002). Differential evolution for optimal design of an auto-thermal ammonia synthesis reactor. *Communicated Computers and Chemical Engineering*.

Babu, B. V., Angira, R., Chakole, P. G., & Mubeen, J. H. S. (2003). Optimal Design of Gas Transmission Network using Differential Evolution. *Proceedings of Second International Conference on Computational Intelligence, Robotics, and Autonomous Systems (CIRAS-2003)*, Singapore, December 15-18. *(Also available via Internet as .pdf file at http://bvbabu.50megs.com/custom.html/#76).*

Babu, B. V., Chakole, P. G., & Mubeen, J. H. S. (2003). Differential Evolution Strategy for Optimal Design of Gas Transmission Network. *Communicated to European Journal of Operational Research. (Also available via Internet as .pdf file at http://bvbabu.50megs.com/custom.html/#77).*

Badin, J., & Kirschner, J. (1998). Biomass greens US power production. *Renewable Energy World, 1*, 40-45.

Bamford, C. H., Crank, J., & Malan, D. H. (1946). The combustion of wood. Part I. *Proceedings of the Cambridge Philosophical Society, 42*, 166-182.

Barooah, J. N., & Long, V. D. (1976). Rates of decomposition of some carbonaceous materials in fluidized bed. *Fuel, 55*, 116.

Beis, S. H., Onay, Ö, & KoçKar, Ö. M. (2002). Fixed-bed pyrolysis of safflower seed: influence of pyrolysis parameters on product yields and compositions. *Renewable Energy, 26*, 21-32.

Bilbao, R., Millera, A., & Murillo, M. B. (1993). Temperature profiles and weight loss in the thermal decomposition of large spherical wood particles. *Industrial & Engineering Chemistry Research, 32*, 1811-1817.

Boroson, M. L., Howard, J. B., Longwell, J. P., & Peters, W. A. (1989). Product yields and kinetics from the vapor phase cracking of wood pyrolysis tars. *AIChE Journal, 35*, 120-128.

Boutin, O., Ferrer, M., & Lédé, J. (2002). Flash pyrolysis of cellulose pellets submitted to a concentrated radiation: experiments and modelling. *Chemical Engineering Science, 57*, 15-25.

Bradbury, A. G. W., Sakai, Y., & Shafizadeh, F. (1979). A kinetic model for pyrolysis of cellulose. *Journal of Applied Polymer Science, 23*, 3271-3280.

Bridgwater, A. V. (2001). *Progress in thermochemical biomass conversion (Volumes 1 & 2)*. CPL Press, United Kingdom, ISBN 0632055332.

Bridgwater, A. V. (2002). *Fast pyrolysis of biomass: A handbook (Volumes 1 & 2)*. CPL Press, United Kingdom, ISBN 1872691072.

Bridgwater, A. V. (2003). *Pyrolysis and gasification of biomass and waste*. CPL Press, United Kingdom, ISBN 1872691773.

Bridgwater, A. V., & Evans, G. D. (1993). An assessment of thermochemical conversion systems for processing biomass and refuse. Rep. ETSU B/T1/00207.

Broek, R., Faaij, A., & Wijk, A. (1996). Biomass combustion power generation technologies. *Biomass and Bioenergy, 11*, 271-281.

Broido, A., & Nelson, M. A. (1975). Char yield on pyrolysis of cellulose. *Combustion and Flame, 24*, 263-268.

Bryden, K. M., Ragland, K. W., & Rutland, C. J. (2002). Modeling thermally thick pyrolysis of wood. *Biomass and Bioenergy, 22*, 41-53.

Buekens, A. G., & Schoeters, J. G. (1980). Basic principles of waste pyrolysis and review of European processes. Thermal conversion of solid waste and biomass, Jones, J. L. & Radding, S. B., Eds.; American Chemical Society: Washington, DC.

Çağlar, A., & Demirbaş, A. (2000). Conversion of cotton cocoon shell to liquid products by pyrolysis. *Energy Conversion and Management, 41*, 1749-1756.

Çağlar, A., & Demirbaş, A. (2001). Conversion of cotton cocoon shell to liquid products by supercritical fluid extraction and low pressure pyrolysis in the presence of alkalis. *Energy Conversion and Management, 42*, 1095-1104.

Çağlar, A., & Demirbaş, A. (2002a). Conversion of cotton cocoon shell to hydrogen rich gaseous products by pyrolysis. *Energy Conversion and Management, 43*, 489-497.

Çağlar, A., & Demirbaş, A. (2002b). Hydrogen rich gas mixture from olive husk via pyrolysis. *Energy Conversion and Management, 43*, 109-117.

Carnahan, B., Luther, H. A., & James, O. W. (1969). *Applied numerical methods*. New York: John Wiley & Sons.

Castets, K., Daguerre, E., & Py, X. (2001). Pithches pyrolysis kinetics: non-isothermal heat treatments, experiments and model. *Fuel, 80*, 2075-2083.

Chan, W. R., Kelbon, M., & Krieger, B. B. (1985). Modeling and experimental verification of physical and chemical processes during pyrolysis of large biomass particle. *Fuel, 64*, 1505-1513.

Chan, W. R., Kelbon, M., & Krieger-Brockett, B. (1988). Single-particle pyrolysis: correlations of reaction products with process conditions. *Industrial & Engineering Chemistry Research, 27*, 2261-2275.

Chaurasia, A. S., & Babu, B. V. (2003a). Modeling & simulation of pyrolysis of biomass: effect of thermal conductivity, reactor temperature and particle size on product concentrations. *Proceedings of International conference on Energy and Environmental Technologies for Sustainable Development (ICEET-2003)*, Jaipur, India, 151-156. *(Also available via Internet as .pdf file at http://bvbabu.50megs.com/custom.html/#65.)*

Chaurasia, A. S., & Babu, B. V. (2003b). Influence of product yields, density, heating conditions and conversion on pyrolysis of biomass. *Proceedings of International Conference on Desert Technology-7 (DT-7)*, Jodhpur, India. *(Also available via Internet as .pdf file at http://bvbabu.50megs.com/custom.html/#67).*

Chaurasia, A. S., Babu, B. V., Kaur, A., & Thiruchitrambalam, V. (2003). Convective and radiative heat transfer through a biomass particle. Communicated to *Indian Chemical Engineer Journal*.

Chiou, J. P., & Wang, F. S. (1999). Hybrid method of evolutionary algorithms for static and dynamic optimization problems with application to a fed-batch fermentation process, *Computers & Chemical Engineering, 23*, 1277-1291.

Curtis, L. J., & Miller, D. J. (1988). Transport model with radiative heat transfer for rapid cellulose pyrolysis. *Industrial and Engineering Chemistry Research, 27*, 1775-1783.

Demirbaş, A. (1998a). Fuel properties and calculation of higher heating values of vegetable oils. *Fuel, 77*, 1117-1120.

Demirbaş, A. (1998b). Yields of oil products from thermochemical biomass conversion processes. *Energy Conversion and Management, 39*, 685-690.

Demirbaş, A. (1998c). Calculation of higher heating values of biomass fuels. *Fuel*, *76*, 431-434.

Demirbaş, A. (1999). Properties of charcoal derived from hazelnut shell and the production of briquettes using pyrolytic oil. *Energy*, *29*, 141-150.

Demirbaş, A. (2000a). Biomass resources for energy and chemical industry. *Energy Education Science and Technology*, *5*, 21-45.

Demirbaş, A. (2000b). Effect of lignin content on aqueous liquefaction products of biomass. *Energy Conversion and Management*, *41*, 1601-1607.

Demirbaş, A. (2001a). Biomass resource facilities and biomass conversion processing for fuels and chemicals. *Energy Conversion and Management*, *42*, 1357-1378.

Demirbaş, A. (2001b). Supercritical fluid extraction and chemicals from biomass with supercritical fluids. *Energy Conversion and Management*, *42*, 279-294.

Demirbaş, A. (2001c). Relationships between lignin contents and heating values of biomass. *Energy Conversion and Management*, *42*, 183-188.

Demirbaş, A. (2002a). Partly chemical analysis of liquid fraction of flash pyrolysis products from biomass in the presence of sodium carbonate. *Energy Conversion and Management*, *43*, 1801-1809.

Demirbaş, A. (2002b). Gaseous products from biomass by pyrolysis and gasification: effects of catalyst on hydrogen yield. *Energy Conversion and Management*, *43*, 897-909.

Demirbaş, A. (2002c). Pyrolysis and steam gasification processes of black liquor. *Energy Conversion and Management*, *43*, 877-884.

Demirbaş, A. (2002d). Mechanisms of liquefaction and pyrolysis reactions of biomass. *Energy Conversion and Management*, *41*, 633-646.

Demirbaş, A., & Çağlar, A. (1998). Catalytic steam reforming of biomass and heavy oil residues to hydrogen. *Energy Education Science and Technology*, *1*, 45-52.

Demirbaş, A., & Güllü, D. (1998). Acetic acid, methanol and acetone from lignocellulosics by pyrolysis. *Energy Education Science and Technology*, *2*, 111-115.

Demirbaş, A., Karslioğlu, S., & Ayas, A. (1996). Hydrogen resources: conversion of black liquor to hydrogen rich gaseous products. *Fuel Science and Technology International*, *14*, 451-463.

Demirbaş, A., Tüzen, M., & Özdemir, M. (1999). Supercritical fluid extraction of phenolics acids in snowdrop. *Energy Education Science and Technology*, *2*, 47-52.

Di Blasi, C. (1993a). Modeling and simulation of combustion processes of charring and non-charring solid fuels. *Progress in Energy and Combustion Science*, *19*, 71-104.

Di Blasi, C. (1993b). Analysis of convection and secondary reaction effects within porous solid fuels undergoing pyrolysis. *Combustion Science and Technology*, *90*, 315-340.

Di Blasi, C. (1994a). Numerical simulation of cellulose pyrolysis. *Biomass and Bioenergy*, *7*, 87-98.

Di Blasi, C. (1994b). *Proceedings of 4th international symposium on fire safety science* (Ed T. Kashiwagi). The International Association of Fire Safety Science, Boston, 229.

Di Blasi, C. (1995). Predictions of wind-opposed flame spread rates and energy feedback analysis for charring of solids in a microgravity environment. *Combustion and Flame*, *100*, 332-340.

Di Blasi, C. (1996a). Influences of model assumptions on the predictions of cellulose pyrolysis in the heat transfer controlled regime. *Fuel, 75*, 58-66.

Di Blasi, C. (1996b). Heat, momentum and mass transport through a shrinking biomass particle exposed to thermal radiation. *Chemical Engineering Science, 51*, 1121-1132.

Di Blasi, C. (1996c). Kinetic and heat transfer control in the slow and flash pyrolysis of solids. *Industrial & Engineering Chemistry Research, 35*, 37-46.

Di Blasi, C. (1997). Influences of physical properties on biomass devolatilization characteristics. *Fuel, 76*, 957-964.

Di Blasi, C. (1998). Physico-chemical processes occurring inside a degrading two-dimensional anisotropic porous medium. *International Journal of Heat and Mass Transfer, 41*, 4139-4150.

Di Blasi, C. (2000a). Dynamic behaviour of stratified downdraft gasifiers. *Chemical Engineering Science, 55*, 2931-2944.

Di Blasi, C. (2000b). Modelling the fast pyrolysis of cellulosic particles in fluid-bed reactors. *Chemical Engineering Science, 55*, 5999-6013.

Do, H. D., & Bell, P. R. F. (1991). The importance of vaporization kinetics in the pyrolysis of solid fuels. *Chemical Engineering Science, 46*, 2895-2904.

Dong, C. Y., & De Pater, C. J. (2002). Numerical modeling of crack reorientation and link-up. *Advances in Engineering Software, 33*, 577-587.

Donskoi, E., & Mcelwain, D. L. S. (1999). Approximate modelling of coal pyrolysis. *Fuel, 78*, 825-835.

Donskoi, E., & Mcelwain, D. L. S. (2000). Optimization of coal pyrolysis modeling. *Combustion and Flame, 122*, 359-367.

Emmons, H. W., & Atreya, A. (1983). The science of wood combustion. *In Wood Heat for Cooking*, edited by K Krishna Prasad and P Verhaart, Bangalore: Indian Academy of Sciences, 259-268.

Fan, L. T., Fan, L. S., Miyanami, K., Chen, T. Y., & Walawender, W. P. (1977). A mathematical model for pyrolysis of a solid particle - effects of the Lewis number. *The Canadian Journal of Chemical Engineering, 55*, 47-53.

Figueiredo, J. L., Valenzuela, C., Bernalte, A., & Encinar, J. M. (1989). Pyrolysis of holm-oak wood: influence of temperature and particle size. *Fuel, 68*, 1012-1016.

Fletcher, D. F., Haynes, B. S., Chen, J., & Joseph, S. D. (1998). Computational fluid dynamics modelling of an entrained flow biomass gasifier. *Applied mathematical modelling, 22*, 747-757.

Font, R., Marcilla, A., Verdu, E. and Devesa, J. (1990). Kinetics of the pyrolysis of almond shells and almond shells impregnated with $CoCl_2$ in a fluidized bed reactor and in a Pyroprobe 100. *Industrial & Engineering Chemistry Research, 29*, 1846-1855.

Galvagno, S., Fortuna, F., Cornacchia, G., Casu, S., Coppola, T., & Sharma, V. K. (2001). Pyrolysis process for treatment of automobile shredder residue: preliminary experimental results. *Energy Conversion and Management, 42*, 573-586.

Ghoshdastidar, P. S. (1998). *Computer simulation of flow and heat transfer*. New Delhi: Tata McGraw-Hill Publishing Company Limited.

Goldberg, D. E. (1989). *Genetic algorithms in search, optimization, and machine learning*, Reading, MA: Addison-Wesley.

Güllü, D., & Demirbaş, A. (2001). Biomass to methanol via pyrolysis. *Energy Conversion and Management*, *42*, 1349-1356.

Hagge, M. J., & Bryden, K. M. (2002). Modeling the impact of shrinkage on the pyrolysis of dry biomass. *Chemical Engineering Science*, *57*, 2811-2823.

Hastaoglu, M. A., & Berruti, F. (1989). A gas-solid reaction model for flash wood pyrolysis. *Fuel*, *68*, 1408-1415.

Hawboldt, K. A., Monnery, W. D., & Svrcek, W. Y. (2000). New experimental data and kinetic expression for H_2S pyrolysis and re-association. *Chemical Engineering Science*, *55*, 957-966.

Haykiri-Açma, H. (2003). Combustion characteristics of different biomass materials. *Energy Conversion and Management*, *44*, 155-162.

Jai, F., Galea, E. R., & Patel, M. K. (1999). The numerical simulation of the noncharring pyrolysis process and fire development within a compartment. *Applied Mathematical Modeling*, *23*, 587-607.

Jain, R. K., & Singh, B. (1999). Fuelwood characteristics of selected indigenous tree species from central India. *Bioresource Technology*, *68*, 305-308.

Jalan, R. K., & Srivastava, V. K. (1999). Studies on pyrolysis of a single biomass cylindrical pellet- kinetic and heat transfer effects. *Energy Conversion and Management*, *40*, 467-494.

Janse, A. M. C., Westerhout, R. W. J., & Prins, W. (2000). Modelling of flash pyrolysis of a single wood particle. *Chemical Engineering and Processing*, *39*, 239-252.

Jegers, H. F., & Klein, M. T. (1985). Primary and secondary lignin pyrolysis reaction pathways. *Industrial & Engineering Chemistry-Process Design & Development*, *24*, 173-183.

Jorapur, R., & Rajvanshi, A. K. (1997). Sugarcane leaf-bagasse gasifiers for industrial heating applications. *Biomass and Bioenergy*, *13*, 141-146.

Kaltschmitt, M., & Bridgwater, A. V. (1997). *Biomass gasification and pyrolysis: State of art and future prospects*. CPL Press, United Kingdom, ISBN 1872691714, EUR 17788.

Kansa, E. J., Perlee, H. E., & Chaiken, R. F. (1977). Mathematical model of wood pyrolysis including internal forced convection. *Combustion and Flame*, *29*, 311-324.

Kanury, A. M. (1972). Thermal decomposition kinetics of wood pyrolysis. *Combustion & Flame*, *18*, 75-83.

Kanury, A. M., & Blackshear, P. L. (1970). Some considerations pertaining to the problem of wood-burning. *Combustion Science and Technology*, *1*, 339.

Kaygusuz, K. (1996). Rural energy resources: applications and consumption in Turkey. *Energy Source*, *19*, 549-557.

Kaygusuz, K. (2002). Sustainable development of hydropower and biomass energy in Turkey. *Energy Conversion and Management*, *43*, 1099-1120.

Khraisha, Y. H. (2000). Flash pyrolysis of oil shales in a fluidized bed reactor. *Energy Conversion and Management*, 41, 1729-1739.

Klose, W., & Wiest, W. (1999). Experiments and mathematical modeling of maize pyrolysis in a rotary kiln. *Fuel*, *78*, 65-72.

Korbitz, W. E. (1998). From the field to the fast lane-biodiesel. *Renewable Energy World*, *1*, 32-37.

Kordylewski, W., & Rybak, W. (1986). Influence of endothermic effect on the rate of pyrolysis of porous materials. *Chemical Engineering Science, 41*, 192-194.

Koufopanos, C. A., Maschio, G. & Lucchesi, A. (1989). Kinetic modelling of the pyrolysis of biomass and biomass components. *The Canadian Journal of Chemical Engineering, 67*, 75-84.

Koufopanos, C. A., Papayannakos, N., Maschio, G., & Lucchesi, A. (1991). Modelling of the pyrolysis of biomass particles. Studies on kinetics, thermal and heat transfer effects. *The Canadian Journal of Chemical Engineering, 69*, 907-915.

Krishna Prasad, K., Sangen, E., & Visser, P. Woodburning cookstoves. *Advances in Heat Transfer*, Academic Press, Inc., New York, 1985, *117*, 159-317.

Küçük, M. M., & Tunç, M. (1999). Supercritical fluid extraction of biomass. *Energy Education Science and Technology, 2*, 1-5.

Kung, H. C. (1972). A mathematical model of wood pyrolysis. *Combustion and Flame, 18*, 185-195.

Larfeldt, J., Leckner, B., & Melaaen, M. C. (2000). Modelling and measurements of the pyrolysis of large wood particles. *Fuel, 79*, 1637-1643.

Lavine, B. K., Moores, A., & Helfend, L. K. (1999). A genetic algorithm for pattern recognition analysis of pyrolysis gas chromatographic data. *Journal of Analytical and Applied Pyrolysis, 50*, 47-62.

Lede, J., Panagopoulos, J., Li, H. Z., & Villermaux, J. (1985). Fast pyrolysis of wood: direct measurement and study of ablation rate. *Fuel, 64*, 1514-1520.

Lee, C. K., Chaiken, R. F., & Singer, J. M. (1976). Charring pyrolysis of wood in fires by laser simulation. *Proceedings of the 16th international symposium on combustion*, Pittsburgh: The Combustion Institute, 1459-1470.

Lee, M. H., Han, C., & Chang, K. S. (1999). Dynamic optimization of a continuous polymer reactor using a modified differential evolution, *Industrial & Engineering Chemistry Research, 38*, 4825-4831.

Lewellen, P. C., Peters, W. A., & Howard, J. B. (1969). Cellulose pyrolysis, kinetics and char formation mechanism. *Proceedings of the 12th international symposium on combustion*, Pittsburgh: The Combustion Institute, 1471-1480.

Li, K., Kennedy, E. M., & Dlugogorski, B. Z. (2000). Experimental and computational studies of the pyrolysis of $CBrF_3$, and the reaction of $CBrF_3$ with CH_4. *Chemical Engineering Science, 55*, 4067-4078.

Li., X., Grace, J. R., Watkinson, A. P., Lim, C. J., & Ergüdenler, L. A. (2001). Equilibrium modeling of gasification: a free energy minimization approach and its application to a circulating fluidized bed coal gasifier. *Fuel, 80*, 195-207.

Liden, A. G., Berruti, F., & Scott, D. S. (1988). A kinetic model for the production of liquids from the flash pyrolysis of biomass. *Chemical Engineering Communications, 65*, 207-221.

Liliedahl, T., & Sjöström, K. (1998). Heat transfer controlled pyrolysis kinetics of a biomass slab, rod or sphere. *Biomass and Bioenergy, 15*, 503-509.

Luss, R. (1978). On the optimization of oil shale pyrolysis. *Chemical Engineering Science, 33*, 1403-1404.

Maa, P. S., & Bailie, R. C. (1973). Influence of particle sizes and environmental conditions on high temperature pyrolysis of cellulosic material-I (theoretical). *Combustion Science and Technology, 7*, 257-269.

Mastral, F. J., Esperanza, E., Garcia, P., & Juste, M. (2002). Pyrolysis of high-density polyethylene in a fluidized bed reactor. Influence of the temperature and residence time. *Journal of Analytical and Applied Pyrolysis, 63*, 1-15.

Mathieu, P., & Dubuisson, R. (2002). Performance analysis of a biomass gasifier. *Energy Conversion and Management*, 43, 1291-1299.

Matsui, I., Kojima, T., Kunii, D., & Furusawa, T. (1987). Study of char gasification by carbon dioxide. 2. Continuous gasification in fluidized bed. *Industrial & Engineering Chemistry Research, 26*, 95-100.

Matsui, I., Kunii, D., & Furusawa, T. (1987). Study of char gasification by carbon dioxide. 1. Kinetic study by thermogravimetric analysis. *Industrial & Engineering Chemistry Research, 26*, 91-95.

Matsumoto, T, Fujiwara, T, & Kondo, J. (1969). *Proceedings of the 12th international symposium on combustion*, Pittsburgh: The Combustion Institute, 515-531.

McKendry, P. (2002). Energy production from biomass (part 2): conversion technologies. *Bioresource Technology, 83*, 47-54.

Meesri, C., & Moghtaderi, B. (2002). Lack of synergetic effects in the pyrolytic characteristics of woody biomass/coal blends under low and high heating rate regimes. *Biomass and Bioenergy, 23*, 55-66.

Melaaen, M. C., & Grønli, M. G. (1997). Modeling and simulation of moist wood drying and pyrolysis. In: A.V. Bridgwater & D.B.G. Boocock (Eds.), Developments in thermochemical biomass conversion (pp. 132-146). London: Blackie.

Mellottee, H., & Richard, J. R. (1983). Pyrolysis and combustion of wood in relation with its chemical composition. *Energy Biomass, Comm. Eur. Communities, EUR 8245, EUR*, 523-529.

Midilli, A., Dogru, M., Howarth, C. R., Ling, M. J., & Ayhan, T. (2001). Combustible gas production from sewage sludge with a downdraft gasifier. *Energy Conversion and Management*, 42, 157-172.

Miyanami, K., Fan, L. S., Fan, L. T., & Walawender, W. P. (1977). A mathematical model for pyrolysis of a solid particle - effects of the heat of reaction. The *Canadian Journal of Chemical Engineering, 55*, 317-325.

Morel, J. I., Amundson, N. R., & Park, S. K. (1990). Dynamics of a single particle during char gasification. *Chemical Engineering Science, 45*, 387-401.

Mousquès, P., Dirion, J. L., & Grouset, D. (2001). Modeling of solid particles pyrolysis. *Journal of Analytical and Applied Pyrolysis, 58-59*, 733-745.

Murty, K. A., & Blackshear, Jr. P. E. (1967). Pyrolysis effects in the transfer of heat and mass in thermally decomposing organic solids. *Proceedings of the 11th international symposium on combustion*, Pittsburgh: The Combustion Institute, 517-523.

Nalon, P. F., Brown, D. J., & Rothwell, E. (1973). *Proceedings of the 4th international symposium on combustion*, Pittsburgh: The Combustion Institute, 1143.

Narvaez, I., Orio, A., Aznar, M. P., & Corella, J. (1996). Biomass gasification with air in an atmospheric bubbling fluidized bed. Effect of six operational variables on the quality of the produced raw gas. *Industrial & Engineering Chemistry Research, 35*, 2110-2120.

Nunn, T. R., Howard, J. B., Longwell, J. P., & Peters, W. A. (1985a). Product compositions and kinetics in the rapid pyrolysis of sweet gum hardwood. *Industrial & Engineering Chemistry-Process Design & Development, 24*, 836-844.

Nunn, T. R., Howard, J. B., Longwell, J. P., & Peters, W. A. (1985b). Product compositions and kinetics in the rapid pyrolysis of milled wood lignin. *Industrial & Engineering Chemistry-Process Design & Development, 24*, 844-852.

Overend, R. P. (1998). Biomass gasification: a growing business. *Renewable Energy World, 1*, 59-63.

Panton, R. L., & Rittman, J. G. (1971). Pyrolysis of slab of a porous material. *Proceedings of the 13th international symposium on combustion*, Pittsburgh: The Combustion Institute, 881-891.

Park, J. Y., & Levenspiel, O. (1975). The crackling core model for the reaction of solid particles. *Chemcal Engineering Science, 30*, 1207-1214.

Price, K., & Storn, R. (1997). Differential evolution-a simple evolution strategy for fast optimization. *Dr. Dobb's Journal, 22*, 18-24 and 78.

Price, K., & Storn, R. (2003). *Home page of differential evolution as on June 25*. URL: http://www.ICSI.Berkeley.edu/~storn/code.html

Pyle, D. L., & Zaror, C. A. (1984). Heat transfer and kinetics in the low temperature pyrolysis of solids. *Chemical Engineering Science, 39*, 147-158.

Ragland, K. W., Boerger, J. C., & Baker, A. J. (1988). A model of chunkwood combustion. *The Forest Products Journal, 38*(2), 27-32.

Ramana Rao, M. V., Plehiers, P. M., & Froment, G. F. (1988). The coupled simulation of heat transfer and reaction in a pyrolysis furnace. *Chemical Engineering Science, 43*, 1223-1229.

Reddy, B. S. (1994). Biomass energy for India: an overview. *Energy Conversion and Management, 35*, 341-361.

Reed, T. B., Milne, T., Diebold, J., & Desrosiers, R. (1981). Biomass gasification for production of gaseous and liquid fuels. *Proceedings of the Eleventh Symposium on Biotechnology and Bioengineering*, Colorado: Solar Energy Research Institute, 137-150.

Roberts, A. F. (1970). The kinetic behavior of intermediate compounds during the pyrolysis of cellulose. *Journal of Applied Polymer Science, 14*, 244-247.

Roberts, A. F. (1971). Problems associated with the theoretical analysis of the burning wood. *Proceedings of the 16th international symposium on combustion*, Pittsburgh: The Combustion Institute, 158-167.

Roberts, A. F., & Clough, G. (1963). Thermal degradation of wood in an inert atmosphere. *Proceedings of the 9th international symposium on combustion*, Pittsburgh: The Combustion Institute, 158-167.

Ruggiero, M., & Manfrida, G. (1999). An equilibrium model for biomass gasification processes. *Renewable Energy, 16*, 1106-1109.

Rustamov, V. R., Kerimov, V. K., Schachbazov, Sh. J., Kerimov, M. K., & Rustamova, L. V. (2002). Mechanism and main regularities of the alkaline pyrolysis of wood. *Energy Conversion and Management, 43*, 1901-1910.

Saastamoinen, J. J. (1993). Model for drying and pyrolysis in an updraft gasifier. In: A.V. Bridgwater (Ed.), *Advances in thermochemical biomass conversion* (pp. 186-200). London: Blackie.

Samaldo, M. C., & Vasalos, L. A. (1991). A kinetic approach to the flash pyrolysis of biomass in a fluidized bed reactor. *Fuel, 70*, 883-889.

Sato, H., Aoki, H., Miura, T., & Patrick, J. W. (1997). Numerical analysis of macrocrack formation behaviour in lump coke. *Fuel, 76*, 879-885.

Scott, D. S., Piskorz, J., Bergougnou, M. A., Graham, R., & Overend, R. P. (1988). The role of temperature in the fast pyrolysis of cellulose and wood. *Industrial & Engineering Chemistry Research, 27*, 8-15.

Şensöz, S., Angin, S., & Yorgun, S. (2000). Influence of particle size on the pyrolysis of rapeseed *(Brassica napus* L.*)*: fuel properties of bio-oil. *Biomass & Bioenergy, 19*, 271-279.

Shafizadeh, F. (1979). Introduction to pyrolysis of biomass. In specialists *workshop on fast pyrolysis of biomass. Proceedings (SERI, Golden, CO)*, SERI/CP-622-1096, p. 79.

Shafizadeh, F. (1982). Introduction to pyrolysis of biomass. *Journal of Analytical and Applied Pyrolysis, 3*, 283-305.

Shafizadeh, F., & Chin, P. P. S. (1977). Thermal deterioration of wood. *ACS Symposium Series, 43*, 57-81.

Shafizadeh, F., Furneaux, R. H., Cochran, T. G., Scholl, J. P., & Sakai, Y. (1979). Production of levoglucosan and glucose from pyrolysis of cellulosic materials. *Journal of Applied Polymer Science*, 23, 3525-3539.

Sinha, S., Jhalani, A., Ravi, M. R., & Ray, A. (2000). Modeling of pyrolysis in wood: a review. *Solar Energy Society of India, 10*, 41-62.

Soltes, E. J., & Elder, T. J. Organic chemicals from biomass. *In Pyrolysis*, Boca Raton, FL, CRC Press, USA, 1981, 63-95.

Soltes, E. J., Wiley, A. T., & Kenny Lin, S. C. (1981). Biomass pyrolysis-towards an understanding of its versatility and potentials. *Proceedings of the Symposium on Biotechnology and Bioengineering*, Texas: Forest Science Laboratory, 125-136.

Sørum, L., Grønli, M. G., & Hustad, J. E. (2001). Pyrolysis characteristics and kinetics of municipal solid wastes. *Fuel, 80*, 1217-1227.

Srivastava, V. K., & Jalan, R. K. (1994). Predictions of concentration in the pyrolysis of biomass materials-I. *Energy Conversion and Management*, 35, 1031-1040.

Srivastava, V. K., Sushil, & Jalan, R. K. (1996). Prediction of concentration in the pyrolysis of biomass material-II. *Energy Conversion and Management, 37*, 473-483.

Storn, R. (1995). Differential evolution design of an IIr-filter with requirements for magnitude and group delay, *International Computer Science Institute, TR*-95-026.

Thurner, F., & Mann, U. (1981). Kinetic investigation of wood pyrolysis. *Industrial and Engineering Chemical Process Design and Development, 20*, 482-488.

Tinney, E. R. (1965). The combustion of wooden dowels in heated air. *Proceedings of the 10th international symposium on combustion*, Pittsburgh: The Combustion Institute, 925-930.

Twidell, J. (1998). Biomass energy. *Renewable Energy World, 3*, 38-39.

Tye, R.D., Ed., (1969). Thermal conductivity. Academic Press, London.

Varhegyi, G., Jakab, E., & Antal, M. J. (1994). Is the Broido-Shafizadeh model for cellulose pyrolysis true? *Energy Fuels, 8*, 1345-1352.

Villermaux, J., Antoine, B., Lede, J., & Soulignac, F. (1986). A new model for thermal volatilization of solid particles undergoing fast pyrolysis. *Chemical Engineering Science, 41*, 151-157.

Violi, A., Anna, A. D., & Alessio, A. D. (1999). Modeling of particulate formation in combustion and pyrolysis. *Chemical Engineering Science, 54*, 3433-3442.

Wang, F. S., & Cheng, W. M. (1999). Simultaneous optimization of feeding rate and operation parameters for fed-batch fermentation processes, *Biotechnology Progress, 15*, 949-952.

Wang, Y., & Kinoshita, C. M. (1993). Kinetic model of biomass gasification. *Solar Energy, 51*, 19-25.

Ward, S. M., & Braslaw, J. (1985). Experimental weight-loss kinetics of wood pyrolysis under vacuum. *Combustion & Flame, 61*, 261-269.

Warnecke, R. (2000). Gasification of biomass: comparison of fixed bed and fluidized bed gasifier. *Biomass and Bioenergy, 18*, 489-497.

Weatherford, W. D, & Sheppard, D. M. (1965). *Proceedings of the 10th international symposium on combustion*, Pittsburgh: The Combustion Institute, 897.

Wen, C. S., & Yen, T. F. (1977). Optimization of oil shale pyrolysis. *Chemical Engineering Science, 32*, 346-349.

Wiktorsson, L. P., & Wanzl, W. (2000). Kinetic parameters for coal pyrolysis at low and high heating rates – a comparison of data from different laboratory equipment. *Fuel, 79*, 701-716.

Yang, J., Tanguy, P. A., & Roy, C. (1995). Heat transfer, mass transfer and kinetics study of the vacuum pyrolysis of a large used tire particle. *Chemical Engineering Science, 50*, 1909-1922.

Zainal, Z. A., Ali, R., Lean, C. H., & Seetharamu, K. N. (2001). Prediction of performance of a downdraft gasifier using equilibrium modeling for different biomass materials. *Energy Conversion and Management*, 42, 1499-1515.

Zaror, C. A., & Pyle, D. L. (1984). Models for low temperature pyrolysis of wood. *Thermochemical Processing of Biomass*. London: Butterworths & Company Publishers Limited.

Zhuo, Y., Messenböck, R., Collot, A. G., Megaritis, A., Paterson, N., Dugwell, D. R., & Kandiyoti, R. (2000). *Fuel, 79*, 793-802.

LIST OF PUBLICATIONS

Research Publications in International Journals:

1. Babu, B. V., & Chaurasia, A. S. (2004). Dominant design variables in pyrolysis of biomass particles of different geometries in thermally thick regime. ***Chemical Engineering Science***, Accepted (In Press). *(Also available via Internet at http://bvbabu.50megs.com/custom.html/#64).*
2. Babu, B. V., & Chaurasia, A. S. (2003). Modeling, simulation, and estimation of optimum parameters in pyrolysis of biomass. ***Energy Conversion and Management***, *44*, 2135-2158. *(Also available via Internet as .pdf file at http://bvbabu.50megs.com/custom.html/#47).*
3. Babu, B. V., & Chaurasia, A. S. (2003). Modeling for pyrolysis of solid particle: kinetics and heat transfer effects. ***Energy Conversion and Management***, 44, 2251-2275. *(Also available via Internet as .pdf file at http://bvbabu.50megs.com/custom.html/#50).*
4. Babu, B. V., & Chaurasia, A. S. (2004). Parametric study of thermal and thermodynamic properties on pyrolysis of biomass in thermally thick regime. ***Energy Conversion and Management***, *45*, 53-72. *(Also available via Internet as .pdf file at http://bvbabu.50megs.com/custom.html/#62).*
5. Babu, B. V., & Chaurasia, A. S. (2004). Pyrolysis of biomass: Improved models for simultaneous kinetics and transport of heat, mass, and momentum. ***Energy Conversion and Management***, Accepted (In Press). *(Also available via Internet as .pdf file at http://bvbabu.50megs.com/custom.html/#60).*
6. Chaurasia, A. S., & Babu, B. V. (2003). Influence of product yields, density, heating conditions and conversion on pyrolysis of biomass. ***Journal of Arid Land Studies***, Accepted, (In Press).
7. Babu, B. V., & Chaurasia, A. S. (2004). Heat transfer and kinetics in the pyrolysis of shrinking biomass particle. Communicated to ***Chemical Engineering Science***.

Research Publications in International Conferences / Proceedings:

8. Babu, B. V., & Chaurasia, A. S. (2002). Modeling & simulation of pyrolysis: influence of particle size and temperature. *Proceedings of International conference*

on multimedia and design (ICMD-2002), **Mumbai**, September 23-25, India, 4, 103-128. *(Also available via Internet as .pdf file at http://bvbabu.50megs.com/custom.html/#51).*

9. Babu, B. V., & Chaurasia, A. S. **(2002)**. Modeling & simulation of pyrolysis: effect of convective heat transfer & orders of reactions. *Proceedings of International symposium & 55th annual session of IIChE (CHEMCON-2002)*, OU, **Hyderabad**, December 19-22, India, 105-106. *(Also available via Internet as .pdf file at http://bvbabu.50megs.com/custom.html/#52).*
10. Babu, B. V., & Chaurasia, A. S. **(2003)**. Modeling & simulation of pyrolysis of biomass: effect of heat of reaction. *Proceedings of International symposium on process systems engineering and control (ISPSEC-2003) - for productivity enhancement through design and optimization*, **IIT-Bombay**, Mumbai, January 3-4, India, 181-186. *(Also available via Internet as .pdf file at http://bvbabu.50megs.com/custom.html/#55).*
11. Babu, B. V., & Chaurasia, A. S. **(2003)**. Optimization of pyrolysis of biomass using differential evolution approach. *Proceedings of Second International Conference on Computational Intelligence, Robotics, and Autonomous Systems (CIRAS-2003)*, **Singapore**, December 15-18. *(Also available via Internet as .pdf file at http://bvbabu.50megs.com/custom.html/#73).*
12. Babu, B. V., & Chaurasia, A. S. **(2003)**. Pyrolysis of shrinking cylindrical biomass pellet. *Proceedings of International symposium & 56th annual session of IIChE (CHEMCON-2003)*, **Bhubhaneswar**, December 19-22, India. *(Also available via Internet as .pdf file at http://bvbabu.50megs.com/custom.html/#70).*
13. Chaurasia, A. S., & Babu, B. V. **(2003)**. Modeling & simulation of pyrolysis of biomass: effect of thermal conductivity, reactor temperature and particle size on product concentrations. *Proceedings of International conference on Energy and Environmental Technologies for Sustainable Development (ICEET-2003)*, **Jaipur**, October 8-10, India, 151-156. *(Also available via Internet as .pdf file at http://bvbabu.50megs.com/custom.html/#65.)*
14. Chaurasia, A. S., & Babu, B. V. **(2003)**. Influence of product yields, density, heating conditions and conversion on pyrolysis of biomass. *Proceedings of International Conference on Desert Technology-7 (DT-7)*, **Jodhpur**, November 9-14, India. *(Also available via Internet as .pdf file at http://bvbabu.50megs.com/custom.html/#67).*

Research Publications in National Journal:

15. Chaurasia, A. S., Babu, B. V., Kaur, A., & Thiruchitrambalam, V. **(2003)**. Convective and radiative heat transfer through a biomass particle. Communicated to ***Indian Chemical Engineer Journal***.

APPENDIX-A

A-1 Runge-Kutta fourth order method

The Taylor's series method of solving differential equations numerically is restricted by the labour involved in finding the higher order derivatives. However there is a class of methods known as Runge-Kutta fourth order method which do no require the calculations of higher order derivatives and give greater accuracy. The Runge-Kutta formulae possess the advantage of requiring only the function values at some points. This method agrees with Taylor's series solution upto the term in h^r where r differs from method to method and is called the order of that method.

A-1.1. Single first order differential equation

Working rule for finding the increment k of y corresponding to an increment h of x by Runge-Kutta method from the differential equation

$$\frac{dy}{dx} = f(x, y)$$

with initial condition $y(x_0) = y_0$ is as follows:

Calculate successively the following:

$$k_1 = hf(x_0, y_0)$$

$$k_2 = hf(x_0 + \frac{1}{2}h, y_0 + \frac{1}{2}k_1)$$

$$k_3 = hf(x_0 + \frac{1}{2}h, y_0 + \frac{1}{2}k_2)$$

$$k_4 = hf(x_0 + h, y_0 + k_3)$$

Finally compute,

$$k = \frac{1}{6}(k_1 + 2k_2 + 2k_3 + k_4)$$

which gives the required approximate value as

$$y_1 = y_0 + k$$

To compute y_2, we simply replace x_0 and y_0 by x_1 and y_1 respectively in the above formulae.

A-1.2. Simultaneous first order differential equations

The simultaneous differential equations of the type

$$\frac{dy}{dx} = f(x, y, z)$$

and $$\frac{dy}{dx} = \phi(x, y, z)$$

with the initial conditions $y(x_0) = y_0$ and $z(x_0) = z_0$ can also be solved by Runge-Kutta fourth order method. Starting at (x_0, y_0, z_0) and taking step sizes for x, y, z to be h, k, l respectively, the Runge-Kutta fourth order method gives,

$$k_1 = hf(x_0, y_0, z_0)$$
$$l_1 = h\phi(x_0, y_0, z_0)$$
$$k_2 = hf(x_0 + \frac{1}{2}h, y_0 + \frac{1}{2}k_1, z_0 + \frac{1}{2}l_1)$$

$$l_2 = h\phi(x_0 + \frac{1}{2}h, y_0 + \frac{1}{2}k_1, z_0 + \frac{1}{2}l_1)$$

$$k_3 = hf(x_0 + \frac{1}{2}h, y_0 + \frac{1}{2}k_2, z_0 + \frac{1}{2}l_2)$$

$$l_3 = h\phi(x_0 + \frac{1}{2}h, y_0 + \frac{1}{2}k_2, z_0 + \frac{1}{2}l_2)$$

$$k_4 = hf(x_0 + h, y_0 + k_3, z_0 + l_3)$$

$$l_4 = h\phi(x_0 + h, y_0 + k_3, z_0 + l_3)$$

Hence,

$$y_1 = y_0 + \frac{1}{6}(k_1 + 2k_2 + 2k_3 + k_4)$$

and

$$z_1 = z_0 + \frac{1}{6}(l_1 + 2l_2 + 2l_3 + l_4)$$

To compute y_2 and z_2, we simply replace x_0, y_0, z_0 by x_1, y_1, z_1 in the above formulae.

A-1.3. Flowchart for kinetic model equations using Runge-Kutta fourth order method

The steps involved in coding the programs for simulations using above methods are shown in the form of flowchart given in Fig. A.1. This is the generalized flowchart where only the model equations need to be changed for various simulations, the detailed programming codes of which are given in sections A-2 and A-3.

A-2 Program for linear non-isothermal Runge-Kutta fourth order method

```
/* Program for Chapter 3 */
/* Modeling, Simulation, and Estimation of Optimum Parameters in Pyrolysis of
Biomass.*/
#include<stdio.h>
#include<math.h>
```

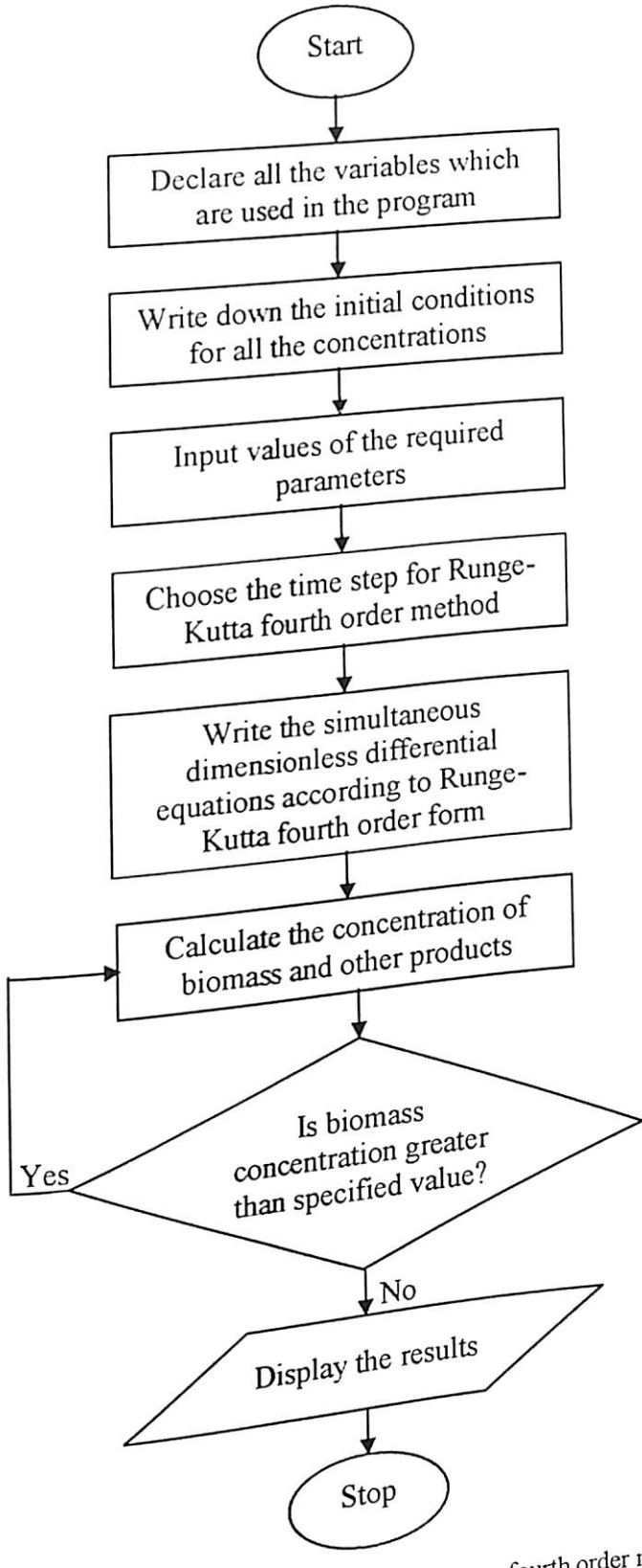

Fig. A.1. Flowchart for kinetic model equations using Runge-Kutta fourth order method.

```
void main()
{
long double T0,HR;
long double T,CB,k1,k2,k3;
int i;
long double A1,A2,A3,D1,D2,L1,L2,E3,R;
long double Cc1,CG1,Cc2,CG2,t;
long double n1,n2,n3,h;
long double a1,b1,c1,d1,e1;
long double a2,b2,c2,d2,e2;
long double a3,b3,c3,d3,e3;
long double a4,b4,c4,d4,e4;

/* Initial condition */
CB=1.0;
Cc1=0.0;
CG1=0.0;
Cc2=0.0;
CG2=0.0;

/* Input */
printf(" Enter the value of initial temp(T0=773.0)\n");
scanf("%Lf",&T0);
printf("Enter the value of heating rate(HR)\n");
scanf("%Lf",&HR);
printf("Enter the value of order of reaction n1,n2,n3\n");
scanf("%Lf %Lf %Lf",&n1,&n2,&n3);
printf("Enter the value of time step h(t)\n");
scanf("%Lf",&h);
printf("\n");
printf("\n  h(t)    T       CB     CG1      Cc1      CG2    Cc2");
t=h;

/* Runge-Kutta method starts here */
while(1)
{
T=(HR)*t+T0;
A1=9.973*pow(10.0,-5.0);
A2=1.068*pow(10.0,-3.0);
A3=5.7*pow(10.0,5.0);
D1=17254.4;
D2=10224.4;
L1=-9061227.0;
L2=-6123081.0;
E3=81000.0;
R=8.314;
```

```
k1=A1*exp((D1/T)+(L1/(T*T)));
k2=A2*exp((D2/T)+(L2/(T*T)));
k3=A3*exp(-E3/(R*T));
a1=(-h)*((k1+k2)*pow(CB,n1));
b1=h*((k1*pow(CB,n1))-(k3*pow(CG1,n2)*pow(Cc1,n3)));
c1=h*((k2*pow(CB,n1))-(k3*pow(CG1,n2)*pow(Cc1,n3)));
d1=h*(k3*pow(CG1,n2)*pow(Cc1,n3));
e1=h*(k3*pow(CG1,n2)*pow(Cc1,n3));
a2=(-h)*((k1+k2)*pow((CB+(a1/2.0)),n1));
b2=h*((k1*pow((CB+(a1/2.0)),n1))-
(k3*pow((CG1+(b1/2.0)),n2)*pow((Cc1+(c1/2.0)),n3)));
c2=h*((k2*pow((CB+(a1/2.0)),n1))-
(k3*pow((CG1+(b1/2.0)),n2)*pow((Cc1+(c1/2.0)),n3)));
d2=h*(k3*pow((CG1+(b1/2.0)),n2)*pow((Cc1+(c1/2.0)),n3));
e2=h*(k3*pow((CG1+(b1/2.0)),n2)*pow((Cc1+(c1/2.0)),n3));
a3=(-h)*((k1+k2)*pow((CB+(a2/2.0)),n1));
b3=h*((k1*pow((CB+(a2/2.0)),n1))-
(k3*pow((CG1+(b2/2.0)),n2)*pow((Cc1+(c2/2.0)),n3)));
c3=h*((k2*pow((CB+(a2/2.0)),n1))-
(k3*pow((CG1+(b2/2.0)),n2)*pow((Cc1+(c2/2.0)),n3)));
d3=h*(k3*pow((CG1+(b2/2.0)),n2)*pow((Cc1+(c2/2.0)),n3));
e3=h*(k3*pow((CG1+(b2/2.0)),n2)*pow((Cc1+(c2/2.0)),n3));
a4=(-h)*((k1+k2)*pow((CB+a3),n1));
b4=h*((k1*pow((CB+a3),n1))-(k3*pow((CG1+b3),n2)*pow((Cc1+c3),n3)));
c4=h*((k2*pow((CB+a3),n1))-(k3*pow((CG1+b3),n2)*pow((Cc1+c3),n3)));
d4=h*(k3*pow((CG1+b3),n2)*pow((Cc1+c3),n3));
e4=h*(k3*pow((CG1+b3),n2)*pow((Cc1+c3),n3));
CB=CB+(1.0/6.0)*(a1+2.0*a2+2.0*a3+a4);
CG1=CG1+(1.0/6.0)*(b1+2.0*b2+2.0*b3+b4);
Cc1=Cc1+(1.0/6.0)*(c1+2.0*c2+2.0*c3+c4);
CG2=CG2+(1.0/6.0)*(d1+2.0*d2+2.0*d3+d4);
Cc2=Cc2+(1.0/6.0)*(e1+2.0*e2+2.0*e3+e4);
if(CB<=0.03)
break;

/* Output */                                %0.6Lf        %0.6Lf        %0.6Lf
printf("\n%0.6Lf        %0.6Lf        %0.6Lf
%0.6Lf",t,T,CB,CG1,Cc1,CG2,Cc2);
t=t+h;
/*getch();*/
}
printf("\n");
getch();
}
```

A-3 Program for linear isothermal Runge-Kutta fourth order method

```
/* Program for Chapter 3 */
/* Modeling, Simulation, and Estimation of Optimum Parameters in Pyrolysis of
Biomass.*/
#include<stdio.h>
#include<math.h>
void main()
{
long double T0,HR;
long double T,CB,k1,k2,k3;
int i;
long double A1,A2,A3,D1,D2,L1,L2,E3,R;
long double Cc1,CG1,Cc2,CG2,t;
long double n1,n2,n3,h;
long double a1,b1,c1,d1,e1;
long double a2,b2,c2,d2,e2;
long double a3,b3,c3,d3,e3;
long double a4,b4,c4,d4,e4;

/* Initial condition */
CB=1.0;
Cc1=0.0;
CG1=0.0;
Cc2=0.0;
CG2=0.0;

/* Input */
printf(" Enter the value of temperature\n");
scanf("%Lf",&T0);
printf("Enter the value of order of reaction n1,n2,n3\n");
scanf("%Lf %Lf %Lf",&n1,&n2,&n3);
printf("Enter the value of time step h(t)\n");
scanf("%Lf",&h);
printf("\n");
printf("\n  h(t)    T       CB     CG1      Cc1      CG2    Cc2");
t=h;

/* Runge-Kutta method starts here */
while(1)
{T=T0;
A1=9.973*pow(10.0,-5.0);
A2=1.068*pow(10.0,-3.0);
A3=5.7*pow(10.0,5.0);
D1=17254.4;
D2=10224.4;
L1=-9061227.0;
```

```
L2=-6123081.0;
E3=81000.0;
R=8.314;
k1=A1*exp((D1/T)+(L1/(T*T)));
k2=A2*exp((D2/T)+(L2/(T*T)));
k3=A3*exp(-E3/(R*T));
a1=(-h)*((k1+k2)*pow(CB,n1));
b1=h*((k1*pow(CB,n1))-(k3*pow(CG1,n2)*pow(Cc1,n3)));
c1=h*((k2*pow(CB,n1))-(k3*pow(CG1,n2)*pow(Cc1,n3)));
d1=h*(k3*pow(CG1,n2)*pow(Cc1,n3));
e1=h*(k3*pow(CG1,n2)*pow(Cc1,n3));
a2=(-h)*((k1+k2)*pow((CB+(a1/2.0)),n1));
b2=h*((k1*pow((CB+(a1/2.0)),n1))-
(k3*pow((CG1+(b1/2.0)),n2)*pow((Cc1+(c1/2.0)),n3)));
c2=h*((k2*pow((CB+(a1/2.0)),n1))-
(k3*pow((CG1+(b1/2.0)),n2)*pow((Cc1+(c1/2.0)),n3)));
d2=h*(k3*pow((CG1+(b1/2.0)),n2)*pow((Cc1+(c1/2.0)),n3));
e2=h*(k3*pow((CG1+(b1/2.0)),n2)*pow((Cc1+(c1/2.0)),n3));
a3=(-h)*((k1+k2)*pow((CB+(a2/2.0)),n1));
b3=h*((k1*pow((CB+(a2/2.0)),n1))-
(k3*pow((CG1+(b2/2.0)),n2)*pow((Cc1+(c2/2.0)),n3)));
c3=h*((k2*pow((CB+(a2/2.0)),n1))-
(k3*pow((CG1+(b2/2.0)),n2)*pow((Cc1+(c2/2.0)),n3)));
d3=h*(k3*pow((CG1+(b2/2.0)),n2)*pow((Cc1+(c2/2.0)),n3));
e3=h*(k3*pow((CG1+(b2/2.0)),n2)*pow((Cc1+(c2/2.0)),n3));
a4=(-h)*((k1+k2)*pow((CB+a3),n1));
b4=h*((k1*pow((CB+a3),n1))-(k3*pow((CG1+b3),n2)*pow((Cc1+c3),n3)));
c4=h*((k2*pow((CB+a3),n1))-(k3*pow((CG1+b3),n2)*pow((Cc1+c3),n3)));
d4=h*(k3*pow((CG1+b3),n2)*pow((Cc1+c3),n3));
e4=h*(k3*pow((CG1+b3),n2)*pow((Cc1+c3),n3));
CB=CB+(1.0/6.0)*(a1+2.0*a2+2.0*a3+a4);
CG1=CG1+(1.0/6.0)*(b1+2.0*b2+2.0*b3+b4);
Cc1=Cc1+(1.0/6.0)*(c1+2.0*c2+2.0*c3+c4);
CG2=CG2+(1.0/6.0)*(d1+2.0*d2+2.0*d3+d4);
Cc2=Cc2+(1.0/6.0)*(e1+2.0*e2+2.0*e3+e4);
if(CB<=0.03)
break;

/* Output */                                %0.6Lf        %0.6Lf        %0.6Lf
printf("\n%0.6Lf        %0.6Lf        %0.6Lf
%0.6Lf",t,T,CB,CG1,Cc1,CG2,Cc2);
t=t+h;
}
printf("\n");
getch();
}
```

APPENDIX-B

Since the numerical treatment of conduction problem depends on the nature of the conduction process, all conduction processes are divided broadly into two categories, namely, steady and unsteady. Steady state means that temperature, density, etc. at all the points of the conduction region is independent of time. Unsteady state means a change with time, usually only of the temperature.

Many difficult problems arise in conduction, for example, variable and thermal conductivity, distributed energy sources, radiation boundary conditions for which analytical solutions are not available. Approximate solution is then obtained by numerical method. The basic approach is to arrive at the relevant governing differential equation based on the physics of the particular problem. They are then converted to required finite difference forms. Here the idea is to show the use of the numerical method. One-dimensional steady state problem can be solved by using tridiagonal matrix algorithm while one-dimensional unsteady state (transient) problem can be solved by using tridiagonal matrix algorithm utilizing pure implicit scheme.

B-1 One-dimensional steady state problem

Consider the one-dimensional steady state heat conduction in an isolated rectangular horizontal fin as shown in Fig. B.1. The base temperature is maintained at $T = T_0$ and the tip of the fin is insulated. The fine is exposed to a convective environment (neglecting radiation heat transfer from the fin) which is at $T_\infty (T_\infty < T_0)$. The average heat transfer coefficient of the fin to the ambient is h. The length of the fin is L and the coordinate axis begins at the base of the fin. The one-dimensionality arises from the fact that thickness of the fin is much small as compared to its length and the width can be considered either too long or the sides of the fin to be insulated.

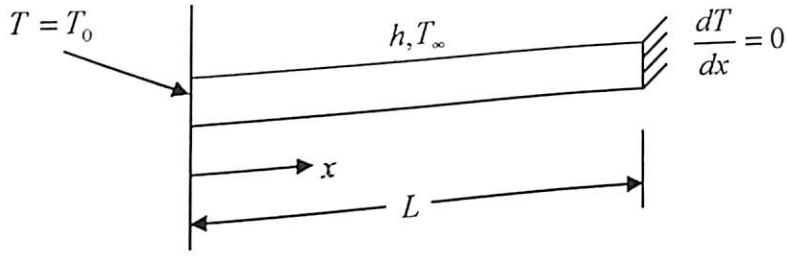

Fig. B.1. Physical domain of the rectangular fin.

B-1.1. Governing differential equation

The energy equation for the fin at the steady state (assuming constant k) is

$$\frac{d^2T}{dx^2} - \frac{hP}{kA}(T - T_\infty) = 0 \tag{B.1}$$

where P and A are the perimeter and the cross-sectional area of the fin respectively.

B-1.2. Boundary conditions

Since equation (B.1) is a linear, second order ordinary differential equation, two boundary conditions are needed to completely describe this problem (which is a

boundary value problem or elliptic problem).

Boundary conditions are

B.C.1: at $x = 0$, $T = T_0$ (B.1a)

B.C.2: at $x = L$, $\frac{dT}{dx} = 0$ (B.1b)

B-1.3. Non-dimensionalisation

Non-dimensionalising equation (B.1) and equations (B.1a) and (B.1b) using the dimensionless variables

$\theta = \frac{T - T_\infty}{T_0 - T_\infty}$ and $X = \frac{x}{L}$,

we obtain

$$\frac{d^2\theta}{dx^2} - (mL)^2\theta = 0 \quad \text{(B.2)}$$

where $m^2 = \frac{hP}{kA}$

and

$\theta(0) = 1$ (B.2a)

$\theta'(1) = 0$ (B.2b)

where $\theta' = \frac{d\theta}{dx}$

B-1.4. Discretization

Equation (B.2) is discretized at any interior grid point i using central difference for $\frac{d^2\theta}{dx^2}$ as follows:

$$\frac{d^2\theta}{dx^2} - (mL)^2\theta = 0$$

or

$$\frac{\theta_{i-1} - 2\theta_i + \theta_{i+1}}{(\Delta X)^2} - (mL)^2\theta_i = 0$$

or

$$\theta_{i-1} - D\theta_i + \theta_{i+1} = 0, \quad i = 2,....M \tag{B.3}$$

where

$$D = 2 + (mL)^2(\Delta X)^2$$

B-1.4.1. Handling of the boundary condition

At $x = L$, i.e. at $i = M$, equation (B.3) reduces to

$$\theta_{M-1} - D\theta_M + \theta_{M+1} = 0 \tag{B.4}$$

A careful look at equation (B.4) reveals that θ_{M+1} represents a fictitious temperature θ at point $M+1$ which lies outside the computational domain. This can be solved by image point technique.

B-1.4.2. Image point technique

It is assumed that θ vs X curve extends beyond $X = 1$ so that at $X = 1$, the condition $\frac{d\theta}{dX} = 0$ is satisfied. In other words, θ vs X curve can be imagined to look as in Fig. B.2. The dotted line represents the mirror-image extension of solid line indicating that a minima exists at $X = 1$. Therefore, the boundary condition at $X = 1$ can be approximately satisfied by taking

$$\theta_{M+1} = \theta_{M-1} \tag{B.5}$$

Equation (B.5) also follows from the central difference approximation of $\frac{d\theta}{dX}$ at $i = M$.

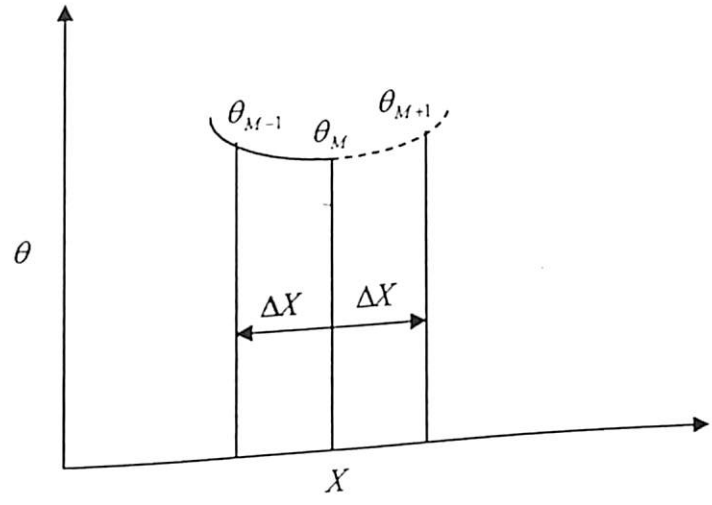

Fig. B.2. Mirror-image extension of θ vs X curve near the tip of the fin.

Substituting equation (B.5) into equation (B.4), we get,

$$2\theta_{M-1} - D\theta_M = 0 \tag{B.6}$$

Therefore, we can write that

$$\begin{aligned} &\theta_1 = 1 && \text{for } i = 1 \text{ (known)} \\ &\theta_{i-1} - D\theta_i + \theta_{i+1} = 0 && \text{for } i = 2,\ldots M-1 \\ &2\theta_{M-1} - D\theta_M = 0 && \text{for } i = M \end{aligned} \tag{B.7}$$

Hence, we have a set of $M-1$ linear simultaneous algebraic equations and $M-1$ unknowns which can be easily solved by standard numerical methods.

For the case in which $M = 5$, we have $N - M - 1 = 4$ equations to solve. The four equations can be written in matrix form as

$$\begin{bmatrix} D & -1 & & \\ -1 & D & -1 & \\ & -1 & D & -1 \\ & & -2 & D \end{bmatrix} \begin{bmatrix} \theta_1 \\ \theta_2 \\ \theta_3 \\ \theta_4 \end{bmatrix} = \begin{bmatrix} 1 \\ 0 \\ 0 \\ 0 \end{bmatrix} \tag{B.8}$$

It should be noted that θ_1 corresponds to temperature at grid point 2 and son on for $\theta_2, \theta_3, \theta_4$.

B-1.5. Method of solution

In equation (B.8), the coefficient matrix has three diagonals – main diagonal, sub-diagonal and super-diagonal, and hence the name tridiagonal matrix (abbreviated as TDM). The set of equations (B.8) is called tridiagonal system of equations.

B-1.5.1. Thomas Algorithm or Tridiagonal Matrix Algorithm or TDMA

Equation (B.7) is actually a special form of the system (using $N = M - 1$)

$$\begin{aligned} & = d_1 \\ b_1 T_1 + c_1 T_2 & = d_2 \\ a_2 T_1 + b_2 T_2 + c_2 T_3 & = d_3 \\ a_3 T_2 + b_3 T_3 + c_3 T_4 & \\ \cdots\cdots\cdots\cdots\cdots\cdots\cdots\cdots & = d_i \\ a_i T_{i-1} + b_i T_i + c_i T_{i+1} & \\ \cdots\cdots\cdots\cdots\cdots\cdots\cdots\cdots & \\ a_{N-1} T_{N-2} + b_{N-1} T_{N-1} + c_{N-1} T_N & = d_{N-1} \\ a_N T_{N-1} + b_N T_N & = d_N \end{aligned} \tag{B.9}$$

In a nut-shell, the complete algorithm for the solution of the tridiagonal system is

$$T_N = \gamma_N \tag{B.10}$$

$$T_i = \gamma_i - \frac{c_i T_{i+1}}{\beta_i}, i = N-1, N-2, \ldots, 1 \tag{B.11}$$

where, β's and γ's are determined from the recursion formulae

$$\beta_1 = b_1 \tag{B.12}$$

$$\gamma_1 = \frac{d_1}{\beta_1} \tag{B.13}$$

$$\beta_i = b_i - \frac{a_i c_{i-1}}{\beta_{i-1}},\ i = 2,3,\ldots,N \tag{B.14}$$

$$\gamma_i = \frac{d_i - a_i \gamma_{i-1}}{\beta_i},\ i = 2,3,\ldots,N \tag{B.15}$$

The above algorithm is also known as Thomas Algorithm.

B-2 One-dimensional unsteady state (transient) problem

Consider a hot infinite plate (Fig. B.3) of finite thickness $2L$, that is suddenly exposed to a cool fluid at T_∞. Initial temperature of the plate is $T_i\,(T_i > T_\infty)$. Heat transfer coefficient is large. We wish to find the temperature of the plate as a function of space and time using numerical method.

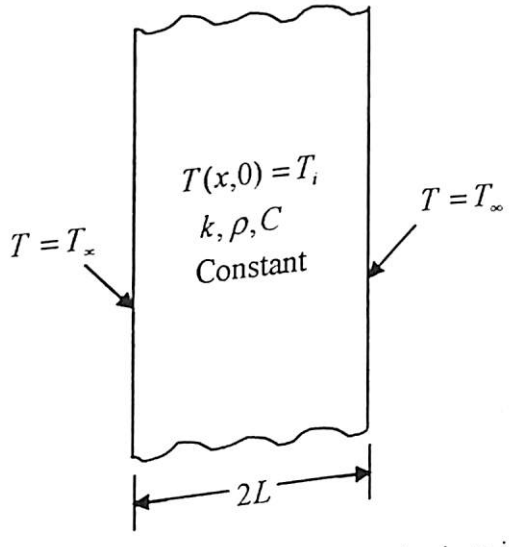

Fig. B.3. Physical domain of the one-dimensional transient conduction in an infinite plane slab.

The problem can be modeled as a one-dimensional unsteady state problem because $\frac{\partial T}{\partial y} = \frac{\partial T}{\partial z} = 0$ as the plate is infinitely long in y and z directions.

B-2.1. Consideration of symmetry

Since the problem is a thermally and geometrically symmetric one, only one half of the plate can be taken as the computational domain with insulation boundary condition at $x = L$ (Fig. B.4).

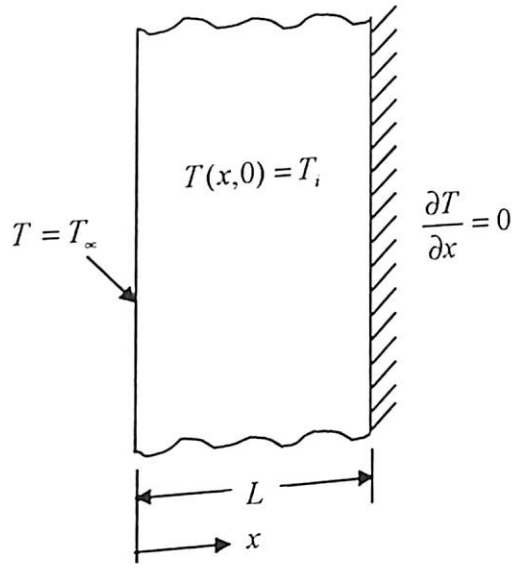

Fig. B.4. Computational domain of the one-dimensional transient conduction problem.

B-2.2. Governing differential equation

For constant thermophysical properties, k, ρ, C the non-dimensional energy equation for the plate is

$$\frac{\partial \theta}{\partial \tau} = \frac{\partial^2 \theta}{\partial X^2} \tag{B.16}$$

where

$$\theta = \frac{T - T_\infty}{T_i - T_\infty}, \quad X = \frac{x}{L}, \quad \tau = \frac{\alpha t}{L^2}$$

B-2.3. Initial and boundary conditions

The initial and boundary conditions are

I.C.: at $\tau = 0$, $\theta = 1$ for all X (B.16a)

For $\tau > 0$,

B.C.1: at $X = 0$, $\theta = 0$ (B.16b)

B.C.2: at $X = 1$, $\frac{\partial \theta}{\partial X} = 0$ (B.16c)

B-2.4. Discretization

For any interior grid point, finite-difference formulation gives,

$$\frac{\partial \theta_i}{\partial \tau} = \frac{\theta_{i-1} - 2\theta_i + \theta_{i+1}}{(\Delta X)^2} \qquad for\ i = 1,...,M \tag{B.17}$$

The equation for $X = 1$ is obtained by using image-point technique, that is, substituting $\theta_{M+1} = \theta_{M-1}$ in equation (B.17) for $i = M$.

Therefore,

$$\frac{\partial \theta_M}{\partial \tau} = \frac{2\theta_{M-1} - 2\theta_M}{(\Delta X)^2} \tag{B.18}$$

For the sake of demonstration, let us take four equal sub-division in the X - direction.

Therefore, $\Delta X = 1/4$.

At $i = 0$, $\theta = 0$ (known).

At $i = 1,2,3$ from equation (B.17), we obtain

$$\frac{\partial \theta_1}{\partial \tau} = \frac{1}{(\Delta X)^2}(\theta_0 - 2\theta_1 - \theta_2) = \frac{1}{(\Delta X)^2}(-2\theta_1 - \theta_2) \tag{B.19}$$

$$\frac{\partial \theta_2}{\partial \tau} = \frac{1}{(\Delta X)^2}(\theta_1 - 2\theta_2 - \theta_3) \tag{B.20}$$

$$\frac{\partial \theta_3}{\partial \tau} = \frac{1}{(\Delta X)^2}(\theta_2 - 2\theta_3 - \theta_4) \tag{B.21}$$

At $i = 4$, from equation (B.18), we obtain,

$$\frac{\partial \theta_4}{\partial \tau} = \frac{1}{(\Delta X)^2}(2\theta_3 - 2\theta_4) \tag{B.22}$$

Thus, we have four simultaneous ordinary differential equations [equations (B.19) to (B.22)] to solve. This system of ordinary differential equations may be classified as initial-value problems. This is because these equations are to be solved for the unknowns as a function of time beginning with an initial value for each of the unknowns. In this case the initial value are obtained from the initial temperature distribution in the plate which is given by

$$\theta_1(0) = \theta_2(0) = \theta_3(0) = \theta_4(0) = 1 \tag{B.23}$$

B-2.5. Method of solution

The initial value problem mentioned above in the section B-4.4 can be solved by pure implicit method.

B-2.5.1. Pure implicit method

In the pure implicit scheme, the time derivative at the new time is used to move ahead in time. Thus,

$$\theta^{p+1} = \theta^p + \left(\frac{\partial \theta}{\partial \tau}\right)^{p+1} \Delta\tau \tag{B.24}$$

From equations (B.19)-(B.22) and equation (B.24), we obtain

$$\frac{\theta_1^{p+1} - \theta_1^p}{\Delta\tau} = \frac{1}{(\Delta X)^2}(-2\theta_1^{p+1} - \theta_2^{p+1}) \tag{B.25}$$

$$\frac{\theta_2^{p+1} - \theta_2^p}{\Delta\tau} = \frac{1}{(\Delta X)^2}(\theta_1^{p+1} - 2\theta_2^{p+1} + \theta_3^{p-1}) \tag{B.26}$$

$$\frac{\theta_3^{p+1}-\theta_3^{p}}{\Delta\tau}=\frac{1}{(\Delta X)^2}(\theta_2^{p+1}-2\theta_3^{p+1}+\theta_4^{p+1}) \tag{B.27}$$

$$\frac{\theta_4^{p+1}-\theta_4^{p}}{\Delta\tau}=\frac{1}{(\Delta X)^2}(2\theta_3^{p+1}-2\theta_4^{p+1}) \tag{B.28}$$

Equations (B.25)-(B.28) are rearranged resulting in a set of four simultaneous algebraic equations in θ_1^{p+1}, θ_2^{p+1}, θ_3^{p-1} and θ_4^{p+1}, represented in matrix form as

$$\begin{bmatrix} 1+2r & -r & & \\ -r & 1+2r & -r & \\ & -r & 1+2r & -r \\ & & -2r & 1+2r \end{bmatrix}\begin{bmatrix}\theta_1\\ \theta_2\\ \theta_3\\ \theta_4\end{bmatrix}^{p-1}=\begin{bmatrix}\theta_1\\ \theta_2\\ \theta_3\\ \theta_4\end{bmatrix}^{p} \tag{B.29}$$

Equation (B.29) is an implicit set of equations to solve for the new temperatures at each step in time. Pure implicit is an unconditionally stable scheme, that is, there is no restriction on time-step in sharp contrast with the Euler and the Crank-Nicholson method.

B-2.6. Flowchart for heat, mass and momentum transfer model equations using pure implicit scheme

The steps involved in coding the programs for simulations using above methods are shown in the form of flowchart given in Fig. B.5. This is the generalized flowchart where only the model equations need to be changed for various simulations, the detailed programming codes of which are given in sections B-3, B-4 and Appendices D, E and F.

B-3 Program for heat transfer model by using finite difference pure implicit scheme and Runge-Kutta fourth order method

```
/* Program for Chapter 4 */
/* Modeling for pyrolysis of solid particle: kinetics and heat transfer effects. */
/* This is the program when wall temperature is constant */
#include<stdio.h>
#include<math.h>
#define M 150                    /* (M+1)=Total number of equations to be solved */
void main()
```

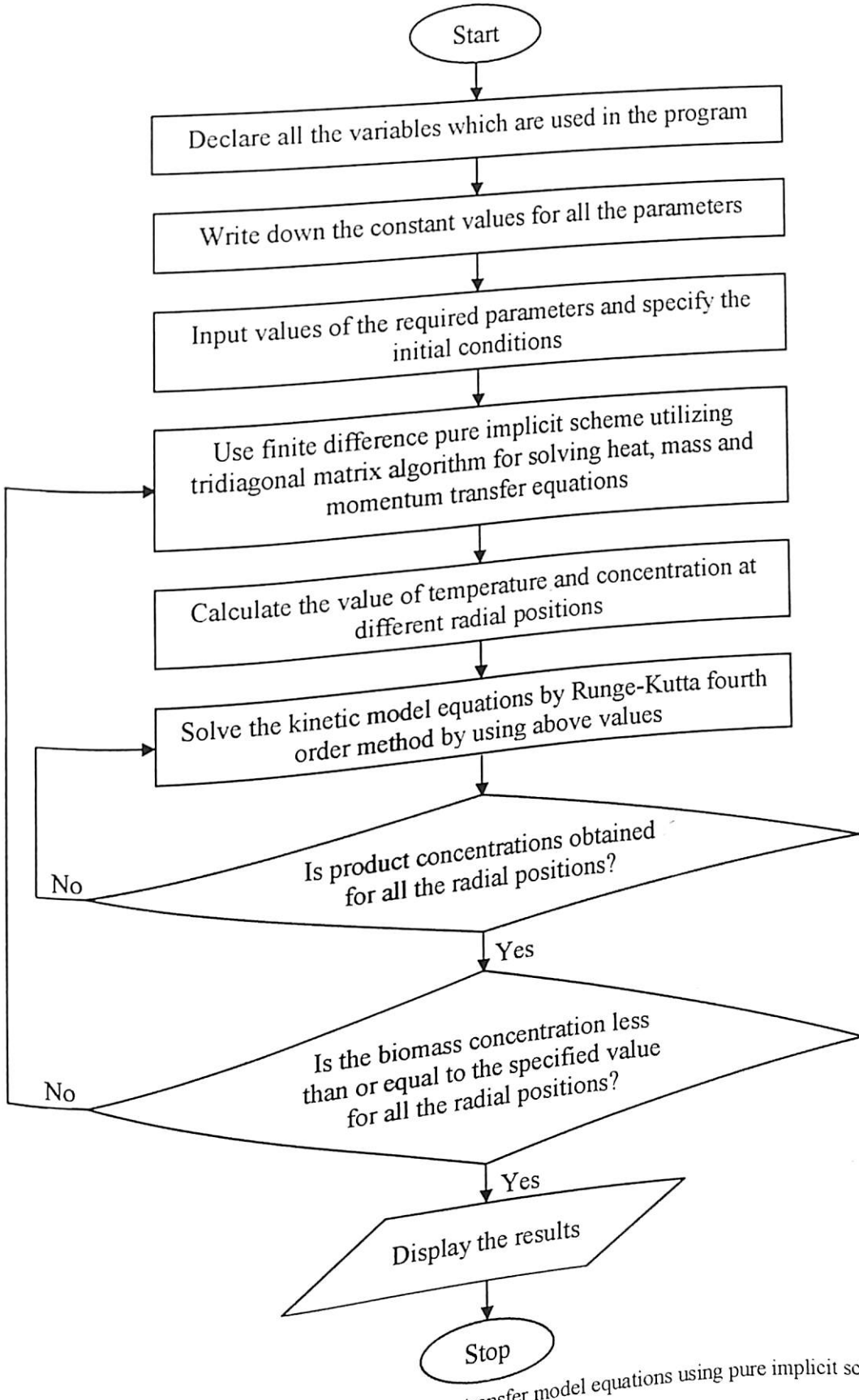

Fig. B.5. Flowchart for heat, mass and momentum transfer model equations using pure implicit scheme

```
{
long double T[M+2];          /* T=Temperature (K) */
long double CB[M+2];         /* CB=Concentration of biomass (kg/m^3) */
long double k1[M+2];         /* k1=Rate constant for reaction 1 (1/s) */
long double k2[M+2];         /* k2=Rate constant for reaction 2 (1/s) */
long double k3[M+2];         /* k3=Rate constant for reaction 3 (1/s) */
int i;                       /* i=integer used in program */
int j;                       /* j=integer used in program */
int eqn[M+2];
long double xx;              /* xx=used for output of dimensionles distance (-) */
long double R;               /* R=radius of cylindrical pellet (m) */
long double A1;              /* A1=Arrhenius frequency factor for reaction 1 (1/s) */
long double A2;              /* A2=Arrhenius frequency factor for reaction 2 (1/s) */
long double A3;              /* A3=Arrhenius frequency factor for reaction 3 (1/s) */
long double D1;              /* D1=Constant used while calculating k1 (K) */
long double D2;              /* D2=Constant used while calculating k2 (K) */
long double L1;              /* L1=Constant used while calculating k1 (K^2) */
long double L2;              /* L2=Constant used while calculating k2 (K^2) */
long double E3;              /* E3=Activation energy (J/gmol) */
long double Rc;              /* Rc=Universal gas constant (J/gmol K)*/
long double Cc1[M+2];        /* Cc1=Concentration of char 1 (-) */
long double CG1[M+2];        /* CG1=Concentration of volatile 1 (-) */
long double Cc2[M+2];        /* Cc2=Concentration of char 2 (-) */
long double CG2[M+2];        /* CG2=Concentration of volatile 2 (-) */
long double t[M+2];          /* t=Time (s) */
long double n1;              /* n1=Order of reaction 1 (-) */
long double n2;              /* n2=Order of reaction 2 (-) */
long double n3;              /* n3=Order of reaction 3 (-) */
long double h;               /* h=step size for RK4 Method (s) */
long double a1;
long double b1;
long double c1;
long double d1;
long double e1;
long double a2;
long double b2;
long double c2;
long double d2;
long double e2;              /*a1-e4=Variables used while solving RK4 method */
long double a3;
long double b3;
long double c3;
long double d3;
long double e3;
long double a4;
long double b4;
```

```
long double c4;
long double d4;
long double e4;
long double dtow;          /* dtow=Dimensionless time step for finite difference
                           method (-) */
long double tow;           /* tow=Dimensionless time for finite difference
                           method (-) */
long double dx;            /* dx=Dimensionless radial distance step for finite
                           difference method (-) */
long double T0;            /* T0=Initial temperature (K) */
long double Tf;            /* Tf=Final temperature (K) */
long double ht;            /* ht=convective heat transfer coefficient (W/m^2K) */
long double ab;            /* ab=emissivity coefficient */
long double sig;           /* sig=Stefan Boltzman constant */
long double dH;            /* dH=heat of reaction (kJ/kg) */
long double k[M+2];        /* k=thermal conductivity (W/m K) */
long double H[M+2];        /* H=modified Biot Number */
long double cp[M+2];       /* cp=specific heat (J/kg K) */
long double ro[M+2];       /* ro=density (kg/m^3) */
long double Q[M+2];        /* Q=heat of reaction number (m^3/kg) */
long double x[M+2];        /* x=Dimensionless radial distance (-) */
long double a[M+2];
long double b[M+2];        /*a-d=Variables used in assigning values in tridiagonal
                           matrix*/
long double c[M+2];
long double d[M+2];
long double theta[M+2];    /* theta=Dimensionless temperature (-) */
long double beta[M+2];     /* beta=used while calculating theta (-) */
long double gamma[M+2];    /* gamma=used while calculating theta (-) */
long double alpha;         /* alpha=used while calculating theta (-) */
long double ft;            /* ft=conversion of dimensionless time second (s) */
long double roin;          /* roin=initial value of density (kg/m^3) */
long double jj;
long double kk;            /* jj-bb=Variables used while calculating the value of H */
long double ll;
long double aa;
long double mm;
long double bb;

/*Constants*/
/*R=0.005;*/
A1=9.973*pow(10.0,-5.0);
A2=1.068*pow(10.0,-3.0);
A3=5.7*pow(10.0,5.0);
D1=17254.4;
D2=10224.4;
```

```
L1=-9061227.0;
L2=-6123081.0;
E3=81000.0;
Rc=8.314;
dx=(1.0/M);
x[1]=(1.0/M);
ht=8.4;
ab=0.95;
/*sig=5.67*pow(10.0,-8.0);*/
roin=650.0;
dH=-255000.0;
alpha=1.79*pow(10.0,-7.0);
/*n1=1.0;
n2=1.5;
n3=1.5;
h=0.01;
tow=0.010024;
dtow=0.010024;
T0=473.0;
Tf=873.0;*/
eqn[0]=1;
for(i=0;i<=M;i++)
{
eqn[i+1]=eqn[i]+1;
}
/*printf("%d",eqn[M]);
getch();*/
/*printf("%Lf %Lf\n",dx,x[1]);
getch();*/

/* Input */
printf("Enter the orders of reactions n1,n2,n3 (1,1.5,1.5)\n");
scanf("%Lf %Lf %Lf",&n1,&n2,&n3);
printf("Enter the value of time step h(t) for RK4 method (0.01)\n");
scanf("%Lf",&h);
printf("Enter the value of radius of cylindrical pellet\n");
scanf("%Lf",&R);
printf("The value of tow can be calculated by the following formula:\n");
printf("t=(tow*R*R)/(alpha)\n");
printf("Here alpha is known i.e. alpha=1.79*pow(10.0,-7.0)\n");
printf("Suppose you want that your output come after every 1sec\n");
printf("Then t=1sec and say R=0.005m,then tow comes out to be 0.00716\n");
printf("Enter the initial value of time step i.e.tow (dimensionless) for\n");
printf("finite difference method \n");
scanf("%Lf",&tow);
printf("Enter the value of dtow(Its value is same as initial value of tow)\n");
```

```
scanf("%Lf",&dtow);
printf("Enter the initial value of temperature\n");
scanf("%Lf",&T0);
printf("Enter the final value of temperature\n");
printf(" (i.e. Constant wall temperature) [600,750,900]\n");
scanf("%Lf",&Tf);
/*printf("\n There are following cases:\n");
printf("\n");
printf("(1) Convection and radiation on wall surface\n");
printf("For this case, put ht=8.4 & ab=0.95\n");
printf("(2) No convection on wall surface (Radiation only)\n");
printf("For this case, put ht=0 & ab=0.95\n");
printf("(3) No radiation on wall surface (Convection only)\n");
printf("For this case, put ht=8.4 & ab=0\n");
printf("(4) No radiation on wall surface (10 Times Convection)\n");
printf("For this case, put ht=84.0 & ab=0\n");
printf("\n");
printf("Read the above cases and then press enter key to continue\n");
getch();
getch();
printf("\nNow enter the value according to the above cases\n");
printf("\n");*/
printf("Enter the value of convective heat transfer coefficient (ht=8.4)\n");
printf("ht=");
scanf("%Lf",&ht);
printf("Enter the value of emissivity coefficient (ab=0.95)\n");
printf("ab=");
scanf("%Lf",&ab);

/* Initial condition */
for(i=0;i<=M;i++)
{
CB[i]=1.0;
Cc1[i]=0.0;
CG1[i]=0.0;
Cc2[i]=0.0;
CG2[i]=0.0;
/*T[i]=473.0;*/
t[i]=h;
theta[i]=1.0;
}
for(i=0;i<=M;i++)
{
T[i]=T0;
}
/*printf("%0.6Lf\n",T[1]);
```

```
getch();*/
/*for(i=0;i<=M;i++)
{
printf("%0.6Lf\n",T[i]);
getch();
}*/

/*Program of finite difference method based on pure implicit scheme*/
while(1)
{
/*printf("%0.6Lf\n",R);
getch();
printf("%0.6Lf %0.6Lf\n",Tf,R);
getch();*/
k[M]=0.13+0.0003*(T[M]-273.0);
jj=pow(T[M],3.0);
kk=pow(T[M],2.0)*Tf;
ll=pow(Tf,2.0)*T[M];
mm=pow(Tf,3.0);
bb=(5.67*pow(10.0,-8.0))*(ab);
aa=ht+(bb*(jj+kk+ll+mm));
/*printf("%0.6Lf %0.6Lf %0.6Lf %0.6Lf  %0.6Lf %0.16Lf",jj,kk,ll,mm,aa,bb);
getch();*/
H[M]=(R/k[M])*(aa);
ft=(tow*pow(R,2.0))/(alpha);
/*printf("The value of k[M],H[M],ft\n");
printf("\n%0.6Lf %0.6Lf %0.6Lf",k[M],H[M],ft);
getch();
getch();
printf("\n%0.6Lf %0.6Lf %d %0.6Lf",Tf,R,M,T[0]);
getch();*/
for(i=0;i<=M;i++)
{
cp[i]=1112.0+4.85*(T[i]-273.0);
ro[i]=roin*(CB[i]+Cc1[i]+Cc2[i]);
Q[i]=((-dH)+(cp[i]*T[i]))/(ro[i]*cp[i]*(Tf-T0));
k1[i]=A1*exp((D1/T[i])+(L1/(T[i]*T[i])));
}
/*for(i=0;i<=M;i++)
{
printf("\n%0.6Lf %0.6Lf %0.6Lf %0.10Lf",cp[i],ro[i],Q[i],k1[i]);
getch();
}*/
for(i=1;i<=M-1;i++)
{
a[i]=((dtow)/(2.0*dx*x[i]))-((dtow)/(dx*dx));
```

```
x[i+1]=x[i]+dx;
}
/*for(i=1;i<=M-1;i++)
{
printf("%0.6Lf\n",a[i]);
getch();
}*/
b[0]=(((4.0*dtow)/(dx*dx))+(1.0));
for(i=1;i<=M-1;i++)
{
b[i]=((2.0*dtow)/(dx*dx)+1.0);
}
/*for(i=0;i<=M-1;i++)
{
printf("%0.6Lf\n",b[i]);
getch();
}*/
c[0]=(-4.0*dtow)/(dx*dx);
for(i=1;i<=M-2;i++)
{
c[i]=(((-dtow)/(2.0*dx*x[i]))-((dtow)/(dx*dx)));
x[i+1]=x[i]+dx;
}
/*for(i=0;i<=M-2;i++)
{
printf("%0.6Lf\n",c[i]);
getch();
}*/
for(i=0;i<=M-1;i++)
{
d[i]=(theta[i])+((dtow*Q[i]*R*R*k1[i]*pow(CB[i],n1))/(alpha));
}
/*for(i=0;i<=M-1;i++)
{
printf("%0.9Lf\n",d[i]);
getch();
}*/
beta[0]=b[0];
for(i=1;i<=M-1;i++)
{
beta[i]=b[i]-(a[i]*c[i-1])/(beta[i-1]);
}
/*for(i=0;i<=M-1;i++)
{
printf("%0.6Lf\n",beta[i]);
getch();
```

```
}*/
gamma[0]=d[0]/beta[0];
for(i=1;i<=M-1;i++)
{
gamma[i]=(d[i]-a[i]*gamma[i-1])/(beta[i]);
}

/*for(i=0;i<=M-1;i++)
{
printf("%0.6Lf\n",gamma[i]);
getch();
}*/
theta[M-1]=gamma[M-1];
i=M-1;
for(j=1;j<=M-1;j++)
{
theta[M-1-j]=(gamma[M-1-j])-((c[M-1-j]*theta[i])/(beta[M-1-j]));
i=i-1;
}
theta[M]=0.0;
/*for(i=0;i<=M;i++)
{
printf("%0.6Lf\n",theta[i]);
getch();
}*/
for(i=0;i<=M;i++)
{
T[i]=Tf-theta[i]*(Tf-T0);
}
/*printf("T\n");
for(i=0;i<=M;i++)
{ printf("%0.6Lf\n",T[i]);
getch(); }*/

/* Runge-Kutta method starts here */      CG1      Cc1      CG2      Cc2");*/
/*printf("\neqn        t        T        CB
for(i=0;i<=M;i++)
{
while(1)
{
k1[i]=A1*exp((D1/T[i])+(L1/(T[i]*T[i])));
k2[i]=A2*exp((D2/T[i])+(L2/(T[i]*T[i])));
k3[i]=A3*exp(-E3/(Rc*T[i]));
a1=(-h)*((k1[i]+k2[i])*pow(CB[i],n1));
b1=h*((k1[i]*pow(CB[i],n1))-(k3[i]*pow(CG1[i],n2)*pow(Cc1[i],n3)));
c1=h*((k2[i]*pow(CB[i],n1))-(k3[i]*pow(CG1[i],n2)*pow(Cc1[i],n3)));
```

```
d1=h*(k3[i]*pow(CG1[i],n2)*pow(Cc1[i],n3));
e1=h*(k3[i]*pow(CG1[i],n2)*pow(Cc1[i],n3));
a2=(-h)*((k1[i]+k2[i])*pow((CB[i]+(a1/2.0)),n1));
b2=h*((k1[i]*pow((CB[i]+(a1/2.0)),n1))-
(k3[i]*pow((CG1[i]+(b1/2.0)),n2)*pow((Cc1[i]+(c1/2.0)),n3)));
c2=h*((k2[i]*pow((CB[i]+(a1/2.0)),n1))-
(k3[i]*pow((CG1[i]+(b1/2.0)),n2)*pow((Cc1[i]+(c1/2.0)),n3)));
d2=h*(k3[i]*pow((CG1[i]+(b1/2.0)),n2)*pow((Cc1[i]+(c1/2.0)),n3));
e2=h*(k3[i]*pow((CG1[i]+(b1/2.0)),n2)*pow((Cc1[i]+(c1/2.0)),n3));
a3=(-h)*((k1[i]+k2[i])*pow((CB[i]+(a2/2.0)),n1));
b3=h*((k1[i]*pow((CB[i]+(a2/2.0)),n1))-
(k3[i]*pow((CG1[i]+(b2/2.0)),n2)*pow((Cc1[i]+(c2/2.0)),n3)));
c3=h*((k2[i]*pow((CB[i]+(a2/2.0)),n1))-
(k3[i]*pow((CG1[i]+(b2/2.0)),n2)*pow((Cc1[i]+(c2/2.0)),n3)));
d3=h*(k3[i]*pow((CG1[i]+(b2/2.0)),n2)*pow((Cc1[i]+(c2/2.0)),n3));
e3=h*(k3[i]*pow((CG1[i]+(b2/2.0)),n2)*pow((Cc1[i]+(c2/2.0)),n3));
a4=(-h)*((k1[i]+k2[i])*pow((CB[i]+a3),n1));
b4=h*((k1[i]*pow((CB[i]+a3),n1))-(k3[i]*pow((CG1[i]+b3),n2)*pow((Cc1[i]+c3),n3)));
c4=h*((k2[i]*pow((CB[i]+a3),n1))-(k3[i]*pow((CG1[i]+b3),n2)*pow((Cc1[i]+c3),n3)));
d4=h*(k3[i]*pow((CG1[i]+b3),n2)*pow((Cc1[i]+c3),n3));
e4=h*(k3[i]*pow((CG1[i]+b3),n2)*pow((Cc1[i]+c3),n3));
CB[i]=CB[i]+(1.0/6.0)*(a1+2.0*a2+2.0*a3+a4);
CG1[i]=CG1[i]+(1.0/6.0)*(b1+2.0*b2+2.0*b3+b4);
Cc1[i]=Cc1[i]+(1.0/6.0)*(c1+2.0*c2+2.0*c3+c4);
CG2[i]=CG2[i]+(1.0/6.0)*(d1+2.0*d2+2.0*d3+d4);
Cc2[i]=Cc2[i]+(1.0/6.0)*(e1+2.0*e2+2.0*e3+e4);
if(CB[i]<0.0)
CB[i]=0.0000001;
if(t[i]>=(ft-h))
break;
t[i]=t[i]+h;
}
}

/* Output */
/*for(i=0;i<=M;i++)
{
printf("\n%d      \t%0.6Lf      %0.6Lf      %0.6Lf      %0.6Lf      %0.6Lf
%0.6Lf",eqn[i],t[i],T[i],CB[i],CG1[i],Cc1[i],CG2[i],Cc2[i]);
getch();
} */
printf("\neqn    xx    t      T      CB      CG1     Cc1     CG2     Cc2  ");
xx=0.0;
for(i=0;i<=M;i=i+15)
{
```

```
printf("\n%d    \t%0.1Lf    %0.6Lf  %0.6Lf  %0.6Lf  %0.6Lf  %0.6Lf  %0.6Lf
%0.6Lf",eqn[i],xx,t[i],T[i
],CB[i],CG1[i],Cc1[i],CG2[i],Cc2[i]);
/*getch();*/
xx=xx+0.1;
}
getch();
tow=tow+dtow;
if(CB[M]<=0.00000001)
if(CB[0]<=0.00000001)
break;
}
}
```

B-4 Program for heat transfer model by using finite difference pure implicit scheme and Runge-Kutta fourth order method (Model-III program)

```
/* Program for Chapter 4 */
/* Modeling for pyrolysis of solid particle: kinetics and heat transfer effects. */
/* This is the program when wall temperature is varying */
#include<stdio.h>
#include<math.h>
#define M 150                    /* (M+1)=Total number of equations to be solved */
main()
{
long double T[M+2];              /* T=Temperature (K) */
long double CB[M+2];             /* CB=Concentration of biomass (kg/m3) */
long double k1[M+2];             /* k1=Rate constant for reaction 1 (1/s) */
long double k2[M+2];             /* k2=Rate constant for reaction 2 (1/s) */
long double k3[M+2];             /* k3=Rate constant for reaction 3 (1/s) */
int i;                           /* i=integer used in program */
int j;                           /* j=integer used in program */
int eqn[M+2];                    /* xx=used for output of dimensionles distance (-) */
long double xx;                  /* R=radius of cylindrical pellet (m) */
long double R;                   /* A1=Arrhenius frequency factor for reaction 1 (1/s) */
long double A1;                  /* A2=Arrhenius frequency factor for reaction 2 (1/s) */
long double A2;                  /* A3=Arrhenius frequency factor for reaction 3 (1/s) */
long double A3;                  /* D1=Constant used while calculating k1 (K) */
long double D1;                  /* D2=Constant used while calculating k2 (K) */
long double D2;                  /* L1=Constant used while calculating k1 (K2) */
long double L1;                  /* L2=Constant used while calculating k2 (K2) */
long double L2;                  /* E3=Activation energy (J/gmol) */
long double E3;                  /* Rc=Universal gas constant (J/gmol K)*/
long double Rc;                  /* Cc1=Concentration of char 1 (-) */
long double Cc1[M+2];
```

```
long double CG1[M+2];      /* CG1=Concentration of volatile 1 (-) */
long double Cc2[M+2];      /* Cc2=Concentration of char 2 (-) */
long double CG2[M+2];      /* CG2=Concentration of volatile 2 (-) */
long double t[M+2];        /* t=Time (s) */
long double n1;            /* n1=Order of reaction 1 (-) */
long double n2;            /* n2=Order of reaction 2 (-) */
long double n3;            /* n3=Order of reaction 3 (-) */
long double h;             /* h=step size for RK4 Method (s) */
long double a1;
long double b1;
long double c1;
long double d1;
long double e1;
long double a2;
long double b2;
long double c2;
long double d2;
long double c2;            /*a1-e4=Variables used while solving rk4 method */
long double a3;
long double b3;
long double c3;
long double d3;
long double e3;
long double a4;
long double b4;
long double c4;
long double d4;
long double e4;
long double dtow;          /* dtow=Dimensionless time step for finite difference
                           method (-) */
                           /* tow = Dimensionless time for finite difference method */
long double tow;
long double dx;            /*  dx=Dimensionless radial distance step for finite
                           difference method (-) */
                           /* T0=Initial temperature (K) */
long double T0;
long double Tf;            /* Tf=Final temperature (K) */
long double ht;            /* ht=convective heat transfer coefficient (W/m2K) */
long double ab;            /* ab=emissivity coefficient */
/*long double sig;*/       /* sig=Stefan Boltzman constant */
long double dH;            /* dH=heat of reaction (kJ/kg) */
long double k[M+2];        /* k=thermal conductivity (W/m K) */
long double H[M+2];        /* H=modified Biot Number */
long double cp[M+2];       /* cp=specific heat (J/kg K) */
long double ro[M+2];       /* ro=density (kg/m3) */
long double Q[M+2];        /* Q=heat of reaction number (m3/kg) */
long double x[M+2];        /* x=Dimensionless radial distance (-) */
long double a[M+2];
```

```
long double b[M+2];          /* a-d=Variables used in assigning values in tridiagonal
                             matrix */
long double c[M+2];
long double d[M+2];
long double theta[M+2];      /* theta=Dimensionless temperature (-) */
long double beta[M+2];       /* beta=used while calculating theta (-) */
long double gamma[M+2];      /* gamma=used while calculating theta (-) */
long double alpha;           /* alpha=used while calculating theta (-) */
long double ft;              /* ft=conversion of dimensionless time second (s) */
long double roin;            /* roin=initial value of density (kg/m3) */
long double jj;
long double kk;              /* jj-bb=Variable used while calculating the value of H */
long double ll;
long double aa;
long double mm;
long double bb;
long double Hc[M+2];
long double kc[M+2];
long double Tc[M+2];
long double Qc[M+2];
long double cpc[M+2];
long double bc[M+2];         /* From Hc-bbc the 'c' is used for char */
long double dc[M+2];
long double thetac[M+2];
long double betac[M+2];
long double gammac[M+2];
long double jjc;
long double kkc;
long double llc;
long double aac;
long double mmc;
long double bbc;             /* To find the sum of biomass at a particular time */
long double sum[M+2];        /* To find the average of biomass at a particular time */
long double avg[M+2];        /* To find the conversion of biomass*/
long double conversion[M+2]; /* bf=geometry factor(slab=1;cylinder=2;sphere=3)
long double bf;
/*long double ss1[M+2];
long double ss2[M+2];
long double ss3[M+2];
long double ss4[M+2];*/

/*Constants*/
/*R=0.005;*/
A1=9.973*pow(10.0,-5.0);
A2=1.068*pow(10.0,-3.0);
A3=5.7*pow(10.0,5.0);
```

```
D1=17254.4;
D2=10224.4;
L1=-9061227.0;
L2=-6123081.0;
E3=81000.0;
Rc=8.314;
dx=(1.0/M);
x[1]=(1.0/M);
/*ht=8.4;
ab=0.95;*/
/*sig=5.67*pow(10.0,-8.0);*/
roin=650.0;
dH=-255000.0;
alpha=1.79*pow(10.0,-7.0);
sum[0]=0.0;
/*n1=0.0;
n2=1.5;
n3=1.5;
h=0.01;
tow=0.010024;
dtow=0.010024;
T0=473.0;
Tf=873.0;*/
eqn[0]=1;
for(i=0;i<=M;i++)
{
eqn[i+1]=eqn[i]+1;
}
/*printf("%d",eqn[M]);
getchar();*/
/*printf("%Lf %Lf\n",dx,x[1]);
getchar();*/

/* Input */
printf("Enter the orders of reactions n1,n2,n3 (0,1.5,1.5)\n");
scanf("%Lf %Lf %Lf",&n1,&n2,&n3);
printf("Enter the value of time step h(t) for RK4 method (0.01)\n");
scanf("%Lf",&h);
printf("Enter the value of geometry factor i.e.bf(slab=1;cylinder=2;sphere=3)\n");
scanf("%Lf",&bf);
printf("Enter the value R (Half the thickness of slab,radius for cylinder & sphere)\n");
scanf("%Lf",&R);
printf("The value of tow can be calculated by the following formula:\n");
printf("t=(tow*R*R)/(alpha)\n");
printf("Here alpha is known i.e. alpha=1.79*pow(10.0,-7.0)\n");
printf("Suppose you want that your output come after every 1sec\n");
```

```
printf("Then t=1sec and say R=0.005m,then tow comes out to be 0.00716\n");
printf("Enter the initial value of time step i.e.tow (dimensionless) for\n");
printf("finite difference method \n");
scanf("%Lf",&tow);
printf("Enter the value of dtow(Its value is same as initial value of tow)\n");
scanf("%Lf",&dtow);
printf("Enter the initial value of temperature\n");
scanf("%Lf",&T0);
printf("Enter the final value of temperature\n");
scanf("%Lf",&Tf);
printf("\n There are following cases:\n");
printf("\n");
printf("(1) Convection and radiation on wall surface\n");
printf("For this case, put ht=8.4 & ab=0.95\n");
printf("(2) No convection on wall surface (Radiation only)\n");
printf("For this case, put ht=0 & ab=0.95\n");
printf("(3) No radiation on wall surface (Convection only)\n");
printf("For this case, put ht=8.4 & ab=0\n");
printf("(4) No radiation on wall surface (10 Times Convection)\n");
printf("For this case, put ht=84.0 & ab=0\n");
printf("\n");
printf("Read the above cases and then press enter key to continue\n");
getchar();
printf("\nNow enter the value according to the above cases\n");
printf("\n");
printf("Enter the value of convective heat transfer coefficient (ht=8.4)\n");
printf("ht=");
scanf("%Lf",&ht);
printf("Enter the value of emissivity coefficient (ab=0.95)\n");
printf("ab=");
scanf("%Lf",&ab);

/* Initial condition */
for(i=0;i<=M;i++)
{
CB[i]=1.0;
Cc1[i]=0.0;
CG1[i]=0.0;
Cc2[i]=0.0;
CG2[i]=0.0;
/*T[i]=473.0;*/
t[i]=h;
theta[i]=1.0;
thetac[i]=1.0;
}
for(i=0;i<=M;i++)
```

```
{
T[i]=T0;
}
for(i=0;i<=M;i++)
{
Tc[i]=T0;
}
/*printf("%0.6Lf\n",T[1]);
getchar();*/
/*for(i=0;i<=M;i++)
{
printf("%0.6Lf\n",T[i]);
getchar();
}*/

/*Program of finite difference method based on pure implicit scheme*/
while(1)
{
/*printf("%0.6Lf\n",R);
getchar();
printf("%0.6Lf %0.6Lf\n",Tf,R);
getchar();*/
for(i=0;i<=M;i++)
{
sum[i+1]=sum[i]+CB[i];
}
avg[1]=sum[M+1]/(M+1);
conversion[1]=(1.0-avg[1])/(1.0);
/*printf("%Lf %Lf %Lf\n",sum[M+1],avg[1],conversion[1]);
getchar();*/
k[M]=0.13+0.0003*(T[M]-273.0);
jj=pow(T[M],3.0);
kk=pow(T[M],2.0)*Tf;
ll=pow(Tf,2.0)*T[M];
mm=pow(Tf,3.0);
bb=(5.67*pow(10.0,-8.0))*(ab);
aa=ht+(bb*(jj+kk+ll+mm));
H[M]=(R/k[M])*(aa);
/*printf("%0.6Lf %0.6Lf %0.6Lf %0.6Lf  %0.6Lf %0.16Lf",jj,kk,ll,mm,aa,bb);
getchar();*/
kc[M]=0.08-0.0001*(Tc[M]-273.0);
jjc=pow(Tc[M],3.0);
kkc=pow(Tc[M],2.0)*Tf;
llc=pow(Tf,2.0)*Tc[M];
mmc=pow(Tf,3.0);
bbc=(5.67*pow(10.0,-8.0))*(ab);
```

```
aac=ht+(bbc*(jjc+kkc+llc+mmc));
Hc[M]=(R/kc[M])*(aac);
ft=(tow*pow(R,2.0))/(alpha);
/*printf("The value of k[M],H[M],ft\n");
printf("\n%0.6Lf %0.6Lf %0.6Lf",k[M],H[M],ft);
getchar();
getchar();
printf("\n%0.6Lf %0.6Lf %d %0.6Lf",Tf,R,M,T[0]);
getchar();*/
for(i=0;i<=M;i++)
{
cp[i]=1112.0+4.85*(T[i]-273.0);
ro[i]=roin*(CB[i]+Cc1[i]+Cc2[i]);
Q[i]=((-dH)+(cp[i]*T[i]))/(ro[i]*cp[i]*(T0-Tf));
k1[i]=A1*exp((D1/T[i])+(L1/(T[i]*T[i])));
}
/*for(i=0;i<=M;i++)
{
printf("\n%0.6Lf %0.6Lf %0.6Lf %0.10Lf",cp[i],ro[i],Q[i],k1[i]);
getchar();
}*/
for(i=0;i<=M;i++)
{
cpc[i]=1003.2+2.09*(Tc[i]-273.0);
Qc[i]=((-dH)+(cpc[i]*Tc[i]))/(ro[i]*cpc[i]*(T0-Tf));
}
for(i=1;i<=M-1;i++)
{
a[i]=(((bf-1.0)*(dtow))/(2.0*dx*x[i]))-((dtow)/(dx*dx));
x[i+1]=x[i]+dx;
}
a[M]=((-2.0*dtow)/(dx*dx));
/*for(i=1;i<=M;i++)
{
printf("%0.6Lf\n",a[i]);
getchar();
}*/
b[0]=(((2.0*bf*dtow)/(dx*dx))+(1.0));
for(i=1;i<=M-1;i++)
{
b[i]=((2.0*dtow)/(dx*dx)+1.0);
}
b[M]=(((2.0*dtow)/(dx*dx))+(1.0)+((2.0*dtow*H[M])/(dx))+((bf-1.0)*dtow*H[M]));
/*for(i=0;i<=M;i++)
{
printf("%0.6Lf\n",b[i]);
```

```
getchar();
}*/
bc[0]=(((2.0*bf*dtow)/(dx*dx))+(1.0));
for(i=1;i<=M-1;i++)
{
bc[i]=((2.0*dtow)/(dx*dx)+1.0);
}
bc[M]=(((2.0*dtow)/(dx*dx))+(1.0)+((2.0*dtow*Hc[M])/(dx))+((bf-1.0)*dtow*Hc[M]));
c[0]=(-2.0*bf*dtow)/(dx*dx);
for(i=1;i<=M-1;i++)
{
c[i]=((((bf-1.0)*(-dtow))/(2.0*dx*x[i]))-((dtow)/(dx*dx)));
x[i+1]=x[i]+dx;
}
/*for(i=0;i<=M-1;i++)
{
printf("%0.6Lf\n",c[i]);
getchar();
}*/
for(i=0;i<=M;i++)
{
d[i]=(theta[i])+((dtow*Q[i]*R*R*k1[i]*pow((roin*CB[i]),n1))/(alpha));
}
/*for(i=0;i<=M;i++)
{
printf("%0.9Lf\n",d[i]);
getchar();
}*/
for(i=0;i<=M;i++)
{
dc[i]=(thetac[i])+((dtow*Qc[i]*R*R*k1[i]*pow((roin*CB[i]),n1))/(alpha));
}
beta[0]=b[0];
for(i=1;i<=M;i++)
{
beta[i]=b[i]-(a[i]*c[i-1])/(beta[i-1]);
}
/*for(i=0;i<=M;i++)
{
printf("%0.6Lf\n",beta[i]);
getchar();
}*/
betac[0]=bc[0];
for(i=1;i<=M;i++)
{
betac[i]=bc[i]-(a[i]*c[i-1])/(betac[i-1]);
```

```
}
gamma[0]=d[0]/beta[0];
for(i=1;i<=M;i++)
{
gamma[i]=(d[i]-a[i]*gamma[i-1])/(beta[i]);
}
/*for(i=0;i<=M;i++)
{
printf("%0.6Lf\n",gamma[i]);
getchar();
}*/
gammac[0]=dc[0]/betac[0];
for(i=1;i<=M;i++)
{
gammac[i]=(dc[i]-a[i]*gammac[i-1])/(betac[i]);
}
theta[M]=gamma[M];
i=M;
for(j=1;j<=M;j++)
{
theta[M-j]=(gamma[M-j])-((c[M-j]*theta[i])/(beta[M-j]));
i=i-1;
}
/*for(i=0;i<=M;i++)
{
printf("%0.6Lf\n",theta[i]);
getchar();
}*/
thetac[M]=gammac[M];
i=M;
for(j=1;j<=M;j++)
{
thetac[M-j]=(gammac[M-j])-((c[M-j]*thetac[i])/(betac[M-j]));
i=i-1;
}
for(i=0;i<=M;i++)
{
T[i]=Tf-theta[i]*(Tf-T0);
}
/*printf("T\n");
for(i=0;i<=M;i++){
printf("%0.6Lf\n",T[i]);
getchar(); }*/
for(i=0;i<=M;i++)
{
Tc[i]=Tf-thetac[i]*(Tf-T0);
```

```
}

/* Runge-Kutta method starts here */
/*printf("\neqn        t       T       CB      CG1     Cc1     CG2     Cc2");*/
for(i=0;i<=M;i++)
{
while(1)
{
k1[i]=A1*exp((D1/T[i])+(L1/(T[i]*T[i])));
k2[i]=A2*exp((D2/Tc[i])+(L2/(Tc[i]*Tc[i])));
k3[i]=A3*exp(-E3/(Rc*Tc[i]));
a1=(-h)*((k1[i]+k2[i])*pow(CB[i],n1));
b1=h*((k1[i]*pow(CB[i],n1))-(k3[i]*pow(CG1[i],n2)*pow(Cc1[i],n3)));
c1=h*((k2[i]*pow(CB[i],n1))-(k3[i]*pow(CG1[i],n2)*pow(Cc1[i],n3)));
d1=h*(k3[i]*pow(CG1[i],n2)*pow(Cc1[i],n3));
e1=h*(k3[i]*pow(CG1[i],n2)*pow(Cc1[i],n3));
a2=(-h)*((k1[i]+k2[i])*pow((CB[i]+(a1/2.0)),n1));
b2=h*((k1[i]*pow((CB[i]+(a1/2.0)),n1))-
(k3[i]*pow((CG1[i]+(b1/2.0)),n2)*pow((Cc1[i]+(c1/2.0)),n3)));
c2=h*((k2[i]*pow((CB[i]+(a1/2.0)),n1))-
(k3[i]*pow((CG1[i]+(b1/2.0)),n2)*pow((Cc1[i]+(c1/2.0)),n3)));
d2=h*(k3[i]*pow((CG1[i]+(b1/2.0)),n2)*pow((Cc1[i]+(c1/2.0)),n3));
e2=h*(k3[i]*pow((CG1[i]+(b1/2.0)),n2)*pow((Cc1[i]+(c1/2.0)),n3));
a3=(-h)*((k1[i]+k2[i])*pow((CB[i]+(a2/2.0)),n1));
b3=h*((k1[i]*pow((CB[i]+(a2/2.0)),n1))-
(k3[i]*pow((CG1[i]+(b2/2.0)),n2)*pow((Cc1[i]+(c2/2.0)),n3)));
c3=h*((k2[i]*pow((CB[i]+(a2/2.0)),n1))-
(k3[i]*pow((CG1[i]+(b2/2.0)),n2)*pow((Cc1[i]+(c2/2.0)),n3)));
d3=h*(k3[i]*pow((CG1[i]+(b2/2.0)),n2)*pow((Cc1[i]+(c2/2.0)),n3));
e3=h*(k3[i]*pow((CG1[i]+(b2/2.0)),n2)*pow((Cc1[i]+(c2/2.0)),n3));
a4=(-h)*((k1[i]+k2[i])*pow((CB[i]+a3),n1));
b4=h*((k1[i]*pow((CB[i]+a3),n1))-(k3[i]*pow((CG1[i]+b3),n2)*pow((Cc1[i]+c3),n3)));
c4=h*((k2[i]*pow((CB[i]+a3),n1))-(k3[i]*pow((CG1[i]+b3),n2)*pow((Cc1[i]+c3),n3)));
d4=h*(k3[i]*pow((CG1[i]+b3),n2)*pow((Cc1[i]+c3),n3));
e4=h*(k3[i]*pow((CG1[i]+b3),n2)*pow((Cc1[i]+c3),n3));
CB[i]=CB[i]+(1.0/6.0)*(a1+2.0*a2+2.0*a3+a4);
CG1[i]=CG1[i]+(1.0/6.0)*(b1+2.0*b2+2.0*b3+b4);
Cc1[i]=Cc1[i]+(1.0/6.0)*(c1+2.0*c2+2.0*c3+c4);
CG2[i]=CG2[i]+(1.0/6.0)*(d1+2.0*d2+2.0*d3+d4);
Cc2[i]=Cc2[i]+(1.0/6.0)*(e1+2.0*e2+2.0*e3+e4);
if(CB[i]<0.0)
{
CB[i]=0.0000001;
/*ss1[i]=CG1[i];
ss2[i]=Cc1[i];
ss3[i]=CG2[i];
```

```
ss4[i]=Cc2[i];*/
}
if(CG1[i]<0.0)
{
CG1[i]=0.0000001;
}
if(Cc1[i]<0.0)
{
Cc1[i]=0.0000001;
}
if(CG2[i]<0.0)
{
CG2[i]=0.0000001;
}
if(Cc2[i]<0.0)
{
Cc2[i]=0.0000001;
}
if(t[i]>=(ft-h))
break;
t[i]=t[i]+h;
}
}

/* Output */
/*for(i=0;i<=M;i++)
{
printf("\n%d      \t%0.6Lf      %0.6Lf      %0.6Lf      %0.6Lf      %0.6Lf
%0.6Lf",eqn[i],t[i],T[i],CB[i],CG1[i],Cc1[i],CG2[i],Cc2[i]);
getchar();
}*/
printf("\neqn    xx    t      T      CB      CG1     Cc1     CG2     Cc2  ");
xx=0.0;
for(i=0;i<=M;i=i+15)
{
/*CG1[i]=ss1[i];
Cc1[i]=ss2[i];
CG2[i]=ss3[i];
Cc2[i]=ss4[i];*/                %0.6Lf  %0.6Lf  %0.6Lf  %0.6Lf  %0.6Lf  %0.6Lf
printf("\n%d      \t%0.1Lf
%0.6Lf",eqn[i],xx,t[i],T[i
],CB[i],CG1[i],Cc1[i],CG2[i],Cc2[i]);
/*getchar();*/
xx=xx+0.1;
}
printf("\nConversion=");
```

```
printf("%Lf",conversion[1]);
printf("\nAverage value of CB=");
printf("%Lf",avg[1]);
/*for(i=0;i<=M;i++)
{
if(CB[i]<0.0)
CB[i]=0.0000001;
}*/
getchar();
tow=tow+dtow;
if(CB[M]<=0.0000000)
if(CB[0]<=0.0000000)
break;}}
```

APPENDIX-C

C-1 Dimensionless groups

$$\alpha = k/\rho C_p \tag{C.1}$$

$$x = r/R \tag{C.2}$$

$$\tau = \alpha t/R^2 \tag{C.3}$$

$$\theta = (T - T_f)/(T_0 - T_f) \tag{C.4}$$

$$Bi_M = (R/k)\left[h + \varepsilon\sigma\left(T^3 + T^2T_f + T_f^2T + T_f^3\right)\right] \tag{C.5}$$

$$H = (R/k_{eff})\left[h + \varepsilon\sigma\left(T^3 + T^2T_f + T_f^2T + T_f^3\right)\right] \tag{C.6}$$

$$Bi = hR/k_{eff} \tag{C.7}$$

$$Q = \left(-\Delta H + C_pT\right)/\left(\rho C_p(T_0 - T_f)\right) \tag{C.8}$$

$$Q'' = QC_B^{n_1} \tag{C.9}$$

$$\overline{C}_B = C_B/C_{B0} \tag{C.10}$$

$$\overline{C}_{B0} = C_{B0}/\rho_0 \tag{C.11}$$

$$\overline{C}_{G1} = C_{G1}/C_{B0} \tag{C.12}$$

$$\overline{C}_{G10} = C_{G10}/C_{B0} \tag{C.13}$$

$$\overline{C}_{C1} = C_{C1}/C_{B0} \tag{C.14}$$

$$\overline{C}_{G2} = C_{G2}/C_{B0} \tag{C.15}$$

$$\overline{C}_{C2} = C_{C2}/C_{B0} \tag{C.16}$$

$$\overline{C}_{pG1} = C_{pG1}/C_{pG10} \tag{C.17}$$

$$\overline{D}_{eG1} = D_{eG1}/D_{eG10} \tag{C.18}$$

$$Le = (k)/(\rho_0 C_{pG10} D_{eG10}) \tag{C.19}$$

$$Sh = (k_{mG1}R)/D_{eG10} \tag{C.20}$$

C-2 Values and correlations used in the numerical solution of the model

Property	Correlation/value	Source
Convective heat transfer coefficient	$h = 8.4$ W m^{-2} K^{-1}	Pyle & Zaror (1984)
Wood specific heat capacity	$C_p = 1112.0 + 4.85(T - 273)$ (J kg^{-1} K^{-1})	Koufopanos *et al.* (1991)
Char specific heat capacity	$C_p = 1003.2 + 2.09(T - 273)$ (J kg^{-1} K^{-1})	Koufopanos *et al.* (1991)
Effective thermal conductivity	$k_{eff} = \eta k_B + (1-\eta)k_C + \varepsilon'' k_g + 13.5\sigma T^3 d/\varepsilon$ (W m^{-1} K^{-1})	Chan *et al.* (1985)
Wood thermal conductivity	$k_B = 0.13 + 0.0003(T - 273)$ (W m^{-1} K^{-1})	Koufopanos *et al.* (1991)
Char thermal conductivity	$k_C = 0.08 - 0.0001(T - 273)$ (W m^{-1} K^{-1})	Koufopanos *et al.* (1991)
Gas thermal conductivity	$k_g = 25.77 \times 10^{-3}$ (W m^{-1} K^{-1})	Di Blasi (1993b)
Pore diameter	$d = 2 \times 10^{-5}$ (m)	Di Blasi (1996a)
Emissivity coefficient	$\varepsilon = 0.95$	Pyle & Zaror (1984)
Rate constant of reaction 1	$k_1 = A_1 \exp[(D_1/T) + (L_1/T^2)]$ (s^{-1}); where, $A_1 = 9.973 \times 10^{-5}$ s^{-1}; $D_1 = 17254.4$ K; $L_1 = -9061227$ K^2	Koufopanos *et al.* (1991)
Rate constant of reaction 2	$k_2 = A_2 \exp[(D_2/T) + (L_2/T^2)]$ (s^{-1}); where, $A_2 = 1.068 \times 10^{-3}$ s^{-1}; $D_2 = 10224.4$ K; $L_2 = -6123081$ K^2	Koufopanos *et al.* (1991)
Rate constant of reaction 3	$k_3 = A_3 \exp[(-E_3/R_c T)]$ (s^{-1}); where, $A_3 = 5.7 \times 10^5$ s^{-1}; $E_3 = 81000$ J mol^{-1}	Koufopanos *et al.* (1991)
Heat capacity of (gases & volatiles)$_1$	$\overline{C}_{pG1} = 1 + P_1(\theta - 1)$; $P_1 = 0.001$	Fan *et al.* (1977)
Effective diffusivity of (gases & volatiles)$_1$	$\overline{D}_{G1} = (\theta)^{P_1} \exp\{P_2(1 - \overline{C}_B)\}$ $P_1 = 1.5, P_2 = 1.0$	Fan *et al.* (1977)
Sherwood number	$Sh = P_1(\theta)^{P_2}$; $P_1 = 50000, P_2 = 0.75$	Koufopanos *et al.* (1991)
Heat of reaction	$\Delta H = -255000$ J kg^{-1}	Koufopanos *et al.* (1991)
Initial density of wood	$\rho_0 = 650$ kg m^{-3}	Jalan & Srivastava (1999)
Initial thermal diffusivity of wood	$\alpha = 1.79 \times 10^{-7}$ m^2 s^{-1}	Fan *et al.* (1977)
Lewis number	$Le = 2.0$	

Initial void fraction of particle	ε_0"= 0.5	Fan *et al.* (1977)
Constant defined by equation of ε"	$\gamma = 0.3$	Fan *et al.* (1977)
Molecular weight of water vapor	$W_v = 18\times10^{-3}$ kg/mol	Hagge & Bryden (2002)
Molecular weight of light hydrocarbons	$W_L = 28\times10^{-3}$ kg/mol	Hagge & Bryden (2002)
Molecular weight of wood	$W_B = 110\times10^{-3}$ kg/mol	Hagge & Bryden (2002)
Viscosity	$\mu = 3\times10^{-5}$ kg/m s	Di Blasi (1998)
Permeability of wood	$\phi_B = 1\times10^{-14}$ m^2	Di Blasi (1998)
Permeability of char	$\phi_{C1} = 5\times10^{-11}$ m^2	Di Blasi (1998)

C-3 Nominal values of parameters employed in the present study

Parameters	Values
Geometry factor (slab, cylinder, & sphere)	b =1, b =2 & b =3
Initial concentration of B	C_{B0}=650 kg/m^3
Order of reaction 1	n_1=0 or n_1=1
Order of reaction 2	n_2=1.5
Order of reaction 3	n_3=1.5
Shrinkage factor	α '=0.2
Shrinkage factor	β '=0
Shrinkage factor	γ '=0.2
Particle radius	R =0.0000125-0.05 m
Initial temperature	T_0=303 K
Final temperature	T_f=303-2800 K
Initial effective solid volume	$V_{S0} = 0.5V_{B0}$
Emissivity coefficient	ε =0.95, dimensionless
Stefan Boltzmann constant	σ=5.67×10^{-8} W m^{-2} K^{-4}

APPENDIX-D

D-1 Program for generalized reference model (Model-I)

```
/* Program for Chapter 5 */
/* Pyrolysis of biomass: improved models for simultaneous kinetics and transport of heat,
mass, and momentum */
#include<stdio.h>
#include<math.h>
#define M 250                    /* (M+1)=Total number of equations to be solved */
void main()
{
long double T[M+2];              /* T=Temperature (K) */
long double CB[M+2];             /* CB=Concentration of biomass (kg/m3) */
long double k1[M+2];             /* k1=Rate constant for reaction 1 (1/s) */
long double k2[M+2];             /* k2=Rate constant for reaction 2 (1/s) */
long double k3[M+2];             /* k3=Rate constant for reaction 3 (1/s) */
int i;                           /* i=integer used in program */
int j;                           /* j=integer used in program */
int eqn[M+2];
long double xx;                  /* xx=used for output of dimensionless distance (-) */
long double R;                   /* R=radius of cylindrical pellet (m) */
long double A1;                  /* A1=Arrhenius frequency factor for reaction 1 (1/s) */
long double A2;                  /* A2=Arrhenius frequency factor for reaction 2 (1/s) */
long double A3;                  /* A3=Arrhenius frequency factor for reaction 3 (1/s) */
long double D1;                  /* D1=Constant used while calculating k1 (K) */
long double D2;                  /* D2=Constant used while calculating k2 (K) */
long double L1;                  /* L1=Constant used while calculating k1 (K2) */
long double L2;                  /* L2=Constant used while calculating k2 (K2) */
long double E3;                  /* E3=Activation energy (J/gmol) */
long double Rc;                  /* Rc=Universal gas constant (J/gmol K)*/
long double Cc1[M+2];            /* Cc1=Concentration of char 1 (-) */
long double CG1[M+2];            /* CG1=Concentration of volatile 1 (-) */
long double Cc2[M+2];            /* Cc2=Concentration of char 2 (-) */
long double CG2[M+2];            /* CG2=Concentration of volatile 2 (-) */
```

```
long double t[M+2];          /* t=Time (s) */
long double n1;              /* n1=Order of reaction 1 (-) */
long double n2;              /* n2=Order of reaction 2 (-) */
long double n3;              /* n3=Order of reaction 3 (-) */
long double h;               /* h=step size for RK4 Method (s) */
long double a1;
/*long double b1;*/
long double c1;
long double d1;
long double e1;
long double a2;
/*long double b2;*/
long double c2;
long double d2;
long double e2;
long double a3;              /* a1-e4=Variables used while solving RK4 method */
/*long double b3;*/
long double c3;
long double d3;
long double e3;
long double a4;
/*long double b4;*/
long double c4;
long double d4;
long double e4;
long double dtow;            /* dtow=Dimensionless time step for finite difference
                                method (-) */
long double tow;             /* tow=Dimensionless time for finite difference method */
long double dx;              /* dx=Dimensionless radial distance step for finite
                                difference method (-) */
long double T0;              /* T0=Initial temperature (K) */
long double Tf;              /* Tf=Final temperature (K) */
long double ht;              /* ht=convective heat transfer coefficient (W/m2K) */
long double ab;              /* ab=emissivity coefficient */
/*long double sig;*/         /* sig=Stefan Boltzmann constant */
long double dH;              /* dH=heat of reaction (kJ/kg) */
long double k[M+2];          /* k=thermal conductivity (W/m K) */
long double H[M+2];          /* H=modified Biot Number */
long double cp[M+2];         /* cp=specific heat (J/kg K) */
long double ro[M+2];         /* ro=density (kg/m3) */
long double Q[M+2];          /* Q=heat of reaction number (m3/kg) */
long double x[M+2];          /* x=Dimensionless radial distance (-) */
long double a[M+2];          /* a-d=Variables used in assigning values in tridiagonal
long double b[M+2];             matrix to find temperature */

long double c[M+2];
```

```
long double d[M+2];
long double theta[M+2];      /* theta=Dimensionless temperature (-) */
long double beta[M+2];       /* beta=used while calculating theta (-) */
long double gamma[M+2];      /* gamma=used while calculating theta (-) */
long double alpha;           /* alpha=used while calculating theta (-) */
long double ft;              /* ft=conversion of dimensionless time second (s) */
long double roin;            /* roin=initial value of density (kg/m3) */
long double jj;
long double kk;
long double ll;              /* jj-bb=Variable used while calculating the value of H */
long double aa;
long double mm;
long double bb;
long double Hc[M+2];
long double kc[M+2];
long double Tc[M+2];
long double Qc[M+2];
long double cpc[M+2];
long double bc[M+2];
long double dc[M+2];         /* From Hc-bbc the 'c' is used for char */
long double thetac[M+2];
long double betac[M+2];
long double gammac[M+2];
long double jjc;
long double kkc;
long double llc;
long double aac;
long double mmc;
long double bbc;             /* To find the sum of biomass at a particular time */
long double sum[M+2];        /* To find the average of biomass at a particular time */
long double avg[M+2];        /* To find the conversion of biomass*/
long double conversion[M+2]; /* bf=geometry factor(slab=1;cylinder=2;sphere=3)
long double bf;
/*long double ss1[M+2];
long double ss2[M+2];
long double ss3[M+2];
long double ss4[M+2];*/      /* Effective diffusivity of (volatile+gases)1 (-) */
long double DG1[M+2];        /* Heat capacity of (volatile+gases)1 (-)*/
long double CpG1[M+2];       /* Concentration of biomass at initial conditon (-)*/
long double CB0;             /* Lewis number */
long double Le;              /* p1d and p2d are the constants used in eq. of DG1*/
long double p1d;
long double p2d;             /* p1c is the constant used in eq. of CpG1*/
long double p1c;             /* dcc=(DG1*CpG1*CB0)/(Le)*/
long double dcc[M+2];        /* Sherwood number*/
long double NshG1[M+2];
```

```
long double p1sh;              /* p1sh and p2sh are the constants used in eq. of NshG1*/
long double p2sh;
long double ttt[M+2];          /* Variable used while calculating NshG1*/
long double aaa[M+2];          /* Used in tridiagonal matrix to find CG1(-)*/
long double bbb[M+2];          /* Used in tridiagonal matrix to find CG1(-)*/
long double ccc[M+2];          /* Used in tridiagonal matrix to find CG1(-)*/
long double ddd[M+2];          /* Used in tridiagonal matrix to find CG1(-)*/
long double vf[M+2];           /* Void fraction of particle (-)*/
long double vf0;               /* Void fraction at initial condition*/
long double constgam;          /* Constant used in equation of vf*/
long double dddcal2[M+2];      /* Constant used while calculating ddd*/
long double dddcal3[M+3];      /* Constant used while calculating ddd*/
long double betaCG1[M+2];      /* Used while calculating CG1*/
long double gammaCG1[M+2];     /* Used while calculating CG1*/
long double k3t[M+2];          /* Used when comparison is made with using CG1and
                               when constant value of CG1 is used*/

long double u[M+2];            /* Gas velocity (m/s)*/
long double B[M+2];            /* permeability (m^2)*/
long double Bb;                /* permeability of biomass (m^2)*/
long double Bc1;               /* permeability of char (m^2)*/
long double mu;                /* viscosity (kg/m/s)*/
long double WG1;               /* mean molecular weight of gas (kg/kgmol)*/
long double Rgg;               /* universal gas constant (Pa m^3/kgmolK)*/
long double eta[M+2];          /* Used in equation of B*/
long double Pg[M+2];           /* Gas pressure (Pa)*/
long double u1[M+2];           /* u1, u2. u2 are used to calculate the value of u */
long double u2[M+2];
long double u3[M+2];

/*Constants*/
/*R=0.005;*/
A1=9.973*pow(10.0,-5.0);
A2=1.068*pow(10.0,-3.0);
A3=5.7*pow(10.0,5.0);
D1=17254.4;
D2=10224.4;
L1=-9061227.0;
L2=-6123081.0;
E3=81000.0;
Rc=8.314;
dx=(1.0/M);
x[1]=(1.0/M);
/*ht=8.4;
ab=0.95;*/
/*sig=5.67*pow(10.0,-8.0);*/
roin=650.0;
```

```
dH=-255000.0;
alpha=1.79*pow(10.0,-7.0);
sum[0]=0.0;
/*n1=0.0;
n2=1.5;
n3=1.5;
h=0.01;
tow=0.010024;
dtow=0.010024;
T0=473.0;
Tf=873.0;*/
CB0=1.0;
p1d=1.5;
p2d=1.0;
p1c=0.001;
p1sh=50000.0;
p2sh=0.75;
eqn[0]=1;
for(i=0;i<=M;i++)
{
eqn[i+1]=eqn[i]+1;
}
vf0=0.5;
constgam=0.3;
alpha=1.79*pow(10.0,-7.0);
Bb=1.0*pow(10.0,-14.0);
Bc1=5.0*pow(10.0,-12.0);
mu=3.0*pow(10.0,-5.0);
WG1=51.33;
Rgg=8314.0;
CB0=650.0;
/*printf("%d",eqn[M]);
getchar();*/
/*printf("%Lf %Lf\n",dx,x[1]);
getchar();*/

/* Input */
printf("Enter the orders of reactions n1,n2,n3 (0,1.5,1.5)\n");
scanf("%Lf %Lf %Lf",&n1,&n2,&n3);
printf("Enter the value of time step h(t) for RK4 method (0.01)\n");
scanf("%Lf",&h);
printf("Enter the value of geometry factor i.e.bf(slab=1;cylinder=2;sphere=3)\n");
scanf("%Lf",&bf);
printf("Enter the value R (Half the thickness of slab,radius for cylinder & sphere)\n");
scanf("%Lf",&R);
printf("The value of tow can be calculated by the following formula:\n");
```

```
printf("t=(tow*R*R)/(alpha)\n");
printf("Here alpha is known i.e. alpha=1.79*pow(10.0,-7.0)\n");
printf("Suppose you want that your output come after every 1sec\n");
printf("Then t=1sec and say R=0.005m,then tow comes out to be 0.00716\n");
printf("Enter the initial value of time step i.e.tow (dimensionless) for\n");
printf("finite difference method \n");
scanf("%Lf",&tow);
printf("Enter the value of dtow(Its value is same as initial value of tow)\n");
scanf("%Lf",&dtow);
printf("Enter the initial value of temperature\n");
scanf("%Lf",&T0);
printf("Enter the final value of temperature\n");
scanf("%Lf",&Tf);
printf("\n There are following cases:\n");
printf("\n");
printf("(1) Convection and radiation on wall surface\n");
printf("For this case, put ht=8.4 & ab=0.95\n");
printf("(2) No convection on wall surface (Radiation only)\n");
printf("For this case, put ht=0 & ab=0.95\n");
printf("(3) No radiation on wall surface (Convection only)\n");
printf("For this case, put ht=8.4 & ab=0\n");
printf("(4) No radiation on wall surface (10 Times Convection)\n");
printf("For this case, put ht=84.0 & ab=0\n");
printf("\n");
printf("Read the above cases and then press enter key to continue\n");
getchar();
printf("\n Now enter the value according to the above cases\n");
printf("\n");
printf("Enter the value of convective heat transfer coefficient (ht=8.4,20.0)\n");
printf("ht=");
scanf("%Lf",&ht);
printf("Enter the value of emissivity coefficient (ab=0.95)\n");
printf("ab=");
scanf("%Lf",&ab);
printf("Enter the value of Lewis number (0.000001)\n");
scanf("%Lf",&Le);

/* Initial condition */
for(i=0;i<=M;i++)
{
CB[i]=1.0;
Cc1[i]=0.0;
CG1[i]=0.0;
Cc2[i]=0.0;
CG2[i]=0.0;
/*T[i]=473.0;*/
```

```
t[i]=h;
theta[i]=1.0;
thetac[i]=1.0;
}
for(i=0;i<=M;i++)
{
T[i]=T0;
}
for(i=0;i<=M;i++)
{
Tc[i]=T0;
}
/*printf("%0.6Lf\n",T[1]);
getchar();*/
/*for(i=0;i<=M;i++)
{
printf("%0.6Lf\n",T[i]);
getchar();
}*/
for(i=0;i<=M;i++)
{
u[i]=0;
}

/* Program of finite difference method based on pure implicit scheme */
while(1)
{
/*printf("%0.6Lf\n",R);
getchar();
printf("%0.6Lf %0.6Lf\n",Tf,R);
getchar();*/
for(i=0;i<=M;i++)
{
sum[i+1]=sum[i]+CB[i];
}
avg[1]=sum[M+1]/(M+1);
conversion[1]=(1.0-avg[1])/(1.0);
printf("%Lf %Lf %Lf\n",sum[M+1],avg[1],conversion[1]);
getchar();
k[M]=0.13+0.0003*(T[M]-273.0);
jj=pow(T[M],3.0);
kk=pow(T[M],2.0)*Tf;
ll=pow(Tf,2.0)*T[M];
mm=pow(Tf,3.0);
bb=(5.67*pow(10.0,-8.0))*(ab);
aa=ht+(bb*(jj+kk+ll+mm));
```

```
H[M]=(R/k[M])*(aa);
/*printf("%0.6Lf %0.6Lf %0.6Lf %0.6Lf  %0.6Lf %0.16Lf",jj,kk,ll,mm,aa,bb);
getchar();*/
kc[M]=0.08-0.0001*(Tc[M]-273.0);
jjc=pow(Tc[M],3.0);
kkc=pow(Tc[M],2.0)*Tf;
llc=pow(Tf,2.0)*Tc[M];
mmc=pow(Tf,3.0);
bbc=(5.67*pow(10.0,-8.0))*(ab);
aac=ht+(bbc*(jjc+kkc+llc+mmc));
Hc[M]=(R/kc[M])*(aac);
ft=(tow*pow(R,2.0))/(alpha);
/*printf("The value of k[M],H[M],ft\n");
printf("\n%0.6Lf %0.6Lf %0.6Lf",k[M],H[M],ft);
getchar();*/
/*printf("\n%0.6Lf %0.6Lf %d %0.6Lf",Tf,R,M,T[0]);
getchar();*/
for(i=0;i<=M;i++)
{
cp[i]=1112.0+4.85*(T[i]-273.0);
ro[i]=roin*(CB[i]+Cc1[i]+Cc2[i]);
Q[i]=((-dH)+(cp[i]*T[i]))/(ro[i]*cp[i]*(T0-Tf));
k1[i]=A1*exp((D1/T[i])+(L1/(T[i]*T[i])));
}
/*for(i=0;i<=M;i++)
{
printf("\n%0.6Lf %0.6Lf %0.6Lf %0.10Lf",cp[i],ro[i],Q[i],k1[i]);
getchar();
}*/
for(i=0;i<=M;i++)
{
cpc[i]=1003.2+2.09*(Tc[i]-273.0);
Qc[i]=((-dH)+(cpc[i]*Tc[i]))/(ro[i]*cpc[i]*(T0-Tf));
}
for(i=0;i<=M;i++)
{
DG1[i]=pow(theta[i],p1d)*exp(p2d*(1.0-CB[i]));
CpG1[i]=1.0+p1c*(theta[i]-1.0);
dcc[i]=(DG1[i]*CpG1[i]*CB0)/(Le);
}
/*printf("\tDG1 \tCpG1  \tdcc \n");
for(i=0;i<=M;i++)
{
printf("%0.6Lf %0.6Lf %0.6Lf\n",DG1[i],CpG1[i],dcc[i]);
getchar();
}*/
```

```
for(i=0;i<=M;i++)
{
ttt[i]=pow(theta[i],p2sh);
NshG1[i]=((p1sh)*(ttt[i]));
}
/*printf("\t NshG1    DG1\n");
for(i=0;i<=M;i++)
{
printf("%0.6Lf%0.6Lf\n",NshG1[i],DG1[i]);
getchar();
}*/
for(i=0;i<=M;i++)
{
vf[i]=((vf0)+(constgam*(1.0-CB[i])));
}
/*printf("vf\n");
for(i=0;i<=M;i++)
{
printf("%0.6Lf\n",vf[i]);
getchar();
}*/
for(i=0;i<=M;i++)
{
eta[i]=CB[i];
B[i]=(eta[i]*Bb)+((1.0-eta[i])*Bc1);
Pg[i]=((CG1[i]*Rgg*T[i])/(WG1));
}
/*printf("eta       B       Pg\n");
for(i=0;i<=M;i++)
{
printf("%0.6Lf%0.14Lf%0.6Lf\n",eta[i],B[i],Pg[i]);
getchar();
}*/
/*u[0]=0;
for(i=1;i<=M-1;i++)
{
u[i]=((-B[i]*Rgg*CB0)/(mu*WG1*R))
     +((theta[i]*(T0-Tf)+Tf)*((CG1[i+1]-CG1[i-1])/(2.0*dx)));
if(u[i]<0.0)
u[i]=(-1.0)*u[i];
}
u[M]=((-B[M]*Rgg*CB0)/(mu*WG1*R))
    +((theta[M]*(T0-Tf)+Tf)*((-NshG1[M]*CG1[M])/(DG1[M])));
printf("u\n");
for(i=0;i<=M;i++)
{
```

```
printf("%0.6Lf\n",u[i]);
getchar();
}*/
u[0]=0.0;
for(i=1;i<=M-1;i++)
{
u1[i]=(-B[i]*Rgg*CB0)/(mu*WG1*R);
u2[i]=(T0-Tf)*CG1[i]*((theta[i+1]-theta[i-1])/(2.0*dx));
u3[i]=(theta[i]*(T0-Tf)+Tf)*((CG1[i+1]-CG1[i-1])/(2.0*dx));
u[i]=(u1[i])*(u2[i]+u3[i]);
if(u[i]<0.0)
u[i]=(-1.0)*u[i];
}
u1[M]=(-B[M]*Rgg*CB0)/(mu*WG1*R);
u2[M]=(T0-Tf)*CG1[M]*(-theta[M]*H[M]);
u3[M]=(theta[M]*(T0-Tf)+Tf)*((-NshG1[M]*CG1[M])/(DG1[M]));
u[M]=(u1[M])*(u2[M]+u3[M]);
/*for(i=0;i<=M;i++)
{
u[i]=0.0;
}*/
/*printf("u1    u2      u3      u\n");
for(i=0;i<=M;i=i+15)
{
printf("%0.9Lf%0.9Lf%0.9Lf%0.9Lf\n",u1[i],u2[i],u3[i],u[i]);
getchar();
}*/
for(i=1;i<=M-1;i++)
{
a[i]=(((bf-1.0)*(dtow))/(2.0*dx*x[i]))-((dtow)/(dx*dx))
+((dtow*dc[i]*CG1[i+1])/(4.0*dx*dx))-((dtow*dc[i]*CG1[i-1])/(4.0*dx*dx));
x[i+1]=x[i]+dx;
}
a[M]=((-2.0*dtow)/(dx*dx));
/*for(i=1;i<=M;i++)
{
printf("%0.6Lf\n",a[i]);
getchar();
}*/
b[0]=(((2.0*bf*dtow)/(dx*dx))+(1.0));
for(i=1;i<=M-1;i++)
{
b[i]=((2.0*dtow)/(dx*dx)+1.0);
}
b[M]=(((2.0*dtow)/(dx*dx))+(1.0)+((2.0*dtow*H[M])/(dx))+((bf-1.0)*dtow*H[M])
-(dtow*CpG1[M]*CB0*H[M]*NshG1[M]*CG1[M])/(Le));
```

```
/*for(i=0;i<=M;i++)
{
printf("%0.6Lf\n",b[i]);
getchar();
}*/
bc[0]=(((2.0*bf*dtow)/(dx*dx))+(1.0));
for(i=1;i<=M-1;i++)
{
bc[i]=((2.0*dtow)/(dx*dx)+1.0);
}
bc[M]=(((2.0*dtow)/(dx*dx))+(1.0)+((2.0*dtow*Hc[M])/(dx))+((bf-1.0)*dtow*Hc[M])
-(dtow*CpG1[M]*CB0*Hc[M]*NshG1[M]*CG1[M])/(Le));
/*for(i=0;i<=M;i++)
{
printf("%0.6Lf\n",bc[i]);
getchar();
}*/
c[0]=(-2.0*bf*dtow)/(dx*dx);
for(i=1;i<=M-1;i++)
{
c[i]=((((bf-1.0)*(-dtow))/(2.0*dx*x[i]))-((dtow)/(dx*dx))
+((dtow*dc[i]*CG1[i-1])/(4.0*dx*dx))-((dtow*dc[i]*CG1[i+1])/(4.0*dx*dx)));
x[i+1]=x[i]+dx;
}
/*for(i=0;i<=M-1;i++)
{
printf("%0.6Lf\n",c[i]);
getchar();
}*/
for(i=0;i<=M;i++)
{
d[i]=(theta[i])+((dtow*Q[i]*R*R*k1[i]*pow((roin*CB[i]),n1))/(alpha));
}
/*for(i=0;i<=M;i++)
{
printf("%0.9Lf\n",d[i]);
getchar();
}*/
for(i=0;i<=M;i++)
{
dc[i]=(thetac[i])+((dtow*Qc[i]*R*R*k1[i]*pow((roin*CB[i]),n1))/(alpha));
}
beta[0]=b[0];
for(i=1;i<=M;i++)
{
beta[i]=b[i]-(a[i]*c[i-1])/(beta[i-1]);
```

```
}
/*for(i=0;i<=M;i++)
{
printf("%0.6Lf\n",beta[i]);
getchar();
}*/
betac[0]=bc[0];
for(i=1;i<=M;i++)
{
betac[i]=bc[i]-(a[i]*c[i-1])/(betac[i-1]);
}
gamma[0]=d[0]/beta[0];
for(i=1;i<=M;i++)
{
gamma[i]=(d[i]-a[i]*gamma[i-1])/(beta[i]);
}
/*for(i=0;i<=M;i++)
{
printf("%0.6Lf\n",gamma[i]);
getchar();
}*/
gammac[0]=dc[0]/betac[0];
for(i=1;i<=M;i++)
{
gammac[i]=(dc[i]-a[i]*gammac[i-1])/(betac[i]);
}
theta[M]=gamma[M];
i=M;
for(j=1;j<=M;j++)
{
theta[M-j]=(gamma[M-j])-((c[M-j]*theta[i])/(beta[M-j]));
i=i-1;
}
/*printf("theta\n");
for(i=0;i<=M;i++)
{
printf("%0.6Lf\n",theta[i]);
getchar();
}*/
thetac[M]=gammac[M];
i=M;
for(j=1;j<=M;j++)
{
thetac[M-j]=(gammac[M-j])-((c[M-j]*thetac[i])/(betac[M-j]));
i=i-1;
}
```

```
for(i=0;i<=M;i++)
{
T[i]=Tf-theta[i]*(Tf-T0);
}
/*printf("T\n");
for(i=0;i<=M;i++)
{
printf("%0.6Lf\n",T[i]);
getchar();
}*/
for(i=0;i<=M;i++)
{
Tc[i]=Tf-thetac[i]*(Tf-T0);
}

/* Runge-Kutta method to find CB(-)*/
/*printf("\neqn        t      T       CB     CG1      Cc1      CG2     Cc2");*/
for(i=0;i<=M;i++)
{
while(1)
{
k1[i]=A1*exp((D1/T[i])+(L1/(T[i]*T[i])));
k2[i]=A2*exp((D2/Tc[i])+(L2/(Tc[i]*Tc[i])));
k3[i]=A3*exp(-E3/(Rc*Tc[i]));
a1=(-h)*((k1[i]+k2[i])*pow(CB[i],n1));
a2=(-h)*((k1[i]+k2[i])*pow((CB[i]+(a1/2.0)),n1));
a3=(-h)*((k1[i]+k2[i])*pow((CB[i]+(a2/2.0)),n1));
a4=(-h)*((k1[i]+k2[i])*pow((CB[i]+a3),n1));
CB[i]=CB[i]+(1.0/6.0)*(a1+2.0*a2+2.0*a3+a4);
if(CB[i]<0.0)
{
CB[i]=0.0000001;
}
if(t[i]>=(ft-h))
break;
t[i]=t[i]+h;
}
}
/*printf("CB(-)\n");
for(i=0;i<=M;i++)
{
printf("%0.6Lf\n",CB[i]);
getchar();
}*/

/* Program of finite difference to find CG1(-) */
```

```
for(i=1;i<=M-1;i++)
{
aaa[i]=(((bf-1.0)*dtow*DG1[i])/(2.0*dx*x[i]*Le*vf[i]))-
((u[i]*R*dtow)/(alpha*2.0*dx))-((dtow*DG1[i])/(dx*dx*Le*vf[i]));
x[i+1]=x[i]+dx;
}
aaa[M]=-((2.0*dtow*DG1[M])/(dx*dx*Le*vf[M]));
/*printf("aaa\n");
for(i=1;i<=M;i++)
{
printf("%0.6Lf\n",aaa[i]);
getchar();
}*/
bbb[0]=((2.0*bf*dtow*DG1[0])/(dx*dx*Le*vf[0]))+(1.0);
for(i=1;i<=M-1;i++)
{
bbb[i]=((2.0*dtow*DG1[i])/(dx*dx*Le*vf[i]))+(1.0);
}
bbb[M]=(((bf-
1.0)*dtow*NshG1[M])/(Le*vf[M]))+((2.0*dtow*NshG1[M])/(dx*Le*vf[M]))+((2.0*dto
w*DG1[M])/(dx*dx*Le*vf[M]))+(1.0)-((NshG1[M]*dtow*u[M]*R)/(DG1[M]*alpha));
/*printf("bbb\n");
for(i=0;i<=M;i++)
{
printf("%0.6Lf\n",bbb[i]);
getchar();
}*/
ccc[0]=((-2.0*bf*dtow*DG1[0])/(dx*dx*Le*vf[0]));
for(i=1;i<=M-1;i++)
{
ccc[i]=(((bf-1.0)*(-
dtow)*DG1[i])/(2.0*dx*x[i]*Le*vf[i]))+((u[i]*R*dtow)/(alpha*2.0*dx))
   -((dtow*DG1[i])/(dx*dx*Le*vf[i]));
x[i+1]=x[i]+dx;
}
/*printf("ccc\n");
for(i=0;i<=M-1;i++)
{
printf("%0.6Lf\n",ccc[i]);
getchar();
}*/
/*printf("CB   CG1  Cc1   vf\n");
for(i=0;i<=M;i++)
{
printf("%0.6Lf %0.6Lf %0.6Lf\n",CB[i],CG1[i],vf[i]);
getchar();
```

```
}*/
for(i=0;i<=M;i++)
{
dddcal2[i]=((dtow*R*R*k1[i]*pow(CB[i],n1))/(vf[i]*alpha));
dddcal3[i]=((dtow*R*R*k3[i]*(pow(CG1[i],n2))*(pow(Cc1[i],n3)))/(alpha));
}
/*printf("T   Tc[i]        k1     k3        dddcal2    dddcal3\n");
for(i=0;i<=M;i++)
{
printf("%0.6Lf          %0.6Lf          %0.11Lf          %0.11Lf          %0.11Lf
%0.11Lf\n",T[i],Tc[i],k1[i],k3[i],dddcal2[i],dddcal3[i]);
getchar();
}*/
for(i=0;i<=M;i++)
{
ddd[i]=CG1[i]+((dtow*R*R*k1[i]*pow(CB[i],n1))/(vf[i]*alpha))-
((dtow*R*R*k3[i]*(pow(CG1[i],n2))*(pow(Cc1[i],n3)))/(alpha));
}
/*printf("ddd\n");
for(i=0;i<=M;i++)
{
printf("%0.9Lf\n",ddd[i]);
getchar();
}*/
betaCG1[0]=bbb[0];
for(i=1;i<=M;i++)
{
betaCG1[i]=bbb[i]-(aaa[i]*ccc[i-1])/(betaCG1[i-1]);
}
/*printf("betaCG1\n");
for(i=0;i<=M;i++)
{
printf("%0.6Lf\n",betaCG1[i]);
getchar();
}*/
gammaCG1[0]=ddd[0]/betaCG1[0];
for(i=1;i<=M;i++)
{
gammaCG1[i]=(ddd[i]-aaa[i]*gammaCG1[i-1])/(betaCG1[i]);
}
/*printf("aaa     ccc     ddd     betaCG1     gammaCG1\n");
for(i=0;i<=M;i++)
{
printf("%0.6Lf          %0.6Lf          %0.6Lf
%0.6Lf\n",aaa[i],ccc[i],ddd[i],betaCG1[i],gammaCG1[i]);
getchar();
```

```
}*/
CG1[M]=gammaCG1[M];
i=M;
for(j=1;j<=M;j++)
{
CG1[M-j]=(gammaCG1[M-j])-((ccc[M-j]*CG1[i])/(betaCG1[M-j]));
i=i-1;
}
/*printf("CG1\n");
for(i=0;i<=M;i++)
{ printf("%0.11Lf\n",CG1[i]);
getchar(); }*/
for(i=0;i<=M;i++)
{
while(1)
{
k1[i]=A1*exp((D1/T[i])+(L1/(T[i]*T[i])));
k2[i]=A2*exp((D2/Tc[i])+(L2/(Tc[i]*Tc[i])));
k3[i]=A3*exp(-E3/(Rc*Tc[i]));
k3t[i]=k3[i]*pow(CG1[i],n2);
a1=(-h)*((k1[i]+k2[i])*pow(CB[i],n1));
c1=h*((k2[i]*pow(CB[i],n1))-(k3t[i]*pow(Cc1[i],n3)));
d1=h*(k3t[i]*pow(Cc1[i],n3));
e1=h*(k3t[i]*pow(Cc1[i],n3));
a2=(-h)*((k1[i]+k2[i])*pow((CB[i]+(a1/2.0)),n1));
c2=h*((k2[i]*pow((CB[i]+(a1/2.0)),n1))-(k3t[i]*pow((Cc1[i]+(c1/2.0)),n3)));
d2=h*(k3t[i]*pow((Cc1[i]+(c1/2.0)),n3));
e2=h*(k3t[i]*pow((Cc1[i]+(c1/2.0)),n3));
a3=(-h)*((k1[i]+k2[i])*pow((CB[i]+(a2/2.0)),n1));
c3=h*((k2[i]*pow((CB[i]+(a2/2.0)),n1))-(k3t[i]*pow((Cc1[i]+(c2/2.0)),n3)));
d3=h*(k3t[i]*pow((Cc1[i]+(c2/2.0)),n3));
e3=h*(k3t[i]*pow((Cc1[i]+(c2/2.0)),n3));
a4=(-h)*((k1[i]+k2[i])*pow((CB[i]+a3),n1));
c4=h*((k2[i]*pow((CB[i]+a3),n1))-(k3t[i]*pow((Cc1[i]+c3),n3)));
d4=h*(k3t[i]*pow((Cc1[i]+c3),n3));
e4=h*(k3t[i]*pow((Cc1[i]+c3),n3));
CB[i]=CB[i]+(1.0/6.0)*(a1+2.0*a2+2.0*a3+a4);
Cc1[i]=Cc1[i]+(1.0/6.0)*(c1+2.0*c2+2.0*c3+c4);
CG2[i]=CG2[i]+(1.0/6.0)*(d1+2.0*d2+2.0*d3+d4);
Cc2[i]=Cc2[i]+(1.0/6.0)*(e1+2.0*e2+2.0*e3+e4);
if(CB[i]<0.0)
{
CB[i]=0.0000001;
/*ss1[i]=CG1[i];
ss2[i]=Cc1[i];
ss3[i]=CG2[i];
```

```
ss4[i]=Cc2[i];*/
}
if(t[i]>=(ft-h))
break;
t[i]=t[i]+h;
}
}

/* Output */
/*for(i=0;i<=M;i++)
{
printf("\n%d      \t%0.6Lf      %0.6Lf      %0.6Lf      %0.6Lf      %0.6Lf
%0.6Lf",eqn[i],t[i],T[i],CB[i],CG1[i],Cc1[i],CG2[i],Cc2[i]);
getchar();
}*/
printf("\neqn   xx   t     T      CB      CG1     Cc1     CG2=Cc2   u ");
xx=0.0;
for(i=0;i<=M;i=i+25)
{
/*CG1[i]=ss1[i];
Cc1[i]=ss2[i];
CG2[i]=ss3[i];
Cc2[i]=ss4[i];*/
printf("\n%0.3d  %0.1Lf %0.2Lf %0.6Lf %0.6Lf %0.6Lf %0.6Lf %0.6Lf  %0.6Lf",
eqn[i],xx,t[i],T[i],CB[i],CG1[i],Cc1[i],CG2[i],u[i]);
/*getchar();*/
/*printf("\nk3 k3t\n");
printf("%0.6Lf %0.6Lf\n",k3[i],k3t[i]);
getchar(); */
/*getchar();*/
xx=xx+0.1;
}
printf("\nConversion=");
printf("%Lf",conversion[1]);
/*for(i=0;i<=M;i++)
{
if(CB[i]<0.0)
CB[i]=0.0000001;
}*/
getchar();
tow=tow+dtow;
if(CB[M]<=0.00000001)
if(CB[0]<=0.00000001)
break;
}
}
```

D-2 Program for Model-II

```
/* Program for Chapter 5 */
/* Pyrolysis of biomass: improved models for simultaneous kinetics and transport of heat,
mass, and momentum */
#include<stdio.h>
#include<math.h>
#define M 150                    /* (M+1)=Total number of equations to be solved */
void main()
{
long double T[M+2];              /* T=Temperature (K) */
long double CB[M+2];             /* CB=Concentration of biomass (kg/m3) */
long double k1[M+2];             /* k1=Rate constant for reaction 1 (1/s) */
long double k2[M+2];             /* k2=Rate constant for reaction 2 (1/s) */
long double k3[M+2];             /* k3=Rate constant for reaction 3 (1/s) */
int i;                           /* i=integer used in program */
int j;                           /* j=integer used in program */
int eqn[M+2];
long double xx;                  /* xx=used for output of dimensionless distance (-) */
long double R;                   /* R=radius of cylindrical pellet (m) */
long double A1;                  /* A1=Arrhenius frequency factor for reaction 1 (1/s) */
long double A2;                  /* A2=Arrhenius frequency factor for reaction 2 (1/s) */
long double A3;                  /* A3=Arrhenius frequency factor for reaction 3 (1/s) */
long double D1;                  /* D1=Constant used while calculating k1 (K) */
long double D2;                  /* D2=Constant used while calculating k2 (K) */
long double L1;                  /* L1=Constant used while calculating k1 (K2) */
long double L2;                  /* L2=Constant used while calculating k2 (K2) */
long double E3;                  /* E3=Activation energy (J/gmol) */
long double Rc;                  /* Rc=Universal gas constant (J/gmol K)*/
long double Cc1[M+2];            /* Cc1=Concentration of char 1 (-) */
long double CG1[M+2];            /* CG1=Concentration of volatile 1 (-) */
long double Cc2[M+2];            /* Cc2=Concentration of char 2 (-) */
long double CG2[M+2];            /* CG2=Concentration of volatile 2 (-) */
long double t[M+2];              /* t=Time (s) */
long double n1;                  /* n1=Order of reaction 1 (-) */
long double n2;                  /* n2=Order of reaction 2 (-) */
long double n3;                  /* n3=Order of reaction 3 (-) */
long double h;                   /* h=step size for RK4 Method (s) */
long double a1;
/*long double b1;*/
long double c1;
long double d1;
long double e1;
long double a2;
/*long double b2;*/
long double c2;
long double d2;
```

```
long double e2;
long double a3;          /* a1-e4=Variables used while solving RK4 method */
/*long double b3;*/
long double c3;
long double d3;
long double e3;
long double a4;
/*long double b4;*/
long double c4;
long double d4;
long double e4;
long double dtow;        /* dtow=Dimensionless time step for finite difference
                            method (-) */
long double tow;         /* tow=Dimensionless time for finite difference method */
long double dx;          /* dx=Dimensionless radial distance step for finite
                            difference method (-) */
long double T0;          /* T0=Initial temperature (K) */
long double Tf;          /* Tf=Final temperature (K) */
long double ht;          /* ht=convective heat transfer coefficient (W/m2K) */
long double ab;          /* ab=emissivity coefficient */
/*long double sig;*/     /* sig=Stefan Boltzmann constant */
long double dH;          /* dH=heat of reaction (kJ/kg) */
long double k[M+2];      /* k=thermal conductivity (W/m K) */
long double H[M+2];      /* H=modified Biot Number */
long double cp[M+2];     /* cp=specific heat (J/kg K) */
long double ro[M+2];     /* ro=density (kg/m3) */
long double Q[M+2];      /* Q=heat of reaction number (m3/kg) */
long double x[M+2];      /* x=Dimensionless radial distance (-) */
long double a[M+2];      /* a-d=Variables used in assigning values in tridiagonal
long double b[M+2];      matrix to find temperature */
long double c[M+2];
long double d[M+2];
long double theta[M+2];  /* theta=Dimensionless temperature (-) */
long double beta[M+2];   /* beta=used while calculating theta (-) */
long double gamma[M+2];  /* gamma=used while calculating theta (-) */
long double alpha;       /* alpha=used while calculating theta (-) */
long double ft;          /* ft=conversion of dimensionless time second (s) */
long double roin;        /* roin=initial value of density (kg/m3) */
long double jj;
long double kk;          /* jj-bb=Variables used while calculating the value of H */
long double ll;
long double aa;
long double mm;
long double bb;
long double Hc[M+2];
```

```
long double kc[M+2];
long double Tc[M+2];
long double Qc[M+2];
long double cpc[M+2];
long double bc[M+2];
long double dc[M+2];          /* From Hc-bbc the 'c' is used for char */
long double thetac[M+2];
long double betac[M+2];
long double gammac[M+2];
long double jjc;
long double kkc;
long double llc;
long double aac;
long double mmc;
long double bbc;
long double sum[M+2];         /* To find the sum of biomass at a particular time */
long double avg[M+2];         /* To find the average of biomass at a particular time */
long double conversion[M+2];  /* To find the conversion of biomass*/
long double bf;               /* bf=geometry factor(slab=1;cylinder=2;sphere=3)
/*long double ss1[M+2];
long double ss2[M+2];
long double ss3[M+2];
long double ss4[M+2];*/
long double DG1[M+2];         /* Effective diffusivity of (volatile+gases)1 (-) */
long double CpG1[M+2];        /* Heat capacity of (volatile+gases)1 (-)*/
long double CB0;              /* Concentration of biomass at initial conditon (-)*/
long double Le;               /* Lewis number */
long double p1d;              /* p1d and p2d are the constants used in eq. of DG1*/
long double p2d;
long double p1c;              /* p1c is the constant used in eq. of CpG1*/
long double dcc[M+2];         /* dcc=(DG1*CpG1*CB0)/(Le)*/
long double NshG1[M+2];       /* Sherwood number*/
long double p1sh;             /* p1sh and p2sh are the constants used in eq. of NshG1*/
long double p2sh;
long double ttt[M+2];         /* Variable used while calculating NshG1*/
long double aaa[M+2];         /* Used in tridiagonal matrix to find CG1(-)*/
long double bbb[M+2];         /* Used in tridiagonal matrix to find CG1(-)*/
long double ccc[M+2];         /* Used in tridiagonal matrix to find CG1(-)*/
long double ddd[M+2];         /* Used in tridiagonal matrix to find CG1(-)*/
long double vf[M+2];          /* Void fraction of particle (-)*/
long double vf0;              /* Void fraction at initial condition*/
long double constgam;         /* Constant used in equation of vf*/
long double dddcal2[M+2];     /* Constant used while calculating ddd*/
long double dddcal3[M+3];     /* Used while calculating ddd*/
long double betaCG1[M+2];     /* Used while calculating CG1*/
long double gammaCG1[M+2];
```

```
long double k3t[M+2];        /* Used when comparison is made with using CG1 and
                                when constant value of CG1 is used */

/*Constants*/
/*R=0.005;*/
A1=9.973*pow(10.0,-5.0);
A2=1.068*pow(10.0,-3.0);
A3=5.7*pow(10.0,5.0);
D1=17254.4;
D2=10224.4;
L1=-9061227.0;
L2=-6123081.0;
E3=81000.0;
Rc=8.314;
dx=(1.0/M);
x[1]=(1.0/M);
/*ht=8.4;
ab=0.95;*/
/*sig=5.67*pow(10.0,-8.0);*/
roin=650.0;
dH=-255000.0;
alpha=1.79*pow(10.0,-7.0);
sum[0]=0.0;
/*n1=0.0;
n2=1.5;
n3=1.5;
h=0.01;
tow=0.010024;
dtow=0.010024;
T0=473.0;
Tf=873.0;*/
CB0=1.0;
p1d=1.5;
p2d=1.0;
p1c=0.001;
p1sh=5.0;
p2sh=0.75;
eqn[0]=1;
for(i=0;i<=M;i++)
{
eqn[i+1]=eqn[i]+1;
}
vf0=0.5;
constgam=0.3;
/*printf("%d",eqn[M]);
getch();*/
```

```
/*printf("%Lf %Lf\n",dx,x[1]);
getch();*/

/* Input */
printf("Enter the orders of reactions n1.n2,n3 (0,1.5,1.5)\n");
scanf("%Lf %Lf %Lf",&n1,&n2,&n3);
printf("Enter the value of time step h(t) for RK4 method (0.01)\n");
scanf("%Lf",&h);
printf("Enter the value of geometry factor i.e.bf(slab=1;cylinder=2;sphere=3)\n");
scanf("%Lf",&bf);
printf("Enter the value R (Half the thickness of slab,radius for cylinder & sphere)\n");
scanf("%Lf",&R);
printf("The value of tow can be calculated by the following formula:\n");
printf("t=(tow*R*R)/(alpha)\n");
printf("Here alpha is known i.e. alpha=1.79*pow(10.0,-7.0)\n");
printf("Suppose you want that your output come after every 1sec\n");
printf("Then t=1sec and say R=0.005m.then tow comes out to be 0.00716\n");
printf("Enter the initial value of time step i.e.tow (dimensionless) for\n");
printf("finite difference method \n");
scanf("%Lf",&tow);
printf("Enter the value of dtow(Its value is same as initial value of tow)\n");
scanf("%Lf",&dtow);
printf("Enter the initial value of temperature\n");
scanf("%Lf",&T0);
printf("Enter the final value of temperature\n");
scanf("%Lf",&Tf);
printf("\n There are following cases:\n");
printf("\n");
printf("(1) Convection and radiation on wall surface\n");
printf("For this case, put ht=8.4 & ab=0.95\n");
printf("(2) No convection on wall surface (Radiation only)\n");
printf("For this case, put ht=0 & ab=0.95\n");
printf("(3) No radiation on wall surface (Convection only)\n");
printf("For this case, put ht=8.4 & ab=0\n");
printf("(4) No radiation on wall surface (10 Times Convection)\n");
printf("For this case, put ht=84.0 & ab=0\n");
printf("\n");
printf("Read the above cases and then press enter key to continue\n");
getchar();
printf("\n Now enter the value according to the above cases\n");
printf("\n");
printf("Enter the value of convective heat transfer coefficient (ht=8.4)\n");
printf("ht=");
scanf("%Lf",&ht);
printf("Enter the value of emissivity coefficient (ab=0.95)\n");
printf("ab=");
```

```
scanf("%Lf",&ab);
printf("Enter the value of Lewis number (2,10,etc...\n");
scanf("%Lf",&Le);

/* Initial condition */
for(i=0;i<=M;i++)
{
CB[i]=1.0;
Cc1[i]=0.0;
CG1[i]=0.0;
Cc2[i]=0.0;
CG2[i]=0.0;
/*T[i]=473.0;*/
t[i]=h;
theta[i]=1.0;
thetac[i]=1.0;
}
for(i=0;i<=M;i++)
{
T[i]=T0;
}
for(i=0;i<=M;i++)
{
Tc[i]=T0;
}
/*printf("%0.6Lf\n",T[1]);
getch();*/
/*for(i=0;i<=M;i++)
{
printf("%0.6Lf\n",T[i]);
getch();
}*/

/*Program of finite difference method based on pure implicit scheme*/
while(1)
{
/*printf("%0.6Lf\n",R);
getch();
printf("%0.6Lf %0.6Lf\n",Tf,R);
getch();*/
for(i=0;i<=M;i++)
{
sum[i+1]=sum[i]+CB[i];
}
avg[1]=sum[M+1]/(M+1);
conversion[1]=(1.0-avg[1])/(1.0);
```

```
/*printf("%Lf %Lf %Lf\n",sum[M+1],avg[1],conversion[1]);
getch();*/
k[M]=0.13+0.0003*(T[M]-273.0);
jj=pow(T[M],3.0);
kk=pow(T[M],2.0)*Tf;
ll=pow(Tf,2.0)*T[M];
mm=pow(Tf,3.0);
bb=(5.67*pow(10.0,-8.0))*(ab);
aa=ht+(bb*(jj+kk+ll+mm));
H[M]=(R/k[M])*(aa);
/*printf("%0.6Lf %0.6Lf %0.6Lf %0.6Lf  %0.6Lf %0.16Lf",jj,kk,ll,mm,aa,bb);
getch();*/
kc[M]=0.08-0.0001*(Tc[M]-273.0);
jjc=pow(Tc[M],3.0);
kkc=pow(Tc[M],2.0)*Tf;
llc=pow(Tf,2.0)*Tc[M];
mmc=pow(Tf,3.0);
bbc=(5.67*pow(10.0,-8.0))*(ab);
aac=ht+(bbc*(jjc+kkc+llc+mmc));
Hc[M]=(R/kc[M])*(aac);
ft=(tow*pow(R,2.0))/(alpha);
/*printf("The value of k[M],H[M],ft\n");
printf("\n%0.6Lf %0.6Lf %0.6Lf",k[M],H[M],ft);
getch();
getch();
printf("\n%0.6Lf %0.6Lf %d %0.6Lf",Tf,R,M,T[0]);
getch();*/
for(i=0;i<=M;i++)
{
cp[i]=1112.0+4.85*(T[i]-273.0);
ro[i]=roin*(CB[i]+Cc1[i]+Cc2[i]);
Q[i]=((-dH)+(cp[i]*T[i]))/(ro[i]*cp[i]*(T0-Tf));
k1[i]=A1*exp((D1/T[i])+(L1/(T[i]*T[i])));
}
/*for(i=0;i<=M;i++)
{
printf("\n%0.6Lf %0.6Lf %0.6Lf %0.10Lf",cp[i],ro[i],Q[i],k1[i]);
getch();
}*/
for(i=0;i<=M;i++)
{
cpc[i]=1003.2+2.09*(Tc[i]-273.0);
Qc[i]=((-dH)+(cpc[i]*Tc[i]))/(ro[i]*cpc[i]*(T0-Tf));
}
for(i=0;i<=M;i++)
{
```

```
DG1[i]=pow(theta[i],p1d)*exp(p2d*(1.0-CB[i]));
CpG1[i]=1.0+p1c*(theta[i]-1.0);
dcc[i]=(DG1[i]*CpG1[i]*CB0)/(Le);
}
/*printf("\tDG1 \tCpG1  \tdcc \n");
for(i=0;i<=M;i++)
{
printf("%0.6Lf %0.6Lf %0.6Lf\n",DG1[i],CpG1[i],dcc[i]);
getch();
}*/
for(i=0;i<=M;i++)
{
ttt[i]=pow(theta[i],p2sh);
NshG1[i]=((p1sh)*(ttt[i]));
}
/*printf("\t NshG1\n");
for(i=0;i<=M;i++)
{
printf("%0.6Lf\n",NshG1[i]);
getch();
}*/
for(i=0;i<=M;i++)
{
vf[i]=((vf0)+(constgam*(1.0-CB[i])));
}
/*printf("vf\n");
for(i=0;i<=M;i++)
{
printf("%0.6Lf\n",vf[i]);
getch();
}*/
for(i=1;i<=M-1;i++)
{
a[i]=(((bf-1.0)*(dtow))/(2.0*dx*x[i]))-((dtow)/(dx*dx))
+((dtow*dc[i]*CG1[i+1])/(4.0*dx*dx))-((dtow*dc[i]*CG1[i-1])/(4.0*dx*dx));
x[i+1]=x[i]+dx;
}
a[M]=((-2.0*dtow)/(dx*dx));
/*for(i=1;i<=M;i++)
{
printf("%0.6Lf\n",a[i]);
getch();
}*/
b[0]=(((2.0*bf*dtow)/(dx*dx))+(1.0));
for(i=1;i<=M-1;i++)
{
```

```
b[i]=((2.0*dtow)/(dx*dx)+1.0);
}
b[M]=(((2.0*dtow)/(dx*dx))+(1.0)+((2.0*dtow*H[M])/(dx))+((bf-1.0)*dtow*H[M])
-(dtow*CpG1[M]*CB0*H[M]*NshG1[M]*CG1[M])/(Le));
/*for(i=0;i<=M;i++)
{
printf("%0.6Lf\n",b[i]);
getch();
}*/
bc[0]=(((2.0*bf*dtow)/(dx*dx))+(1.0));
for(i=1;i<=M-1;i++)
{
bc[i]=((2.0*dtow)/(dx*dx)+1.0);
}
bc[M]=(((2.0*dtow)/(dx*dx))+(1.0)+((2.0*dtow*Hc[M])/(dx))+((bf-1.0)*dtow*Hc[M])
-(dtow*CpG1[M]*CB0*Hc[M]*NshG1[M]*CG1[M])/(Le));
/*for(i=0;i<=M;i++)
{
printf("%0.6Lf\n",bc[i]);
getch();
}*/
c[0]=(-2.0*bf*dtow)/(dx*dx);
for(i=1;i<=M-1;i++)
{
c[i]=((((bf-1.0)*(-dtow))/(2.0*dx*x[i]))-((dtow)/(dx*dx))
+((dtow*dc[i]*CG1[i-1])/(4.0*dx*dx))-((dtow*dc[i]*CG1[i+1])/(4.0*dx*dx)));
x[i+1]=x[i]+dx;
}
/*for(i=0;i<=M-1;i++)
{
printf("%0.6Lf\n",c[i]);
getch();
}*/
for(i=0;i<=M;i++)
{
d[i]=(theta[i])+((dtow*Q[i]*R*R*k1[i]*pow((roin*CB[i]),n1))/(alpha));
}
/*for(i=0;i<=M;i++)
{
printf("%0.9Lf\n",d[i]);
getch();
}*/
for(i=0;i<=M;i++)
{
dc[i]=(thetac[i])+((dtow*Qc[i]*R*R*k1[i]*pow((roin*CB[i]),n1))/(alpha));
}
```

```
beta[0]=b[0];
for(i=1;i<=M;i++)
{
beta[i]=b[i]-(a[i]*c[i-1])/(beta[i-1]);
}
/*for(i=0;i<=M;i++)
{
printf("%0.6Lf\n",beta[i]);
getch();
}*/
betac[0]=bc[0];
for(i=1;i<=M;i++)
{
betac[i]=bc[i]-(a[i]*c[i-1])/(betac[i-1]);
}
gamma[0]=d[0]/beta[0];
for(i=1;i<=M;i++)
{
gamma[i]=(d[i]-a[i]*gamma[i-1])/(beta[i]);
}
/*for(i=0;i<=M;i++)
{
printf("%0.6Lf\n",gamma[i]);
getch();
}*/
gammac[0]=dc[0]/betac[0];
for(i=1;i<=M;i++)
{
gammac[i]=(dc[i]-a[i]*gammac[i-1])/(betac[i]);
}
theta[M]=gamma[M];
i=M;
for(j=1;j<=M;j++)
{
theta[M-j]=(gamma[M-j])-((c[M-j]*theta[i])/(beta[M-j]));
i=i-1;
}
/*for(i=0;i<=M;i++)
{
printf("%0.6Lf\n",theta[i]);
getch();
}*/
thetac[M]=gammac[M];
i=M;
for(j=1;j<=M;j++)
{
```

```
thetac[M-j]=(gammac[M-j])-((c[M-j]*thetac[i])/(betac[M-j]));
i=i-1;
}
for(i=0;i<=M;i++)
{
T[i]=Tf-theta[i]*(Tf-T0);
}
/*printf("T\n");
for(i=0;i<=M;i++)
{
printf("%0.6Lf\n",T[i]);
getch();
}*/
for(i=0;i<=M;i++)
{
Tc[i]=Tf-thetac[i]*(Tf-T0);
}

/* Runge-Kutta method to find CB(-)*/      CG1      Cc1      CG2    Cc2");*/
/*printf("\neqn        t      T       CB
for(i=0;i<=M;i++)
{
while(1)
{
k1[i]=A1*exp((D1/T[i])+(L1/(T[i]*T[i])));
k2[i]=A2*exp((D2/Tc[i])+(L2/(Tc[i]*Tc[i])));
k3[i]=A3*exp(-E3/(Rc*Tc[i]));
a1=(-h)*((k1[i]+k2[i])*pow(CB[i],n1));
a2=(-h)*((k1[i]+k2[i])*pow((CB[i]+(a1/2.0)),n1));
a3=(-h)*((k1[i]+k2[i])*pow((CB[i]+(a2/2.0)),n1));
a4=(-h)*((k1[i]+k2[i])*pow((CB[i]+a3),n1));
CB[i]=CB[i]+(1.0/6.0)*(a1+2.0*a2+2.0*a3+a4);
if(CB[i]<0.0)
{
CB[i]=0.0000001;
}
if(t[i]>=(ft-h))
break;
t[i]=t[i]+h;
}
}
/*printf("CB(-)\n");
for(i=0;i<=M;i++)
{
printf("%0.6Lf\n",CB[i]);
getch();
```

```
}*/

/* Program of finite difference to find CG1(-) */
for(i=1;i<=M-1;i++)
{
aaa[i]=(((bf-1.0)*dtow*DG1[i])/(2.0*dx*x[i]*Le*vf[i]))
    -((dtow*DG1[i])/(dx*dx*Le*vf[i]));
x[i+1]=x[i]+dx;
}
aaa[M]=-((2.0*dtow*DG1[M])/(dx*dx*Le*vf[M]));
/*printf("aaa\n");
for(i=1;i<=M;i++)
{
printf("%0.6Lf\n",aaa[i]);
getch();
}*/
bbb[0]=((2.0*bf*dtow*DG1[0])/(dx*dx*Le*vf[0]))+(1.0);
for(i=1;i<=M-1;i++)
{
bbb[i]=((2.0*dtow*DG1[i])/(dx*dx*Le*vf[i]))+(1.0);
}
bbb[M]=(((bf-
1.0)*dtow*NshG1[M])/(Le*vf[M]))+((2.0*dtow*NshG1[M])/(dx*Le*vf[M]))
   +((2.0*dtow*DG1[M])/(dx*dx*Le*vf[M]))+(1.0);
/*printf("bbb\n");
for(i=0;i<=M;i++)
{
printf("%0.6Lf\n",bbb[i]);
getch();
}*/
ccc[0]=((-2.0*bf*dtow*DG1[0])/(dx*dx*Le*vf[0]));
for(i=1;i<=M-1;i++)
{
ccc[i]=(((bf-1.0)*(-dtow)*DG1[i])/(2.0*dx*x[i]*Le*vf[i]))
    -((dtow*DG1[i])/(dx*dx*Le*vf[i]));
x[i+1]=x[i]+dx;
}
/*printf("ccc\n");
for(i=0;i<=M-1;i++)
{
printf("%0.6Lf\n",ccc[i]);
getch();
}*/
/*printf("CB   CG1  Cc1   vf\n");
for(i=0;i<=M;i++)
{
```

```
printf("%0.6Lf %0.6Lf %0.6Lf\n",CB[i],CG1[i],vf[i]);
getch();
}*/
for(i=0;i<=M;i++)
{
dddcal2[i]=((dtow*R*R*k1[i]*pow(CB[i],n1))/(vf[i]*alpha));
dddcal3[i]=((dtow*R*R*k3[i]*(pow(CG1[i],n2))*(pow(Cc1[i],n3)))/(alpha));
}
/*printf("T   Tc[i]        k1     k3        dddcal2    dddcal3\n");
for(i=0;i<=M;i++)
{                                                    %0.11Lf          %0.11Lf
printf("%0.6Lf          %0.6Lf          %0.11Lf
%0.11Lf\n",T[i],Tc[i],k1[i],k3[i],dddcal2[i],dddcal3[i]);
getch();
}*/
for(i=0;i<=M;i++)
{
ddd[i]=CG1[i]+((dtow*R*R*k1[i]*pow(CB[i],n1))/(vf[i]*alpha))
   -((dtow*R*R*k3[i]*(pow(CG1[i],n2))*(pow(Cc1[i],n3)))/(alpha));
}
/*printf("ddd\n");
for(i=0;i<=M;i++)
{
printf("%0.9Lf\n",ddd[i]);
getch();
}*/
betaCG1[0]=bbb[0];
for(i=1;i<=M;i++)
{
betaCG1[i]=bbb[i]-(aaa[i]*ccc[i-1])/(betaCG1[i-1]);
}
/*printf("betaCG1\n");
for(i=0;i<=M;i++)
{
printf("%0.6Lf\n",betaCG1[i]);
getch();
}*/
gammaCG1[0]=ddd[0]/betaCG1[0];
for(i=1;i<=M;i++)
{
gammaCG1[i]=(ddd[i]-aaa[i]*gammaCG1[i-1])/(betaCG1[i]);
}
/*printf("aaa     ccc     ddd        betaCG1     gammaCG1\n");
for(i=0;i<=M;i++)
{
```

```
printf("%0.6Lf %0.6Lf %0.6Lf %0.6Lf
%0.6Lf\n",aaa[i],ccc[i],ddd[i],betaCG1[i],gammaCG1[i]);
getch();
}*/
CG1[M]=gammaCG1[M];
i=M;
for(j=1;j<=M;j++)
{
CG1[M-j]=(gammaCG1[M-j])-((ccc[M-j]*CG1[i])/(betaCG1[M-j]));
i=i-1;
}
/*printf("CG1\n");
for(i=0;i<=M;i++)
{
printf("%0.6Lf\n",CG1[i]);
getch();
}*/
for(i=0;i<=M;i++)
{
while(1)
{
k1[i]=A1*exp((D1/T[i])+(L1/(T[i]*T[i])));
k2[i]=A2*exp((D2/Tc[i])+(L2/(Tc[i]*Tc[i])));
k3[i]=A3*exp(-E3/(Rc*Tc[i]));
k3t[i]=k3[i]*pow(CG1[i],n2);
a1=(-h)*((k1[i]+k2[i])*pow(CB[i],n1));
c1=h*((k2[i]*pow(CB[i],n1))-(k3t[i]*pow(Cc1[i],n3)));
d1=h*(k3t[i]*pow(Cc1[i],n3));
e1=h*(k3t[i]*pow(Cc1[i],n3));
a2=(-h)*((k1[i]+k2[i])*pow((CB[i]+(a1/2.0)),n1));
c2=h*((k2[i]*pow((CB[i]+(a1/2.0)),n1))-(k3t[i]*pow((Cc1[i]+(c1/2.0)),n3)));
d2=h*(k3t[i]*pow((Cc1[i]+(c1/2.0)),n3));
e2=h*(k3t[i]*pow((Cc1[i]+(c1/2.0)),n3));
a3=(-h)*((k1[i]+k2[i])*pow((CB[i]+(a2/2.0)),n1));
c3=h*((k2[i]*pow((CB[i]+(a2/2.0)),n1))-(k3t[i]*pow((Cc1[i]+(c2/2.0)),n3)));
d3=h*(k3t[i]*pow((Cc1[i]+(c2/2.0)),n3));
e3=h*(k3t[i]*pow((Cc1[i]+(c2/2.0)),n3));
a4=(-h)*((k1[i]+k2[i])*pow((CB[i]+a3),n1));
c4=h*((k2[i]*pow((CB[i]+a3),n1))-(k3t[i]*pow((Cc1[i]+c3),n3)));
d4=h*(k3t[i]*pow((Cc1[i]+c3),n3));
e4=h*(k3t[i]*pow((Cc1[i]+c3),n3));
CB[i]=CB[i]+(1.0/6.0)*(a1+2.0*a2+2.0*a3+a4);
Cc1[i]=Cc1[i]+(1.0/6.0)*(c1+2.0*c2+2.0*c3+c4);
CG2[i]=CG2[i]+(1.0/6.0)*(d1+2.0*d2+2.0*d3+d4);
Cc2[i]=Cc2[i]+(1.0/6.0)*(e1+2.0*e2+2.0*e3+e4);
if(CB[i]<0.0)
```

```
{
CB[i]=0.0000001;
/*ss1[i]=CG1[i];
ss2[i]=Cc1[i];
ss3[i]=CG2[i];
ss4[i]=Cc2[i];*/
}

if(t[i]>=(ft-h))
break;
t[i]=t[i]+h;
}
}

/* Output */
/*for(i=0;i<=M;i++)
{
printf("\n%d      \t%0.6Lf      %0.6Lf      %0.6Lf      %0.6Lf      %0.6Lf      %0.6Lf
%0.6Lf",eqn[i],t[i],T[i],CB[i],CG1[i],Cc1[i],CG2[i],Cc2[i]);
getch();
}*/
printf("\neqn xx   t      T      Tc      CB      CG1     Cc1     CG2     Cc2  ");
xx=0.0;
for(i=0;i<=M;i=i+15)
{
/*CG1[i]=ss1[i];
Cc1[i]=ss2[i];
CG2[i]=ss3[i];
Cc2[i]=ss4[i];*/
printf("\n%d      %0.1Lf  %0.2Lf  %0.6Lf  %0.6Lf  %0.6Lf  %0.6Lf  %0.6Lf  %0.6Lf
%0.6Lf",eqn[i],xx,t[i],T[i
],Tc[i],CB[i],CG1[i],Cc1[i],CG2[i],Cc2[i]);
/*getch();*/
/*printf("\nk3 k3t\n");
printf("%0.6Lf %0.6Lf\n",k3[i],k3t[i]);
getch(); */
/*getch();*/
xx=xx+0.1;
}
printf("\nConversion=");
printf("%Lf",conversion[1]);
/*for(i=0;i<=M;i++)
{
if(CB[i]<0.0)
CB[i]=0.0000001;
}*/
```

```
getchar();
tow=tow+dtow;
if(CB[M]<=0.00000001)
if(CB[0]<=0.00000001)
break;
}
}
```

APPENDIX-E

E-1 Program for heat of reaction number

```
/* Program used in Chapter 6 */
/* Dominant design variables in pyrolysis of biomass particles of different geometries in
thermally thick regime */
#include<stdio.h>
#include<math.h>
#define M 150                    /* (M+1)=Total number of equations to be solved */
main()
{
long double T[M+2];              /* T=Temperature (K) */
long double CB[M+2];             /* CB=Concentration of biomass (kg/m3) */
long double k1[M+2];             /* k1=Rate constant for reaction 1 (1/s) */
long double k2[M+2];             /* k2=Rate constant for reaction 2 (1/s) */
long double k3[M+2];             /* k3=Rate constant for reaction 3 (1/s) */
int i;                           /* i=integer used in program */
int j;                           /* j=integer used in program */
int eqn[M+2];
long double xx;                  /* xx=used for output of dimensionless distance (-) */
long double R;                   /* R=radius of cylindrical pellet (m) */
long double A1;                  /* A1=Arrhenius frequency factor for reaction 1 (1/s) */
long double A2;                  /* A2=Arrhenius frequency factor for reaction 2 (1/s) */
long double A3;                  /* A3=Arrhenius frequency factor for reaction 3 (1/s) */
long double D1;                  /* D1=Constant used while calculating k1 (K) */
long double D2;                  /* D2=Constant used while calculating k2 (K) */
long double L1;                  /* L1=Constant used while calculating k1 (K2) */
long double L2;                  /* L2=Constant used while calculating k2 (K2) */
long double E3;                  /* E3=Activation energy (J/gmol) */
long double Rc;                  /* Rc=Universal gas constant (J/gmol K)*/
long double Cc1[M+2];            /* Cc1=Concentration of char 1 (-) */
long double CG1[M+2];            /* CG1=Concentration of volatile 1 (-) */
long double Cc2[M+2];            /* Cc2=Concentration of char 2 (-) */
long double CG2[M+2];            /* CG2=Concentration of volatile 2 (-) */
```

```
long double t[M+2];          /* t=Time (s) */
long double n1;              /* n1=Order of reaction 1 (-) */
long double n2;              /* n2=Order of reaction 2 (-) */
long double n3;              /* n3=Order of reaction 3 (-) */
long double h;               /* h=step size for RK4 Method (s) */
long double a1;
long double b1;
long double c1;
long double d1;
long double e1;
long double a2;
long double b2;
long double c2;
long double d2;
long double e2;              /*a1-e4=Variables used while solving rk4 method */
long double a3;
long double b3;
long double c3;
long double d3;
long double e3;
long double a4;
long double b4;
long double c4;
long double d4;
long double e4;
long double dtow;            /* dtow=Dimensionless time step for finite difference
                             method (-) */
long double tow;             /* tow = Dimensionless time for finite difference method */
long double dx;              /*  dx=Dimensionless radial distance step for finite
                             difference method (-) */
long double T0;              /* T0=Initial temperature (K) */
long double Tf;              /* Tf=Final temperature (K) */
long double ht;              /* ht=convective heat transfer coefficient (W/m2K) */
long double ab;              /* ab=emissivity coefficient */
/*long double sig;*/         /* sig=Stefan Boltzmann constant */
long double dH;              /* dH=heat of reaction (kJ/kg) */
long double k[M+2];          /* k=thermal conductivity (W/m K) */
long double H[M+2];          /* H=modified Biot Number */
long double cp[M+2];         /* cp=specific heat (J/kg K) */
long double ro[M+2];         /* ro=density (kg/m3) */
long double Q[M+2];          /* Q=heat of reaction number (m3/kg) */
long double x[M+2];          /* x=Dimensionless radial distance (-) */
long double a[M+2];          /* a-d=Variables used in assigning values in tridiagonal
long double b[M+2];          matrix */

long double c[M+2];
```

```
long double d[M+2];
long double theta[M+2];     /* theta=Dimensionless temperature (-) */
long double beta[M+2];      /* beta=used while calculating theta (-) */
long double gamma[M+2];     /* gamma=used while calculating theta (-) */
long double alpha;          /* alpha=used while calculating theta (-) */
long double ft;             /* ft=conversion of dimensionless time second (s) */
long double roin;           /* roin=initial value of density (kg/m3) */
long double jj;
long double kk;
long double ll;             /* jj-bb=Variable used while calculating the value of H */
long double aa;
long double mm;
long double bb;
long double Hc[M+2];
long double kc[M+2];
long double Tc[M+2];
long double Qc[M+2];
long double cpc[M+2];
long double bc[M+2];        /* From Hc-bbc the 'c' is used for char */
long double dc[M+2];
long double thetac[M+2];
long double betac[M+2];
long double gammac[M+2];
long double jjc;
long double kkc;
long double llc;
long double aac;
long double mmc;
long double bbc;
long double sum[M+2];       /* To find the sum of biomass at a particular time */
long double avg[M+2];       /* To find the average of biomass at a particular time */
long double conversion[M+2]; /* To find the conversion of biomass*/
long double bf;             /* bf=geometry factor(slab=1;cylinder=2;sphere=3)
/*long double ss1[M+2];
long double ss2[M+2];
long double ss3[M+2];
long double ss4[M+2];*/

/*Constants*/
/*R=0.005;*/
A1=9.973*pow(10.0,-5.0);
A2=1.068*pow(10.0,-3.0);
A3=5.7*pow(10.0,5.0);
D1=17254.4;
D2=10224.4;
L1=-9061227.0;
```

```
L2=-6123081.0;
E3=81000.0;
Rc=8.314;
dx=(1.0/M);
x[1]=(1.0/M);
/*ht=8.4;
ab=0.95;*/
/*sig=5.67*pow(10.0,-8.0);*/
roin=650.0;
dH=-255000.0;
alpha=1.79*pow(10.0,-7.0);
sum[0]=0.0;
/*n1=0.0;
n2=1.5;
n3=1.5;
h=0.01;
tow=0.010024;
dtow=0.010024;
T0=473.0;
Tf=873.0;*/
eqn[0]=1;
for(i=0;i<=M;i++)
{
eqn[i+1]=eqn[i]+1;
}
/*printf("%d",eqn[M]);
getchar();*/
/*printf("%Lf %Lf\n",dx,x[1]);
getchar();*/

/* Input */
printf("Enter the orders of reactions n1,n2,n3 (0,1.5,1.5)\n");
scanf("%Lf %Lf %Lf",&n1,&n2,&n3);
printf("Enter the value of time step h(t) for RK4 method (0.01)\n");
scanf("%Lf",&h);
printf("Enter the value of geometry factor i.e.bf(slab=1;cylinder=2;sphere=3)\n");
scanf("%Lf",&bf);
printf("Enter the value R (Half the thickness of slab,radius for cylinder & sphere)\n");
scanf("%Lf",&R);
printf("The value of tow can be calculated by the following formula:\n");
printf("t=(tow*R*R)/(alpha)\n");
printf("Here alpha is known i.e. alpha=1.79*pow(10.0,-7.0)\n");
printf("Suppose you want that your output come after every 1sec\n");
printf("Then t=1sec and say R=0.005m,then tow comes out to be 0.00716\n");
printf("Enter the initial value of time step i.e.tow (dimensionless) for\n");
printf("finite difference method \n");
```

```
scanf("%Lf",&tow);
printf("Enter the value of dtow(Its value is same as initial value of tow)\n");
scanf("%Lf",&dtow);
printf("Enter the initial value of temperature\n");
scanf("%Lf",&T0);
printf("Enter the final value of temperature\n");
scanf("%Lf",&Tf);
printf("\n There are following cases:\n");
printf("\n");
printf("(1) Convection and radiation on wall surface\n");
printf("For this case, put ht=8.4 & ab=0.95\n");
printf("(2) No convection on wall surface (Radiation only)\n");
printf("For this case, put ht=0 & ab=0.95\n");
printf("(3) No radiation on wall surface (Convection only)\n");
printf("For this case, put ht=8.4 & ab=0\n");
printf("(4) No radiation on wall surface (10 Times Convection)\n");
printf("For this case, put ht=84.0 & ab=0\n");
printf("\n");
printf("Read the above cases and then press enter key to continue\n");
getchar();
printf("\nNow enter the value according to the above cases\n");
printf("\n");
printf("Enter the value of convective heat transfer coefficient (ht=8.4)\n");
printf("ht=");
scanf("%Lf",&ht);
printf("Enter the value of emissivity coefficient (ab=0.95)\n");
printf("ab=");
scanf("%Lf",&ab);
printf("Enter the value of Heat of Reaction number(Q)\n");
printf("Q=");
scanf("%Lf",&Q);

/* Initial condition */
for(i=0;i<=M;i++)
{
CB[i]=1.0;
Cc1[i]=0.0;
CG1[i]=0.0;
Cc2[i]=0.0;
CG2[i]=0.0;
/*T[i]=473.0;*/
t[i]=h;
theta[i]=1.0;
thetac[i]=1.0;
}
for(i=0;i<=M;i++)
```

```
{
T[i]=T0;
}
for(i=0;i<=M;i++)
{
Tc[i]=T0;
}
/*printf("%0.6Lf\n",T[1]);
getchar();*/
/*for(i=0;i<=M;i++)
{
printf("%0.6Lf\n",T[i]);
getchar();
}*/

/* Program of finite difference method based on pure implicit scheme*/

while(1)
{
/*printf("%0.6Lf\n",R);
getchar();
printf("%0.6Lf %0.6Lf\n",Tf,R);
getchar();*/
for(i=0;i<=M;i++)
{
sum[i+1]=sum[i]+CB[i];
}
avg[1]=sum[M+1]/(M+1);
conversion[1]=(1.0-avg[1])/(1.0);
/*printf("%Lf %Lf %Lf\n",sum[M+1],avg[1],conversion[1]);
getchar();*/
k[M]=0.13+0.0003*(T[M]-273.0);
jj=pow(T[M],3.0);
kk=pow(T[M],2.0)*Tf;
ll=pow(Tf,2.0)*T[M];
mm=pow(Tf,3.0);
bb=(5.67*pow(10.0,-8.0))*(ab);
aa=ht+(bb*(jj+kk+ll+mm));
H[M]=(R/k[M])*(aa);
/*printf("%0.6Lf %0.6Lf %0.6Lf %0.6Lf  %0.6Lf %0.16Lf",jj,kk,ll,mm,aa,bb);
getchar();*/
kc[M]=0.08-0.0001*(Tc[M]-273.0);
jjc=pow(Tc[M],3.0);
kkc=pow(Tc[M],2.0)*Tf;
llc=pow(Tf,2.0)*Tc[M];
mmc=pow(Tf,3.0);
```

```
bbc=(5.67*pow(10.0,-8.0))*(ab);
aac=ht+(bbc*(jjc+kkc+llc+mmc));
Hc[M]=(R/kc[M])*(aac);
ft=(tow*pow(R,2.0))/(alpha);
/*printf("The value of k[M],H[M],ft\n");
printf("\n%0.6Lf %0.6Lf %0.6Lf",k[M],H[M],ft);
getchar();
getchar();
printf("\n%0.6Lf %0.6Lf %d %0.6Lf",Tf,R,M,T[0]);
getchar();*/
for(i=0;i<=M;i++)
{
/*cp[i]=1112.0+4.85*(T[i]-273.0);
ro[i]=roin*(CB[i]+Cc1[i]+Cc2[i]);
Q[i]=((-dH)+(cp[i]*T[i]))/(ro[i]*cp[i]*(Tf-T0));*/
k1[i]=A1*exp((D1/T[i])+(L1/(T[i]*T[i])));
}
/*for(i=0;i<=M;i++)
{
printf("\n%0.6Lf %0.6Lf %0.6Lf %0.10Lf",cp[i],ro[i],Q[i],k1[i]);
getchar();
}*/
/*for(i=0;i<=M;i++)
{
cpc[i]=1003.2+2.09*(Tc[i]-273.0);
Qc[i]=((-dH)+(cpc[i]*Tc[i]))/(ro[i]*cpc[i]*(Tf-T0));
}*/
for(i=1;i<=M-1;i++)
{
a[i]=(((bf-1.0)*(dtow))/(2.0*dx*x[i]))-((dtow)/(dx*dx));
x[i+1]=x[i]+dx;
}
a[M]=((-2.0*dtow)/(dx*dx));

/*for(i=1;i<=M;i++)
{
printf("%0.6Lf\n",a[i]);
getchar();
}*/
b[0]=(((2.0*bf*dtow)/(dx*dx))+(1.0));
for(i=1;i<=M-1;i++)
{
b[i]=((2.0*dtow)/(dx*dx)+1.0);
}
b[M]=(((2.0*dtow)/(dx*dx))+(1.0)+((2.0*dtow*H[M])/(dx))+((bf-1.0)*dtow*H[M]));
/*for(i=0;i<=M;i++)
```

```
{
printf("%0.6Lf\n",b[i]);
getchar();
}*/
bc[0]=(((2.0*bf*dtow)/(dx*dx))+(1.0));
for(i=1;i<=M-1;i++)
{
bc[i]=((2.0*dtow)/(dx*dx)+1.0);
}
bc[M]=(((2.0*dtow)/(dx*dx))+(1.0)+((2.0*dtow*Hc[M])/(dx))+((bf-1.0)*dtow*Hc[M]));
c[0]=(-2.0*bf*dtow)/(dx*dx);
for(i=1;i<=M-1;i++)
{
c[i]=((((bf-1.0)*(-dtow))/(2.0*dx*x[i]))-((dtow)/(dx*dx)));
x[i+1]=x[i]+dx;
}
/*for(i=0;i<=M-1;i++)
{
printf("%0.6Lf\n",c[i]);
getchar();
}*/
for(i=0;i<=M;i++)
{
d[i]=(theta[i])+((dtow*Q*R*R*k1[i])/(alpha));
}
/*for(i=0;i<=M;i++)
{
printf("%0.9Lf\n",d[i]);
getchar();
}*/
for(i=0;i<=M;i++)
{
dc[i]=(thetac[i])+((dtow*Q*R*R*k1[i])/(alpha));
}
beta[0]=b[0];
for(i=1;i<=M;i++)
{
beta[i]=b[i]-(a[i]*c[i-1])/(beta[i-1]);
}
/*for(i=0;i<=M;i++)
{
printf("%0.6Lf\n",beta[i]);
getchar();
}*/
betac[0]=bc[0];
for(i=1;i<=M;i++)
```

```
{
betac[i]=bc[i]-(a[i]*c[i-1])/(betac[i-1]);
}
gamma[0]=d[0]/beta[0];
for(i=1;i<=M;i++)
{
gamma[i]=(d[i]-a[i]*gamma[i-1])/(beta[i]);
}
/*for(i=0;i<=M;i++)
{
printf("%0.6Lf\n",gamma[i]);
getchar();
}*/
gammac[0]=dc[0]/betac[0];
for(i=1;i<=M;i++)
{
gammac[i]=(dc[i]-a[i]*gammac[i-1])/(betac[i]);
}
theta[M]=gamma[M];
i=M;
for(j=1;j<=M;j++)
{
theta[M-j]=(gamma[M-j])-((c[M-j]*theta[i])/(beta[M-j]));
i=i-1;
}
/*for(i=0;i<=M;i++)
{
printf("%0.6Lf\n",theta[i]);
getchar();
}*/
thetac[M]=gammac[M];
i=M;
for(j=1;j<=M;j++)
{
thetac[M-j]=(gammac[M-j])-((c[M-j]*thetac[i])/(betac[M-j]));
i=i-1;
}
for(i=0;i<=M;i++)
{
T[i]=Tf-theta[i]*(Tf-T0);
}
/*printf("T\n");
for(i=0;i<=M;i++)
{
printf("%0.6Lf\n",T[i]);
getchar();
```

```
}*/
for(i=0;i<=M;i++)
{ Tc[i]=Tf-thetac[i]*(Tf-T0);
}

/* Runge-Kutta method starts here */

/*printf("\neqn        t       T       CB      CG1      Cc1      CG2     Cc2");*/

for(i=0;i<=M;i++)
{ while(1)
{
k1[i]=A1*exp((D1/T[i])+(L1/(T[i]*T[i])));
k2[i]=A2*exp((D2/Tc[i])+(L2/(Tc[i]*Tc[i])));
k3[i]=A3*exp(-E3/(Rc*Tc[i]));
a1=(-h)*((k1[i]+k2[i])*pow(CB[i],n1));
b1=h*((k1[i]*pow(CB[i],n1))-(k3[i]*pow(CG1[i],n2)*pow(Cc1[i],n3)));
c1=h*((k2[i]*pow(CB[i],n1))-(k3[i]*pow(CG1[i],n2)*pow(Cc1[i],n3)));
d1=h*(k3[i]*pow(CG1[i],n2)*pow(Cc1[i],n3));
e1=h*(k3[i]*pow(CG1[i],n2)*pow(Cc1[i],n3));
a2=(-h)*((k1[i]+k2[i])*pow((CB[i]+(a1/2.0)),n1));
b2=h*((k1[i]*pow((CB[i]+(a1/2.0)),n1))-
(k3[i]*pow((CG1[i]+(b1/2.0)),n2)*pow((Cc1[i]+(c1/2.0)),n3)));
c2=h*((k2[i]*pow((CB[i]+(a1/2.0)),n1))-
(k3[i]*pow((CG1[i]+(b1/2.0)),n2)*pow((Cc1[i]+(c1/2.0)),n3)));
d2=h*(k3[i]*pow((CG1[i]+(b1/2.0)),n2)*pow((Cc1[i]+(c1/2.0)),n3));
e2=h*(k3[i]*pow((CG1[i]+(b1/2.0)),n2)*pow((Cc1[i]+(c1/2.0)),n3));
a3=(-h)*((k1[i]+k2[i])*pow((CB[i]+(a2/2.0)),n1));
b3=h*((k1[i]*pow((CB[i]+(a2/2.0)),n1))-
(k3[i]*pow((CG1[i]+(b2/2.0)),n2)*pow((Cc1[i]+(c2/2.0)),n3)));
c3=h*((k2[i]*pow((CB[i]+(a2/2.0)),n1))-
(k3[i]*pow((CG1[i]+(b2/2.0)),n2)*pow((Cc1[i]+(c2/2.0)),n3)));
d3=h*(k3[i]*pow((CG1[i]+(b2/2.0)),n2)*pow((Cc1[i]+(c2/2.0)),n3));
e3=h*(k3[i]*pow((CG1[i]+(b2/2.0)),n2)*pow((Cc1[i]+(c2/2.0)),n3));
a4=(-h)*((k1[i]+k2[i])*pow((CB[i]+a3),n1));
b4=h*((k1[i]*pow((CB[i]+a3),n1))-(k3[i]*pow((CG1[i]+b3),n2)*pow((Cc1[i]+c3),n3)));
c4=h*((k2[i]*pow((CB[i]+a3),n1))-(k3[i]*pow((CG1[i]+b3),n2)*pow((Cc1[i]+c3),n3)));
d4=h*(k3[i]*pow((CG1[i]+b3),n2)*pow((Cc1[i]+c3),n3));
e4=h*(k3[i]*pow((CG1[i]+b3),n2)*pow((Cc1[i]+c3),n3));
CB[i]=CB[i]+(1.0/6.0)*(a1+2.0*a2+2.0*a3+a4);
CG1[i]=CG1[i]+(1.0/6.0)*(b1+2.0*b2+2.0*b3+b4);
Cc1[i]=Cc1[i]+(1.0/6.0)*(c1+2.0*c2+2.0*c3+c4);
CG2[i]=CG2[i]+(1.0/6.0)*(d1+2.0*d2+2.0*d3+d4);
Cc2[i]=Cc2[i]+(1.0/6.0)*(e1+2.0*e2+2.0*e3+e4);
if(CB[i]<0.0)
{
CB[i]=0.0000001;
```

```
/*ss1[i]=CG1[i];
ss2[i]=Cc1[i];
ss3[i]=CG2[i];
ss4[i]=Cc2[i];*/
}
if(t[i]>=(ft-h))
break;
t[i]=t[i]+h;
}
}

/* Output */
/*for(i=0;i<=M;i++)
{
printf("\n%d      \t%0.6Lf      %0.6Lf      %0.6Lf      %0.6Lf      %0.6Lf
%0.6Lf",eqn[i],t[i],T[i],CB[i],CG1[i],Cc1[i],CG2[i],Cc2[i]);
getchar();
}*/
printf("\neqn    xx    t      T      CB     CG1    Cc1    CG2    Cc2  "):
xx=0.0;
for(i=0;i<=M;i=i+15)
{
/*CG1[i]=ss1[i];
Cc1[i]=ss2[i];
CG2[i]=ss3[i];
Cc2[i]=ss4[i];*/
printf("\n%d      \t%0.1Lf      %0.6Lf  %0.6Lf  %0.6Lf  %0.6Lf  %0.6Lf  %0.6Lf
%0.6Lf",eqn[i],xx,t[i],T[i
],CB[i],CG1[i],Cc1[i],CG2[i],Cc2[i]):
/*getchar();*/
xx=xx+0.1;
}
printf("\nConversion=");
printf("%Lf",conversion[1]);
/*for(i=0;i<=M;i++)
{
if(CB[i]<0.0)
CB[i]=0.0000001;
}*/
getchar();
tow=tow+dtow;
if(CB[M]<=0.00000001)
if(CB[0]<=0.00000001)
break;
}
}
```

E-2 Program for thermal conductivity of biomass

```
/* Program used in Chapter 6 */
/* Dominant design variables in pyrolysis of biomass particles of different geometries in
thermally thick regime */
#include<stdio.h>
#include<math.h>
#define M 150                    /* (M+1)=Total number of equations to be solved */
main()
{
long double T[M+2];              /* T=Temperature (K) */
long double CB[M+2];             /* CB=Concentration of biomass (kg/m3) */
long double k1[M+2];             /* k1=Rate constant for reaction 1 (1/s) */
long double k2[M+2];             /* k2=Rate constant for reaction 2 (1/s) */
long double k3[M+2];             /* k3=Rate constant for reaction 3 (1/s) */
int i;                           /* i=integer used in program */
int j;                           /* j=integer used in program */
int eqn[M+2];
long double xx;                  /* xx=used for output of dimensionless distance (-) */
long double R;                   /* R=radius of cylindrical pellet (m) */
long double A1;                  /* A1=Arrhenius frequency factor for reaction 1 (1/s) */
long double A2;                  /* A2=Arrhenius frequency factor for reaction 2 (1/s) */
long double A3;                  /* A3=Arrhenius frequency factor for reaction 3 (1/s) */
long double D1;                  /* D1=Constant used while calculating k1 (K) */
long double D2;                  /* D2=Constant used while calculating k2 (K) */
long double L1;                  /* L1=Constant used while calculating k1 (K2) */
long double L2;                  /* L2=Constant used while calculating k2 (K2) */
long double E3;                  /* E3=Activation energy (J/gmol) */
long double Rc;                  /* Rc=Universal gas constant (J/gmol K)*/
long double Cc1[M+2];            /* Cc1=Concentration of char 1 (-) */
long double CG1[M+2];            /* CG1=Concentration of volatile 1 (-) */
long double Cc2[M+2];            /* Cc2=Concentration of char 2 (-) */
long double CG2[M+2];            /* CG2=Concentration of volatile 2 (-) */
long double t[M+2];              /* t=Time (s) */
long double n1;                  /* n1=Order of reaction 1 (-) */
long double n2;                  /* n2=Order of reaction 2 (-) */
long double n3;                  /* n3=Order of reaction 3 (-) */
long double h;                   /* h=step size for RK4 Method (s) */
long double a1;
long double b1;
long double c1;
long double d1;
long double e1;
long double a2;
long double b2;
long double c2;
long double d2;
```

```
long double Hc[M+2];
long double kc[M+2];
long double Tc[M+2];
long double Qc[M+2];
long double cpc[M+2];
long double bc[M+2];
long double dc[M+2];          /* From Hc-bbc the 'c' is used for char */
long double thetac[M+2];
long double betac[M+2];
long double gammac[M+2];
long double jjc;
long double kkc;
long double llc;
long double aac;
long double mmc;
long double bbc;
long double sum[M+2];         /* To find the sum of biomass at a particular time */
long double avg[M+2];         /* To find the average of biomass at a particular time */
long double conversion[M+2];  /* To find the conversion of biomass*/
long double bf;               /* bf=geometry factor(slab=1;cylinder=2;sphere=3)
/*long double ss1[M+2];
long double ss2[M+2];
long double ss3[M+2];
long double ss4[M+2];*/

/*Constants*/
/*R=0.005;*/
A1=9.973*pow(10.0,-5.0);
A2=1.068*pow(10.0,-3.0);
A3=5.7*pow(10.0,5.0);
D1=17254.4;
D2=10224.4;
L1=-9061227.0;
L2=-6123081.0;
E3=81000.0;
Rc=8.314;
dx=(1.0/M);
x[1]=(1.0/M);
/*ht=8.4;
ab=0.95;*/
/*sig=5.67*pow(10.0,-8.0);*/
roin=650.0;
dH=-255000.0;
alpha=1.79*pow(10.0,-7.0);
sum[0]=0.0;
/*n1=0.0;
```

```
n2=1.5;
n3=1.5;
h=0.01;
tow=0.010024;
dtow=0.010024;
T0=473.0;
Tf=873.0;*/
eqn[0]=1;
for(i=0;i<=M;i++)
{
eqn[i+1]=eqn[i]+1;
}
/*printf("%d",eqn[M]);
getchar();*/
/*printf("%Lf %Lf\n",dx,x[1]);
getchar();*/

/* Input */
printf("Enter the orders of reactions n1,n2,n3 (0,1.5,1.5)\n");
scanf("%Lf %Lf %Lf",&n1,&n2,&n3);
printf("Enter the value of time step h(t) for RK4 method (0.01)\n");
scanf("%Lf",&h);
printf("Enter the value of geometry factor i.e.bf(slab=1;cylinder=2;sphere=3)\n");
scanf("%Lf",&bf);
printf("Enter the value R (Half the thickness of slab,radius for cylinder & sphere)\n");
scanf("%Lf",&R);
printf("The value of tow can be calculated by the following formula:\n");
printf("t=(tow*R*R)/(alpha)\n");
printf("Here alpha is known i.e. alpha=1.79*pow(10.0,-7.0)\n");
printf("Suppose you want that your output come after every 1sec\n");
printf("Then t=1sec and say R=0.005m.then tow comes out to be 0.00716\n");
printf("Enter the initial value of time step i.e.tow (dimensionless) for\n");
printf("finite difference method \n");
scanf("%Lf",&tow);
printf("Enter the value of dtow(Its value is same as initial value of tow)\n");
scanf("%Lf",&dtow);
printf("Enter the initial value of temperature\n");
scanf("%Lf",&T0);
printf("Enter the final value of temperature\n");
scanf("%Lf",&Tf);
printf("\n There are following cases:\n");
printf("\n");
printf("(1) Convection and radiation on wall surface\n");
printf("For this case, put ht=8.4 & ab=0.95\n");
printf("(2) No convection on wall surface (Radiation only)\n");
printf("For this case, put ht=0 & ab=0.95\n");
```

```
printf("(3) No radiation on wall surface (Convection only)\n");
printf("For this case, put ht=8.4 & ab=0\n");
printf("(4) No radiation on wall surface (10 Times Convection)\n");
printf("For this case, put ht=84.0 & ab=0\n");
printf("\n");
printf("Read the above cases and then press enter key to continue\n");
getchar();
printf("\nNow enter the value according to the above cases\n");
printf("\n");
printf("Enter the value of convective heat transfer coefficient (ht=8.4)\n");
printf("ht=");
scanf("%Lf",&ht);
printf("Enter the value of emissivity coefficient (ab=0.95)\n");
printf("ab=");
scanf("%Lf",&ab);
printf("Enter the value of thermal conductivity (kkw) of wood (W/m K)\n");
scanf("%Lf",&kkw);

/* Initial condition */

for(i=0;i<=M;i++)
{
CB[i]=1.0;
Cc1[i]=0.0;
CG1[i]=0.0;
Cc2[i]=0.0;
CG2[i]=0.0;
/*T[i]=473.0;*/
t[i]=h;
theta[i]=1.0;
thetac[i]=1.0;
}
for(i=0;i<=M;i++)
{
T[i]=T0;
}
for(i=0;i<=M;i++)
{
Tc[i]=T0;
}
/*printf("%0.6Lf\n",T[1]);
getchar();*/
/*for(i=0;i<=M;i++)
{
printf("%0.6Lf\n",T[i]);
getchar(); }*/
```

```
/* Program of finite difference method based on pure implicit scheme*/

while(1)
{
/*printf("%0.6Lf\n",R);
getchar();
printf("%0.6Lf %0.6Lf\n",Tf,R);
getchar();*/
for(i=0;i<=M;i++)
{
sum[i+1]=sum[i]+CB[i];
}
avg[1]=sum[M+1]/(M+1);
conversion[1]=(1.0-avg[1])/(1.0);
/*printf("%Lf %Lf %Lf\n",sum[M+1],avg[1],conversion[1]);
getchar();*/
/*k[M]=0.13+0.0003*(T[M]-273.0);*/
k[M]=kkw;
jj=pow(T[M],3.0);
kk=pow(T[M],2.0)*Tf;
ll=pow(Tf,2.0)*T[M];
mm=pow(Tf,3.0);
bb=(5.67*pow(10.0,-8.0))*(ab);
aa=ht+(bb*(jj+kk+ll+mm));
H[M]=(R/k[M])*(aa);
/*printf("%0.6Lf %0.6Lf %0.6Lf %0.6Lf  %0.6Lf %0.16Lf",jj,kk,ll,mm,aa,bb);
getchar();*/
kc[M]=0.08-0.0001*(Tc[M]-273.0);
jjc=pow(Tc[M],3.0);
kkc=pow(Tc[M],2.0)*Tf;
llc=pow(Tf,2.0)*Tc[M];
mmc=pow(Tf,3.0);
bbc=(5.67*pow(10.0,-8.0))*(ab);
aac=ht+(bbc*(jjc+kkc+llc+mmc));
Hc[M]=(R/kc[M])*(aac);
ft=(tow*pow(R,2.0))/(alpha);
/*printf("The value of k[M],H[M],ft\n");
printf("\n%0.6Lf %0.6Lf %0.6Lf",k[M],H[M],ft);
getchar();
getchar();
printf("\n%0.6Lf %0.6Lf %d %0.6Lf",Tf,R,M,T[0]);
getchar();*/
for(i=0;i<=M;i++)
{
cp[i]=1112.0+4.85*(T[i]-273.0);
```

```
ro[i]=roin*(CB[i]+Cc1[i]+Cc2[i]);
Q[i]=((-dH)+(cp[i]*T[i]))/(ro[i]*cp[i]*(Tf-T0));
k1[i]=A1*exp((D1/T[i])+(L1/(T[i]*T[i])));
}
/*for(i=0;i<=M;i++)
{
printf("\n%0.6Lf %0.6Lf %0.6Lf %0.10Lf",cp[i],ro[i],Q[i],k1[i]);
getchar();
}*/
for(i=0;i<=M;i++)
{
cpc[i]=1003.2+2.09*(Tc[i]-273.0);
Qc[i]=((-dH)+(cpc[i]*Tc[i]))/(ro[i]*cpc[i]*(Tf-T0));
}
for(i=1;i<=M-1;i++)
{
a[i]=(((bf-1.0)*(dtow))/(2.0*dx*x[i]))-((dtow)/(dx*dx));
x[i+1]=x[i]+dx;
}
a[M]=((-2.0*dtow)/(dx*dx));
/*for(i=1;i<=M;i++)
{
printf("%0.6Lf\n",a[i]);
getchar();
}*/
b[0]=(((2.0*bf*dtow)/(dx*dx))+(1.0));
for(i=1;i<=M-1;i++)
{
b[i]=((2.0*dtow)/(dx*dx)+1.0);
}
b[M]=(((2.0*dtow)/(dx*dx))+(1.0)+((2.0*dtow*H[M])/(dx))+((bf-1.0)*dtow*H[M]));
/*for(i=0;i<=M;i++)
{
printf("%0.6Lf\n",b[i]);
getchar();
}*/
bc[0]=(((2.0*bf*dtow)/(dx*dx))+(1.0));
for(i=1;i<=M-1;i++)
{
bc[i]=((2.0*dtow)/(dx*dx)+1.0);
}
bc[M]=(((2.0*dtow)/(dx*dx))+(1.0)+((2.0*dtow*Hc[M])/(dx))+((bf-1.0)*dtow*Hc[M]));
c[0]=(-2.0*bf*dtow)/(dx*dx);
for(i=1;i<=M-1;i++)
{
c[i]=((((bf-1.0)*(-dtow))/(2.0*dx*x[i]))-((dtow)/(dx*dx)));
```

```
x[i+1]=x[i]+dx;
}
/*for(i=0;i<=M-1;i++)
{
printf("%0.6Lf\n",c[i]);
getchar();
}*/
for(i=0;i<=M;i++)
{
d[i]=(theta[i])+((dtow*Q[i]*R*R*k1[i]*pow((roin*CB[i]),n1))/(alpha));
}
/*for(i=0;i<=M;i++)
{
printf("%0.9Lf\n",d[i]);
getchar();
}*/
for(i=0;i<=M;i++)
{
dc[i]=(thetac[i])+((dtow*Qc[i]*R*R*k1[i]*pow((roin*CB[i]),n1))/(alpha));
}
beta[0]=b[0];
for(i=1;i<=M;i++)
{
beta[i]=b[i]-(a[i]*c[i-1])/(beta[i-1]);
}
/*for(i=0;i<=M;i++)
{
printf("%0.6Lf\n",beta[i]);
getchar();
}*/
betac[0]=bc[0];
for(i=1;i<=M;i++)
{
betac[i]=bc[i]-(a[i]*c[i-1])/(betac[i-1]);
}
gamma[0]=d[0]/beta[0];
for(i=1;i<=M;i++)
{
gamma[i]=(d[i]-a[i]*gamma[i-1])/(beta[i]);
}
/*for(i=0;i<=M;i++)
{
printf("%0.6Lf\n",gamma[i]);
getchar();
}*/
gammac[0]=dc[0]/betac[0];
```

```
for(i=1;i<=M;i++)
{
gammac[i]=(dc[i]-a[i]*gammac[i-1])/(betac[i]);
}
theta[M]=gamma[M];
i=M;
for(j=1;j<=M;j++)
{
theta[M-j]=(gamma[M-j])-((c[M-j]*theta[i])/(beta[M-j]));
i=i-1;
}
/*for(i=0;i<=M;i++)
{
printf("%0.6Lf\n",theta[i]);
getchar();
}*/
thetac[M]=gammac[M];
i=M;
for(j=1;j<=M;j++)
{
thetac[M-j]=(gammac[M-j])-((c[M-j]*thetac[i])/(betac[M-j]));
i=i-1;
}
for(i=0;i<=M;i++)
{
T[i]=Tf-theta[i]*(Tf-T0);
}
/*printf("T\n");
for(i=0;i<=M;i++)
{
printf("%0.6Lf\n",T[i]);
getchar();
}*/
for(i=0;i<=M;i++)
{
Tc[i]=Tf-thetac[i]*(Tf-T0);
}

/* Runge-Kutta method starts here */                    CG2    Cc2");*/

/*printf("\neqn        t      T       CB      CG1       Cc1
for(i=0;i<=M;i++)
{
while(1)
{
```

```
k1[i]=A1*exp((D1/T[i])+(L1/(T[i]*T[i])));
k2[i]=A2*exp((D2/Tc[i])+(L2/(Tc[i]*Tc[i])));
k3[i]=A3*exp(-E3/(Rc*Tc[i]));
a1=(-h)*((k1[i]+k2[i])*pow(CB[i],n1));
b1=h*((k1[i]*pow(CB[i],n1))-(k3[i]*pow(CG1[i],n2)*pow(Cc1[i],n3)));
c1=h*((k2[i]*pow(CB[i],n1))-(k3[i]*pow(CG1[i],n2)*pow(Cc1[i],n3)));
d1=h*(k3[i]*pow(CG1[i],n2)*pow(Cc1[i],n3));
e1=h*(k3[i]*pow(CG1[i],n2)*pow(Cc1[i],n3));
a2=(-h)*((k1[i]+k2[i])*pow((CB[i]+(a1/2.0)),n1));
b2=h*((k1[i]*pow((CB[i]+(a1/2.0)),n1))-
(k3[i]*pow((CG1[i]+(b1/2.0)),n2)*pow((Cc1[i]+(c1/2.0)),n3)));
c2=h*((k2[i]*pow((CB[i]+(a1/2.0)),n1))-
(k3[i]*pow((CG1[i]+(b1/2.0)),n2)*pow((Cc1[i]+(c1/2.0)),n3)));
d2=h*(k3[i]*pow((CG1[i]+(b1/2.0)),n2)*pow((Cc1[i]+(c1/2.0)),n3));
e2=h*(k3[i]*pow((CG1[i]+(b1/2.0)),n2)*pow((Cc1[i]+(c1/2.0)),n3));
a3=(-h)*((k1[i]+k2[i])*pow((CB[i]+(a2/2.0)),n1));
b3=h*((k1[i]*pow((CB[i]+(a2/2.0)),n1))-
(k3[i]*pow((CG1[i]+(b2/2.0)),n2)*pow((Cc1[i]+(c2/2.0)),n3)));
c3=h*((k2[i]*pow((CB[i]+(a2/2.0)),n1))-
(k3[i]*pow((CG1[i]+(b2/2.0)),n2)*pow((Cc1[i]+(c2/2.0)),n3)));
d3=h*(k3[i]*pow((CG1[i]+(b2/2.0)),n2)*pow((Cc1[i]+(c2/2.0)),n3));
e3=h*(k3[i]*pow((CG1[i]+(b2/2.0)),n2)*pow((Cc1[i]+(c2/2.0)),n3));
a4=(-h)*((k1[i]+k2[i])*pow((CB[i]+a3),n1));
b4=h*((k1[i]*pow((CB[i]+a3),n1))-(k3[i]*pow((CG1[i]+b3),n2)*pow((Cc1[i]+c3),n3)));
c4=h*((k2[i]*pow((CB[i]+a3),n1))-(k3[i]*pow((CG1[i]+b3),n2)*pow((Cc1[i]+c3),n3)));
d4=h*(k3[i]*pow((CG1[i]+b3),n2)*pow((Cc1[i]+c3),n3));
e4=h*(k3[i]*pow((CG1[i]+b3),n2)*pow((Cc1[i]+c3),n3));
CB[i]=CB[i]+(1.0/6.0)*(a1+2.0*a2+2.0*a3+a4);
CG1[i]=CG1[i]+(1.0/6.0)*(b1+2.0*b2+2.0*b3+b4);
Cc1[i]=Cc1[i]+(1.0/6.0)*(c1+2.0*c2+2.0*c3+c4);
CG2[i]=CG2[i]+(1.0/6.0)*(d1+2.0*d2+2.0*d3+d4);
Cc2[i]=Cc2[i]+(1.0/6.0)*(e1+2.0*e2+2.0*e3+e4);
if(CB[i]<0.0)
{
CB[i]=0.0000001;
/*ss1[i]=CG1[i];
ss2[i]=Cc1[i];
ss3[i]=CG2[i];
ss4[i]=Cc2[i];*/
}
if(t[i]>=(ft-h))
break;
t[i]=t[i]+h;
}
}
```

```
/* Output */

/*for(i=0;i<=M;i++)
{
printf("\n%d      \t%0.6Lf      %0.6Lf      %0.6Lf      %0.6Lf      %0.6Lf      %0.6Lf
%0.6Lf",eqn[i],t[i],T[i],CB[i],CG1[i],Cc1[i],CG2[i],Cc2[i]);
getchar();
}*/
printf("\neqn    xx    t      T      CB      CG1    Cc1    CG2    Cc2  ");
xx=0.0;
for(i=0;i<=M;i=i+15)
{
/*CG1[i]=ss1[i];
Cc1[i]=ss2[i];
CG2[i]=ss3[i];
Cc2[i]=ss4[i];*/
printf("\n%d      \t%0.1Lf      %0.6Lf  %0.6Lf  %0.6Lf  %0.6Lf  %0.6Lf  %0.6Lf
%0.6Lf",eqn[i],xx,t[i],T[i
],CB[i],CG1[i],Cc1[i],CG2[i],Cc2[i]);
/*getchar();*/
xx=xx+0.1;
}
/*avgCB=0.0;
for(i=0;i<=M;i=i+15)
{
avgCB=avgCB+CB[i];
}
avgCB=((avgCB)/(11.0));
avgCG1=0.0;
for(i=0;i<=M;i=i+15)
{
avgCG1=avgCG1+CG1[i];
}
avgCG1=((avgCG1)/(11.0));
avgCc1=0.0;
for(i=0;i<=M;i=i+15)
{
avgCc1=avgCc1+Cc1[i];
}
avgCc1=((avgCc1)/(11.0));
avgCG2=0.0;
for(i=0;i<=M;i=i+15)
{
avgCG2=avgCG2+CG2[i];
}
avgCG2=((avgCG2)/(11.0));
```

```
avgCc2=0.0;
for(i=0;i<=M;i=i+15)
{
avgCc2=avgCc2+Cc2[i];
}
avgCc2=((avgCc2)/(11.0));
printf("\nConversion avgCB  avgCG1   avgCc1   avgCG2  avgCc2");
printf("\n%0.6Lf          %0.6Lf          %0.6Lf          %0.6Lf          %0.6Lf
%0.6Lf",conversion[1],avgCB,avgCG1,
avgCc1,avgCG2,avgCc2); */
printf("\nConversion");
printf("\n%0.6Lf",conversion[1]);
/*for(i=0;i<=M;i++)
{
if(CB[i]<0.0)
CB[i]=0.0000001;
}*/
getchar();
tow=tow+dtow;
if(CB[M]<=0.00000001)
if(CB[0]<=0.00000001)
break;
}
}
```

APPENDIX-F

F-1 Program for model with shrinkage

```
/* Program used in Chapter 7 */
/* Heat transfer and kinetics in the pyrolysis of shrinking biomass particle */
#include<stdio.h>
#include<math.h>
#define M 150                    /* (M+1)=Total number of equations to be solved */
main()
{
long double T[M+2];              /* T=Temperature (K) */
long double CB[M+2];             /* CB=Concentration of biomass (kg/m3) */
long double k1[M+2];             /* k1=Rate constant for reaction 1 (1/s) */
long double k2[M+2];             /* k2=Rate constant for reaction 2 (1/s) */
long double k3[M+2];             /* k3=Rate constant for reaction 3 (1/s) */
int i;                           /* i=integer used in program */
int j;                           /* j=integer used in program */
int eqn[M+2];
long double xx;                  /* xx=used for output of dimensionless distance (-) */
long double R;                   /* R=radius of cylindrical pellet (m) */
long double A1;                  /* A1=Arrhenius frequency factor for reaction 1 (1/s) */
long double A2;                  /* A2=Arrhenius frequency factor for reaction 2 (1/s) */
long double A3;                  /* A3=Arrhenius frequency factor for reaction 3 (1/s) */
long double D1;                  /* D1=Constant used while calculating k1 (K) */
long double D2;                  /* D2=Constant used while calculating k2 (K) */
long double L1;                  /* L1=Constant used while calculating k1 (K2) */
long double L2;                  /* L2=Constant used while calculating k2 (K2) */
long double E3;                  /* E3=Activation energy (J/gmol) */
long double Rc;                  /* Rc=Universal gas constant (J/gmol K)*/
long double Cc1[M+2];            /* Cc1=Concentration of char 1 (-) */
long double CG1[M+2];            /* CG1=Concentration of volatile 1 (-) */
long double Cc2[M+2];            /* Cc2=Concentration of char 2 (-) */
long double CG2[M+2];            /* CG2=Concentration of volatile 2 (-) */
long double t[M+2];              /* t=Time (s) */
```

```
long double n1;          /* n1=Order of reaction 1 (-) */
long double n2;          /* n2=Order of reaction 2 (-) */
long double n3;          /* n3=Order of reaction 3 (-) */
long double h;           /* h=step size for RK4 Method (s) */
long double a1;
long double b1;
long double c1;
long double d1;
long double e1;
long double a2;
long double b2;
long double c2;
long double d2;
long double e2;          /*a1-e4=Variable used while solving RK4 method */
long double a3;
long double b3;
long double c3;
long double d3;
long double e3;
long double a4;
long double b4;
long double c4;
long double d4;
long double e4;
long double dtow;        /*dtow=Dimensionless time step for finite difference
                         method (-) */
long double tow;         /* tow=Dimensionless time for finite difference method */
long double dx;          /*dx=Dimensionless radial distance step for finite
                         difference method (-) */
long double T0;          /* T0=Initial temperature (K) */
long double Tf;          /* Tf=Final temperature (K) */
long double ht;          /* ht=convective heat transfer coefficient (W/m2K) */
long double ab;          /* ab=emissivity coefficient */
/*long double sig;*/     /* sig=Stefan Boltzmann constant */
long double dH;          /* dH=heat of reaction (kJ/kg) */
long double k[M+2];      /* k=thermal conductivity (W/m K) */
long double H[M+2];      /* H=modified Biot Number */
long double cp[M+2];     /* cp=specific heat (J/kg K) */
long double ro[M+2];     /* ro=density (kg/m3) */
long double Q[M+2];      /* Q=heat of reaction number (m3/kg) */
long double x[M+2];      /* x=Dimensionless radial distance (-) */
long double a[M+2];      /* a-d=Varible used in assigning values in tridiagonal
long double b[M+2];      matrix */

long double c[M+2];
long double d[M+2];
```

```
long double theta[M+2];      /* theta=Dimensionless temperature (-) */
long double beta[M+2];       /* beta=used while calculating theta (-) */
long double gamma[M+2];      /* gamma=used while calculating theta (-) */
long double alpha;           /* alpha=used while calculating theta (-) */
long double ft;              /* ft=conversion of dimensionless time second (s) */
long double roin;            /* roin=initial value of density (kg/m3) */
long double jj;
long double kk;
long double ll;              /* jj-bb=variable used while calculating the value of H */
long double aa;
long double mm;
long double bb;
/*long double Hc[M+2];*/
/*long double kc[M+2];*/
long double Tc[M+2];
long double Qc[M+2];
long double cpc[M+2];
long double bc[M+2];         /* From Hc-bbc the 'c' is used for char */
long double dc[M+2];
long double thetac[M+2];
long double betac[M+2];
long double gammac[M+2];
/*long double jjc;
long double kkc;
long double llc;
long double aac;
long double mmc;
long double bbc;*/
long double sum[M+2];        /* To find the sum of biomass at a particular time */
long double avg[M+2];        /* To find the average of biomass at a particular time */
long double conversion[M+2]; /* To find the conversion of biomass*/
long double bf;              /* bf=geometry factor(slab=1;cylinder=2;sphere=3)
/*long double ss1[M+2];
long double ss2[M+2];
long double ss3[M+2];
long double ss4[M+2];*/
long double length;          /* Length (Thickness) of slab (m) */
long double breadth;         /* Breadth of slab (m) */
long double height;          /* Height of slab (m) */
long double Vs0;             /* Initial volume of solid (wood and char) at any time t
                             (m3) */
long double Vs[M+2];         /* Volume of solid (wood and char) at any time t (m3) */
long double Vg0;             /* Initial volume occupied by volatiles and gases at any
                             time t (m3) */
long double Vg[M+2];         /* Volume occupied by volatiles and gases at any time t
                             (m3) */
```

```
long double Vgb[M+2],      /* Vgb=Vg/VB0 (-) */
long double VB0,           /* Initial volume of biomass (m3) */
long double V[M+2];        /* Volume of biomass at any time t (m3) */
long double Vb[M+2];       /* Vb=V/VB0 (-) */
long double dp;            /* Diameter of the pore or crack (m) */
long double MB0;           /* Initial mass of biomass (kg) */
long double MB[M+2];       /* Mass of biomass (wood) at any time t (kg) */
long double Mc[M+2];       /* Mass of the char at any time t (kg) */
long double rob[M+2];      /* Density of biomass at any time t (kg/m3) */
long double roc[M+2];      /* Density of char at any time t (kg/m3) */
long double shralpha;      /* Shrinkage factor */
long double shrbeta;       /* Shrinkage factor */
long double shrgamma;      /* Shrinkage factor */
long double eta[M+2];      /* Ratio of current to initial biomass (-) */
long double kB[M+2];       /* Thermal conductivity of biomass (W/mK) */
long double kc[M+2];       /* Thermal conductivity of char (W/mK) */
long double kg;            /* Thermal conductivity of gas and volatiles (W/mK) */
long double voidfr[M+2];   /* Void fraction (-) */

/*Constants*/
/*R=0.005;*/
A1=9.973*pow(10.0,-5.0);
A2=1.068*pow(10.0,-3.0);
A3=5.7*pow(10.0,5.0);
D1=17254.4;
D2=10224.4;
L1=-9061227.0;
L2=-6123081.0;
E3=81000.0;
Rc=8.314;
dx=(1.0/M);
x[1]=(1.0/M);
/*ht=8.4;
ab=0.95;*/
/*sig=5.67*pow(10.0,-8.0);*/
/*roin=650.0;*/
dH=-255000.0;
alpha=1.79*pow(10.0,-7.0);
sum[0]=0.0;
/*n1=0.0;
n2=1.5;
n3=1.5;
h=0.01;
tow=0.010024;
dtow=0.010024;
T0=473.0;
```

```
scanf("%Lf",&Tf);
printf("\n There are following cases:\n");
printf("\n");
printf("(1) Convection and radiation on wall surface\n");
printf("For this case, put ht=8.4 & ab=0.95\n");
printf("(2) No convection on wall surface (Radiation only)\n");
printf("For this case, put ht=0 & ab=0.95\n");
printf("(3) No radiation on wall surface (Convection only)\n");
printf("For this case, put ht=8.4 & ab=0\n");
printf("(4) No radiation on wall surface (10 Times Convection)\n");
printf("For this case, put ht=84.0 & ab=0\n");
printf("\n");
printf("Read the above cases and then press enter key to continue\n");
getchar();
printf("\n Now enter the value according to the above cases\n");
printf("\n");
printf("Enter the value of convective heat transfer coefficient (ht=8.4)\n");
printf("ht=");
scanf("%Lf",&ht);
printf("Enter the value of emissivity coefficient (ab=0.95)\n");
printf("ab=");
scanf("%Lf",&ab);
printf("Enter the value of initial density (roin=650,_ _ _ _)\n");
printf("roin=");
scanf("%Lf",&roin);
printf("Enter the value of diameter of pore (crack) [0.00002,_ _ _ _]\n");
printf("dp=");
scanf("%Lf",&dp);
printf("Enter the value of shrinkage factor i.e. shralpha, shrgamma and shrbeta\n");
scanf("%Lf %Lf %Lf",&shralpha,&shrgamma,&shrbeta);

/* Initial condition*/
for(i=0;i<=M;i++)
{
CB[i]=1.0;
Cc1[i]=0.0;
CG1[i]=0.0;
Cc2[i]=0.0;
CG2[i]=0.0;
/*T[i]=473.0;*/
t[i]=h;
theta[i]=1.0;
thetac[i]=1.0;
}
for(i=0;i<=M;i++)
{
```

```
T[i]=T0;
}
for(i=0;i<=M;i++)
{
Tc[i]=T0;
}
for(i=0;i<=M;i++)
{
Vb[i]=1.0;
Vgb[i]=0.5;
}
/*for(i=0;i<=M;i++)
{
printf("%0.6Lf %0.6Lf\n",Vb[i],Vgb[i]);
getchar();
}*/
if(bf==1)
VB0=length*breadth*height;
else
if(bf==2)
VB0=31.416*R*R*R;
else
VB0=(4.0/3.0)*3.1416*R*R*R;
/*printf("The value of VB0 is\n");
printf("%0.12Lf\n",VB0);
getchar();*/
for(i=0;i<=M;i++)
{
V[i]=VB0;
}
/*for(i=0;i<=M;i++)
{
printf("%0.12Lf\n",V[i]);
getchar();
}*/
MB0=roin*VB0;
/*printf("%0.12Lf\n",MB0);
getchar();*/
/*printf("%0.6Lf\n",T[1]);
getchar();*/
/*for(i=0;i<=M;i++)
{
printf("%0.6Lf\n",T[i]);
getchar();
}*/
```

```
/* Program of finite difference method based on pure implicit scheme*/
while(1)
{
for(i=0;i<=M;i++)
{
rob[i]=roin*CB[i];
roc[i]=roin*(Cc1[i]+Cc2[i]);
MB[i]=rob[i]*V[i];
Mc[i]=roc[i]*V[i];
Vs0=0.5*VB0;
Vs[i]=Vs0*(MB[i]/MB0)+shralpha*Vs0*(Mc[i]/MB0);
eta[i]=MB[i]/MB0;
Vg0=0.5*VB0;
Vg[i]=eta[i]*Vg0+(1.0-eta[i])*shrgamma*Vg0+shrbeta*(Vs0-Vs[i]);
V[i]=Vg[i]+Vs[i];
Vb[i]=Vg[i]/VB0;
Vgb[i]=Vg[i]/VB0;
voidfr[i]=Vg[i]/V[i];
}
/*for(i=0;i<=M;i=i+15)
{
printf("%0.12Lf %0.12Lf %0.12Lf %0.12Lf\n",rob[i],roc[i],MB[i],Mc[i]);
getchar();
}*/
/*for(i=0;i<=M;i=i+15)
{
printf("%0.12Lf %0.12Lf %0.12Lf %0.12Lf\n",Vs[i],eta[i],Vg[i],V[i]);
getchar();
}*/
/*printf("%0.6Lf\n",R);
getchar();
printf("%0.6Lf %0.6Lf\n",Tf,R);
getchar();*/
for(i=0;i<=M;i++)
{
sum[i+1]=sum[i]+CB[i];
}
avg[1]=sum[M+1]/(M+1);
conversion[1]=(1.0-avg[1])/(1.0);
/*printf("%Lf %Lf %Lf\n",sum[M+1],avg[1],conversion[1]);
getchar();*/
kB[M]=0.13+0.0003*(T[M]-273.0);
kc[M]=0.08-0.0001*(Tc[M]-273.0);
kg=0.02577;
jj=pow(T[M],3.0);
kk=pow(T[M],2.0)*Tf;
```

```
ll=pow(Tf,2.0)*T[M].
mm=pow(Tf,3.0).
bb=(5.67*pow(10.0,-8.0))*(ab).
aa=ht+(bb*(jj+kk+ll+mm)).
k[M]=eta[M]*kB[M]+(1.0-
eta[M])*kc[M]+voidfr[M]*kg+(13.5*bb*pow(T[M],3.0)*dp)/ab;
H[M]=(R/k[M])*(aa).
/*printf("%0.6Lf %0.6Lf %0.6Lf %0.6Lf  %0.6Lf %0.16Lf",jj,kk,ll,mm,aa,bb);
getchar();*/
/*kc[M]=0.08-0.0001*(Tc[M]-273.0).
jjc=pow(Tc[M],3.0).
kkc=pow(Tc[M],2.0)*Tf.
llc=pow(Tf,2.0)*Tc[M].
mmc=pow(Tf,3.0).
bbc=(5.67*pow(10.0,-8.0))*(ab).
aac=ht+(bbc*(jjc+kkc+llc+mmc)).
Hc[M]=(R/kc[M])*(aac);*/
ft=(tow*pow(R,2.0))/(alpha).
/*printf("The value of k[M],H[M],ft\n").
printf("\n%0.6Lf %0.6Lf %0.6Lf",k[M],H[M],ft);
getchar();
getchar();
printf("\n%0.6Lf %0.6Lf %d %0.6Lf",Tf,R,M,T[0]);
getchar();*/
for(i=0;i<=M;i++)
{
cp[i]=1112.0+4.85*(T[i]-273.0);
ro[i]=roin*(CB[i]+Cc1[i]+Cc2[i]).
Q[i]=((-dH)+(cp[i]*T[i]))/(ro[i]*cp[i]*(T0-Tf));
k1[i]=A1*exp((D1/T[i])+(L1/(T[i]*T[i])));
}
/*for(i=0;i<=M;i++)
{
printf("\n%0.6Lf %0.6Lf %0.6Lf %0.10Lf",cp[i],ro[i],Q[i],k1[i]);
getchar();
}*/
for(i=0;i<=M;i++)
{
cpc[i]=1003.2+2.09*(Tc[i]-273.0);
Qc[i]=((-dH)+(cpc[i]*Tc[i]))/(ro[i]*cpc[i]*(T0-Tf));
}
for(i=1;i<=M-1;i++)
{
a[i]=(((bf-1.0)*(dtow))/(2.0*dx*x[i]))-((dtow)/(dx*dx));
x[i+1]=x[i]+dx;
}
```

```
a[M]=((-2.0*dtow)/(dx*dx));
/*for(i=1;i<=M;i++)
{
printf("%0.6Lf\n",a[i]);
getchar();
}*/
b[0]=(((2.0*bf*dtow)/(dx*dx))+(1.0));
for(i=1;i<=M-1;i++)
{
b[i]=((2.0*dtow)/(dx*dx)+1.0);
}
b[M]=(((2.0*dtow)/(dx*dx))+(1.0)+((2.0*dtow*H[M])/(dx))+((bf-1.0)*dtow*H[M]));
/*for(i=0;i<=M;i++)
{
printf("%0.6Lf\n",b[i]);
getchar();
}*/
bc[0]=(((2.0*bf*dtow)/(dx*dx))+(1.0));
for(i=1;i<=M-1;i++)
{
bc[i]=((2.0*dtow)/(dx*dx)+1.0);
}
bc[M]=(((2.0*dtow)/(dx*dx))+(1.0)+((2.0*dtow*H[M])/(dx))+((bf-1.0)*dtow*H[M]));
c[0]=(-2.0*bf*dtow)/(dx*dx);
for(i=1;i<=M-1;i++)
{
c[i]=((((bf-1.0)*(-dtow))/(2.0*dx*x[i]))-((dtow)/(dx*dx)));
x[i+1]=x[i]+dx;
}
/*for(i=0;i<=M-1;i++)
{
printf("%0.6Lf\n",c[i]);
getchar();
}*/
for(i=0;i<=M;i++)
{
d[i]=(theta[i])+((dtow*Q[i]*R*R*k1[i]*pow((roin*CB[i]),n1))/(alpha));
}
/*for(i=0;i<=M;i++)
{
printf("%0.9Lf\n",d[i]);
getchar();
}*/
for(i=0;i<=M;i++)
{
dc[i]=(thetac[i])+((dtow*Qc[i]*R*R*k1[i]*pow((roin*CB[i]),n1))/(alpha));
```

```
}
beta[0]=b[0];
for(i=1;i<=M;i++)
{
beta[i]=b[i]-(a[i]*c[i-1])/(beta[i-1]);
}
/*for(i=0;i<=M;i++)
{
printf("%0.6Lf\n",beta[i]);
getchar();
}*/
betac[0]=bc[0];
for(i=1;i<=M;i++)
{
betac[i]=bc[i]-(a[i]*c[i-1])/(betac[i-1]);
}
gamma[0]=d[0]/beta[0];
for(i=1;i<=M;i++)
{
gamma[i]=(d[i]-a[i]*gamma[i-1])/(beta[i]);
}
/*for(i=0;i<=M;i++)
{
printf("%0.6Lf\n",gamma[i]);
getchar();
}*/
gammac[0]=dc[0]/betac[0];
for(i=1;i<=M;i++)
{
gammac[i]=(dc[i]-a[i]*gammac[i-1])/(betac[i]);
}
theta[M]=gamma[M];
i=M;
for(j=1;j<=M;j++)
{
theta[M-j]=(gamma[M-j])-((c[M-j]*theta[i])/(beta[M-j]));
i=i-1;
}
/*for(i=0;i<=M;i++)
{
printf("%0.6Lf\n",theta[i]);
getchar();
}*/
thetac[M]=gammac[M];
i=M;
for(j=1;j<=M;j++)
```

```
{
thetac[M-j]=(gammac[M-j])-((c[M-j]*thetac[i])/(betac[M-j]));
i=i-1;
}
for(i=0;i<=M;i++)
{
T[i]=Tf-theta[i]*(Tf-T0);
}
/*printf("T\n");
for(i=0;i<=M;i++)
{
printf("%0.6Lf\n",T[i]);
getchar();
}*/
for(i=0;i<=M;i++)
{
Tc[i]=Tf-thetac[i]*(Tf-T0);
}

/* Runge-kutta method starts here */
/*printf("\neqn        t      T       CB      CG1       Cc1       CG2     Cc2");*/
for(i=0;i<=M;i++)
{
while(1)
{
k1[i]=A1*exp((D1/T[i])+(L1/(T[i]*T[i])));
k2[i]=A2*exp((D2/Tc[i])+(L2/(Tc[i]*Tc[i])));
k3[i]=A3*exp(-E3/(Rc*Tc[i]));
a1=(-h)*((k1[i]+k2[i])*pow(CB[i],n1));
b1=h*((k1[i]*(Vb[i]/Vgb[i])*pow(CB[i],n1))-
(k3[i]*Vb[i]*pow(CG1[i],n2)*pow(Cc1[i],n3)));
c1=h*((k2[i]*pow(CB[i],n1))-(k3[i]*Vgb[i]*pow(CG1[i],n2)*pow(Cc1[i],n3)));
d1=h*(k3[i]*Vb[i]*pow(CG1[i],n2)*pow(Cc1[i],n3));
e1=h*(k3[i]*Vgb[i]*pow(CG1[i],n2)*pow(Cc1[i],n3));
a2=(-h)*((k1[i]+k2[i])*pow((CB[i]+(a1/2.0)),n1));
b2=h*((k1[i]*(Vb[i]/Vgb[i])*pow((CB[i]+(a1/2.0)),n1))-
(k3[i]*Vb[i]*pow((CG1[i]+(b1/2.0)),n2)*pow((Cc1[i]+(c1/2.0)),n3)));
c2=h*((k2[i]*pow((CB[i]+(a1/2.0)),n1))-
(k3[i]*Vgb[i]*pow((CG1[i]+(b1/2.0)),n2)*pow((Cc1[i]+(c1/2.0)),n3)));
d2=h*(k3[i]*Vb[i]*pow((CG1[i]+(b1/2.0)),n2)*pow((Cc1[i]+(c1/2.0)),n3));
e2=h*(k3[i]*Vgb[i]*pow((CG1[i]+(b1/2.0)),n2)*pow((Cc1[i]+(c1/2.0)),n3));
a3=(-h)*((k1[i]+k2[i])*pow((CB[i]+(a2/2.0)),n1));
b3=h*((k1[i]*(Vb[i]/Vgb[i])*pow((CB[i]+(a2/2.0)),n1))-
(k3[i]*Vb[i]*pow((CG1[i]+(b2/2.0)),n2)*pow((Cc1[i]+(c2/2.0)),n3)));
c3=h*((k2[i]*pow((CB[i]+(a2/2.0)),n1))-
(k3[i]*Vgb[i]*pow((CG1[i]+(b2/2.0)),n2)*pow((Cc1[i]+(c2/2.0)),n3)));
```

```
d3=h*(k3[i]*Vb[i]*pow((CG1[i]+(b2/2.0)),n2)*pow((Cc1[i]+(c2/2.0)),n3));
e3=h*(k3[i]*Vgb[i]*pow((CG1[i]+(b2/2.0)),n2)*pow((Cc1[i]+(c2/2.0)),n3));
a4=(-h)*((k1[i]+k2[i])*pow((CB[i]+a3),n1));
b4=h*((k1[i]*(Vb[i]/Vgb[i])*pow((CB[i]+a3),n1))-
(k3[i]*Vb[i]*pow((CG1[i]+b3),n2)*pow((Cc1[i]+c3),n3)));
c4=h*((k2[i]*pow((CB[i]+a3),n1))-
(k3[i]*Vgb[i]*pow((CG1[i]+b3),n2)*pow((Cc1[i]+c3),n3)));
d4=h*(k3[i]*Vb[i]*pow((CG1[i]+b3),n2)*pow((Cc1[i]+c3),n3));
e4=h*(k3[i]*Vgb[i]*pow((CG1[i]+b3),n2)*pow((Cc1[i]+c3),n3));
CB[i]=CB[i]+(1.0/6.0)*(a1+2.0*a2+2.0*a3+a4);
CG1[i]=CG1[i]+(1.0/6.0)*(b1+2.0*b2+2.0*b3+b4);
Cc1[i]=Cc1[i]+(1.0/6.0)*(c1+2.0*c2+2.0*c3+c4);
CG2[i]=CG2[i]+(1.0/6.0)*(d1+2.0*d2+2.0*d3+d4);
Cc2[i]=Cc2[i]+(1.0/6.0)*(e1+2.0*e2+2.0*e3+e4);
if(CB[i]<0.0)
{
CB[i]=0.0000001;
/*ss1[i]=CG1[i];
ss2[i]=Cc1[i];
ss3[i]=CG2[i];
ss4[i]=Cc2[i];*/
}
if(CG1[i]<0.0)
{
CG1[i]=0.0000001;
}
if(Cc1[i]<0.0)
{
Cc1[i]=0.0000001;
}
if(CG2[i]<0.0)
{
CG2[i]=0.0000001;
}
if(Cc2[i]<0.0)
{
Cc2[i]=0.0000001;
}
if(t[i]>=(ft-h))
break;
t[i]=t[i]+h;
}
}

/* Output */
/*for(i=0;i<=M;i++)
```

```
{
printf("\n%d \t%0.6Lf %0.6Lf %0.6Lf %0.6Lf %0.6Lf
%0.6Lf",eqn[i],t[i],T[i],CB[i],CG1[i],Cc1[i],CG2[i],Cc2[i]);
getchar();
}*/
printf("\neqn xx t T CB CG1 Cc1 CG2 Cc2 ");
xx=0.0;
for(i=0;i<=M;i=i+15)
{
/*CG1[i]=ss1[i];
Cc1[i]=ss2[i];
CG2[i]=ss3[i];
Cc2[i]=ss4[i];*/
printf("\n%d \t%0.1Lf %0.6Lf %0.6Lf %0.6Lf %0.6Lf %0.6Lf %0.6Lf
%0.6Lf",eqn[i],xx,t[i],T[i
],CB[i],CG1[i],Cc1[i],CG2[i],Cc2[i]);
/*getchar();*/
xx=xx+0.1;
}
printf("\nConversion=");
printf("%Lf",conversion[1]);
printf("\nAverage value of CB=");
printf("%Lf",avg[1]);
/*for(i=0;i<=M;i++)
{
if(CB[i]<0.0)
CB[i]=0.0000001;
}*/
getchar();
tow=tow+dtow;
if(CB[M]<=0.0000000)
if(CB[0]<=0.0000000)
break;
}
}
```

APPENDIX-G

G-1 Program to estimate optimum parameters using differential evolution

```
/* Program used in Chapter 8 */
/* Optimization of pyrolysis of biomass using differential evolution approach */
#define gen_max 1000
#define D 1
#define NP D*10
#define F 0.5
#define CR 0.7
#define inibound_l 0.2
#define inibound_h 1.2

/*----Constant for rnd_uni()----------*/
#define IM1 2147483563
#define IM2 2147483399
#define AM  (1.0/IM1)
#define IMM1  (IM1-1)
#define IA1   40014
#define IA2   40692
#define IQ1   53668
#define IQ2   52774
#define IR1   12211
#define IR2   3791
#define NTAB  32
#define NDIV  (1+IMM1/NTAB)
#define EPS1   1.2e-7
#define RNMX   (1.0-EPS1)
#include<stdlib.h>
#include<stdio.h>
#include<time.h>
#include<math.h>
```

```
#include<conio.h>
long double R;                  /* Radius of the particle (m) */
long double alpha;              /* alpha=used while calculating costmin i.e. dimensionless
                                time (m/s^2) */
long double HR;                 /* Heating rate (K/s) */
long double T0;                 /* Initial value of temperature (K) */
long double T;                  /* T=Temperature (K) */
long double CB;                 /* CB=Concentration of biomass (kg/m^3) */
long double k1;                 /* k1=Rate constant for reaction 1 (1/s) */
long double k2;                 /* k2=Rate constant for reaction 2 (1/s) */
long double k3;                 /* k3=Rate constant for reaction 3 (1/s) */
long double A1;                 /* A1=Arrhenius frequency factor for reaction 1 (1/s) */
long double A2;                 /* A2=Arrhenius frequency factor for reaction 2 (1/s) */
long double A3;                 /* A3=Arrhenius frequency factor for reaction 3 (1/s) */
long double D1;                 /* D1=Constant used while calculating k1 (K) */
long double D2;                 /* D2=Constant used while calculating k2 (K) */
long double L1;                 /* L1=Constant used while calculating k1 (K2) */
long double L2;                 /* L2=Constant used while calculating k2 (K2) */
long double E3;                 /* E3=Activation energy (J/gmol) */
long double Rc;                 /* Rc=Universal gas constant (J/gmol K)*/
long double Cc1;                /* Cc1=Concentration of char 1 (-) */
long double CG1;                /* CG1=Concentration of volatile 1 (-) */
long double Cc2;                /* Cc2=Concentration of char 2 (-) */
long double CG2;                /* CG2=Concentration of volatile 2 (-) */
long double t;                  /* t=Time (s) */
long double n1;                 /* n1=Order of reaction 1 (-) */
long double n2;                 /* n2=Order of reaction 2 (-) */
long double n3;                 /* n3=Order of reaction 3 (-) */
long double h;                  /* h=step size for RK4 Method (s) */
long double a1;
long double b1;
long double c1;
long double d1;
long double e1;
long double a2;
long double b2;
long double c2;
long double d2;
long double e2;                 /* a1-e4=Variable used while solving RK4 method */
long double a3;
long double b3;
long double c3;
long double d3;
long double e3;
long double a4;
long double b4;
```

```
long double c4;
long double d4;
long double e4;
long double store;                  /* To store the time (s) */
double evaluate(double [],long *);
double evaluate(double tmp[],long *nfe)
 {    double cost;  (*nfe)++;    /**** tmp[0]=x1, tmp[1]=x3; tmp[2]=x4;******/
       cost=2.4617*pow(tmp[0],4)-8.886*pow(tmp[0],3)+12.583*pow(tmp[0],2)-
7.7199*(tmp[0])+3.4088;
      return(cost);
        }

   /************** end of evaluate() ******************/

float rnd_uni(long *);
float rnd_uni(long *idum)
     {
     long j; long k;
     static long idum2=123456789;
     static long iy=0;static long iv[NTAB]; float temp;
     if(*idum<=0)
     {
       if(-(*idum)<1)   *idum=1; else *idum=-(*idum);  idum2=(*idum);
       for(j=NTAB+7;j>=0;j--)
       {
        k=(*idum)/IQ1;
        *idum=IA1*(*idum-k*IQ1)-k*IR1;
        if(*idum<0)      *idum+=IM1;
        if(j<NTAB)       iv[j]=*idum;
       }
       iy=iv[0];
     }
     k=(*idum)/IQ1;
     *idum=IA1*(*idum-k*IQ1)-k*IR1;
     if(*idum<0)    *idum+=IM1;
     k=idum2/IQ2;
     idum2=IA2*(idum2-k*IQ2)-k*IR2;
     if(idum2<0)
      idum2+=IM2;
      j=iy/NDIV;
      iy=iv[j]-idum2;
      iv[j]=*idum;
     if(iy<1)
      iy+=IMM1;
     if((temp=AM*iy)>RNMX)
      return RNMX;
```

```
    else
      return temp;
   }

void main()
{
  int i,j,k,a,b,c,good,count=0,seed; long nfe=0;
  double x1[NP][D],x2[NP][D],cost[NP],trial[D],cost_trial,costmax,costmin;
 printf("\nseed=");
 scanf("%d",&seed);
 long  rnd_uni_init= -(long)seed;
for (i=0;i<NP;i++)
{
    for (j=0;j<D;j++)
     {
     x1[i][j]=inibound_l + rnd_uni(&rnd_uni_init)*(inibound_h-inibound_l);
     }

  cost[i]=evaluate(x1[i], &nfe);
}
while (count<gen_max)
 {
    for (i=0;i<NP;i++)
    {
      do a=int ((rnd_uni(&rnd_uni_init))*NP); while (a==i);
      do b=int (rnd_uni(&rnd_uni_init)*NP); while (b==i || b==a);
      do c=int (rnd_uni(&rnd_uni_init)*NP); while (c==i || c==a || c==b);
      j=int (rnd_uni(&rnd_uni_init)*D);
      for (k=1;k<=D;k++)
       {
        if(rnd_uni(&rnd_uni_init)<CR  || k==D)
          {
          trial[j]=x1[c][j]+F*(x1[a][j]-x1[b][j]);
          }
          else trial[j]=x1[i][j];
         if(trial[j]>1.2    ||    trial[j]<0.2)    trial[j]=rnd_uni(&rnd_uni_init)*(inibound_h-
 inibound_l);
          j=(j+1)%D;
        }
     cost_trial=evaluate(trial, &nfe);
      if(cost_trial<=cost[i])
       {
          for (j=0;j<D;j++)
          x2[i][j]=trial[j];
          cost[i]=cost_trial;
         if(cost_trial<costmin)
```

```
        {
         costmin=cost_trial;
          /* imin=i;
         assignd(best,trial); */
        }
      }
      else for (j=0;j<D;j++)
          x2[i][j]=x1[i][j];

  }
/************* end of for loop ***************/


    for (i=0;i<NP;i++)
    {
       for (j=0;j<D;j++)
       x1[i][j]=x2[i][j];
    }
     costmax=cost[0];
     for(i=1;i<NP;i++)
      {  if(costmax<cost[i])
      costmax=cost[i];
      }
    costmin=cost[0];
     for(i=1;i<NP;i++)
      {  if(costmin>cost[i])
      costmin=cost[i];
      }
    if((costmax-costmin)<=0.00000001)
      break;
   count++;
 for(i=0;i<NP;i++)
 {
  for(j=0;j<D;j++)
  printf("\n HR[%d]=%lf",j,x1[i][j]);
  printf("\t Time[%d]=%lf   ",i,cost[i]);
  printf("gen=%d\n",count);
 }
 getch();

 }

 /************* end of while loop ***************/

 for(i=0;i<NP;i++)
```

```
{
 for(j=0;j<D;j++)
 printf("\n HR(dimensionless)[%d]=%lf",j,x1[i][j]);
 printf("\t Time(dimensionless)[%d]=%lf    ",i,cost[i]);
}
printf("\nTime_minimum(dimensionless)=%lf",costmin);
printf("\ngen=%d\n",count);
getch();

/* Constants */
alpha=1.79*pow(10.0,-7.0);
R=0.001;
T0=773.0;
t=(costmin*pow(R,2))/(alpha);
HR=((x1[0][0])*T0)/(t);
printf("\nThe optimum value of time in sec is ");
printf("%0.4Lf\n",t);
printf("\nThe optimum value of heating rate in K/sec is ");
printf("%0.4Lf\n",HR);
getch();
store=t;
/*printf("%0.6Lf\n",store);*/

/* Initial condition */
CB=1.0;
Cc1=0.0;
CG1=0.0;
Cc2=0.0;
CG2=0.0;

/* Input */
n1=1.0;
n2=1.5;
n3=1.5;
h=0.0001;
t=h;
printf("\n The optimum value of various parameters are as follows:\n");
printf("\nh(t)      HR  T    CB     CG1     Cc1      CG2     Cc2");

/* Runge-Kutta method starts here */
while(1)
{
T=(HR)*t+T0;
A1=9.973*pow(10.0,-5.0);
A2=1.068*pow(10.0,-3.0);
A3=5.7*pow(10.0,5.0);
```

```
D1=17254.4;
D2=10224.4;
L1=-9061227.0;
L2=-6123081.0;
E3=81000.0;
Rc=8.314;
k1=A1*exp((D1/T)+(L1/(T*T)));
k2=A2*exp((D2/T)+(L2/(T*T)));
k3=A3*exp(-E3/(Rc*T));
a1=(-h)*((k1+k2)*pow(CB,n1));
b1=h*((k1*pow(CB,n1))-(k3*pow(CG1,n2)*pow(Cc1,n3)));
c1=h*((k2*pow(CB,n1))-(k3*pow(CG1,n2)*pow(Cc1,n3)));
d1=h*(k3*pow(CG1,n2)*pow(Cc1,n3));
e1=h*(k3*pow(CG1,n2)*pow(Cc1,n3));
a2=(-h)*((k1+k2)*pow((CB+(a1/2.0)),n1));
b2=h*((k1*pow((CB+(a1/2.0)),n1))-
(k3*pow((CG1+(b1/2.0)),n2)*pow((Cc1+(c1/2.0)),n3)));
c2=h*((k2*pow((CB+(a1/2.0)),n1))-
(k3*pow((CG1+(b1/2.0)),n2)*pow((Cc1+(c1/2.0)),n3)));
d2=h*(k3*pow((CG1+(b1/2.0)),n2)*pow((Cc1+(c1/2.0)),n3));
e2=h*(k3*pow((CG1+(b1/2.0)),n2)*pow((Cc1+(c1/2.0)),n3));
a3=(-h)*((k1+k2)*pow((CB+(a2/2.0)),n1));
b3=h*((k1*pow((CB+(a2/2.0)),n1))-
(k3*pow((CG1+(b2/2.0)),n2)*pow((Cc1+(c2/2.0)),n3)));
c3=h*((k2*pow((CB+(a2/2.0)),n1))-
(k3*pow((CG1+(b2/2.0)),n2)*pow((Cc1+(c2/2.0)),n3)));
d3=h*(k3*pow((CG1+(b2/2.0)),n2)*pow((Cc1+(c2/2.0)),n3));
e3=h*(k3*pow((CG1+(b2/2.0)),n2)*pow((Cc1+(c2/2.0)),n3));
a4=(-h)*((k1+k2)*pow((CB+a3),n1));
b4=h*((k1*pow((CB+a3),n1))-(k3*pow((CG1+b3),n2)*pow((Cc1+c3),n3)));
c4=h*((k2*pow((CB+a3),n1))-(k3*pow((CG1+b3),n2)*pow((Cc1+c3),n3)));
d4=h*(k3*pow((CG1+b3),n2)*pow((Cc1+c3),n3));
e4=h*(k3*pow((CG1+b3),n2)*pow((Cc1+c3),n3));
CB=CB+(1.0/6.0)*(a1+2.0*a2+2.0*a3+a4);
CG1=CG1+(1.0/6.0)*(b1+2.0*b2+2.0*b3+b4);
Cc1=Cc1+(1.0/6.0)*(c1+2.0*c2+2.0*c3+c4);
CG2=CG2+(1.0/6.0)*(d1+2.0*d2+2.0*d3+d4);
Cc2=Cc2+(1.0/6.0)*(e1+2.0*e2+2.0*e3+e4);
t=t+h;
if(store<t)
break;

/* Output */                                                %0.6Lf        %0.6L
/*printf("\n%0.6Lf        %0.6Lf        %0.6Lf
%0.6Lf",t,T,CB,CG1,Cc1,CG2,Cc2);*/
/*getchar();*/
```

```
}
printf("\n"),
printf("\n%0 4Lf      %0 4Lf      %0 6Lf      %0.6Lf      %0.6Lf      %0.6Lf      %0.6Lf
%0.6Lf",t,HR,T,CB,CG1,Cc1,CG2,Cc2),
getchar(),
getchar(),
getchar(),

} /************ end of main() ******************/
```